UNIVERSITY OF NAIROBI
School of Engineering

Department of Electrical and Information Engineering

MSC (ELECTRICAL AND ELECTRONIC ENGINEERING)

OPTIMAL SIZING AND ANALYSIS OF A STAND-ALONE HYBRID SOLAR PV – WIND POWER SYSTEM WITH STORAGE

By

Victor Omondi Okinda

F56/69159/2013

Signature ..... Date .....

Supervisor

Prof. Nicodemus Abungu Odero

Signature ..... Date .....

A thesis submitted in partial fulfilment of the degree of Masters of Science in Electrical and Electronic Engineering of the University of Nairobi.

Declaration

This MSC research work is my original work and has not been presented for a degree award in this or any other university.

Victor Omondi Okinda

F56/69159/2013

This MSC research work has been submitted to the School of Engineering, Department of Electrical and Information Engineering, The University of Nairobi with my approval as supervisor.

Prof. Nicodemus Abungu Odero

Date……..

DECLARATION OF ORIGINALITY

NAME OF STUDENT: VICTOR OMONDI OKINDA

REGISTRATION NUMBER:F56/69159/2013

COLLEGE: ARCHITECTURE AND ENGINEERING

FACULTY: ENGINEERING

DEPARTMENT: ELECTRICAL AND INFORMATION ENGINEERING

COURSE NAME: MASTERS OF SCIENCE IN ELECTRICAL AND ELECTRONIC ENGINEERING

TITLE OF WORK: OPTIMAL SIZING, MODELLING, SIMULATION AND SENSITIVITY ANALYSIS FOR A STAND-ALONE HYBRID SOLAR PV – WIND RENEWABLE ENERGY POWER SYSTEM WITH ENERGY STORAGE

1. I understand what plagiarism is and I am aware of the university policy in this regard.
2. I declare that this final year project report is my original work and has not been submitted elsewhere for examination, award of a degree. Where other people's work or my own work has been used, this has properly been acknowledged and referenced in accordance with the University of Nairobi's requirements.
3. I have not sought or used the services of any professional agencies to produce this work
4. I have not allowed, and shall not allow anyone to copy my work with the intention of passing it off as his/her own work.
5. I understand that any false claim in respect of this work shall result in disciplinary action, in accordance with University anti-plagiarism policy.

Signature:

……..……

Date:

……..

Dedication

This research work is dedicated to my mother and father, fiancée, friends and all benefactors for having faith in me.

Acknowledgement

First and foremost, I wish to thank the Almighty God for being by my side throughout the duration of this intense and laborious research.

I would like to acknowledge and state my immense gratitude to my supervisor Prof. Nicodemus Abungu Odero, the Dean-Faculty of Engineering, Chairman-Department of Electrical and Information Engineering and all my lecturers and support staff at the University of Nairobi for their support which contributed greatly to the provision of knowledge as well as the completion of this thesis.

Finally, I extend special thanks to my parents, Mr. and Mrs. Okinda, fiancée Ms. Nyakundi, friends and benefactors for their mutual, emotional and material support throughout the duration of this work.

Table of contents

List of tables

List of figures

Abbreviations

A

AMPL: A Mathematical Programming Language, 10, 11

ARMA: AutoRegressive Moving Average, 125

B

BESS: Battery Energy Storage System, 2, 11, 16, 23, 59, 66, 67, 68, 70, 71, 79, 80, 151, 153, 154, 162

C

CAES: Compressed Air Energy Systems, 16, 23, 59, 60, 126

COE: Cost of Energy, 7

D

DFIG: Doubly Fed Induction Generators, 55

DG: Distributed Generation, 10, 124

DIRECT: DIviding RECTangles Search Algorithm, 6, 7, 123

DNI: Direct Normal Irradiance, 25, 26, 29

DPSP. *See* LPSP

DSM: Demand Side Management, 79, 88, 89, 97, 100, 104, 108, 114, 117, 118, 151, 152

E

EENS: Expected Energy Not Served, 17, 18, 19

ELF: Equivalent Loss Factor, 18, 19

EPA: (Model) Equilibrium Point Analysis, 9

ESS: Energy Storage System, 8, 9, 10, 11, 16, 17

F

FCWT: Full Converter Wind Turbine, 55, 56

FES: Flywheel Energy Storage, 16, 59, 60, 61

FLNS: Fractional Load Not Served, 19

G

GA: Genetic Algorithm, 5, 7, 9, 22, 80, 81, 82, 83, 121, 145, 155, 157, 159, 161

GHG: Green House Gases, 3, 4

GHI: Global Horizontal Irradiation, 25, 26, 29, 87

H

HRES: Hybrid Renewable Energy Source, 5

K

KiBaM: Kinetic Battery Model, 69

U

UC: Ultra Capacitors, 16, 59

UNDP: United Nations Development Program, 4, 123

USDM: Million United States Dollars, 114

W

WSB-HPS: Wind, Solar, Battery Hybrid Power System, 13

WTG: Wind Turbine Generator, 58, 151

Abstract

There is a global push towards green and sustainable energy which has seen several initiatives being developed to spearhead and promote development of renewable energy generation sources. However, this has not been without challenge. Solar and wind, the most abundant renewable energy resources are still expensive to deploy and unreliable as they suffer from intermittency.

It has long been postulated in open published literature that solar and wind have complementary regimes and that it is possible to make headways in reliability of renewable energy systems by hybridization sources that have complementary regimes. A hybrid solution however is only viable if optimally sized. This thesis examines the problem of optimally sizing a Hybrid Solar and Wind Renewable Energy Power System (HSWREPS). A target location was first identified and meteorological data collected. Components of the system were then mathematically modelled from which an objective function was developed. A parallel multi-deme implementation of genetic algorithms was used to perform the optimization. Multiple scenarios were prepared and simulated to obtain an optimal configuration of the HSWREPS. The results obtained were validated against openly published results from real word projects. A conclusion was then drawn on the basis of the results obtained. The research was successful as all objectives were met. The key findings were first and foremost that in deed on some locations wind and solar have complementary regimes and can thus be hybridized. To this end an optimal configuration of the system consisting of 16,000 PV modules, 10 wind turbine units and 23,809 battery units was developed with an attractive levelized cost of energy of 17 US cents per kWh. Secondly, the research from the results obtained decoupled resource optimal solutions from cost optimal solutions. It was shown that the least cost configuration didn't necessary maximize on utility of the abundant resource. Lastly a clear direction for future research was proposed.

Chapter 1 Introduction

1.1 Background

With the price of oil and associated conflict resulting therefrom in rapid ascent, the threat of global warming and climate change all too apparent, renewable energy technologies are emerging as the answer to power our future. However, Geothermal, hydro power and biomass are limited by resource availability and are plagued by high development costs. Wind and solar have thus emerged as promising technologies for achieving a green powered future, however wind and solar are intermittent sources of energy. A robust power system should be able to meet its demand wholly and reliably, and this is a challenge for intermittent sources of energy. Hybridization of renewable energy sources with complimentary regimes is a new emergent trend being utilized to improve reliability. In some locations for example, a strong solar irradiance is experienced in summer when wind speeds are poor whereas in winter when solar irradiance is poor, stronger winds are recorded. Moreover, on an intra-day basis, wind and solar pick up, and slack at different times hence a plant that combines the two in a hybrid system should theoretically provide a better utilization factor for the available energy [1].

A Hybrid Solar photovoltaic and Wind Renewable Energy Power System (HSWREPS) with battery storage is proposed. The battery banks which store energy are a vital part of this as they convert the jerky intermittent power produced into a smoother and dispatch-able form by storing excess energy when the sun and/ or wind are very strong and releasing this back when there is a shortfall in generation, thus providing a ride-through capacity to the systems in cases of generation insufficiency.

For this work, a remote town in the Northern region of Kenya is selected as a case study. It has been realized that some of these regions have an abundant untapped potential for wind and solar that can be harnessed to power small remote towns and outposts in Kenya. This is thus a promising area of application as these remote towns are either powered by diesel generators which are costly to operate and maintain due to associated high fuel and fuel transport costs or are without power as they are usually cut off from the grid.

1.2 Problem Statement

This research thesis attempts to provide a solution to the problem of optimal size configuration for hybrid renewable energy power plants. Since wind and solar have complementary regimes in some locations, they particularly lend themselves well to hybridization. The key problem here then is that of optimal capacity selection to ensure the total cost of the system is minimized while maximizing system reliability.

However before optimal sizing procedures are carried out, a necessary first step is to mathematically model the components to be hybridized. Energy generated from Wind will be modelled as well as energy generated from PV cells. The expected inputs to these models will be prevailing speed of wind at the desired mast height and solar irradiance for the specific location taken as a case study. A model for energy storage will also be necessary to evaluate adequacy of proposed energy storage capacity.

Finally a model of the load to be served will also be made. The load model is necessary as power demand varies at different times of the day. These models are then used to evaluate the fitness and reliability of a proposed system.

Simulation of the proposed optimal system is then done. This will be necessary for the system's sensitivity analysis. Various conditions are simulated and the systems response is observed.

1.3 Objectives

The study's broad objective is to determine an optimal size configuration for a HSWREPS with battery storage intended to supply electricity to a remote town. Specific objectives to be met include

1) To mathematically model the hybrid power system components

   Mathematical modelling of the system components will be necessary in order to come up with the necessary cost function to be minimized or fitness function to be maximized. The researcher is obliged to fully and comprehensively understand the modelling method in order to employ it in this work

2) To develop an appropriate fitness function to evaluate suitability of the proposed systems

   After careful modelling of RE sources, BESS and Load, the researcher then needs to develop a proper fitness function for maximization of desirable system attribute, and

proper boundary conditions to ensure that resulting systems from the optimization procedure meet the set system constraints.

3) To simulate and perform multiple scenario analysis to arrive at an optimal size configuration for the power system developed.

   Multiple scenarios are analysed to arrive at an optimal solution using a parallel genetic algorithm implementation.

1.4 Research Questions

To meet these objectives, the researcher sought to answer the following questions;

1) Is it possible to design a hybrid wind and solar power system (HSWREPS) for the selected location?
2) Can the components of the HSWREPS be modelled mathematically?
3) Can an objective function be developed from the models developed of the components
4) Can the objective function developed be minimized to arrive at an optimal solution?

Answering these research questions helped the researcher meet the objectives stated above.

1.5 Justification for the Study

Rapid depletion of fossil fuels, political instability amongst other reasons have kept the price of conventional fossil fuels sky high. Moreover, carbon emissions resulting from burning of fossil based fuels has led to global warming and resulted in climate change, a major catastrophe that has already led to the extinction of some species as well as geographical changes such as rising ocean levels.

The World Bank Report on climate change, "Turn Down the Heat" , highlights the key effects of global warming as being, unusual and unprecedented heat extremes, rainfall regime changes and decline in water availability, decline in agricultural yields and nutritional quality, threats on terrestrial eco systems, sea level rise and damages to marine eco systems [5]. The report further states that if current trends continue, a 4°C warmer world will be a reality by the turn of the century and further warming will continue in the 22nd century. The report proposes development of cleaner energy technologies as a possible mitigant in reducing the GHG emission rates. In fact a key area

of focus for the World Bank has been in improving energy efficiency and performance of renewable energy technologies. This is a compelling reason to focus research in renewable energy generation technologies.

Separately, the United Nations millennium development goals [6], and goal number 7 in particular advocates for ensuring environmental sustainability. One of the target areas for promoting environmental sustainability especially in energy production is through the development of clean energy sources [6]. Moreover, the United Nations Development Program (UNDP), has Sustainable Energy as one of its key focus areas [7]. One of its three key areas of intervention is the promotion of the development of low emission climate resilient technologies such as those that this research intends to better understanding on.

It is my view thus that this research work is justified in view of current knowledge needs of mankind. It is focussing on an area of significant potential in terms of benefiting mankind. Renewable energy technologies having been accepted as methods for curtailing GHG emission and curbing climate change are still expensive and in some cases less efficient than conventional fossil fuel based generation methods. By hybridizing wind and solar and capitalizing on the complementary nature in their regimes, coupled with optimal sizing using state of the art heuristic based computational methods, this research hopes to improve knowledge in the field and to chart ways towards more affordable green power generation technologies.

1.6 Scope of work

This research is on optimal size configuration of components of a hybrid solar PV and wind renewable energy power system which incorporates battery energy storage. To see this through, the researcher envisions having to properly understand and apply a modelling method to model the components of the system to be hybridized. A geospatial resource assessment will then follow, the scope of which entails collection of relevant climate data for the selected site. Demand modelling will be carried out based on available data for a model metropolis. The researcher intends to take great care and effort to improve any of the modelling methods in use in open literature and to suitably apply them to this problem. An optimization program will be written in Matlab, implementing a parallel multi-deme Genetic Algorithm optimization. Major improvement to existing methods is expected as the researcher will implement this algorithm to take advantages

of recent advances in parallel programming. Simulation will then be carried out and multiple scenario analysis conducted.

Key milestones in this research will be: Completion of Literature Review, Proposal documentation, presentation and defence, model construction for components of the HRES, Implementation of GA based parallel optimization software in Matlab®, Presentation of Simulation results, thesis documentation, presentation and defence.

At the end of the research, expected deliverables will be: publications in peer reviewed journals, thesis document, optimization software based on a parallel implantation of GA, results of the optimal configuration of a HRES

1.7 Organization of Thesis

This thesis is organized into 5 broad chapters each with a distinct purpose. Chapter 1 provides an introduction to the work, the problem statement, objectives and scope of the work. Chapter 2, titled literature review, is a review of open published research work in the field. It provides a backdrop of method for analysis and results from other researchers that can be drawn from for inspiration or comparison. The third chapter, methodology is broken down into 3 sub chapters. The first, geospatial resource assessment recognizes that the study has to be based on a specific geographical location, based on resource availability and not only pin points such suitable locations but also examines the resources at those locations. The second part, component modelling, takes on the solution to the problem of mathematically modelling the components of the hybrid power system. The final part of chapter 3, addresses the algorithm used to optimally size the power system.

The fourth chapter presents the results of the work and discussion of those results, and the final chapter presents the conclusion, contributions of this work and recommendations for further work.

Chapter 2 Literature Review

The problem of optimal size configuration for hybrid renewable energy systems is very common in recent published works. Various authors have proposed various methods to solving the problem. In this review of current literature on the topic, the various approaches have been categorized by:

- Method used for the optimization of the size of the components of the system
- Generation technologies considered for hybridization,
- Energy storage system employed,
- Reliability index used to ascertain reliability of system designed,
- Modelling method used to represent the individual parts of the system and to develop the objective function,
- Simulation method used to simulate the design concept and validation method used.

2.1 Classification by optimal sizing methodology.

Various methods for performing optimization exist in literature. Some methods take a gradient based optimization approaches while others follow heuristic approaches. The methods presented in the literature reviewed include:

- Genetic Algorithms
- Fuzzy genetic algorithms
- Particle Swarm Optimization
- Simulated Annealing
- Dividing Rectangles (DIRECT) Search Algorithm
- Commercial Software
- Integer Programming
- Response Surface Methodology
- Hybridized Solutions

2.1.1 Dividing Rectangles (DIRECT)

Focussing on the development of a methodology for determining the optimal size of a stand-alone hybrid system, **Zhang et al (2011)** [8] used DIRECT search algorithm to select the optimal number

and type of units from a list of commercially available system devices, for a configuration that ensured availability of energy to meet energy demands. Their case study was the French commune of Le Havre. In a similar fashion to [8], **Yassine et al (2012)** [9] also used DIRECT to select the optimal number and size of system components in a manner ensuring that the objective cost function is minimized from a list of commercially available solutions,. They considered 4 different combinations of hybrid systems. Similarly, **Belfkira et al (2007)** [10] presented a methodology for the design of a HSWREPS with Battery Storage. Using DIRECT they determined the optimal configuration wind turbine generators, solar PV modules and storage units that ensured the system cost was minimized and reliability maximized to guarantee permanent availability. They developed their solution using Matlab®.

2.1.2 Optimal Sizing using Genetic Algorithms

Genetic Algorithms are metaheuristic search algorithms that mimic nature in particular evolution and Natural selection. They usually start with a random generation of an initial population of chromosomes with or without domain specific knowledge. The chromosomes are represented as a data structure of binary numbers or real numbers depending on the encoding method and are parameters of possible solutions to the problem at hand. Encoding is a process of representing the solution parameters in terms of a string, just as in a real chromosome .The entire population, with all the chromosomes is referred to as the search space and it is from therein that an optimal solution is to be located. A problem specific fitness function is used to map the chromosomes into a fitness value which is a representation of the quality of the solution [81].

GA operators are then used to evolve the population from its current generation to the next whose average fitness value should ideally be better. The selection operator, which mimics the process of selecting a mate to sire the future generation, determines good solutions that are to be preserved in the population and bad solutions that are to be pruned from it. The selection operator's objective is to emphasize positive traits in the population and discard negative ones. Some of the selection techniques include: Tournament selection, Roulette Wheel Selection, Rank Selection etc.

After suitable parents are selected, crossover occurs. It mimics the successful mating event whereby offspring are created from the suitable parents selected for mating. Gene information is exchanged between the solutions in the mating pool. There exists single point and multi point crossover, the difference being the amount of gene information exchanged and point of exchange. Multipoint crossover is disruptive and appears to encourage the exploration. Exploration is the

ability to discover new regions of the solution space whilst trying to locate the optimum. On the other hand, exploitation is the ability to converge to the optimum after discovering the region containing the optimum. To prevent premature convergence to a sub-optimal solution, exploration should always precede exploitation [82]. The probability of occurrence of crossover is dictated by the crossover rate P_c.

After crossover, just as in real life, a random but very rare event mutation occurs. Mutation is a shift from norm, it involves the introduction of new features into the solution string of the population pool. Mutation encourages exploration in genetic algorithms. The probability of occurrence of mutation is governed by the mutation rate P_m.

New generations are thus evolved from the knowledge of previous generations and since the fitter individuals in the population are the ones selected for mating (crossover), their good genes (good solutions) overtime dominate the population and the algorithm converges to an optimum. With proper parameter selection ($P_c, P_m, popsize$), GA's are capable of obtaining a global optimum to solution.

(1) Adaptive Genetic Algorithms

Use of static control parameters for GA has been a limitation requiring proper tuning of the algorithm to find the right value that reaches an optimal solution. As observed by Skinner et al [82], the domain of artificial genetic search, as in the process of evolution is an inherently dynamic and adaptive process and the use of static parameters contradicts the evolutionary idea.

Consequently in order to maintain a balance and precedence between exploration and exploitation strategies to dynamically adapt parameters of genetic algorithms have been developed.

A dynamic deterministic approach involves modification of the parameter values according to some decreasing value as the GA evolution proceeds. An example is decreasing the mutation probability as the generation count increase to enhance exploitation.

A dynamic adaptive approach relies on feedback from the GA. This approach would adapt mutation rate and crossover rate simultaneously. For instance, for individuals with a low fitness value, to enhance exploration P_C and P_m would be kept large whereas they would be kept small for individuals with high fitness values to protect good solutions from distortion.

Finally, a dynamic self-adaptive technique, encodes parameters into the genotype and evolves them together with the chromosomes. It is aimed at exploiting the indirect link between favorable control parameters and individual fitness values. This strategy has however met limited success.

(2) Parallel Genetic Algorithms (PGA)

GA's have been used for since their invention in the 80's for solving nonlinear problems with a great number of possible solutions, that are typically very difficult to solve with classical mathematical methods [14]. However when applied to very large scale problems, genetic algorithms due to increased complexity, exhibit high computational costs and degradation of the quality of solutions [81]. To solve this and take advantage of developments in distributed computing, research on parallel genetic algorithms has gained quite a footing. What follows below is a brief of the categories or parallelization strategies in use today.

A global parallelization strategy or the global single population master slave PGA, parallelizes GA by assigning a fraction of the population to each processor for evaluation. A master process performs the genetic operators and distributes the individuals among a set of slave processors that evaluate fitness values. It is particularly effective for complicated fitness functions and it can yield improvements in computational time with regard to sequential genetic algorithms. [81] It does not require additional genetic operators and therefore does not modify the fundamental search behavior of GA. [82]

A single population fine grained PGA or simply fine grained parallelization, assigns exactly one individual to a processing node. Only adjacent individuals participate in genetic operators, hence the topology of the network is crucial to the performance of the GA. This approach is only practical in massively parallel architectures and for solving problems that easily lend themselves to parallelism and are designed with low communication overhead.

The coarse grained parallelization approach partitions the entire population into subpopulations called **demes** [81]. The subpopulations in multi-deme PGA's are relatively large, a defining characteristic. Moreover, when the GA is run, exchange of information between demes is performed in a process termed **migration**. Migration is a very crucial aspect of coarse grained PGA's and is characterized by: period of migration, selection and replacement strategy of individuals, and the number of migrants [82]. As in fine grained PGA's the network topology used is important as it determines the cost of migration in terms of communication overhead and the

rate at which good solutions are disseminated to other demes. This approach is also referred to as island model PGA.

(3) Coarse Grained Adaptive PGA

For this research work, a coarse grained adaptive PGA will be implemented for the purpose of optimal sizing of the renewable hybrid energy system and its associated energy storage requirements. This is advised mainly by the complicated nature of the problem which may render traditional GA inefficient and slow. Moreover Adaptive PGA has been shown to converge faster than PGA as in [83]. Skinner et al [82] also reported significant improvement on convergence velocity and solution quality over ordinary serial Genetic Algorithms when using multi-deme "coarse grained" parallel GA on a set of three benchmark problems: Sphere function, Rastrigin's function and Ackley's path function.

(4) Applications in reviewed literature

Using GA for optimization of the size and configuration of a hybrid solar PV and wind system with battery storage, **Yang et al** [11] had 2 main considerations, these being the cost of the designed system and its reliability under different weather conditions. In parallel **Bilal et al** [12] used a multi-objective GA approach to find an optimal size configuration of a HSWREPS with battery storage. They selected a remote location in the Northern coast of Senegal as a case study for the problem of optimal sizing of a hybrid renewable power system. The problem was formulated as a multi-objective optimization problem solved using genetic algorithms. Their twin objectives were to minimize system cost and maximize reliability by minimizing the loss of power supply probability (LPSP). Their key finding was that the optimal configuration had a strong dependence on the load profile, a conclusion arrived at after investigating different load curves with similar total energy consumption. Separately, **Jemaa et al (2013)** [14] using fuzzy adaptive GA, developed a technique to optimally configure a HSWREPS. In their technique, a fuzzy logic mechanism was used to dynamically change crossover and mutation rates so as to guarantee diversity of the population and hence prevent arbotive convergence. Their objective was to minimize the cost of the system whilst ensuring an invariable availability of supply to meet demand. Components of the system were stochastically modelled using hourly historical data. In similar strides a novel technique for determining the optimal unit size for distributed generators in a micro-grid was developed by **Tafreshi et al** [13]. They used GA to optimize the system to achieve a desired LPSP at a minimum Cost of Energy (COE).

2.1.3 Particle Swarm Optimization

Pirhaghshenasvali et al [15] presented a paper in which a hybrid system for a practical standalone renewable energy generation system was proposed. They employed Wind, PV, Battery banks and Diesel Generators in their hybridization. The Wind PV Battery system was intended as the primary system with the diesel generator provided as a backup system. The goal of their optimization was to minimize investment cost and fuel cost while ensuring availability of the energy needed by the customers and sufficiency to meet peak demand. The design was based on solar radiation data, wind speed data and load curves and Particle Swarm Optimization algorithm was used for optimal sizing.

Bashir and Sadeh [16]argued that capacity sizing was important to fully meet demand due to uncertainty of wind and solar PV. They proposed a method for determining capacity of hybrid wind, PV with battery storage. Their proposed method considered uncertainty in generation of wind energy and of solar PV. They formulated the algorithm for determining the capacity of wind, PV and battery ESS as an optimization problem with the objective of minimizing the system cost whilst constrained to having a given reliability for a given load. This was solved using the PSO algorithm.

Bashir and Sadeh [17] also presented a paper in which they considered a hybrid system of wind, PV and tidal energy with battery storage. In this paper they highlight the benefits of tidal energy which is energy harnessed from rising and falling of ocean water levels as being highly predictable compared to wind and solar. They consider a 20 year plant life and optimize the design with the objective of minimizing the annualized cost of generated energy of the life of the plant, with the constraint of having a specific reliability index. They used PSO algorithm for optimization. Simulation carried out in Matlab environment and revealed that in comparison to stand alone wind and solar systems the new system was more economical.

Saber and Venayagamoorthy [18] presented a paper suggesting the introduction of controllable loads with intelligent optimization as a necessity for the implementation of smart micro grids (SMG). They noted that over or under estimation of resources when considering reliability of the smart micro grid would make it not feasible, thus the optimization problem for sizing of SMG components was presented as a complex multi-objective optimization problem considering minimization of capital cost and operations costs as objectives subject to constraints such as net zero emission, historical wind speed and solar irradiation data and load profiles over a long period

of time. They used the PSO algorithm to solve the optimization problem, and an intelligent energy management system for dispatch of the resources.

Navaerfad et al [19], presented an optimal sizing approach for Distributed energy resources in a micro grid consisting of Wind, solar hybrid system with electrolizer, hydrogen tank, fuel cell and batteries. They proposed the uncertainty of wind power alongside a reliability index as constraints and used PSO algorithm to obtain the global optimal solution.

He, Huang and Deng [20] postulated that low carbon power technologies such as Solar - PV, Wind etc. are gaining a lot of interest and concern worldwide, and because these technologies are mainly adopted in micro grids, they emphasized on the importance of considering the low carbon factor in the generation planning of micro grids. In this paper they use the levelized cost of electricity (LCOE) analysis method to compare the variation trends of power supplies which use different energy sources to generate in the future, and to build the energy price equilibrium point analysis model (EPA) of high carbon energy and low carbon energy. Based on the above research, the authors develop a full life cycle dynamic model for optimal sizing of components in an integrated power generation model. Modified particle Swarm optimization was used to perform optimization. Based on the three cases considered, low carbon, high carbon and equilibrium, results show that a balanced system is most suitable for clean energy production with an equilibrium point of energy consumption and carbon consumption.

2.1.4 Simulated Annealing

Ekren and Ekren [21] used simulated annealing method for size optimization of a hybrid PV / Wind energy conversion system. Simulated annealing is a heuristic approach that uses stochastic gradient search approach for optimization. The objective function to be minimized was the hybrid system's total energy cost, with the key parameters being the PV area, wind turbine rotor sweep area and battery capacity. Results from simulated annealing were compared with those of RSM for an earlier study [22] and it was shown that simulated annealing obtained better results.

2.1.5 Hybridized Meta-heuristics

Crăciunescu et al [23] reckoned using Wind and Solar PV technology with battery ESS in optimally sized combination can help overcome the problem of intermittency that each of these technologies face. In the review of literature they presented, it was shown that GA and PSO were the most popular heuristic methods for optimal sizing of a hybrid wind solar power system with

battery storage. In this paper, mathematical models of hybrid wind and solar were developed and multi-objective optimization performed using the intelligent search methods GA and PSO.

Arabali et al [24] proposed a stochastic framework for optimal sizing and reliability analysis of a hybrid power system including renewable energy sources and energy storage. Uncertainties of wind and PV power generations were modeled stochastically using Auto Regressive Moving Average. A pattern search optimization method was then used in combination with sequential Monte Carlo Simulation (SMCS) to minimize system cost and satisfy system reliability requirements. SMCS simulates chronological behavior of system and emulates the reliability indices from a series of simulated experiments. They then proposed Load shifting strategies to provide some flexibility and reduce mismatch between Renewable Energy generation and Heating Ventilation and Cooling loads in the hybrid power systems. A compromise solution method was then used to arrive at the best compromise between reliability and cost.

2.1.6 Commercial Software, HOMER

Roy et al [25] estimated the optimal sizing for a hybrid solar - wind system for distributed generation for utilization of resources available at Sagar, a remote off grid Island. They optimized the feasibility and size of the generation units and evaluated them using Hybrid Optimization of Multiple Energy Resources (HOMER) software. Sensitivity analysis was performed on the optimal configuration obtained. A comparison between the different modes of the hybrid system was also studied. It was estimated that the solar PV -Wind Hybrid system provided lesser cost per unit of electricity. The capital investment cost was also observed to be less when the system ran with wind DG compared to solar PV DG.

El Badawe et al [26] aimed to optimize and model a hybrid wind solar diesel generator power system for use on remote microwave repeaters. They noted that microwave repeaters were the main energy consumers in the telecommunication industry and are usually powered by diesel generators and when these were located on remote sites, then maintenance and operations costs were even higher due to the added cost of transportation. They used HOMER software for sizing and performed sensitivity analysis to obtain the most feasible configuration, which was then modelled in SIMULINK and results presented to demonstrate system performance.

2.1.7 Integer Programming

Chen and Gooi, [27] proposed a new method for optimal sizing of an energy storage system. The ESS was to be used for storage of energy at times of surplus and for re-dispatch later when needed. They considered the Unit commitment problem with spinning reserve for micro grids. Their total cost function took account of the cost of the Energy Storage System (ESS), the cost of output power and the cost of spinning reserve. They formulated the main method as a mixed nonlinear integer problem (MNIP) which was solved in AMPL (A mathematical programming language). Effectiveness of the proposed method was then validated by a case study where optimal ESS rating for a micro grid were determined. Results indicated that a properly sized ESS not only stored and re-dispatched renewable energy appropriately but also reduced the total cost of the micro grid.

Bahramirad and Reder's [28] view on Energy Storage systems was that they are fast response devices that add flexibility to the control of micro grids and provide security and economic benefits to the micro grid. They thus have a major role in the long term and short term operation of micro grids. In the paper, they evaluated the benefits of ESS in islanded operation of micro grids. Long term unit commitment was then used to obtain the optimal unit scheduling. A practical model for an Energy Storage System was used and probabilistic reliability calculation method used to find expected energy not served and accordingly calculate cost of reliability of the micro grid. They solved the optimization problem using mixed integer programming method.

Chen, Gooi and Wang [29] presented a cost benefit analysis based method for optimal sizing of an energy storage system in a micro grid. They considered the unit commitment problem with spinning reserve for micro grids. Wind speed was modelled using a time series whereas solar irradiance is modelled via feed forward neural network techniques with forecasting errors being accounted for. They also presented two mathematical models for islanded and grid operation. The main problem was formulated as a mixed linear integer problem (MLIP) which is solved in AMPL. Effectiveness of the proposed method was then validated via a case study. Quantitative results indicated that optimal size for a BESS existed but differed for both grid connected and islanded mode of operation.

2.1.8 Response Surface Methodology

Ekren and Ekren (2008) [22] presented a paper aimed at showing the use of response surface methodology (RSM) in size optimization of an autonomous Wind / PV system with battery storage. The response surface output performance measure was the hybrid system cost whilst the design

parameters were PV size, wind turbine rotor sweep area and battery capacity. A commercial simulation software (ARENA 10.0) was used to simulate the case study of a GSM base station. The optimal results obtained by RSM were then confirmed using loss of load probability (LLP) and autonomy analysis. In a later paper [21], they compared these results with those obtained using simulated annealing method for optimization.

Ekren, Ekren and Baris [30] presented a paper to show an optimum sizing procedure for an autonomous PV/Wind hybrid energy system with battery storage. They presented a break even analysis of the system including extension of a transmission line using the net present value (NPV) method. They present a case study of a hybrid system powering a mobile communication base station. The Hybrid PV Wind system was first optimized using a response surface methodology (RSM), which is a collection of statistical and mathematical methods relying on optimization of response surface with design parameters. Optimum PV area, wind turbine rotor sweep area and battery capacity were optimally obtained using RSM, from which the total system cost was obtained. A break even analysis was then carried out to determine the distance at which transmission line extension was less economical compared to development of the hybrid power supply system. Their results showed that if the distance from the transmission line to the point of use was more than 4817m then the hybrid system was more economical than the electricity network.

2.1.9 Other Techniques

Hearn et al [31], Presented a method for sizing of grid level flywheel energy storage using optimal control law. The method allows the loss dynamics of the flywheel to be incorporated into the sizing procedure. This permits data driven trade studies which trade peak grid power requirements and flywheel storage capacity to be performed. A case study based on home consumption and solar generation data from the largest smart grid in Austin Texas was presented.

Anagnostopoulos and Papantonis [32] advocated the attractiveness of hybrid wind hydro generation, in order to increase wind energy penetration and cost effectiveness in autonomous electric grid. In this work they developed a numerical method for the optimum sizing of the various components of a reversible hydraulic system designed to recover excess electrical energy produced by wind farms and not absorbed due to grid limitations. Time variation for rejected wind farm power from a number of wind farms in Crete was used as the case study, while the free parameters considered for optimization were turbine size, size and number of pumps, penstock diameter and

thickness and reservoir capacity. The proposed numerical procedure consisted of an evaluation algorithm to simulate plant operation for a 12 month period and automated optimization software based on Evolutionary Algorithms. Economic evaluation, constrained optimization, sensitivity analysis and various parametric tests were carried out on the case study. The conclusion drawn was that a well optimized design was be crucial for technical and economic viability of the system.

2.2 Classification by generation technologies considered in the hybrid system.

In designing a hybrid renewable energy power system, selection of what is to be hybridized is a very important step. It is very important to be able to select the resources that can best be utilized for a particular case. Other considerations can also be made before selecting technologies to hybridize. In the recent literature reviewed, a trend of hybridizing wind and solar was observed, however other sources were also considered on a case by case basis. Below is a review of generation technologies that have been hybridized in recent published literature.

2.2.1 Hybrid of Solar PV with Wind

A number of Authors have considered hybridization of solar PV with wind. Some cite the complementary characteristics of wind and solar, other make this decision based on resources available at a particular site.

Zhang et al [33] determined that Life-cycle cost and power supply reliability were dependent on proper sizing for a hybrid solar, wind power system with battery storage. They proposed an improved capacity ratio design method for Wind Solar Battery Hybrid Power System (WSB-HPS) that took advantage of the complementary characteristics of wind and solar to greatly improve power supply reliability while requiring less battery capacity. Their proposed method also took account of and reduced the depth of charge/ discharge cycles of the battery. In a similar fashion, **Xu et al** [34] developed an improved optimal sizing method for Wind Solar hybrid power systems with battery storage. They put forward two considerations for standalone operation and for grid tied operation, with key objectives under consideration including a high power supply reliability, full utilization of complementary characteristics of wind and solar, minimization of the fluctuation of power injected to the grid, optimization of battery charge and discharge states and minimization of the total cost. They compared their proposed method to traditional methods and revealed that it achieved higher power supply reliability while requiring less battery capacity in standalone mode.

In grid connected mode it achieved much smaller fluctuation in power injected to the grid. They then used an energy filter method to optimize the battery capacity.

Roy et al [25], specifically pointed out on the economic benefit of hybrid wind and solar generation when compared to pure wind or solar PV. Their results when designing a distributed hybrid renewable energy power system for Sagar Island indicated that hybrid Wind and Solar PV systems with battery storage provided the least cost per unit of electricity compared to pure wind or solar systems.

Yang et al [11] Optimally sized a hybrid combination of wind and solar PV to supply a remote telecommunication station. Their key concerns were to maximize power reliability whilst minimizing cost hence the need for an optimally sized hybrid system.

Kamjoo et al [35] Proposed tackling the challenge of uncertainty in maintaining a high quality power supply by hybridizing renewable energy sources.

Other authors who considered hybridizing wind and Solar PV for renewable energy generation include [23], [16], [24], [36], [37], [38], [27], [39], [12], [22], [21], [30], [29], [40], [26], [41], [14], [10], [42],

2.2.2 Hybrid of Solar PV, Wind and Biofuels

Tafreshi et al [13], hybridized wind, solar PV and biogas. They developed models for the various components of their micro grid, optimized the sizing using genetic Algorithms, performed sensitivity analysis and validated their results using HOMER software.

2.2.3 Hybrid of Solar, Wind and Diesel Generator

A more practical emergent approach in literature has been to hybridize renewable energy with conventional thermal sources. In literature reviewed, Solar PV with Wind renewable energy sources have been hybridized with diesel generators. The diesel generators are mostly intended to supply shortfalls in renewable energy generation hence meeting energy needs at peak demand. The objective of optimization in this case has mostly been to reduce fuel consumption and minimize cost.

Pirhaghshenasvali and Asaei [15] developed a hybrid renewable energy generation system incorporating Wind generation turbines, solar PV, Battery banks and Diesel Generators. The Wind PV Battery system was intended as the primary system with the diesel generator provided as a

backup system. The goal of their optimization was to minimize investment cost and fuel cost while ensuring availability of the energy and sufficiency to meet peak demand

Zhang, Belfkira and Barakat [8] developed a hybrid renewable energy power system consisting of Wind, Solar PV and Diesel Generator for a site in Le Havre, France. Their research focused on the optimal number and type of units ensuring availability of energy to meet energy demands.

Yassine et al [9] for the same site in an earlier study by Zhang et al [8], considered a number of different hybrid renewable energy generation systems with different compositions. Their results indicated that hybrid PV, Wind, Diesel Generator with Battery Energy storage was the most optimum combination for their site. They attributed this finding to good complementary effect between solar energy and wind energy.

Kadda et al [43] presented a mini autonomous hybrid system comprising of wind energy generation, solar PV and Diesel generators with Battery banks. They estimated wind and solar potential first to obtain the optimal sizing for the components of the system.

2.2.4 Hybrid of Solar, Wind and Electrolyzer with Fuel Cell

Navaerfad et al [19] presented a hybrid distributed renewable energy resources for micro grid consisting of Wind, solar hybrid system with electrolizer, hydrogen tank, fuel cell and batteries.

2.2.5 Hybrid of Solar, wind and Tidal Energy

Bashir and Sadeh [17] presented a hybrid system of wind, PV and tidal energy with battery storage. They stated the benefits of tidal energy as being highly predictable compared to wind and solar hence a complementary addition to their hybrid generation solution.

2.2.6 Hybrid of Wind and Hydroelectric Power

Scarlatache et al [44] lamented on the volatility and intermittency of wind as an energy source. In a bid to balance electricity generation with demand at all times and with regard for compliance requirements set forth by system operators, they investigated the influence of coordination of wind and hydro plants on power losses in the electric system based on the correlation between the electrical energy outputs of these sources.

Anagnostopoulos and Papantonis [32] also considered hybridization of wind and hydro power. They proposed the use of a pumped storage hydroelectric plant for recovery of excess energy generated by wind farms on the island of Crete.

2.3 Classification by energy storage system employed

Energy storage solutions are important in a renewable energy power system. They have many uses among them being to integrate renewable energy sources within the power system by converting them from volatile and intermittent source to smoother dispatch-able forms of energy [45]. They also provide ride through capability when distributed generation sources fail to supply required energy. Moreover they are useful in managing the amount of power required to supply during peak hour demand by storing it during off peak demand hours [46]. Different Energy Storage Systems have different applications based on their cost, weight, efficiency, technology, handling, amount of energy stored, duration of storage, etc. For application in micro grids and for hybrid renewable energy systems, various Energy Storage technologies have appeared in literature. These technologies include Battery Energy Storage Systems (BESS), Flywheel Energy Storage (FES), Compressed Air Energy Systems (CAES), Pumped Hydro Storage (PHS), Ultra Capacitors (UC), Super Magnetic Energy Storage Systems (SMES) and Hydrogen. These storage systems with respect to their use in hybrid renewable energy systems are reviewed here.

2.3.1 Battery Energy Storage

From reviewed literature, Battery Energy Storage Systems (BESS) or Battery Banks appear to be the most popular. **Yang et al** [11] incorporated battery Energy storage in their case study of a hybrid power system supply to a remote telecommunications relay station. Crăciunescu et al [23] overcame intermittency and variability of wind and solar by incorporating a battery energy storage solution. **Zhang et al** [33] proposed a method to improve the capacity ratio for Wind and Solar generation whilst reducing the size of battery banks installed. Their method also reduced the depth of charge / discharge cycles of the battery.

Other authors who incorporated BESS as their preferred Energy Storage Solution include [35] ,[15],[16],[24],[36],[8],[37],[9],[27],[34],[43],[12],[13],[22],[17],[21],[30],[29],[26],[19],[41], [14],[10],[47]. Below is an overview of some of the different battery technologies that are available;

(1) Sodium-Sulphur (NaS)

NaS batteries belong to a class of rechargeable batteries known as molten salt batteries. It utilizes molten Sulphur and metallic sodium for the electrolyte and electrodes respectively. As the electrolyte is molten, these batteries require a high operating temperature of between 300 and

350℃ [68]. When idling as much as 14% of the batteries stored energy is consumed parasitically in maintaining operating conditions. This requirement for high temperature operation is probably this battery's key disadvantage and has resulted in a secondary requirement of proper thermal management when designing or installing these batteries. Their other disadvantage is high cost and the fact that there's only one established manufacturer (NGK Insulators) at megawatt scales.

However NaS batteries have gained significant traction due to their other attractive characteristics such as a high charge/discharge efficiency ranging from 75-86% [68]. In addition to efficiency, NaS batteries also boast a very high energy density and long life cycle compared to other mature technologies such as lead acid batteries.

NaS batteries have found acceptance in non-mobile large scale applications such as grid energy storage and renewables integration.

(2) Lead-Acid

These batteries were invented in 1859 by French physicist Gastone Plate. They are technically simple and cheap to manufacture. They boast a mature and well understood technology and in most cases offer the cheapest cost per kW of installed capacity compared to the other systems. They have been successfully modified for both power and energy applications. These batteries however suffer from slow charge rates, cannot be fully discharged and have very limited charge/ discharge cycles [68]. They also have lower energy to weight ratio and energy to volume ratios compared to the other technologies e.g. lithium ion.

They are the most versatile in terms of applications with various modern and more efficient designs available. Two key developments are the Absorbed Glass Mat (AGM) versions and the Gel version. Both of these have made significant improvement on the battery's life and efficiency and by reducing need for maintenance.

(3) Lithium-Ion (Li-Ion)

Li-ion batteries have in recent years emerged as the most preferred battery option for the consumer electronics market due to their high energy density that allows them to be very compact and portable. They have also set precedence in hybrid and all electric vehicle space and are slowly making inroads in the grid applications space. Recent developments in these batteries are targeted towards controllability and safety of these batteries in large applications, lowering of operating and maintenance costs.

(4) Nickel-Cadmium (NiCad / Ni-Cd)

These batteries employ Nickel oxide hydroxide and cadmium and metallic cadmium as the electrodes. Ni-Cd batteries are among the oldest and most mature battery technologies available. They are ideal for mitigating effects of voltage sags and for providing backup power in harsh conditions. Their ability to withstand high temperatures has also seen them adopted in solar generation applications. They however do not excel in peak shaving and energy management solutions [68].

(5) Flow Batteries

In these batteries, the electrolyte which is usually stored externally in tanks, flows through either by gravity or pumping, an electrochemical cell in a reactor that converts the chemical energy directly to electricity. Flow batteries however have a high self-discharge rate and suffer from low energy densities in comparison to other battery types especially Li-Ion. Moreover, flow batteries tend to be more complicated as they require pumps, sensors and control units.

Two categories of flow batteries are considered here,

- Redox Flow Batteries and
- Hybrid Flow Batteries

(a) Vanadium Redox-Flow

The Vanadium Redox Flow battery is an example of a redox flow battery. A redox (reduction oxidation) flow battery is a reversible fuel cell in which all the electro-active components are dissolved in the electrolyte. The energy of a redox flow battery is decoupled from power as the energy is a function of electrolyte volume which is generally stored in tanks external to the fuel cell system. This means it is possible to increase energy storage capacity just by increasing volume of electrolyte and storage tanks. Power on the other hand is a function of the fuel cell capacity. This means redox flow batteries are very scalable in terms of energy storage capacity. Another inherent advantage is the possibility of instant replenishment by topping up with unspent electrolyte charged from a different system. Vanadium redox flow batteries can thus in theory have unlimited capacity, their other advantage is that they can be left discharged for long periods of time without any ill effects, however as stated earlier above they suffer the same flaws as other flow batteries.

Their main intended application in lieu of their complexity and theoretically unlimited storage capacity is in grid energy storage and renewables integration.

(b) Zinc Bromine Battery

The Zinc Bromine battery is a hybrid type of flow battery with one battery electrode and one fuel cell electrode. The result consequently is that in its operation, one or more electroactive components are deposited on the battery electrode [68]. It is noteworthy that energy and power are not fully decoupled in a hybrid flow battery as in a redox flow battery. The energy in these batteries are limited to the size of the electrode. Structurally, the Zinc Bromine battery is constructed from 2 tanks, one holding the electrolyte for the positive electrode reactions and the other for the negative electrode reactions. Compared to lead acid batteries, the Zinc Bromine battery has some critical advantages such as a high energy density, has a higher life cycle of more than 2000 cycles and allows to be operated up to 100% depth of discharge. Additionally, Zinc bromine batteries have unlimited shelf life and are easily scalable. According to Poulikas [68], they also provide the lowest overall energy storage cost when compared to other technologies such as Lead acid, Sodium-Sulphur and Lithium ion.

(6) BESS Installations worldwide

Saez-de-Ibarra et al, [70] presented an overview of BESS installations across the world in their review of BESS technologies for grid applications. Their findings are presented in the table below.

Table 2-1: BESS installations worldwide for grid applications

Location	Technology	Provider	Connection date	Peak power and energy capacity	Functionalities
JAPAN	NaS	NGK	July 2004	9,6MW–58MWh	Demand Charge Management, Area Regulation
USA (HI)	Adv. Pb acid	Xtreme Power	Sept. 2012	10MW–20MWh	Renewable Energy Time Shift and Capacity Firming, Electric Supply Reserve Capacity, Area Regulation
CHINA	Li-ion	BYD	Dec. 2011	6MW–36MWh	Renewable Energy Time Shift and Capacity Firming
SPAIN	Li-ion	Saft	Oct. 2012	1,1MW–560kWh (30min)	Renewable Energy Time Shift and Capacity Firming, Area Regulation
USA (WV)	NaS	NGK	June 2006	1,2MW–7,2MWh	Area Regulation, Electric Supply Reserve Capacity
USA (MA)	ZnBr	Premium Power	Apr. 2012	500kW–2,8MWh	Renewable Energy Time Shift and Capacity Firming, Transmission Congestion Relief
USA (CA)	Li-ion	A123	June 2012	8MW–32MWh	Renewable Energy Time Shift and Capacity Firming, Area Regulation, Voltage Support
USA (TX)	Adv. Pb acid	Xtreme Power	May 2012	36MW –24MWh	Area Regulation, Renewable Energy Time Shift and Capacity Firming
USA (NY)	NaS	NGK	Mar. 2009	1MW –7,2MWh	Demand Charge Management
USA (MI)	Li-ion	A123	July 2011	500kW –1MWh	Electric Energy Time Shift, Area Regulation
JAPAN	NaS	NGK	Aug. 2008	34MW–245MWh	Renewable Energy Time Shift and Capacity Firming
USA (MI)	Adv. Pb acid	Xtreme Power	June 2011	0,75MW–2MWh	Renewable Energy Time Shift and Capacity Firming, Area Regulation
CHINA	Li-ion	BYD	Sept. 2011	3MW–12MWh	Area Regulation, Demand Charge Management
USA (AK)	Ni-Cd	ABB (Saft)	Aug. 2003	27MW-6,75MWh (15min)	Electric Supply Reserve Capacity, Load Following
USA (OH)	VRB	Ashlawn Energy	Dec. 2012	1MW–8MWh	Electric Energy Time Shift, Load Following, Electric Supply Reserve Capacity, Voltage Support, Transmission Congestion Relief
USA(WV)	Li-ion	AES (A123)	Oct. 2011	32MW – 8MWh (15min)	Renewable Energy Time Shift and Capacity Firming

2.3.2 Other ESS

Panahandeh et al [39] considered hydrogen energy storage in the development of a hybrid energy system. They used the Alternative Power Library (APL) to investigate the integration of a hydrogen storage path in hybrid system operation.

Emori et al [48] Described the proceedings of their research on a Carbon Hydride Energy Storage System (CHES). CHES presents a step forward in Hydrogen storage. Since hydrogen is notoriously difficult to handle in natural gaseous state they proposed its storage in the form of the stable liquid methylcyclohexane thereby making it easy to transport and keep in long term storage as an energy medium.

Navaerfad et al [19]**,** considered a hybrid renewable energy generation system that was tied to an electrolyzer – hydrogen-fuel cell energy recovery system that worked in hand with a battery storage system.

Hearn et al [31], used flywheel energy storage for grid level storage of energy in smart grids. They considered a case study of one such smart grid in Austin Texas.

Scarlatache et al [44] and Anagnostopoulos et al [32] Both used Pumped storage hydro as their Energy Storage system for power systems with wind energy generation.

Wang and Yu [49], presented an optimal sizing procedure for a compressed air storage system in a power system with high wind power penetration.

Pedram et al [50] listed the desirable attributes that an Energy Storage System should possess as high Energy density, high Power Delivery Capacity, low cost per unit of storage capacity, long cycle life and low leakage. They realized that of the currently available ESS solutions, none had all those attributes in totality. Thus they presented a hybrid ESS comprising heterogeneous ESS elements. Their proposed system was built on the concept of computer memory systems architecture management in order to achieve the attributes of an ideal ESS system through appropriate allocation and organization of various ESS elements. **Chouhan and Ferdowsi** [46] also reviewed different Energy storage solutions noting their special characteristics with regard to power systems requirements. They draw the conclusion that no single ESS met all power systems requirements in totality. They also proposed a combining ESS with complementary characteristics as a good energy storage solution for the design of a self-regulating renewable energy power system.

2.4 Reliability Index Used

In most studies to optimize the sizing components of a hybrid renewable energy power system, reliability of the designed system is presented as either a constraint or a goal to be achieved in the optimization process. In either case, a method is usually presented for evaluating the reliability of the proposed system. Some of the methods that appear in recent published literature that are presented here include:

- Loss of power supply probability (LPSP)
- Expected Energy Not Served (EENS)
- Loss of Load Probability (LLP)
- Equivalent Loss Factor (ELF)

- Levelized Cost of Electricity (LCOE)

2.4.1 Loss of Power Supply Probability (LPSP)

Yang et al [11] used the Loss of Power Supply probability as a reliability criteria. In designing a hybrid power system to supply a remote telecommunications relay station their objective was to achieve a required loss of power supply probability (LPSP) at a minimum annualized cost of the System (ACS).

Kamjoo et al [35] recognized the uncertainty in maintaining a high quality of supply as the main challenge in standalone hybrid renewable energy systems. They considered the Loss of Power Supply Probability as a reliability measure for their optimization.

Bashir and Sadeh [16] appreciated the importance of capacity sizing in order to fully meet demand due to uncertainty of wind and solar PV. As a measure of reliability they also used LPSP.

Zhang et al [33] postulated that power supply reliability depended on optimum sizing of Solar PV, wind and Battery storage in a hybrid renewable energy supply system. They used LPSP as a reliability index and designed a system for a case study in Shengyang region.

Belmilli et al [37] developed a software based on Loss of power supply probability algorithms for techno-economic analysis and optimization of hybrid systems.

Other authors who considered LPSP in their work are quoted in references [43] and [10]

2.4.2 LPSP with other Indices

LPSP has also been used alongside other indices in written literature. This usually done as a means of ensuring that the proposed system fulfills other criteria other than reliability. **Bilal et al** [12] desired to minimize the cost of their system whilst ensuring it was reliable enough. They used LPSP as reliability index alongside the annualized cost of the system which was to be maximized. Other authors aimed at reducing the cost of electricity generated by their system whilst meeting the required reliability index **Tafreshi et al** [13] , **Paudel et al** [41] and **Dial et al** [42] all used LPSP with levelized cost of electricity (LCE). **Testa et al** [40] used LPSP alongside loss of power produced (LPP).

2.4.3 Expected Energy Not Served (EENS)

Arabali et al [24] developed a stochastic framework for optimal sizing and reliability analysis of a hybrid power system including renewable energy source and energy storage. They used the

Expected Energy Not Served index (EENS) with Energy Index of Reliability (EIR) to measure reliability of the system and a compromise solution method to arrive at the best compromise between reliability and cost. **Bahramirad and Reder** [28] also used EENS as a probabilistic reliability calculation method to evaluate reliability of micro grids with energy storage systems in islanded operation.

2.4.4 Loss of Load Probability (LLP)

Ekren and Ekren [22] applied loss of load probability and autonomy analysis to determine the validity of their optimal sizing. In a later paper with a different optimization approach [21] they again used LLP to validate the reliability of their system.

2.4.5 Equivalent Loss Factor

Bashir and Sadeh [17] used the equivalent loss factor (ELF) as a reliability index to evaluate a hybrid system they had optimally sized. ELF was also used in [19]

2.4.6 Levelized Cost of Electricity

Huang et al [20] used the levelized cost of electricity (LCOE) analysis method to compare the variation trends of power supplies which use different energy sources to generate.

Zhang et al [8] used levelized cost of electricity (LCOE) with Deficiency of Power Supply Probability (DPSP) in the development of a methodology for calculation of the sizing and optimization of a stand-alone hybrid system.

2.4.7 Other Indices

Puri [47] considered the problem of sizing battery storage with renewable energy sources such as solar PV and wind using Fractional Load Not Served (FLNS) as a reliability criterion. He went ahead to demonstrate the characteristic differences between FLNS and LPSP which is the most common reliability index in written literature. He showed that for a fixed FLNS requirement, the minimum battery size required was a decreasing convex function of the size of the renewable energy source and that for a fixed size of renewable energy source, minimum battery size required was a decreasing convex function of FLNS. This is in contrast in his opinion to LPSP which does not display any convex relation to battery size.

Xydis [38] presented Exergetic Capacity Factor (ExCF) as a new parameter that can be used for better classification and evaluation of renewable energy sources. He examined both energy and

exergy characteristics of wind and solar to determine factors that affect the exergy of a hybrid Wind Solar system

2.5 Modelling Method Used

A review of modelling methods used in recent literature follows. In solving the optimal sizing problem for hybridized renewable energy generation, modelling is an important step as it provides the mathematical relation between inputs and expected outputs. Key component usually modelled is the output power generation from wind and solar. Specific characteristic of an energy source eg the wind speed can be modelled and a correlation to equivalent power generation from wind obtained. Below a cross section of methods used in literature read has been presented.

Kamjoo et al [35] used Autoregressive Moving Average models to characterize wind speed and solar irradiance variations. **Arabali et al** [24] modelled uncertainties of wind and PV power generations stochastically using Auto Regressive Moving Average.

Separately, **Ekren and Ekren** [22] used a Box Behnken Regression model to model expected output of wind and solar generation which are intermittent.

Other authors used a combination of various modelling techniques, **Chen et al** [29] used a combination of stochastic time series and feed forward neural networks. They modelled wind speed using a time series whereas solar irradiance was modelled using a feed forward neural network with forecasting errors accounted for.

2.6 Simulation method used

Panahandeh et al [39] emphasized the importance of simulation on engineering research and development of hybrid systems for rural electrification. They used different simulation models from the Alternative Power Library (APL) developed by the Institute for Wind Energy and Energy Systems (IWES) for simulation of regenerative power supply systems. They used APL to investigate the integration of a hydrogen storage path in hybrid system operation

Ekren and Ekren [22], [21] used a commercial simulation software (ARENA 10.0) for the simulation case study of a GSM base station. In [30] when investigating the break-even analysis for hybrid solar PV wind system with consideration for grid extension they used ARENA

simulation to demonstrate the break-even distance from the transmission for which the system was more economical than connection to the grid.

Monte Carlo Simulation (MCS) appears frequently in recent literature especially with regard to optimal sizing of components of a hybrid solar PV and wind power system. **Kamjoo et al** [35] Evaluated the performance of various design candidates using Monte Carlo simulation method. **Bashir and Sadeh** [16] used the probability density of wind speed and solar radiation to consider uncertainty in wind and PV power using Monte Carlo Simulation. **Arabali et al** [24] Used Sequential Monte Carlo to arrive at the best compromise between reliability and cost after optimal sizing using a pattern search method.

2.7 Validation Method

In optimization of sizing of components of a hybrid renewable energy power system, the commercial software Hybrid Optimization of Multiple Energy Resources (HOMER) is the most cited in literature. It has been used both for optimization and for validation of optimal designs [51] [52]. It is a time-step simulator that uses hourly load and environmental data inputs for renewable energy assessment and performs optimization based on Net Present Cost for a given set of constraints and sensitivity variables [51]. For this reason and its wide acceptance, a number of authors have used it as a tool to validate their optimal design. Dufo-Lopez and Bernal-Augustine [53] used HOMER to validate their optimal configuration of diesel generator with solar PV. Zhang et al [33] used HOMER to validate the results of their improved capacity ratio selection method for their case study of a hybrid Wind-Solar battery system for Shengyang. Belmili et al [37] proposed a sizing method for PV wind hybrid systems that was validated by counter designing in HOMER and comparing results. Tafreshi et al [13], used HOMER to validate and perform sensitivity analysis on a genetic algorithms based system configuration optimizer.

2.8 Summary of Literature Review

Optimal sizing of hybrid renewable energy generation sources is a study area that has gained a lot of traction in recent times. From the literature reviewed clear distinctions can be seen in terms of methods used for optimization, generation technologies considered for hybridization, energy storage system employed, reliability index used to gauge the result of optimization, modelling methods used, simulation approaches and validation methods used.

The first clear distinction in the literature reviewed can be seen in the methods used for optimal sizing of capacities of key components of the hybrid renewable energy generation system. Search algorithms such as the dividing rectangles search algorithm are seen to be popular especially in circumstances where an optimal configuration is selected from a pool of possible configurations. Metaheuristics, especially GA, PSO and their derivatives are seen to have significantly increased utilization from the reviewed works. This is a result of their relative maturity compared to other metaheuristics and their suitability to problems with large, non-smooth multimodal search spaces, the kind encountered in this research. Consequently for this same reason traditional gradient based approaches are not popular as they excel in smooth, small unimodal search spaces. Simulated Annealing, a heuristic method based on stochastic gradient search is also used in some works but doesn't seem to have the traction of GA and PSO in the field. A number of authors have also resorted to hybridized metaheuristics such as GA-PSO or PS-SMCS with GA initialization, these have had some success in reducing the time it takes to converge to an acceptable optimal solution. Some studies have also focused purely on optimization using available commercial software packages such as using Hybrid Optimization of Multiple Energy Resources (HOMER). Other software programs of similar nature that occur in literature as reviewed by Sunanda and Chandel [1] include HYBRID 2, RETScreen, iHOGA, INSEL, TRNSYS, iGRHYSO, HYBRIDS, RAPSIM, SOMES, SOLSTOR, HySim, HybSim, IPSYS, HySys, Dymola/Modelica, ARES, SOLSIM, and HYBRID DESIGNER. Moreover, a number of authors have used these commercial tools to validate their results. Other notable approaches for optimization encountered are Integer Programming methods, with both Mixed Nonlinear Integer Programing (MNIP) method and Mixed Linear Integer Programing (MLIP) method being encountered.

The second obvious distinction in the reviewed literature is on the technologies chosen for hybridization. The key principle behind the idea of hybridization is to take two intermittent sources with complementary characteristics, optimally size them and use them in collaboration, this should consequently improve the overall system reliability. A key finding from the literature reviewed is that selection of technologies to be reviewed lies squarely on two factors: the available resources at the specific location considered and whether those resources have complementary regimes hence justify need for hybridization. From the literature reviewed the most popular resources considered for hybridization was wind with solar. This was implemented purely as wind and solar hybrid or in some cases with diesel generation, or with biofuel based generators, electrolizer with

fuel cell and even tidal energy. Interestingly one author hybridized wind and pump storage hydro as well as conventional hydro power. The dominance of wind solar hybrids is clearly attributed to their widespread availability when compared to other sources. Diesel generation added to the mix is usually to reduce system cost by reducing amount of capital spent on energy storage and in most cases the renewable components only serve to reduce fuel consumption. This approach is widely employed in industry today and in areas where diesel prices are fair. In this work the researcher's intention is to keep a pure renewable energy mix hence only wind and solar are considered.

The type or nature of energy storage system used is another line of possible classification of past works in this area. It was observed that energy storage was essential to converting renewable energy sources from their jerky intermittent state to a smoother and more reliable state by storing energy during peak production hours to provide ride through capability later on when renewable energy generation is insufficient to meet demand. Energy storage schemes from the literature reviewed have been seen to be application dependent in that, the suitability of a storage scheme depends solely on its intended application. Nonetheless it was observed that battery energy storage systems (BESS) were more versatile and found application in most situations in the literature reviewed. Other energy storage schemes encountered include: Hydrogen Storage both as gas and ingeniously in the form of the more stable methylcyclohexane as proposed in the Carbon Hydride Energy Storage System (CHES). Other popular storage schemes include Pumped Hydro Schemes which incidentally are the most efficient storage schemes but are only practical at very large scales, Flywheel Energy Storage Systems (FESS), Supercapacitors, and Compressed Air Energy Storage Systems (CAES). A noteworthy approach of hybridizing energy storage systems based on complementary characteristics was also encountered.

A performance index is necessary to evaluate the performance of the system in meeting its objectives. In most literature reviewed, there are two objectives along the lines of technical performance or reliability and economic performance. Consequently the indices used can be broadly and in very general terms classified into reliability performance indices and cost performance indices. Of the reliability indices used, the one with most traction is the loss of power supply probability. On the other hand, the common cost index in literature is the Levelized cost of electricity.

Other distinctions though not of significant importance as the above include choice of modelling method, simulation method and even validation method. This is because not all literature reviewed

included these aspects in their study. Nonetheless, in a nutshell, the literature presented has given an overview on the trends, directions and possible inclination of research into optimal sizing of hybrid renewable energy systems. It has demonstrated that stand alone renewable energy generation is a viable alternative to grid supply or conventional fossil fuel based power generation for remote areas world over. Hybridizing two or more sources with complementary characteristics has emerged as an important technique for improving reliability and reducing cost of renewable energy generation in spite of the intermittency of the individual sources such as wind or solar. Additionally incorporation of a suitable energy storage solution has been shown to be key in converting the jerky intermittent energy sources to smoother forms that can allow despatch. However the design, control and optimization of the hybrid power system is not a trivial task. Optimal sizing of the components of a hybrid system is crucial for the feasibility of such a system in terms of cost and reliability.

Chapter 3 Methodology

The methodology used is separated into three section each covering the methodology used for each facet of the study. These 3 sections are;

- Geospatial resource assessment section, outlining justification for the choice of location and analysing the resource data for that location.
- Component modelling section, outlining the process of mathematical modelling of the components of the hybrid power system and
- Optimal sizing algorithm section, detailing the algorithm used and its parameters.

3.1 Geospatial Resource Assessment

3.1.1 Required Data

To optimally size a hybrid renewable energy source, as is evident from reviewed literature, a sufficient understanding of the underlying resource potential of the target area is necessary. One will need to obtain data that quantifies the available resources that are to be hybridized. For this study, solar and wind resource quantification is necessary for a target area. At minimum, previous studies have relied on solar irradiance data and wind speed data. Additionally ambient temperature at the selected site will also be of importance. This is because solar PV performance has a negative correlation with ambient temperature. Various energy storage systems also display varying relation with ambient temperature. Battery energy storage systems proposed herein for example display reduced useful life when operated above rated temperatures.

3.1.2 Solar Resource Data

Knowledge of irradiance on a collector's surface is critical for solar resource assessment. Most weather station record the total irradiation on a horizontal surface also known as Global Horizontal Irradiation (GHI). On some instances, the Direct Normal Irradiance (DNI) is also available.

DNI represents the sun's radiation striking the earth incident on the direction of the sun and is a vital parameter for the design of concentrated solar power systems (CSP). GHI on the other hand represent the sum of the sun's radiation directly incident on the surface of the earth and the diffuse horizontal irradiance (DHI). It is an important parameter for design of panel based photovoltaic systems. Diffuse Horizontal Irradiance is the sun's radiation that doesn't strike the earth's surface directly but rather has been scattered by clouds, dust or other particles in the earth's atmosphere.

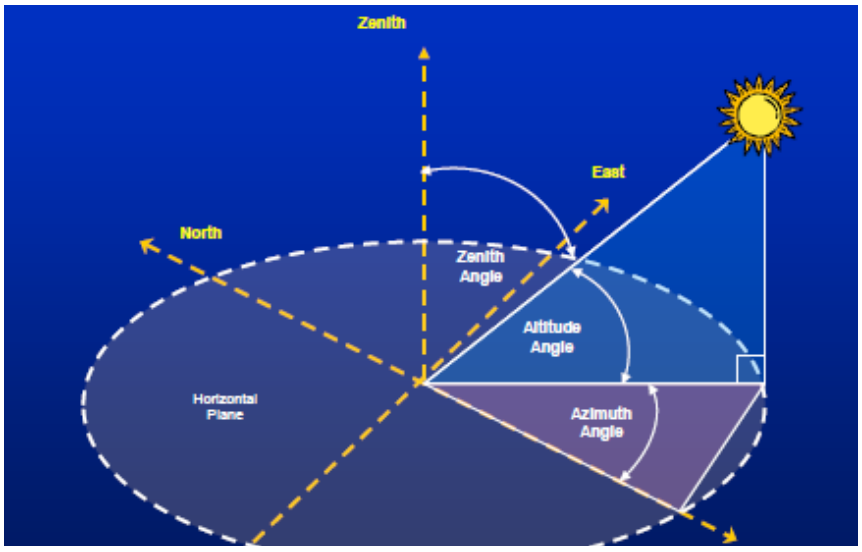

Figure 3-1: Visualization of solar angles

The equation below summarizes the relationship between GHI, DNI and DHI.

$$GHI = DNIcos(\theta_z) + DHI \quad (3.1)$$

Where θ_z, in this expression is known as the solar zenith angle.

The solar zenith angle is illustrated in Figure 3-1. It is the angle between a skyward vertical from the surface and the sun. It is the complementary angle to the elevation and directly determines the amount of radiation absorbed or reflected by the earth. The solar zenith angle varies diurnally with the maximum elevation angle (minimum zenith angle) occurring at solar noon and coincident with peak irradiance over the day. The azimuth angle which is a pointer to which direction the sun is shining is also an important parameter that has to be chosen wisely. It determines the panel orientation and if not properly chosen could lead to a drop in production. Moreover improper panel orientation as in the case of East –West oriented panels would also lead to poor results due to great variance in the Zenith angle as the earth rotates.

GHI data and sometimes DNI data are collected at synoptic weather stations across the globe. In Kenya, this data is available for 36 different locations with synoptic stations. A possible way forward with this study would have been to visit all the 36 stations to collect this data or perhaps to visit the national meteorological department to request for this data. However as with most data

collected at national level, a lot of inconsistencies and missing data should be expected. The approach taken in this study with regard to obtaining solar resource data is explained in detail in section 3.1.4 below and involves relying on results obtained from a previous reputable and trusted study.

3.1.3 Wind Resource Data

Just like solar, to quantify wind potential in an area, wind speeds at certain hub heights are required. Wind data measurement at meteorological weather stations is usually done at a hub height of 10m or less and is intended mainly for weather prediction purposes. For energy prospecting, it is usually necessary to have measurement equipment installed at the required hub height to collect data for a sufficient duration of time so as to enable resource availability modelling and feasibility studies. In addition to wind speed, wind direction is also an important parameter especially in determining the alignment of wind turbines so as to minimize on wake losses.

Two important approaches to assessing the wind potential at a given location are the use of wind frequency rose diagrams to establish frequency of wind blowing from a specific direction and the use of the Weibull distribution function to predict wind speed distribution – an important metric in estimating the amount of energy that will be generated by the wind turbines. Figure 3-2 is an example of a wind frequency rose diagram. It shows the wind speeds in knots divided into speed classes distinguished by different colour codes and the directions from which these winds originate.

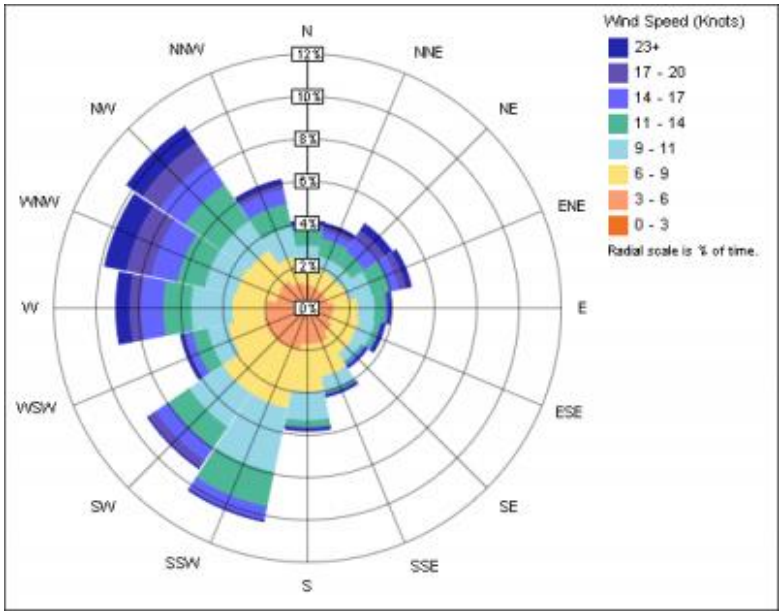

Figure 3-2: Typical windrose

The Weibull Distribution is a very good approximation for the wind speed distribution that can be used to calculate the mean power generated by a wind turbine given wind speeds. The Weibull probability distribution function is given in equation (3.2) below.

$$f(v) = \frac{k}{A}\left(\frac{v}{A}\right)^{k-1} \exp\left(-\left(\frac{v}{A}\right)^{k}\right) \quad (3.2)$$

where A, Is the Weibull scale parameter and is a measure of the characteristic wind speed distribution. It is proportional to the mean speed and is presented in m/s.

k, Is the Weibull slope parameter or form parameter and determines the overall shape of the distribution. It takes on values between 1 and 3. It shows the variability of wind speeds with distributions characterised by highly variable wind speeds having smaller values of k whereas those with constant wind speed having a larger k.

For this study, a model that relates wind speed to the power generated by the wind turbines will be developed. Wind potential for various areas will be evaluated by fitting available data via a Weibull distribution from which input to the model will be obtained.

3.1.4 SWERA Database

The SWERA database is a product of the Solar Wind Energy Resource Assessment (SWERA) initiative started in 2001 with the objective to advance large scale deployment of solar and wind renewable energy technologies by increasing availability and accessibility of high quality solar and wind resource information [54]. It was funded by the Global Energy Facility (GEF) and managed by the Division of Technology, Industry and Economics (DTIE) of the United Nations Environment Program (UNEP).

The project was a highly collaborative researching and analytical project involving experts from different nations who reviewed and validated different available data sets as well as models for the determination of parameters such as surface temperature, relative humidity, aerosol optical depth. The project's efforts led to the creation of a highly interactive GIS toolkit for use in geospatial resource assessment. Additionally on a country by country basis, additional datasets representing wind resources and solar resources were presented. For the 36 synoptic weather stations in Kenya in addition to the above, accompanying metadata and data sets for wind and solar including typical meteorological years and time series were presented.

Earlier work did this analysis at a very low resolution level of a 100Km x 100Km, this was not very helpful for detailed analysis of technical or financial viability of potential solar and wind energy projects let alone hybrid wind and solar projects. The outcome of the SWERA project however was ground-breaking for Kenya as it availed high resolution solar radiation assessment

based on data of the geostationary satellite Meteosat 7 located at an orbit at 0° latitude and 0° longitude and scans a specific area every 30 minutes with a spatial resolution of 5x5 km² [54].

The climate data for the 36 synoptic meteorological weather stations are presented in an epw format and includes the station number, elevation in masl, location in terms of latitude and longitudes. The data collated in this resource file include; average hourly GHI, DNI, and DHI; maximum hourly GHI, DHI, and DNI; average monthly Dry Bulb temperature, Dew point temperature, ground temperature and wind speed. Additionally the monthly mode of wind direction is also collated in the files. A separate epw file exists for each of the 36 synoptic weather stations. Data is exported from epw format to csv for further analysis in excel for the selected region.

3.1.5 Geospatial Resource Assessment

Figure 3-3: Base Map of Kenya

Technical feasibility of renewable energy generation projects are usually highly dependent on geographical location. This is because different locations have different resource potentials.

For this study, a region with strong potential for both solar and wind is preferable. The SWERA GIS toolkit available at http://en.openei.org/wiki/SWERA/Data is used to zero in on a location with promising solar and wind potential. The German Aerospace Centre (DLR) Global Horizontal Irradiance Layer is first overlaid over the digital map. To locate areas of suitable resource, a base map of the country shown in Figure 3-3 is used as as starting point. A map showing the distribution of daily normal irradiance (DNI) is then overlaid over the base map, this is shown in Figure 3-4. A wind resource distribution map in the form of mean wind speeds at 50 meters above ground level is overlaid on the base map as shown in Figure 3-5.

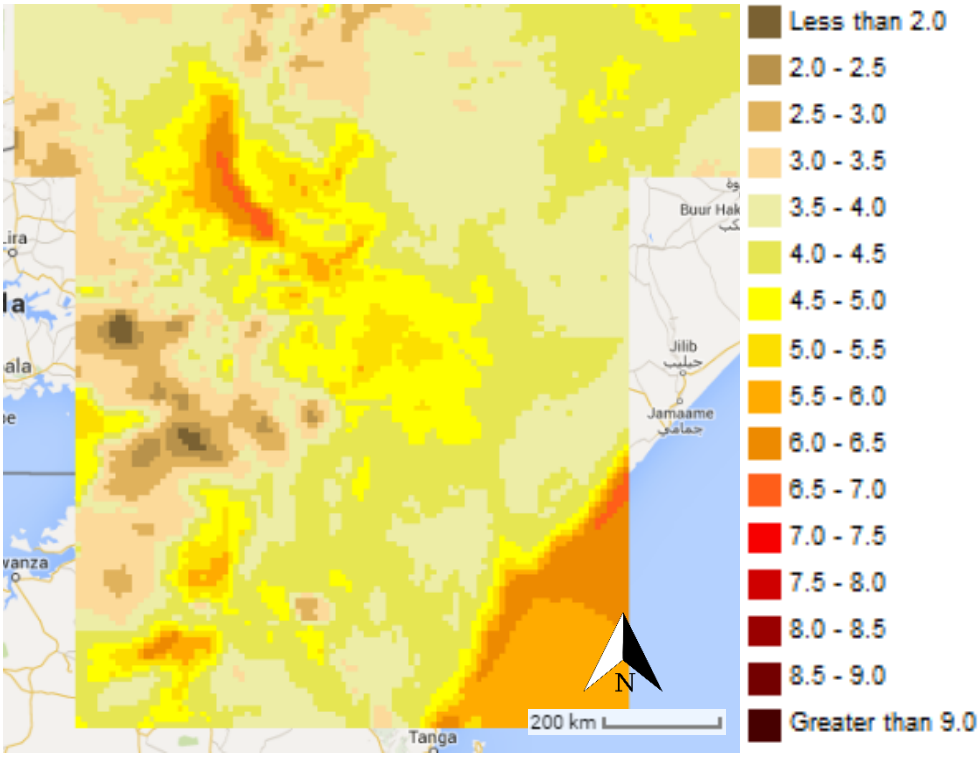

Figure 3-4: DNI Map of Kenya

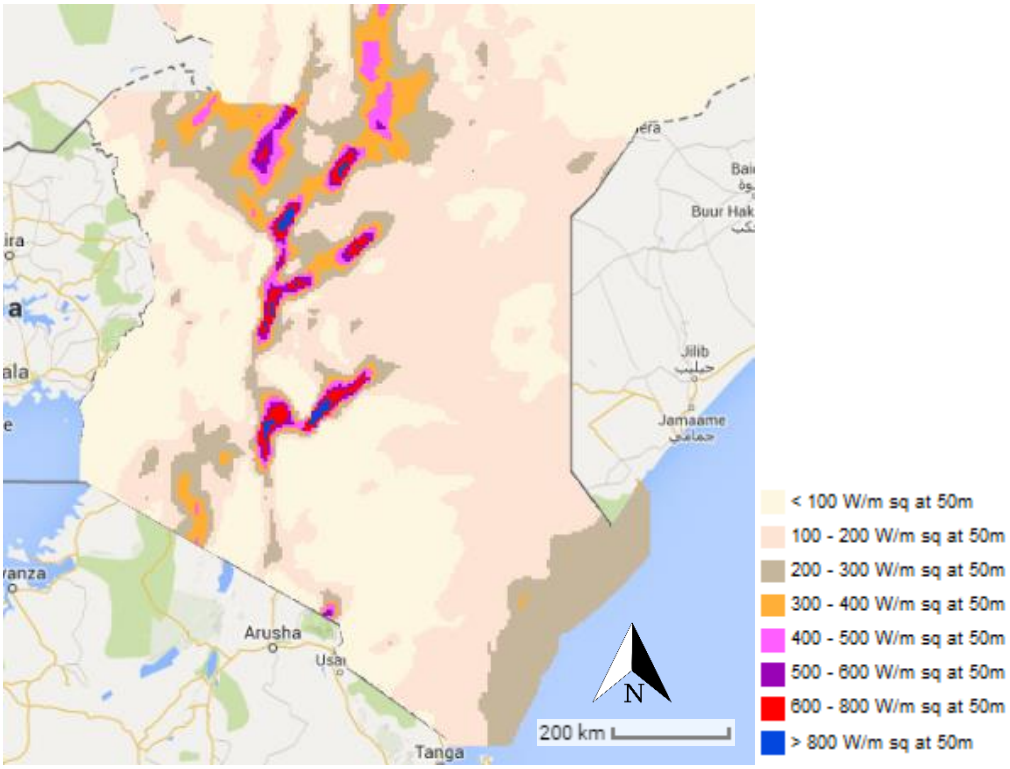

Figure 3-5: Kenya wind atlas at 50 magl

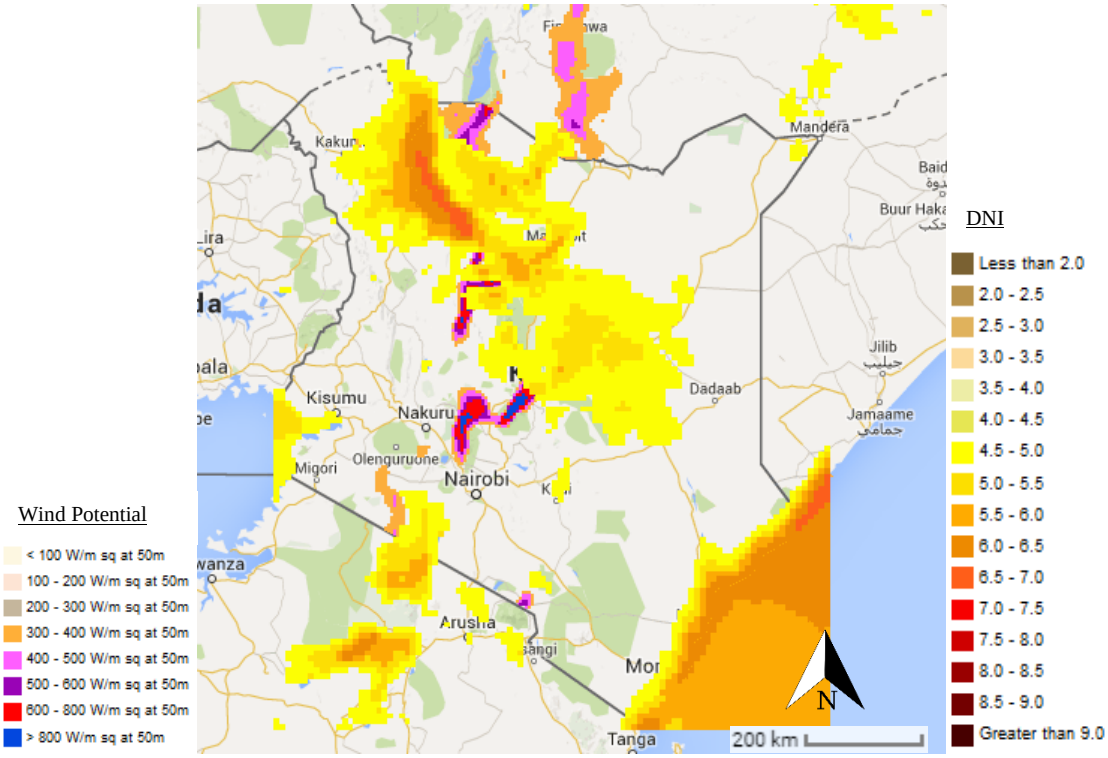

Figure 3-6: Geospatial overlay of commercially viable wind and solar potential in Kenya (areas of overlap)

Finally both wind and solar resource are overlaid on to the base map as shown in Figure 3-6, the distributions are also filetered to display only resources viable for exploitation. It is clear that a suitable location for a pilot project on hybrid renewable wind and solar PV generation would need to have great potential for both solar and wind power generation. As already identified in the SWERA study for Kenya [54] areas around Lake Turkana, East and North East of Kenya have incredible potential for solar PV generation. The area around Lake Turkana and some areas of the Rift Valley and coastal region have significant potential for wind power development. Having overlaid both resource maps onto the base map and filtered for only areas with significant wind and solar resource potential it emerges that the Lake Turkana area would be suitable for a hybrid wind and solar generation project. Coincidentally, a synoptic weather station exists in this region at Marsabit and a typical meteorological year (TMY) dataset exist. This data will be used as input to the component models used in the sizing procedure. This data is analysed below.

3.1.1 Data Analysis and Visualization

The Marsabit Station is located at 2.3° North and 37.9° East at an elevation of 1345 masl. Its World Meteorological Organization (WMO) station number is 636410 and is the point of observation for data used in this study. A wide range of data is available from this station and this data is graphically presented in ANNEX 5: Data visualization. **Error! Reference source not found.**

shows the dry bulb temperature which is the ambient air temperature, the dew point which is the temperature below which moisture condenses out of the air.

3.2 Hybrid System Model

The hybrid power system consists of an array of solar photovoltaic generators, wind turbine generators, and a battery bank and associated power regulation and conversion accessories, protection and switching equipment. Only the generation components are modelled in this study as they represent the key plant components.

Figure 3-7 shows the system's simplified single line diagram. Hybridization is carried out at the DC bus independent of phase and frequency constraints that would need to be overcome on an AC bus.

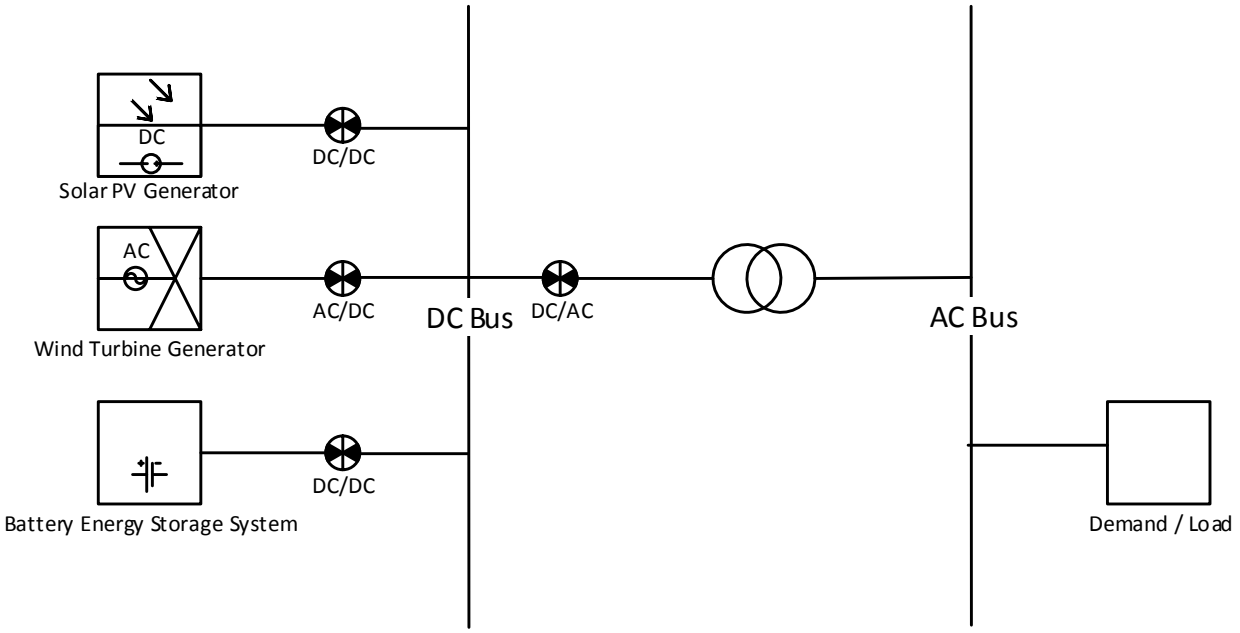

Figure 3-7: Hybrid Power System Model

3.3 Solar PV Model

In order to properly size hybrid renewable energy sources involving Photovoltaic (PV) arrays, a proper understanding of the PV device is necessary. Villalva et al [55], provides a basic introduction to the functioning of PV cells, the mathematical equations involved and the modelling and simulation of PV arrays. They state that PV devices display non-linear current voltage relationships hence several parameters of a PV model have to be obtained or adjusted from experimental data of practical devices. It is for this reason that the analysis below is a necessary precursor to the buildup of a PV generator / array model.

The most fundamental unit in solar PV generation is the solar cell. Numerous solar cells are connected in series parallel configuration to achieve a desired working voltage in what is referred to as a solar PV module. A solar PV array may consist of one or more modules in series parallel connections to achieve a desired peak power output and or a desired generation DC voltage.

3.3.1 The Solar Photovoltaic Cell

In a nutshell, a solar photovoltaic cell is basically a semiconductor diode whose p-n junction is exposed to light [55]. Incident light on the cell generates charge carriers that originate an electric current when the circuit is completed. The rate of generation of these carriers hence current produced by the cell depends on two things; the flux of incident light and the capacity of absorption of the semiconductor.

The semiconductor's capacity of absorption is mainly determined by the semiconductor material's band gap, the reflectance of the cell surface – determined by treatment and shape of surface, other factors such as the recombination rate, electron mobility and temperature.

On the incident light flux, photons of light with energies lower than the band gap of the PV cell do not generate any voltage or electric current. Only photons with energy corresponding to the band gap energy of the solar cell are used to generate voltage and current, those exceeding it are dissipated as heat. Semiconductors with lower band gaps can take advantage of a larger radiation spectrum but will generate lower voltages [55].

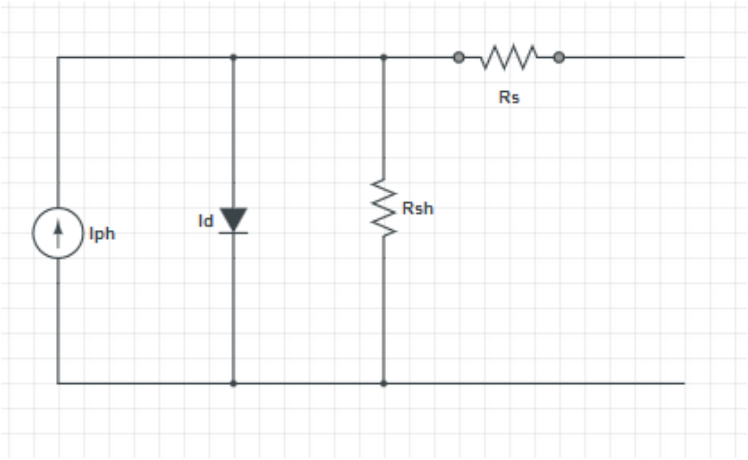

Figure 3-8: Solar photovoltaic cell

As highlighted by Tsai et al [56] and illustrated on Figure 3-8, a solar cell can be modelled as a photo current diode, a parallel resistor to express leakage current and a series resistor to represent

the internal resistance of the cell towards current flow. The voltage –current characteristics of this solar cell model is given as;

$$I = I_{ph} - I_S \left[e^{\frac{q(V+IR_S)}{kT_C A}} - 1 \right] - \frac{V + IR_s}{R_{sh}} \quad (3.3)$$

In this case, I_{PH} is known as the photocurrent, or current generated as a result of the impact of solar radiation on the cell. The cell saturation dark current is expressed as I_S, T_C is the cell's working temperature which influences the saturation current. A is the ideality factor.

The constants $q = 1.6x10^{-19}C$ is the electron charge whereas $k = 1.38x10^{-23}J/K$ is the Boltzmann's constant.

This single diode model however assumes a constant value for the ideality factor, A [57]. The ideality factor which is a measure of how closely the diode follows the ideal diode equation however is usually a function of the voltage across the device and at high voltage, recombination in the device is dominant at the surface and bulk regions, the ideality factor is close to one. However at lower voltages, recombination in the junction dominates and the ideality factor approaches two. The two exponential diode model as in eq.(3.4), factors in junction recombination by adding a second diode in parallel with the first and setting the ideality factor typically to two. This results in a more exact mathematical description of a solar cell.

$$I = I_{ph} - I_{S_1} \left[e^{\frac{q(V+IR_S)}{kT_C A_1}} - 1 \right] - I_{S_2} \left[e^{\frac{q(V+IR_S)}{kT_C A_2}} - 1 \right] - \frac{V + IR_s}{R_{sh}} \quad (3.4)$$

However there are limitations to developing expressions of this model's V-I curve parameters due to the implicit and nonlinear nature of the model [56]. Moreover, according to Honsberg and Bowden [57], analysis using a single diode, but allowing both the ideality factor and the saturation current to vary with voltage provides for more accurate results than a double diode model which yields erroneous values due to the recombination components being a complex function of carrier concentration in actual silicon devices. This model is thus not used in the development of the generalized PV model

3.3.2 Understanding and Improving the Single Diode Model

Most literature on solar PV modelling resort to use the single diode model despite the necessary compromises [57] [56] [55]. However to improve it an understanding of the various parameters

and their implications is necessary. The series resistance of the model R_s whose influence is stronger when the device operates in the voltage source region is a result of the sum of several structural resistances of the device. These include junction and contact resistances found at the various material interfaces in the cell [55]. The shunt resistance R_{sh} dominant in the current source region, exists mainly due to the leakage current of the $p-n$ junction and depends on the fabrication method of the PV cell. This value is generally high.

The light generated current of the PV cell is linearly dependent on solar irradiation but influenced by temperature. This dependence is illustrated in equation (3.5) by Villalva et al [55]

$$I_{ph} = \left(I_{ph,n} + K_I \Delta_T\right) G/G_n \tag{3.5}$$

$$and$$

$$\Delta_T = T - T_n \tag{3.6}$$

where, $I_{ph,n}$ is the light generated current at standard test conditions (STC), T being actual temperature in K and T_n temperature at STC. G, is the irradiation on the device surface and G_n nominal radiation at STC.

$$I_s = I_{s,n} \left(\frac{T_n}{T}\right)^3 \exp[\frac{qE_g}{ak}\left(\frac{1}{T_n} - \frac{1}{T}\right)] \tag{3.7}$$

$$and$$

$$I_{s,n} = \frac{I_{sc,n}}{\exp\left(\frac{V_{oc,n}}{aV_{t,n}}\right) - 1} \tag{3.8}$$

The diode saturation current I_S is also dependent on temperature as per eq.(3.7) but is mainly dependent on the current density J_S. J_s depends on the intrinsic characteristics of the PV cell dependent on such factors as the coefficient of diffusion of electrons in the semiconductor, lifetime of the minority carriers of electrons in the semiconductor, intrinsic carrier density inter alia . $I_{s,n}$, is the nominal saturation current calculated as per equation (3.8) in [55] using experimental data and evaluating equation (3.7) at nominal open-circuit conditions with;

$V = V_{OC}$,$I = 0$ and $I_{ph} \approx I_{SC,n}$

To improve the model, according to [55], I_s can be evaluated as shown in eq.(3.9) below. The idea behind this is to match open circuit voltages of the model with experimental data for a very large

range of temperatures achieved by inclusion of current/temperature and voltage/temperature coefficients K_I and K_V . The result is a simplification of the model and cancellation of errors at the vicinities of the open circuit voltages and other regions of the I-V curve K_I , and K_V are read from manufacturer's datasheets.

$$I_s = \frac{I_{sc,n} + K_I \Delta_T}{\exp\left(\frac{V_{oc,n} + K_V \Delta_T}{aV_t}\right) - 1} \tag{3.9}$$

With the assumptions and simplifications made thus far, the only outstanding unknowns are the resistance R_{sh} and R_s which are seldom provided by manufacturers. Other authors have proposed methods involving iterative adjustment of the series resistance value of the model until the resulting $I - V$ curve visually fits the experimental data and adjusting the shunt resistance value of the model *ad modum.* Villalva et al however believe that this method results in a poor $I - V$ model, instead they capitalize on the fact that there only exists one pair of shunt and series resistance for which the maximum power evaluated via their mathematical model and that obtained experimentally and recorded on the datasheet are equal and equivalent to the peak power at the maximum power point (MPP). With this basis they develop the below two equations used to solve for R_{sh} and R_s in an iterative fashion.

$$P_{max,m} = V_{mp}\left\{I_{ph} - I_s\left[\exp\left(\frac{\frac{q}{kT}\left(V_{mp} + R_s I_{mp}\right)}{aN_s}\right) - 1\right] - \frac{V_{mp} + R_s I_{mp}}{R_{sh}}\right\} = P_{max,e} \tag{3.10}$$

From which,

$$R_{sh} = \frac{V_{mp}\left(V_{mp} + I_{mp}R_s\right)}{\left\{V_{mp}I_{ph} - V_{mp}I_s \exp\left[\frac{V_{mp} + I_{mp}R_s}{N_s a} \times \frac{q}{kT}\right] + V_{mp}I_s - P_{max,e}\right\}} \tag{3.11}$$

where $P_{max,e}$, refers to experimentally evaluated peak power at MPP as recorded in the datasheet. $P_{max,m}$, refers to peak power mathematically evaluated by the model.

An iterative technique is then required to solve the eq. (3.11) above. By substituting parameters from the datasheet, the model can be enumerated. Further improvements can then be made to the model by utilizing solutions for R_{sh} and R_s obtained to better model or represent items estimated earlier. The nominal photocurrent for one can be re-evaluated as

$$I_{ph,n} = \frac{R_{sh} + R_s}{R_{sh}} . I_{sc,n} \tag{3.12}$$

From which, I_{ph} which is light dependent can be rewritten as,

$$I_{ph} = \left(\frac{R_{sh} + R_s}{R_{sh}} . I_{sc,n} + K_I \Delta_T\right) G/G_n \tag{3.13}$$

3.3.3 Solar Array Model

A single cell does not produce enough power to be of significant use, as such the cells are connected in a series parallel configuration to produce enough power at the required working voltage. Such configuration of cells is called a module. A panel would constitute one or more PV modules factory assembled and pre wired ready for field installation, they are usually sold commercially at set sizes by wattage say 120 W, 200W or 250W etc. A similar series parallel configuration of panels forms an array and is the generating unit of a solar PV plant. The wattage rating of a PV module is usually the maximum DC power output in watts under standard test conditions defined by a standard cell operating temperature of 25C and incident irradiance level of $1000W/M^2$.

Thus for N_p parallel circuits and N_s Series circuits, the equivalent model equation for the array becomes,

$$I_{ar} = N_p I_{ph} - N_p I_s \left[\exp\left(\frac{\frac{q}{kT}\left(V_{mp} + R_s I_{mp}\right)}{aN_s}\right) - 1\right] - \frac{V_{mp} N_p + R_s I_{mp} N_p}{R_{sh}} \tag{3.14}$$

The peak array power can be presented as

$$P_{max,ar} = V_{mp}N_p\left\{I_{ph} - I_s\left[\exp\left(\frac{\frac{q}{kT}\left(V_{mp} + R_sI_{mp}\right)}{aN_s}\right) - 1\right] - \frac{V_{mp} + R_sI_{mp}}{R_{sh}}\right\} \quad (3.15)$$

The nominal power of the array at a given operating voltage V_n is thus determined as

$$P_{n,ar} = V_nN_p\left\{I_{ph} - I_s\left[\exp\left(\frac{\frac{q}{kT}\left(V_n + R_sI_{mp}\right)}{aN_s}\right) - 1\right] - \frac{V_n + R_sI_{mp}}{R_{sh}}\right\} \quad (3.16)$$

The critical required parameter in studies of optimal unit sizing for a hybrid power system is the number of PV modules to deploy in the array. This is given by N_p. Thus for a known required amount of power to be supplied by solar, then

$$N_p = \frac{P_{PV}}{V_n\left\{I_{ph} - I_s\left[\exp\left(\frac{\frac{q}{kT}\left(V_n + R_sI_{mp}\right)}{aN_s}\right) - 1\right] - \frac{V_n + R_sI_{mp}}{R_{sh}}\right\}} \quad (3.17)$$

Assuming a maximum power point tracker of efficiency η_{mppt} then,

We can assume, all operating points will be at the determined maximum power point minus the losses of the tracker thus,

$$P_{n,ar} = \eta_{mppt} \times P_{max} \quad (3.18)$$

Consequently,

$$N_p = \frac{P_{PV}}{V_{mp}\eta_{mppt}\left\{I_{ph} - I_s\left[\exp\left(\frac{\frac{q}{kT}\left(V_{mp} + R_sI_{mp}\right)}{aN_s}\right) - 1\right] - \frac{V_{mp} + R_sI_{mp}}{R_{sh}}\right\}} \quad (.319)$$

More completely, the number of modules required will be

$$N_p = \frac{P_{PV}}{V_{mp}\eta_{mppt}\left\{\left(\frac{R_{sh}+R_s}{R_{sh}}.I_{sc,n}+K_I\Delta_T\right)G/G_n - I_s\left[\exp\left(\frac{\frac{q}{kT}\left(V_{mp}+R_sI_{mp}\right)}{aN_s}\right)-1\right]-\frac{V_{mp}+R_sI_{mp}}{R_{sh}}\right\}} \quad (3.20)$$

Of course it is imperative that N_p be an integer, and if a mixed number value is obtained, this should be rounded up to the nearest integer.

3.3.4 Modelling Power Output of a Kyocera KD 200 SX Series Panel

A sample commercially available solar panel is then modelled below, with the model parameters obtained from the panel datasheet [58] an excerpt of which is presented on Table 3-1 . This model is chosen due to its extensively informative datasheet useful for modelling the PV generator. It is also the choice of several authors and is a popular choice in field application as well.

Table 3-1: Kyocera KD 200 SX Parameters

Parameter	Value (Units)
$\boldsymbol{P_{max}}$	200.143 (W)
$\boldsymbol{V_{mp}}$	26.3 (V)
$\boldsymbol{I_{mp}}$	7.61 (A)
$\boldsymbol{V_{OC}}$	32.9 (V)
$\boldsymbol{I_{SC}}$	8.21 (A)
$\boldsymbol{P_{tolerance}}$	$+7/-0$ (%)
K_V	-0.1230 V/ K
K_I	0.0032 A/K
N_s	54

Calculated parameters based on the Algorithm of Villalva et al result in the following additional parameters presented on Table 3-2 for the model at STC.

Table 3-2: Calculated parameters for the Kyocera KD 200 SX

Parameter	Value (Units)

$I_{s,n}$	$9.825 \times 10^{-8}\ A$
I_{pv}	$8.214\ A$
a	1.3
R_{sh}	$415.405\ \Omega$
R_s	0.221Ω

According to [32] assuming the PV arrays are equipped with MPPT trackers then for modelling simplicity, the equation below sufficiently models the array power output.

$$P_{PV}(t) = f_{PV} P_{PVR} \frac{G(t)}{G_{STC}} (1 + \propto_T (T(t) - T_{STC})) \quad (3.21)$$

Where,

The output power of the panel array at time instance t is $P_{PV}(t)$, the rated power of which is P_{PVR}, the derating factor considering shading and wiring losses is f_{PV}. The inputs to the model are the temperature at time instance t represented by $T(t)$ and the solar radiation represented by $G(t)$. G_{STC}, and T_{STC} respectively are the solar radiation and temperature for the panel at standard test conditions. $\propto_T$, is the temperature coefficient which is provided by the manufacturer's datasheets.

The de-rating factor f_{PV} is determined from solar PV modelling best practice [59]. It is assumed in this research that shading is negligible and hence is not accounted for in determination of f_{PV}. This is somewhat true for utility scale PV applications as the layout can be such that shading from adjacent panels is eliminated or minimized by proper spacing, whereas that due to features in the topography of the surrounding site avoided by proper site selection and preparation. The remaining contributing factors are summarized in Table 3-3 below.

Table 3-3: Panel derating factors

Parameter	Value
AC wiring	99.00%
Array soiling	95.00%
DC wiring	98.00%
Diodes and Connections	99.50%
Inverter and transformer	92.00%
Mismatch	98.00%

Panel de-rating factor, f_{PV}	82.68%

3.4 Wind Turbine Generator Model

Wind turbine technology is maturing fast and the penetration of wind in electric grids has been on a steep increase with some countries such as Germany shutting down conventional fossil fuel and nuclear powered plants in favor of renewable energy generation via wind and solar. However as Literature cited by [59] indicates, increasing penetration of wind in electricity grids has brought with it concerns on its effect on the stability of the grid.

To this end, a lot of work has gone into developing wind turbine models intended for use in grid stability studies. Most of these models so far have been manufacturer specific which unfortunately implies that they are subject and limited to terms of non-disclosure agreements. This has impeded sharing and open development of these models [59]. In recent times however, newer work keen on developing generic open wind turbine models have emerged. These include but are not limited to [60] [61] [62] [63] [64] [65] [59] [66]. The general objective for these works has been development of wind turbine models suitable for stability and transient analysis in power systems. In this research more simplistic models are required for mapping out available wind resource quantified in terms of wind speeds to energy generation potential based on specific class of wind turbine generators.

3.4.1 Power in Wind

The power in wind can be evaluated from Newton's second law of motion as highlighted in [60].

$$F = ma \tag{3.22}$$

Where

F , is exerted force;

m , is mass of air;

a , the acceleration of the mass of air.

From which,

$$E = m \times a \times s \tag{3.23}$$

But

$$v^2 = u^2 + 2as \tag{3.24}$$

Or

$$a = \frac{v^2 - u^2}{2s} \tag{3.25}$$

Assuming initial velocity u as zero then $a = \frac{v^2}{2s}$ substituting in equation (3.23)(3.25) then,

$$E = \frac{1}{2} \times m \times v^2 \tag{3.26}$$

Power in wind is thus formulated as

$$P = \frac{dE}{dt} = \frac{1}{2}\frac{dmv^2}{dt} = \frac{1}{2}\rho \times A \times v^3 \tag{3.27}$$

However, actual mechanical power extracted by turbine blades from the wind is evaluated from the difference between the upstream and downstream wind speeds. Thus,

$$P = \frac{1}{2} \times \rho \times A \times v_w(v_u^2 - v_d^2) \tag{3.28}$$

v_u , is the upstream wind speed in m/s while v_d is the downstream wind speed. These two together give rise to the **blade tip speed ratio** an important metric in wind engineering. This will be demonstrated later. Also, $v_w = \frac{v_u + v_d}{2}$ thus

$$P = \frac{1}{2} \times \rho \times A \times (\frac{v_u + v_d}{2})(v_u^2 - v_d^2) \tag{3.29}$$

$$P = \frac{1}{2}\{\rho A v_u^3 \times \frac{(1 + \frac{v_d}{v_u})(1 - \left(\frac{v_d}{v_u}\right)^2)}{2}\} \tag{3.30}$$

or

$$P = \frac{1}{2}\ \rho A v_u^3 C_p \tag{3.31}$$

where

$$C_p = \frac{(1 + \frac{v_d}{v_u})(1 - \left(\frac{v_d}{v_u}\right)^2)}{2} \tag{3.32}$$

C_p , is referred to as the turbine power coefficient or coefficient of performance, and its varies with the blade tip speed ratio and the blade pitch angle β. The blade tip speed ratio is given as

$$\lambda = \frac{v_u}{v_d} \tag{3.33}$$

And the blade pitch angle β is as illustrated in Figure 3-9 [63].

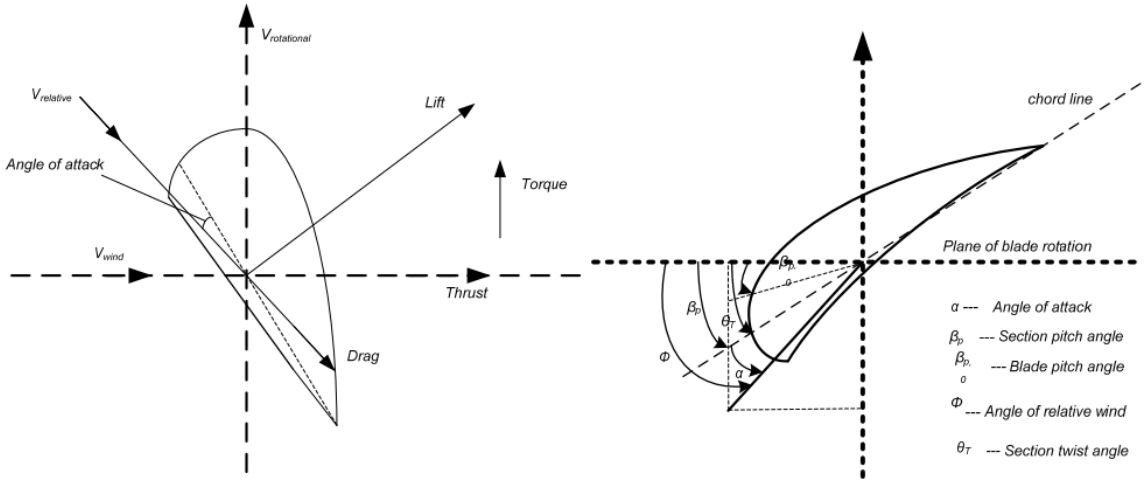

Figure 3-9: Cross-section of wind turbine blade airfoil and relevant angles

3.4.2 Ideal Wind Turbine

Power calculation for an ideal turbine as in [65] assumes a circular tube of air flow through an ideal turbine as illustrated in Figure 3-10

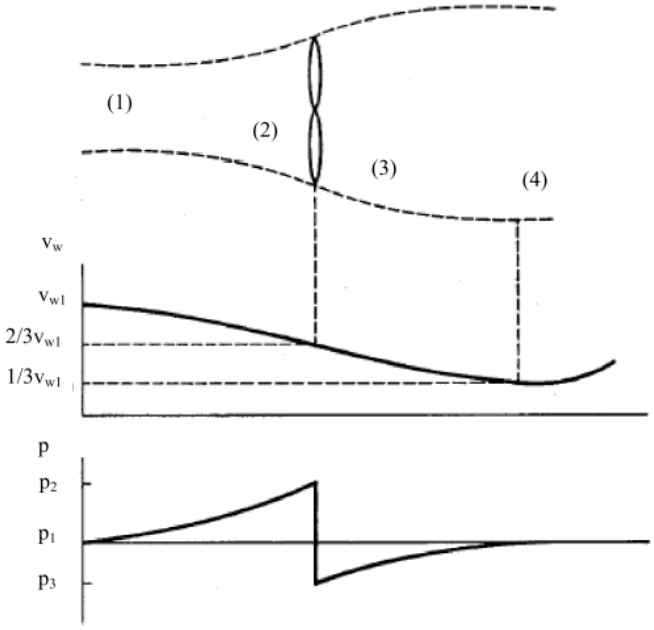

Figure 3-10: Circular airflow through an ideal turbine

Then under optimal conditions,

$$v_{w2} = v_{w3} = \frac{2}{3} v_{w1} \tag{3.34}$$

$$v_{w4} = \frac{1}{3} v_{w1} \tag{3.35}$$

$$A_2 = A_3 = \frac{3}{2} A_1 \tag{3.36}$$

$$A_4 = 3\, A_1 \tag{3.37}$$

Thus the mechanical power extracted can be given as

$$P_{m,ideal} = P_1 - P_4 \tag{3.38}$$

$$P_{m,ideal} = \frac{1}{2}\rho(A_1 v_{w1}^3 - A_4 v_{w4}^3) = \frac{1}{2}\rho\left(\frac{8}{9} A_1 v_{w1}^3\right) \tag{3.39}$$

Expressed in terms of undisturbed wind speed,

$$P_{m,ideal} = \frac{1}{2}\rho\left[\frac{8}{9}\left(\frac{2}{3} A_2\right) v_{w1}^3\right] = \frac{1}{2}\,\rho\,\left(\frac{16}{27}\, A_2 v_{w1}^3\right) \tag{3.40}$$

This shows that an ideal turbine cannot extract more than 59.3% of the power in an undisturbed tube of air [65] and the factor $\frac{16}{27} = 0.593$ is referred to as the **Betz coefficient.**

The existing models of various wind turbine classes are examined in order to develop the simplified model needed for this work.

3.4.3 Practical Wind Turbines

Practical turbines do not reach the 59.3% limit that can be achieved by an ideal turbine in extracting power from the wind. In fact practical turbine depending on the type can only extract between 10 and 40% of the power in the wind. Fractions of between 35 and 40% are considered good although fraction as high as 50% have been claimed according to [65].

Practical wind turbines can be classified according to their rotor axis orientation. This yields two categories of wind turbines. These are vertical axis and horizontal axis type turbines. Vertical axis type turbines are usually setup in urban environments are typically of small capacity compared to available horizontal axis turbines. The advantage to vertical axis wind turbines is that they are able to take advantage of wind blowing in any direction. Their key disadvantage however is that

massive amount of vibrations are set to the supporting structures hence need for reinforced structures. Horizontal axis turbines are the most popular in this classification in terms of commercial deployment.

Horizontal Axis Wind Turbines (HAWT) are further classified into 4 classes.

Type 1 Turbines, are also known as fixed speed wind turbines [59]. They are the most basic type of utility scale wind turbines and are referred to as fixed because they operate within 1% variation of the rated rotor speed. Squirrel cage machines directly connected to the grid are usually employed. Their main advantage is that they are low cost, robust, reliable and simple to maintain [59]. Their key disadvantage is their sub-optimal performance in terms of power extraction this is because in most cases wind speed varies well beyond the acceptable variance for these turbines. Figure 3-11 is a representation of type 1 wind turbines.

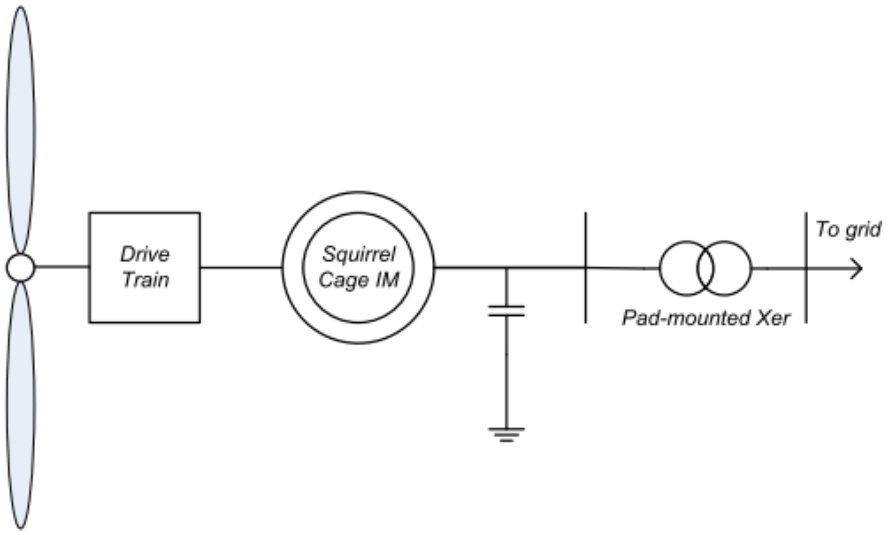

Figure 3-11: A type 1 (Fixed Speed) Wind Turbine

Type 2 Turbines are also known as variable slip wind turbine generators [59]. They resemble type 1 wind turbines in most respects but are however able to generate rated power at higher than rated wind speeds. They are thus known as variable speed wind turbines as the range of speeds within which the turbine can continue generating rated power is large. These machines usually employ wound rotor induction machines with external rotor resistance which is used to regulate power

output. A clear advantage here is the ability to harness the power in wind with speeds above the rated rotor speed. Figure 3-12 is a representation of a type2 wind turbine.

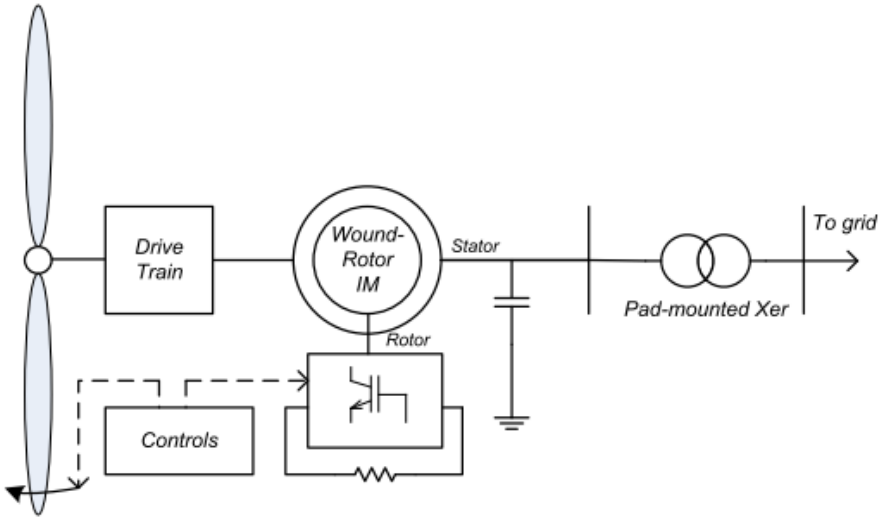

Figure 3-12: Type 2 (Variable- slip) Wind Turbine

Type 3 Turbines are also known as doubly fed induction generators (DFIG). DFIGs have emerged as the preferred technology for Wind Power Plants [59]. DFIGs are similar to conventional wound rotor induction generators albeit with additional external power electronics circuitry on the rotor and stator windings to optimize the wind turbine operation [61]. A three-phase supply voltage at the power system frequency typically feeds the stator winding. The rotor winding is separately powered via a back to back (AC-DC-AC) converter at the desired system frequency. This circuit process only the slip power, and because this is only a fraction of the rated turbine output, the converter circuit need only be rated at about 20%-30% of the rated turbine output. According to [59] DFIGs present the below advantages over Type 1 and 2 WTGs.

- They enable independent active and reactive power control.
- They can utilize wind speeds $\pm 30\%$ of rates wind speed to generate power with minimal slip losses.
- They have maximized aerodynamic power extraction.
- They can be controlled to reduce mechanical stress.

Figure 3-13 is a representation of a type 3 (DFIG) wind turbine.

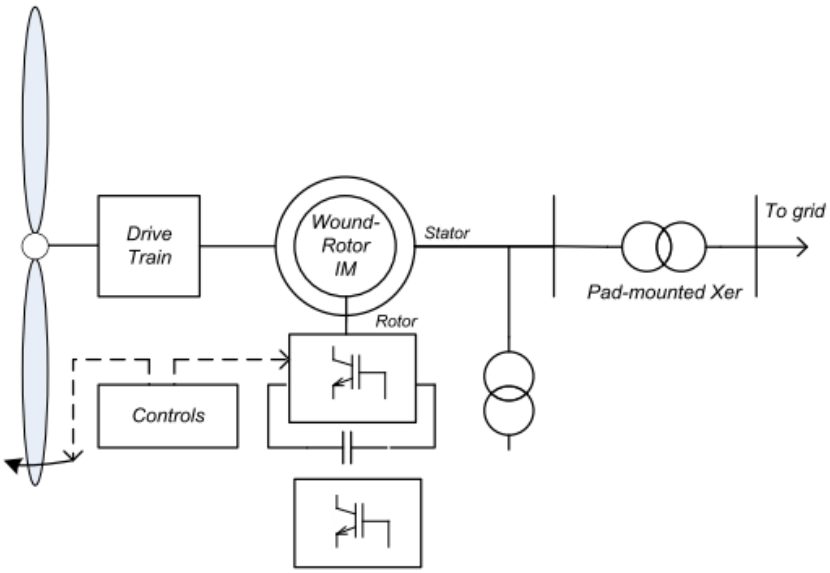

Figure 3-13: Type 3 (DFIG) wind turbine

Type 4 Turbines are also known as Full Converter Wind Turbines (FCWT), the most popular of which employ a permanent magnet alternator (PMA). These turbines present a number of advantages over other types earlier mentioned key among them according to [59] being.

- Decoupling of the generator from the grid hence improving fault response
- Larger wind speed operation range for the turbine
- More headroom to supply reactive power to the grid.
- For FCWT using PMAs, the absence of rotor windings reduces excitation losses and the need for slip rings which translates in reduced maintenance requirements. This is a key advantage especially for offshore installations.

FCWTs however compared to DFIGs and the other types of wind turbines are more costly as the full converter is connected to the stator and must process / handle the entire rating of the turbine.

Figure 3-14 is a representation of a type 4 wind turbine.

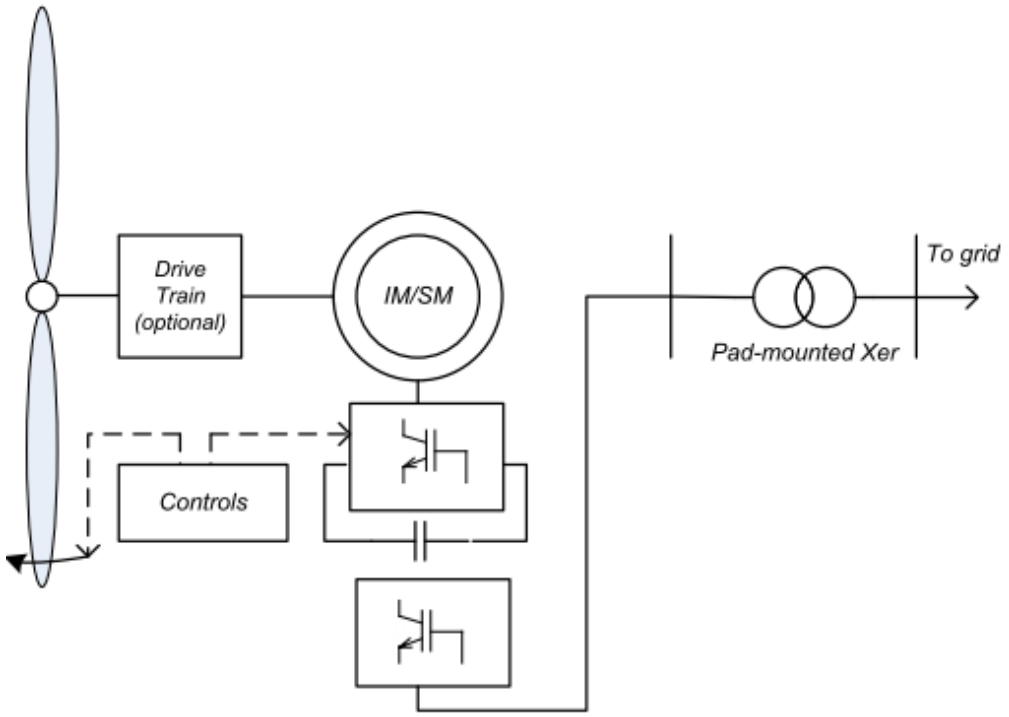

Figure 3-14: Type 4 (Full Converter) Wind Turbine

3.5 Wind Turbine Model

A simplistic yet realistic model is required that follows the typical characteristics of a practical turbine. i.e.

- If the wind speed range is below the cut-in speed for the turbine, then output power is zero.
- If the wind speed range is between the cut-in and the rated speed for the turbine, then the power output is the maximum extractable from the wind based on the C_p and wind speed relation for the turbine.
- If the wind speed range is between the rated and cut-out speed for the turbine, then the power generated is the rated output of the plant.
- If the wind speed range is above the cut-out speed, then the power generated is zero.

Governing equations earlier developed are used with realistic experimental C_p figures from a datasheet of an actual wind turbine.

The model block is represented in Figure 3-15 below.

Equation (3.41) governs the power output as derived by the model, however for computational efficiency, equation (3.42) can be used without loss of meaning as a consequence of its implicit generalization.

$$P = \begin{cases} 0 & 0 \le v_u < v_{in} \\ \frac{1}{2}\ \rho A v_u^3 C_p & v_{in} \le v_u \le v_r \\ P_r & v_r \le v_u < v_{out} \\ 0 & v_u \ge v_{out} \end{cases} \quad (3.41)$$

$$P = \begin{cases} 0 & 0 \le v_u < v_{in} \\ P_r \frac{v_u - v_{in}}{v_r - v_{in}} & v_{in} \le v_u \le v_r \\ P_r & v_r \le v_u < v_{out} \\ 0 & v_u \ge v_{out} \end{cases} \quad (3.42)$$

where P_r, is the rated power output of the wind turbine,

$C_p(v_u)$, is the coefficient of performance of the turbine, simplistically modelled from the turbine datasheet to be a function of wind speed only,

v_u, is the prevailing incident wind speed adjusted to mast height,

v_{in}, is the cut-in speed of the wind turbine taken from the turbine datasheet.

v_r, is the rated speed of the turbine taken from the turbine datasheet.

v_{out}, is the cut-off / out speed of the turbine taken from the turbine datasheet.

Figure 3-15: WTG model block diagram

3.6 Energy Storage

Interest in energy storage is surging in recent times as a consequence of a confluence of industry drivers such as increased deployment of renewable energy generation, demands large investments on grid infrastructure for reliability and mini-grid initiatives and high capital cost of managing peak grid [67].

An energy storage scheme is a technology or device that can take in energy in a charging process and hold this energy for some finite time and later release this energy in a discharging process when required. Energy storage systems are diverse and of different natures. Some scheme involve conversion of energy from one form to another whereas others don't. In general all practical energy storage schemes involve some energy loss, consequently different schemes have different efficiencies.

The two fundamental characteristics of an energy storage scheme are:

- The Power Rating of the Scheme / Discharge Capacity: Refers to the maximum amount of power that can be drawn from the scheme during discharge when properly configured.
- The Energy Rating of the Scheme / Storage Capacity; Refers to the amount of energy that can be stored in the scheme. This is usually specified in either KWh or Ah, but both have the same inference.

Subsequently, [68] identifies two main applications of energy storage systems as being Energy applications – discharge over periods of hours and corresponding long charging periods and Power application – short discharge periods (seconds to minutes) and short recharging periods resulting in many cycles over a day.

For application in micro grids and for hybrid renewable energy systems, various Energy Storage technologies have appeared in literature. These technologies include Battery Energy Storage Systems (BESS), Flywheel Energy Storage (FES), Compressed Air Energy Systems (CAES), Pumped Hydro Storage (PHS), Ultra Capacitors (UC), Super Magnetic Energy Storage Systems (SMES) and Hydrogen. Each is briefly highlighted below;

3.6.1 Battery Energy Storage Systems (BESS)

Include an array of different electrochemical technologies for energy storage such as Lead Acid, Nickel Cadmium, Sodium Sulphur, Lithium Ion etc. Battery energy storage technologies are very

versatile and can be used for both power and energy applications depending on the specific technology. They are also the easiest to scale down for portable applications as is seen with Lithium Ion (Li-Ion) batteries on virtually every portable electronic gadget today. Their biggest downside so far has been cost. Their applications depending on type range from power supply for electric vehicles, energy smoothing from renewable energy sources such as wind and solar, voltage support and frequency stabilization, provision of spinning reserve, power quality improvement, ramp control and curtailment mitigation.

3.6.2 Flywheel Energy Storage Systems (FES)

In these energy storage systems, a rotor is rotated to a very high speed. The energy capacity of a flywheel is the maximum speed it can attain. A typical FES would consist of a rotor / flywheel and a generator/ motor combination set in vacuum on magnetic or mechanical bearings. When the supply exceeds demand, the flywheel picks up speed and stores this extra energy in form of rotational energy. When demand exceeds supply or in the absence of supply the kinetic rotational energy spins the generator to supply back power. In grid setups they are mainly used in power applications and in frequency stabilization. They also feature in the automotive and aviation industries.

3.6.3 Compressed Air Energy Storage Systems (CAES)

These plants compress air and store it under pressure in underground caverns. During the stored energy recovery phase the compressed air is then heated and expanded in an expansion turbine to drive a generator for electricity production. The compression stage results in the air heating up, in diabatic systems this energy is lost and the compressed air has to be heated by say natural gas in the expansion turbine to drive generators which produce electricity. The two large scale plants in existence are of this type. In adiabatic CAES systems, the heat energy generated during the air compression stage that is usually lost is recovered and later used in the stored energy recovery phase to reheat the compressed air being expanded. These storage schemes depend on the existence of natural caverns for storing the compressed air and their energy storage capacity depends on the cavern size. Their key applications are in grid energy storage and energy arbitrage. A stellar example of a CAES is the 321MW Huntorf plant in Germany, able to reach its rated output power of 321 MW in 6 minutes and supply this for up to 2 hours. Smaller capacity applications are also available using artificial pressurized containers for storage of air and have applications in automotive (locomotive) industry.

3.6.4 Pumped Hydro Storage (PHS)

This is a very mature energy storage application that involves pumping of water from a lower reservoir to a higher level reservoir. Its power rating is based on the nameplate rating of the turbine / pumps usually determined from the design discharge up or down the reservoirs and the elevation differences between the reservoirs. PHS is highly dependent on geography, i.e. availability of water to pump, and availability of naturally occurring reservoirs within close proximity and at an elevation difference. Where the terrain and geography allow, PHS tend to be the largest scale energy storage systems both in terms of energy and power rating, however such locations are limited around the globe. Their key applications are in grid energy storage and in energy arbitrage.

3.6.5 Hydrogen

Hydrogen has been proposed in various research and experimented on as a potential energy storage system. The concept is relatively straight forward and simple. Excess energy e.g. that generated by wind farms is used to electrolyze water to produce hydrogen. Hydrogen is then stored and later used as a fuel either in fuel cells or combusted to drive engines or generate steam that turns turbines that in turn drive generators that produce electricity. The application are very versatile especially when the hydrogen generation and recovery of energy stored in it are decoupled. It then can be applied in hydrogen vehicles or as fossil fuel substitute etc. The key challenge with this scheme are the low efficiencies and difficulties in storing hydrogen gas. It is also only applicable for energy applications.

Other Schemes mentioned in literature but not explored here are Ultra-Capacitors and Super Capacitors and Super Magnetic Energy Storage Systems (SMES). These are not dealt with as the technologies are very new and not well proven especially for grid applications.

3.6.6 Criteria for Selecting an Energy Storage Scheme

As each energy storage scheme has its advantages and disadvantages and an inherent proper application, it is imperative that on a case by case a qualitative and quantitative criteria be developed and observed for selecting the appropriate energy storage scheme to use. Barin et. al. [69], developed a multiple criteria analysis for selecting the most appropriate energy storage system from a power quality perspective. From their work it is emergent that the intended application be clear first then therefrom a criterion can be developed. In their work, FES and Li-ion emerged as the preferred technologies as determined by an Analytic Hierarchy Process (AHP) and fuzzy logic approach.

The qualitative criteria they considered included

- Load management in consideration of load following and load levelling, which will also be a consideration in this study.
- Maturity of the technology from a technical standpoint, also a consideration in this study
- Environmental Impact and
- Power quality

The quantitative criteria they considered included

- The roundtrip efficiency, also considered in this study.
- The cost of the technology in US $ per kW, also considered in this study.

In addition to the criteria listed above, other criteria considered in this study include:

- The technology lifetime an important factor in determining lifecycle costs of a technology
- Feasible power rating and
- Feasible energy rating (in terms of discharge time)

The result of this review is presented on Table 3-4, Table 3-5, Table 3-6 and Table 3-7.

Table 3-4: Large scale energy storage systems comparison

Energy storage technology	Advantages	Disadvantages	Power applications	Energy applications
Lead–acid batteries	Low power density and capital cost	Limited life cycle when deeply discharged	Fully capable and suitable	Feasible but not quite practical or economical
Lithium-ion batteries	High power and energy densities, high efficiency	High production cost, requires special charging circuit	Fully capable and suitable	Feasible but not quite practical or economical
Sodium–sulfur batteries	High power and energy densities, high efficiency	Production cost, safety concerns (addressed in design)	Fully capable and suitable	Fully capable and suitable
Flow batteries	High energy density, independent power and energy ratings	Low capacity	Suitable for this application	Fully capable and suitable
Flywheels	High efficiency and power density	Low energy density	Fully capable and suitable	Feasible but not quite practical or economical
Pumped hydro-energy storage systems	High capacity	Special site requirement	Not feasible or economical	Fully capable and suitable
Compressed air energy storage systems	High capacity, low cost	Special site requirement, needs gas fuel	Not feasible or economical	Fully capable and suitable

Table 3-5: Large scale energy storage systems, technical characteristics

Technology	Power rating (MW)	Discharge duration	Response time	Efficiency (%)	Lifetime
Lead–acid batteries	< 50	1 min–8 h	< 1/4 cycle	85	3–12 years
Nickel–cadmium batteries	< 50	1 min–8 h	N/A	60–70	15–20 years
Sodium–sulfur batteries	< 350	< 8 h	N/A	75–86	5 years
Vanadium redox flow batteries	< 3	< 10 h	N/A	70–85	10 years
Zinc–bromine flow batteries	< 1	< 4 h	< 1/4 cycle	75	2000 cydes
Flywheels	< 1.65	3–120 s	< 1 cyde	90	20 years
Pumped hydro energy storage systems	100–4000	4–12 h	s–min	70–85	30–50 years
Compressed air energy storage systems	100–300	6–20 h	s–min	64	30 years

Table 3-6: Technical suitability of large scale energy storage systems

Storage application	Lead-acid batteries	Flow batteries	Flywheels	Pumped hydro energy storage systems	Compressed air energy storage systems
Transit and end-use ride-through	▯	▯	▯		
Uninterruptible power supply	▯	▯	▯		
Emergency back-up	▯	▯			▯
Transmission and distribution stabilization and regulation	▯	▯			
Load leveling[a]	▯	▯		▯	▯
Load following[b]	▯	▯			
Peak generation	▯	▯	▯	▯	▯
Fast response spinning reserve	▯	▯	▯		
Conventional spinning reserve	▯	▯	▯	▯	▯
Allow for renewable integration	▯	▯	▯	▯	▯
Suitable for renewables back-up	▯	▯		▯	▯

[a] Reducing the large fluctuations that occur in electricity demand.
[b] Adjusting power output as demand for electricity fluctuates throughout the day.

Table 3-7: Large scale energy storage systems, economic and environmental characteristics

Technology	Capital cost (US$/kWh)	Environmental issues
Lead–acid batteries	50–310	Lead disposal
Nickel–cadmium batteries	400–2400	Toxic cadmium
Sodium–sulfur batteries	180–500	Chemical handling
Vanadium redox flow batteries	175–1000	Chemical handling
Zinc–bromine flow batteries	200–600	Chemical handling
Flywheels	400–800	Slight
Pumped hydro-energy storage systems	8–100	Reservoir
Compressed air energy storage systems	2–100	Gas emissions

From which it is clear that a battery energy storage system would be the favored option due to its versatility. However as there are various battery energy storage solutions the appropriate battery energy storage technology also needs to be selected. Below is an overview of battery storage technologies.

3.7 Generic Model of a Battery Energy Storage System.

BESS modelling is necessary to predict given a set of parameter the operational characteristics of a given battery. The parameters determining the operational characteristics of a battery include: the Discharge rate, charge rate, battery age, battery type and temperature [71].

Two classes of battery models are explored here:

- The electrochemical model and
- The equivalent circuit model.

Electrochemical models are usually more precise and complex as they take into account the chemical, thermodynamic and physical qualities of the batteries. They are not considered in this research, however a short overview can be found in [71].

Equivalent circuit models are usually used in circuit modelling software as they are usually much easier to model. Two classes exist, dynamic – where the primary parameter; voltage, charge, current and temperature all vary as a function of one another and static -where primary parameters are predetermined and then remain constant through the simulation.

Simpler generic equivalent circuit models are documented in [72] and include the ideal model, the linear model and the Thevenin model.

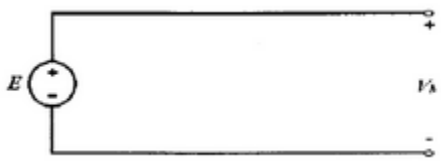

Figure 3-16: Ideal Model

The ideal model, Figure 3-16 is characterized only by an ideal voltage source and does not factor in internal battery resistance.

The linear model, Figure 3-17 includes to the ideal model a series resistance to model the battery internal resistance.

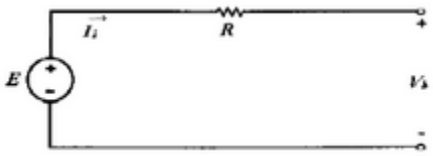

Figure 3-17: Linear Model

The Thevenin model, Figure 3-18 improves on the linear model by addition of an RC circuit in series with the series resistance that models the battery internal resistance. The resistor in parallel with the capacitor is referred to as an overvoltage resistor.

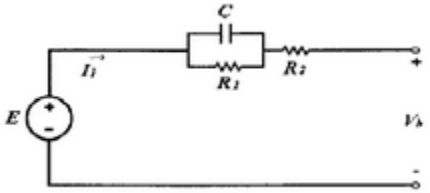

Figure 3-18: Thevenin Model

Additionally specific models have been developed for the different battery types usually taken in to account the various

behavioral characteristics of the battery types. These have not reached perfection yet but can be reliably used in modelling BESS with better accuracy than the generic models mentioned above [71]. Examples include a Lead Acid model developed in [73], a Sodium Sulphur model developed in [74] and a Zinc Bromine battery model developed in [75].

3.8 The Kinetic Battery Model (KiBaM)

This model developed by Manwel and McGowan [76] is based on a chemical kinetic process. It models the battery charge as distributed over two tanks: an available energy tank and a bound energy tank. The available energy tanks supplies electrons directly to the load as its energy is available. The bound energy tanks contains energy that is still chemically bound and can only supply electrons to the available energy tank. This model is simple and particularly useful at modeling batteries where the state of charge and depth of discharge are important. The maximum battery capacity Q_{MAX} is the sum of the capacity of the available energy Q_A and bound energy Q_B.

$$Q_{MAX} = Q_A + Q_B \tag{3.43}$$

and

$$c = \frac{Q_A}{Q_{MAX}} \tag{3.44}$$

The conductance between the two tanks, and indication of the rate at which charge flows between the two states is dependent on a parameter k as well as the height difference between the two tanks [77]. The ratio of the capacities of the two tanks is expressed as c.

The change of charge in both tanks is given by the following system of differential equations,

$$\frac{dQ_A}{dt} = -I + k(h_B - h_A) \tag{3.45}$$

$$\frac{dQ_B}{dt} = -k(h_B - h_A) \tag{3.46}$$

With initial conditions, $Q_A(0) = c.Q_{MAX}$ and $Q_B(0) = (1-c).Q_{MAX}$ for $h_A = \frac{Q_A}{c}$ and $h_B = \frac{Q_B}{1-c}$ on application of a load I , the available charge reduces and the height difference between the two tanks increases. Charge only flows back from the bound energy tank to the available energy tank when the load I is removed. Eq. (3.45) and (3.46) can be solved using Laplace transforms which results in;

$$Q_A = Q_{A_0} e^{-k\Delta t} + \frac{(Q_{MAX_0} k' c - I)(1 - e^{-k' t})}{k'} + \frac{cI(k'\Delta t - 1 + e^{-k'\Delta t})}{k'} \quad (3.47)$$

$$Q_{B-end} = Q_{B_0} e^{-k'\Delta t} + Q_{MAX_0}(1 - c)\left(1 - e^{-k'\Delta t}\right) + \frac{I(c-1)(k'\Delta t - 1 + e^{-k'\Delta t})}{k'} \quad (3.48)$$

Where $Q_{MAX_0} = Q_{A_0} + Q_{B_0}$ and are the charge quantities at $t = 0$

A linear model as in Figure 3-17 is used to model the terminal voltage of the battery, thus

$$V_{BESS} = E - IR_O \quad (3.49)$$

Where the discharge current is I and E the internal voltage and R_0 is the internal resistance. The internal voltage is expressed as;

$$E = E_0 + AX + \frac{CX}{D - X} \quad (3.50)$$

The initial linear variation of battery voltage with state of charge is represented by the parameter A. The decrease in battery voltage with progressive discharge of the battery is represented by the parameter C and D whereas X represents the normalized charge removed from the battery.

These parameters are usually obtained from battery discharge curves, hence this model has to be modified for the different batteries available [77].

The BESS's state of charge is determined as:

$$SOC(t) = SOC(t-1)(1 - \frac{\sigma\Delta t}{24}) + \frac{P_{WTG}(t) + P_{PVG}(t) - P_L(t)}{C_{BESS} V_{BESS}} \quad (3.51)$$

Eq. (3.64) is used to update the state of charge of the BESS at the end of each time step.

Where the battery self-discharge rate is given by σ and Δt is the length of the time step, C_{BESS} is the BESS capacity in Ampere hours and V_{BESS} the terminal battery voltage as defined in eq.(3.49). The State of charge is an energy ratio hence cannot be plugged in directly to a power flow equation. It would be necessary to multiply it with the BESS energy rating. For simplicity in calculation, the researcher makes an assumption here that the BESS is able to deliver constant power over the duration of the time step (1 hour), the internal self-discharge rate is also ignored as it is negligible relative to the other quantities (depends on the battery technology but typically assumed at 0.2% per day for generic models [78]), while not the case in reality it greatly simplifies computational requirements without adversely affecting the results. With this assumption, the power rating and

the energy rating in a time step are equally treated. Thus the corresponding available power flow from the BESS can be determined as;

$$P_{BESS}(t) = (SOC(t) + DOD_{MAX} - 1) \times P_{BESS\_rated} \quad (3.52)$$

In this expression, DOD_{MAX} is the maximum depth of discharge and is the equivalent of the absolute minimum state of charge for the proper functioning of the BESS. It varies with the BESS technology used.

The BESS charge-discharge algorithm can thus be written in the form of the pseudo code below;

1. If $(P_{PVG} + P_{WTG}) > P_D$
    a. Then , all demand has been met, extra power generated to charge BESS
    b. Update SOC as;$SOC(t) = SOC(t-1)\left(1 - \frac{\sigma\Delta t}{24}\right) + \frac{\eta_{conv} * RTEF * (P_{PVG} + P_{WTG} - P_D}{N_{BESS} * P_{BR}}$
2. Else if $(P_{PVG} + P_{PWTG}) < P_D$
    a. Check if Demand will be met with BESS addition
    b. If $(P_{PVG} + P_{PWTG} + \eta_{conv} N_{BESS} P_{BR}(SOC(t-1) + DOD_{max} - 1)) > P_D$
    c. Demand has been met
    d. Update SOC as $SOC(t) = SOC(t-1)\left(1 - \frac{\sigma\Delta t}{24}\right) - \frac{(P_{PVG} + P_{WTG} - P_D}{\eta_{conv} * N_{BESS} * P_{BR}}$
    e. Provided that maximum Depth of Discharge is not violated: thus
        i. If $SOC(t) < 1 - DOD\_max$ then
        ii. Revert and declare Demand not met, overwrite SOC as

$$SOC(t) = SOC(t-1)\left(1 - \frac{\sigma\Delta t}{24}\right)$$

3. Else
    a. Demand not met
    b. Nonetheless , update SOC on account of self-discharge as

$$SOC(t) = SOC(t-1)\left(1 - \frac{\sigma\Delta t}{24}\right)$$

3.9 Load Model

A hypothetical load model is used. It is derived from data made available to the researcher by the national power utility, Kenya Power. The data covers the month of September for the years 2009 to 2012. It is used to derive a typical metropolitan daily load curve which is plotted in Figure 3-19 for weekdays and Figure 3-20 for weekends. This data is sufficient as there is very little interseasonal variation demand resulting from heating and cooling loads for location close to the equator like Nairobi. For improved accuracy, two load curves are used one to represent typical weekdays and one to represent typical weekends and holidays. A base consumption figure is derived from the data above and adjusted to reflect growth as covered in [79].

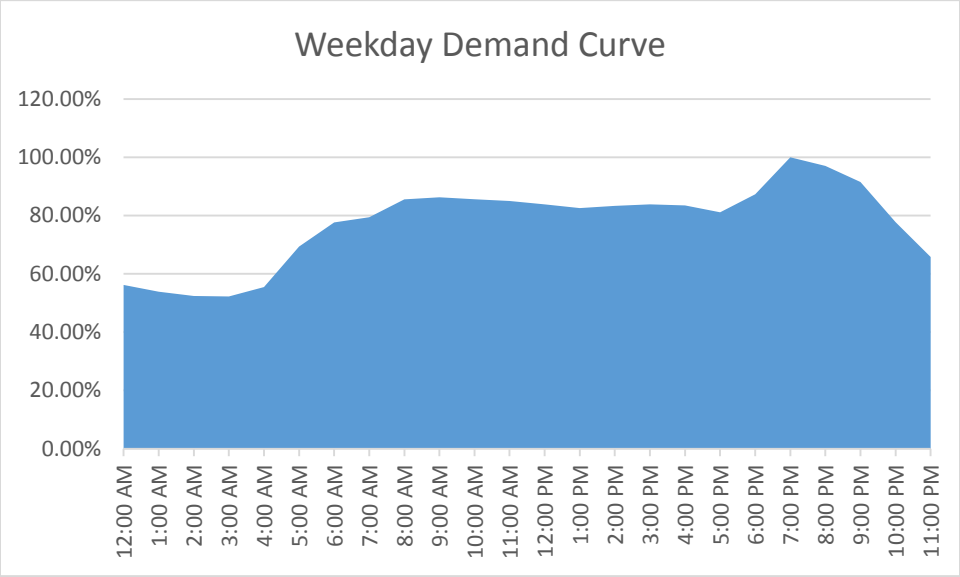

Figure 3-19: Demand curve for a typical weekday

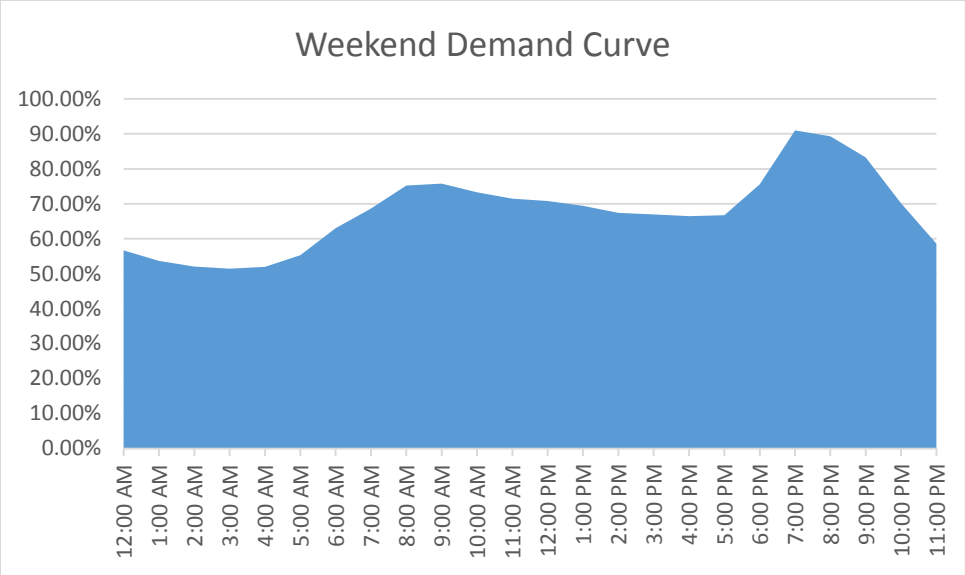

Figure 3-20: Demand curve for a typical weekend or holiday

3.10 Problem Formulation

From the models above, the cost function is derived. It is desired that a technical feasible system is sized at a minimum cost. The objective function is thus in this case an economic cost function that is constrained with technical boundary conditions. These boundary conditions are discussed in the next section. The optimization problem is modelled around one technical index the Loss of Power Supply Probability (LPSP) to model system reliability and one economic index the Levelized cost of Energy (LCoE) to model cost of energy produced by the system. These are from here on referred to as the reliability objective and the cost objective.

3.10.1 The Reliability Objective

The Loss of Power Supply Probability (LPSP) introduced in the literature review is used here. LPSP is the probability that over a certain period of study, the power demand is not fully met by the generated power. Mathematically it is represented as shown below

$$LPSP = \frac{\sum_{i=1}^{N}[P_L(t_i) - P_G(t_i)]}{\sum_{i=1}^{N} P_L(t_i)} \quad (3.53)$$

The period of consideration is one year in time steps of an hour, hence $N = 8760$

In the equation above $P_L(t_i)$, represents the load at a given time step on hour i .

$P_G(t_i)$, in the same equation represents the energy generation from the hybrid power system. In actual implementation, $P_L(t_i)$ is generated from daily load curves for weekdays and weekends and

factors in monthly anticipated load growth as deduced from the 10 year power sector expansion plan for Kenya covering the years 2014 – 2024 [79]. This is covered under the load model above.

$$P_G(t_i) = \begin{cases} P_{WTG}(t_i) + P_{PVG}(t_i) + P_{BESS}(t_i) & \dots case\ 1 \\ P_{WTG}(t_i) + P_{PVG}(t_i) & \dots case\ 2 \\ P_{WTG}(t_i) + P_{PVG}(t_i) - P_{BESS}(t_i) & \dots case\ 3 \end{cases} \quad (3.54)$$

Case1, applies when the total power generation from both the wind turbines and solar PV cells is less than the load is. The shortfall in power is then met by the stored energy in the batteries.

Case 2, applies when the total power generation from both the wind turbines and solar PV cells is equal to the demand, and

Case 3, applies when the total power generation from both the wind turbines and solar PV cells is greater than the demand, in this case, the surplus power is used to charge the batteries.

$P_{WTG}(t_i)$, is the power generated by the wind turbines in the time step i. This is expressed as in eq.(3.41) .$P_{PVG}(t_i)$, is the power generated by the solar photovoltaic generator in the time step i. This is expressed as in eq.(3.21) .$P_{BESS}(t_i)$, is the power flow equation from or to the battery energy storage system in the time step i. This is expressed as in equation (3.54)

Eq. (3.54) can be further simplified using the Heaviside step function as;

$$P_G(t_i) = P_{WTG}(t_i) + P_{PVG}(t_i) + 2.P_{BESS}(t_i).(H(P_L - P_{WTG} - P_{PVG}) - \frac{1}{2}) \quad (3.55)$$

From the definition of LPSP, it is clear that an LPSP of 1 indicates that the load is never met whereas that of 0 indicates the load is fully met. The reliability objective is passed as an inequality constraint in the minimization of the cost objective. An LPSP of 5 % corresponding to approximately 500hrs in a year of unmet demand is chosen as the low threshold for any solution to be valid.

3.10.2 The Cost Objective

The Levelized Cost of Energy (LCOE) introduced in chapter 1 is used here. The LCOE is a convenient metric for measuring the overall cost competitiveness of a generating technology. It represents the overall project cost both in terms of overnight capex, operation and maintenance cost and discounted negative cash flows, inter alia over the project life divided by the total energy

generated by the project over its entire life and is presented as dollars per kWh. In deriving the LCOE the following consideration are made:

Costs; The initial invested capital, operating and maintenance costs (fixed and variable), Financing costs, insurance costs, Taxes, Lifecycle or Major replacement costs, decommissioning costs. Etc.

Rebates and Incentives; Tax credits, Accelerated depreciation (MACRS), Incentives .etc.

Energy; Annual energy production, annual degradation, system availability.

The LCOE is then expressed as;

$$LCOE = \frac{\sum Life\ Cycle\ Costs(USD) - \sum Life\ Cycle\ Rebates\ (USD)}{\sum Life\ Cycle\ Energy} \quad (3.56)$$

Moreover, the LCOE can be expressed either as nominal LCOE or as real LCOE where the real LCOE has been inflation adjusted to cater for the macroeconomic factors. In this evaluation the LCOE has not been inflation adjusted as its principle purpose is to be a fitness function for comparing multiple options in a similar setting which implies the macroeconomic environment remains the same hence no need for the adjustment. Furthermore, for efficiency in execution of the algorithm a simplified version of the LCOE is used as an objective function. The simplified LCOE does not factor in financing costs, insurance costs, future replacements and degradation as it is thought that these differences among the options will be marginal yet the savings in terms of computational resources will be substantial. The LCOE used is thus expressed as:

$$LCOE = \left[\frac{CC \times CRF + FOM}{8760 \times CF}\right] + FC + VOM \quad (3.57)$$

Where CC refers to capital costs in USD/ kW and is deduced as shown in below.

$$CC = \frac{N_{PV}}{N_{TIC}} CC_{PV} + \frac{N_{WT}}{N_{TIC}} CC_{WT} + \frac{N_{BESS}}{N_{TIC}} CC_{BESS} \quad (3.58)$$

From which;

N_{TIC} , is the total installed capacity in kW,

N_{PV} , is the PV installed capacity in kW,

N_{WT} , is the installed capacity of wind turbines in kW,

N_{BESS} , is the power rating of the installed battery energy storage units,

And CRF is the capital recovery factor. The capital recovery factor is the ratio of a constant annuity to the present value of receiving that annuity for a given length of time. In this evaluation CRF has been based on a nominal discount rate as opposed to a real discount rate as the researcher has settled for evaluation of a nominal LCOE. CRF , is calculated as shown in the equation below;

$$CRF = \frac{i(1+i)^n}{(1+i)^n - 1} \quad (3.59)$$

Where the nominal annual discount rate is i and n is the project life in years.

The other key cost consideration is the operations and maintenance costs (O&M). O&M is divided into Fixed and Variable components. The Fixed Operations and Maintenance costs, FOM in equation (3.57) refers to those O&M costs that relate to the installed capacity of the plant and has the units of USD/kW.

$$FOM = \frac{N_{PV}}{N_{TIC}} FOM_{PV} + \frac{N_{WT}}{N_{TIC}} FOM_{WT} + \frac{N_{BESS}}{N_{TIC}} FOM_{BESS} \quad (3.60)$$

From which;

N_{PV} , $N_{WT}, N_{BESS}, and\ N_{TIC}$, retain their definitions from eq.(3.58) above.

The fixed O&M cost associated with PV technology are represented by FOM_{PV}.

The fixed O&M cost associated with wind turbines are represented by FOM_{WTG}.

The fixed O&M cost associated with battery energy storage technology are represented by FOM_{BESS}.

The other component of the Operations and maintenance costs, the Variable O&M or VOM as in eq. (3.57) is the O&M component relative to the amount of energy generated by the power plant. The Variable O&M costs are defined in a similar manner to eq.(3.60). Thus;

$$VOM = \frac{E_{PV}}{E_{TIC}} VOM_{PV} + \frac{E_{WT}}{E_{TIC}} VOM_{WT} \quad (3.61)$$

From which;

E_{TIC} , is the total energy **generated** in the plant life in kWh, thus

$$E_{TIC} = E_{PV} + E_{WT} \quad (3.62)$$

E_{PV} , is the PV generated energy in kWh,

E_{WT} , is the energy generated by the wind turbines in kWh,

The Operations and maintenance costs relating to the battery storage unit are all modelled as Fixed O&M. This approach allows for simplicity in evaluation of the objective function. It is also the researcher's postulation that the variable component in the O&M cost for the battery energy storage system is negligible compared to the fixed component.

The Fuel Cost is represented by FC. In this assessment since generation is based on wind and solar, for which the energy sources are wind and solar irradiation respectively and which are free and abundant in nature, the fuel cost component is thus zero and is eliminated from the implemented cost objective function.

CF in eq. (3.57) refers to the plant capacity factor, evaluated as

$$CF = \frac{Total\ Energy\ Generated\ annually\ by\ HRES(kWh)}{Total\ Installed\ Capacity\ of\ Power\ Units\ (kW)\ \times 8760} \quad (3.63)$$

$$CF = \frac{Energy_{PV} + Energy_{WT} + Energy_{BESS}}{(N_{TIC}) \times 8760} \quad (3.64)$$

The cost objective function to be minimized can thus be presented in full as:

$$minimize\ LCoE,$$

$$where\ LCOE = \frac{((N_{PV}CC_{PV} + N_{WT}CC_{WT} + N_{BESS}CC_{BESS}) \times \frac{i(1+i)^n}{(1+i)^n - 1}) + (N_{PV}FOM_{PV} + N_{WT}FOM_{WT} + N_{BESS}FOM_{BESS})}{Energy_{PV} + Energy_{WT} + Energy_{BESS}} + \frac{VOM_{PV}E_{PV} + VOM_{WT}E_{WT}}{Energy_{PV} + Energy_{WT}} \quad (3.65)$$

$$subject\ to\ Boundary\ Conditions\ defined\ in\ 3.10.3.$$

3.10.3 Boundary Conditions

These are imposed on the proposed optimal solutions to ensure adherence to physical feasible limits and safe operating conditions of the power plant. The following conditions below are considered;

That the reliability objective is met, an inequality constraint is defined as;

$$LPSP_i < 0.05 \quad (3.66)$$

A configuration i is only a viable candidate solution if its Loss of Power Supply Probability (LPSP) is less than 5%. This corresponds only 500 hours annually of unmet demand, much better than the existing distribution grids nationally.

Maximum installed capacity is benchmarked to the demand. A peak demand of 2 MW after factoring load growth over a 20 year period is considered. A suitable system configuration would then be sought to supply this peak demand at the least cost. Sizing constraints are also applied on the individual generation technologies.

(1) Option 1 – Land Size based Constraints

The number of wind turbine units is constrained by consideration of losses due to wake effect. Thus as developed by [34], for a region with area S_1 , length L , and width W , the maximum number of wind turbines that can be installed is then evaluated as

$$N_{WT} \leq \left[\frac{L}{L_M d} + 1\right] \times \left[\frac{W}{W_M d} + 1\right] \quad (3.67)$$

Where L_M , is a multiplier between 6 and 10 and W_M is a multiplier between 3 and 5.

N_{WT} , is evaluated to 14 units assuming a 10 acre piece of land.

The maximum number of PV panels will also be constrained by the size of the land acquired for the project. Thus assuming a land area S_A , and a PV panel size S_{PV};

$$N_{PV} \leq \frac{S_A(1 - \alpha_{BOP})}{S_{PV}} \quad (3.68)$$

The ratio of land size requirements of the balance of plant to the whole plant is represented by the factor α_{BOP}. This based on research documented in [80] has been evaluated at around 0.276.

This evaluates to 117,430 units based on a 10 acre parcel of land.

Minimum installed capacity is set as a lower bound of zero indicating that at least some capacity must be installed.

Battery charge/ discharge constraints are handled using the state of charge. There is a correlation between the state of charge and a battery's state of health. The higher the minimum state of charge, the more cycles a battery in proper operating conditions has. The charge / discharge constraints of the battery have been modelled into the performance objective function.

The number of battery units N_{BAT}, Number of installed panels N_{PV} and number of installed wind turbines N_{WT} are all bound as positive integers. This ensures only true hybrid systems with battery storage are considered.

(2) Option 2 – Algorithm Evaluated Constraints

A second set of constraints is also applied. These constraints are engineered to constrain the optimization algorithm to resolve to minimum in less time.

The Matlab code written to achieve this is in the appendix. The pseudocode is listed below;

1. Set BESS units to 0
2. Run optimal sizing algorithm with random but reasonable upper bounds for wind and solar (base case assumptions used)
3. Iterate through 8760 time steps to work out wind and solar potential
4. Calculate approximate lower bounds using;
   a. $Solar_{LB} = \frac{SP_{PVG}(1-LPSP)\times P_{LMAX}}{SP_{PVG}+SP_{WTG}}$
   b. $Wind_{LB} = \frac{SP_{WTG}(1-LPSP)\times P_{LMAX}}{SP_{PVG}+SP_{WTG}}$
   c. $BESS_{LB} = LPSP * P_{LMAX}$
5. Calculate approximate upper bounds using a scale factor of 10 as;

$$UB = LB * SF$$

The matrix of lower bounds as determined via this method are listed on Table 3-8.

Table 3-8: Boundary parameters

Case	DSM	Trackers	Lower Bounds			Upper Bounds		
			Solar	Wind	BESS	Solar	Wind	BESS
D	No	No	1,975	4	7,879	19,750	40	7,890
E	Yes	No	2,438	4	3,230	24,380	40	32,300
F	Yes	Yes	3,041	3	2,103	30,410	30	21,030

(3) Base Case

As the trivial solution would involve, scaling a generation and storage sources to match the load plus a margin, upper constraints are set on the installed capacities of the solar PV generation units, wind turbine generation units and battery storage system as below;

The maximum Number of wind turbines, is set to the 1.2 times the maximum demand divided by the rated capacity of a single unit. This evaluates to 10 units.

The maximum number of PV panels is set to 2 times the maximum demand divided by the rated capacity of a single unit. This evaluates to 16000 units.

The maximum number of battery units is calculated at 1 times the maximum demand divided the rated power delivery in a single hour of each unit. This evaluates to 23809 units. These parameters are listed on Table 3-9.

Table 3-9: Base case assumptions

Base Case Assumptions		
Solar	Wind	BESS
16,000	10	23,809

3.11 Flow Chart and Initial Algorithm Parameters

3.11.1 Process Flow Chart

The process flow chart for coarse grained parallel genetic algorithms is illustrated on Figure 3-21

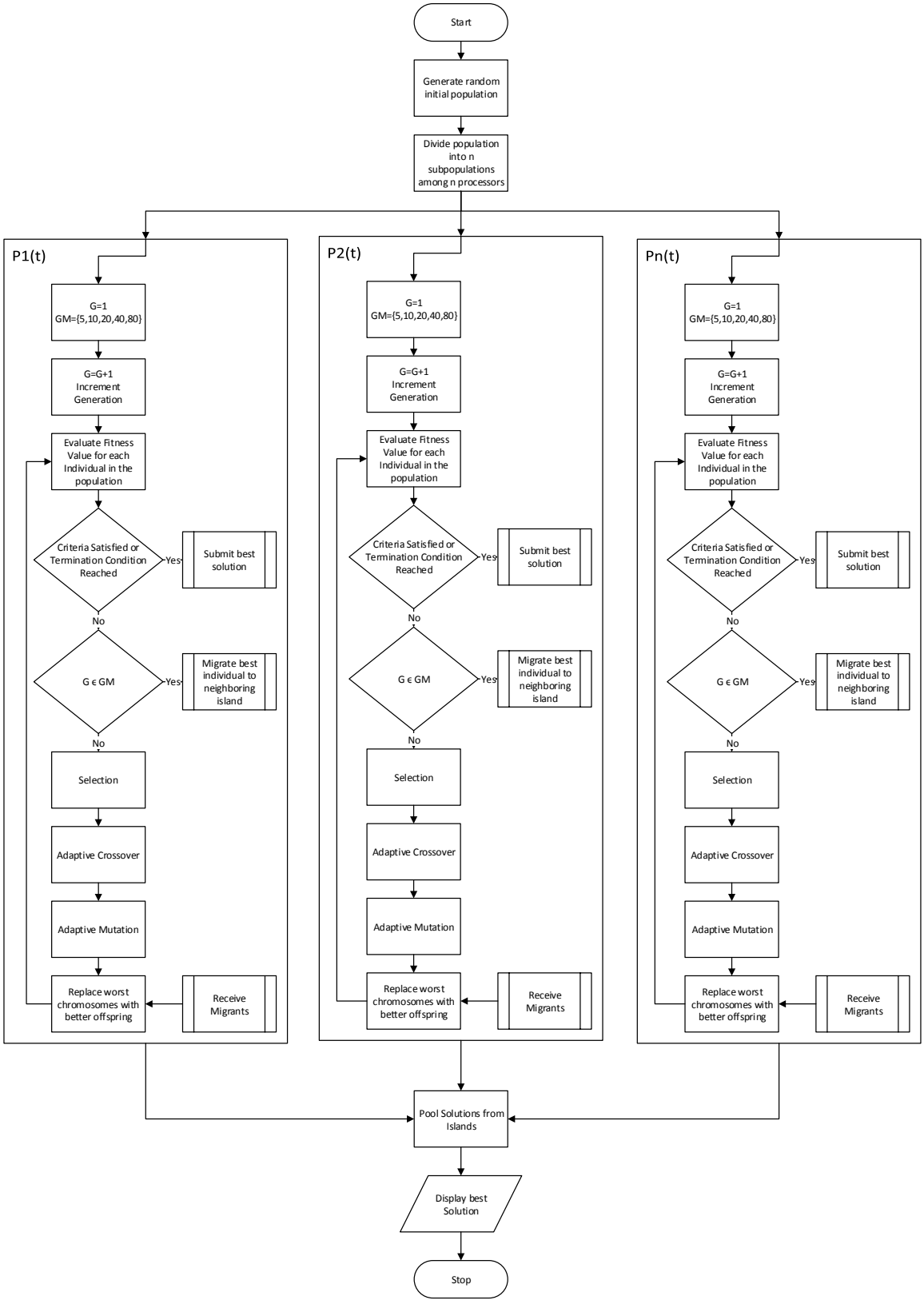

Figure 3-21: Flow chart CGPAGA

3.11.2 Population

Population is an important parameter in a genetic algorithm implementation. The population defines the quality of solution arrived at as well as how good the solution is. A population with a large diversity at the earlier generations of the genetic algorithm will ensure exploration of the search space. As the search progresses over several generations, the diversity should reduce to enable exploitation of a potential region of the search space near the optimal solution. An important characteristic of the population is its size; which directly affects the quality of the solutions obtained and how fast the algorithm converges towards an optimal solution, however a large population will overburden computational resources. A total population of 150 across 5 equal demes of 30 members each is applied. The initial population is created randomly but in a manner that ensures all bounds and constraints are satisfied.

3.11.3 Fitness Scaling and Selection

The selection function is used to select parents for the next generation based on their fitness. The fitness function values are scaled using a fitness scaling function to enable easy comparison hence selection. Various ways exist to perform fitness function scaling each with its advantages and disadvantages. In this work, rank selection is used on account of its simplicity. Rank selection sorts the raw fitness function scores and ranks the individuals based on their scores. A roulette wheel selection is then used to select the parents for the next generation. In roulette wheel selection, a roulette wheel is simulated with the area of each segment of the wheel proportional in expectation to that of the individual it represents, a random number then selects one of the segments in a manner which like natural selection gives a higher likelihood to the fittest individual being selected to pass its gene's to the next generation.

3.11.4 Reproduction, Elitism, Crossover and Mutation

The next generation of individuals is produced from the selected parents via the reproduction process. In this work, Elitism is used. This is a procedure where by a number of very fit individuals (elite) are guaranteed to survive into the next generation. To encourage exploration of the search space only the 3 (2% of the initial population) fittest individuals are allowed as elite.

Crossover then is the procedure by which genetic information from both parents are combined to form an offspring. The crossover fraction determines what percentage of the population in the next

generation are generated as result of crossover with the remainder being a result of mutation. Crossover enables exploitation of the search space and as in real life the crossover fraction is usually a large fraction much closer to 1, whereas the mutation fraction is it's complementary. In this work a crossover fraction of 0.98 has been chosen to promote refinement of good solutions and discovery of better ones. A heuristic approach is used for the crossover mechanism. This approach creates offspring that randomly lie on the line containing the two parents, closer to the parent with better fitness values hence generally ensuring an improved fitness over the present generation over the past.

The mutation function is used to ensure genetic diversity in the population and is very important in exploration of the search space. The method employed adds a random number taken from a Gaussian distribution centred on zero to an individual's genes. The Gaussian distribution is defined by a scale parameter which specifies the standard deviation away from the initial population and a shrink factor which controls how the deviations shrink with successive generations. This is an important parameter which ensures that the algorithm decreases explorative behaviours with successive generation and promoting more exploitative behaviours. A scale factor of 1 and a similar shrink factor have been selected.

3.11.5 Migration

As this implementation of the genetic algorithm is coarse grained (implies the population is composed of sub populations that "evolve" independent of each other, a novel real life concept of migration is introduced. The best individuals from one sub population moves (in actual sense is copied) to another and replaces the worst in the other subpopulation. This movement is set to happen both ways from subpopulation n to n+1 and to n-1. Migration promotes sharing of good solutions that have been discovered among the demes. The number of individuals participating in the migration should be limited to promote diversity of the overall population and to maintain the integrity of the individual demes evolution direction. A fraction of 0.1 (10% of the deme) is applied. The frequency of the migration is also an important parameter in ensuring the demes follow unique evolution patterns that can promote discovery of good solutions. Migration is therefore set in this study to occur after every 15 generations.

3.11.6 Stopping Criteria

The stopping criterion is the method used to determine when the algorithm needs to stop. A function tolerance method has been used to stop the algorithm when the weighted average change

in the fitness function value of a number of generation taken as 50 in this case is less than 10^{-6}. An upper limit of 500 has also been set on the generations and the algorithm will stop on exceedance.

3.12 Data Pre-processing

Data pre-processing was done using Microsoft Excel. The purpose of this step was to set up static data required by the software program developed to an acceptable form that would reduce need for further computation in the algorithm itself, so as to free the algorithm to only perform optimization hence be more efficient.

An input matrix was created, the matrix is preloaded with data records that correspond to the simulation time steps. The data records include incident wind speed, wind speed adjusted to hub height, GHI, proxy demand figures based on a typical daily demand curve for weekdays and weekends for Kenya and dry bulb temperature.

Chapter 4 Results and Discussion

The results of select simulation runs are documented in this chapter. Six configuration scenarios are simulated, starting with the base configuration as A. Scenario B, then is an improvement of A in which the effects of a proper demand side management are simulated, resulting in a demand profile that follows the generation profile. Scenario C improves scenario B by including single axis tracking on the PV generation side. For each scenario two cases 1 and 2 are run for each of the 2 strategis around boundary conditions as explained in 3.10.3.

4.1 Simulation Results

4.1.1 A: Base Configuration without DSM Simulation

The base configuration is run without any optimization conducted. The results are shown in Table 4-1. It is clear that the resulting system does not work as the the cost is very high and the reliability requirements are not met.

Table 4-1: Base Configuration without DSM

		Solar PV Panels	Wind Turbines	PV Batteries	LPSP requirements not met
a	Number	16000	10	23809	
	Rating	4,000 kW	2,500 kW	2,000 kWh	
	LPSP	0.2318			
	LCOE	Not Evaluated	US cents/ kWh		
	OCC	$ 79,811,947.31	$ 21,163.71	$ 5,101,928.57	**$ 84,935,039.59**

4.1.2 B: Base Configuration with DSM Simulation

The base case is improved by including a simulation of a successful demand side management scheme (DSM). The results are presented in Table 4-2.The DSM tries to approximate a load pattern that matches the generation pattern. No optimization is performed and the cost of the DSM is not factored in. The overall solution has a remarkably improved reliability but still fails to meet the acceptance criteria, optimization is thus still necessary.

Table 4-2: Base Configuration with DSM Simulation

		Solar PV Panels	Wind Turbines	PV Batteries	LPSP requirements not met
b	Number	16000	10	23809	
	Rating	4,000 kW	2,500 kW	2,000 kWh	
	LPSP	0.0838			
	LCOE	Not Evaluated	US cents/ kWh		
	OCC	$ 79,811,947.31	$ 21,163.71	$ 5,101,928.57	**$ 84,935,039.59**

4.1.3 C: Base Configuration with DSM Simulation and PV Tracking

Case B is further improved by utilizing single axis trackers to enhance PV generation. Single axis trackers have been shown to improve generation at a marginal incremental cost in both CAPEX and OPEX. The results of these are highlighted in table Table 4-3. With increased generation, the reliability criteria is now met, however the system cost is still prohibitive hence the case for optimization.

Table 4-3: Base configuration with DSM Simulation and PV Trackers

		Solar PV Panels	Wind Turbines	PV Batteries	
c	Number	16000	10	23809	
	Rating	4,000 kW	2,500 kW	2,000 kWh	
	LPSP	0.0484			
	LCOE	31.9	US cents/ kWh		
	OCC	$ 79,811,947.31	$ 21,163.71	$ 5,101,928.57	**$ 84,935,039.59**

4.1.4 D: Optimal Configuration without DSM Simulation

(1) Current Best Individual, algorithm constrained.

A series of simulations are carried on the configuration on scenario A and the best solution with an algorithm defined set of boundary conditions is tabulated on Table 4-4. The overall cost of the system attained is 39 million USD with a levelized costs of energy of 21.51 US cents per kWH.

Table 4-4: Optimal Configuration without DSM

		Solar PV Panels	Wind Turbines	PV Batteries	
d.1	Number	4459	33	78580	
	Rating	1,115 kW	8,250 kW	6,601 kWh	
	LPSP	0.0498			
	LCOE	21.51	US cents/ kWh		
	OCC	$ 22,242,592.06	$ 69,840.24	$ 16,838,571.43	**$ 39,151,003.73**

The interim results of the optimization process are also documented. Figure 4-1, shows the fitness value across generations, the pattern is indicative of a proper convergence towards a global minimum. This convergence can also be interpretd in the similarity of individual within the search space. Figure 4-2 shows this similarity in terms of the aveerage distance between solution over iterated generations.Figure 4-3, shows the fitness value of each individual at the final iteration, the similarity of heights of the bar charts further indicate a convergence of the solution towards a global minimum. This is also clear across the different demes which are represented with different colors. Figure 4-4 shows the fitness scaling and Figure 4-5 is a score histogram indicating the distribution in the range of scores. Figure 4-6 illustrates the satisfaction of the stopping criteria defined in 3.11.6.

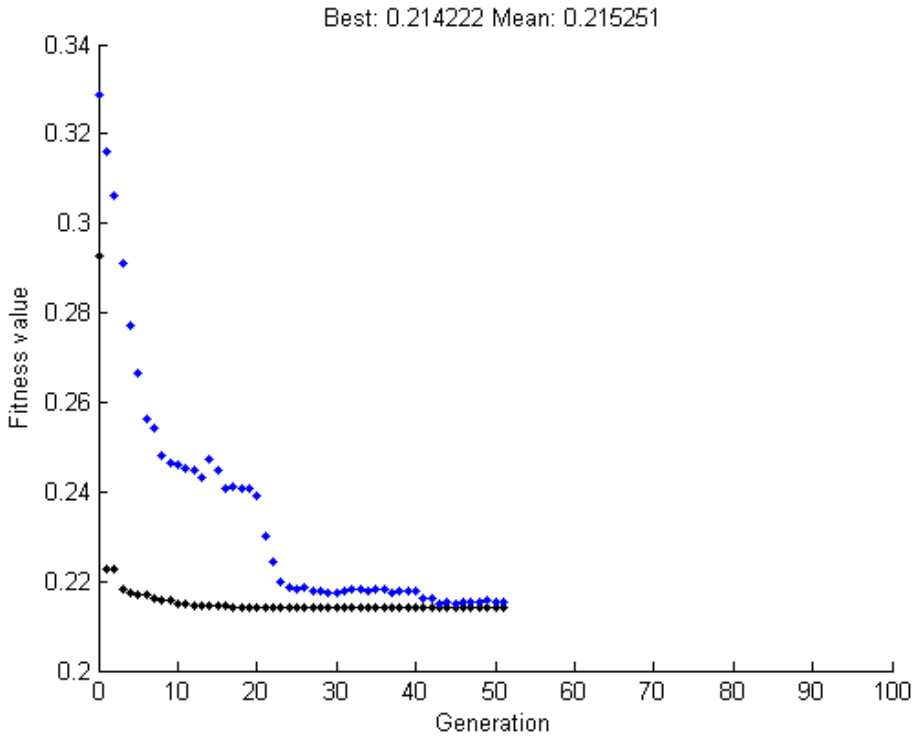

Figure 4-1: Fitness value vs generation

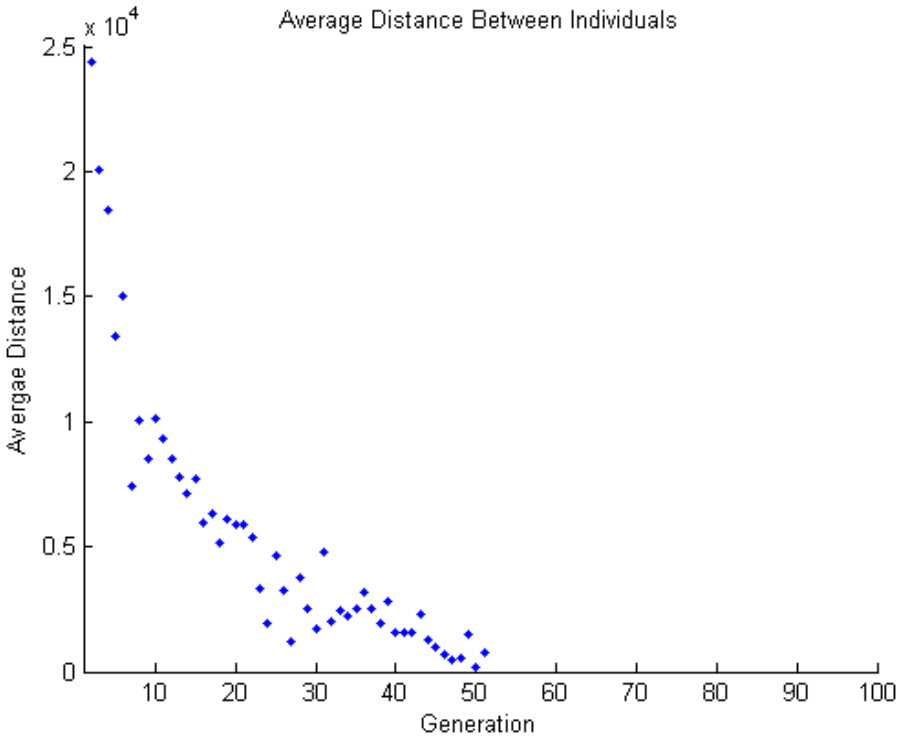

Figure 4-2: Average distance between individuals

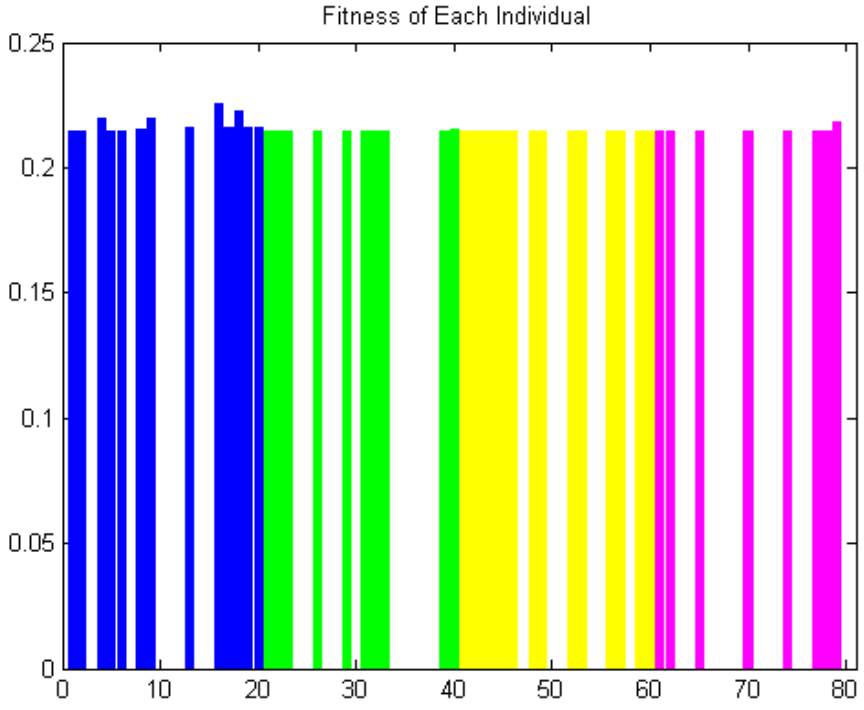

Figure 4-3: Fitness of Each individual at final iteration

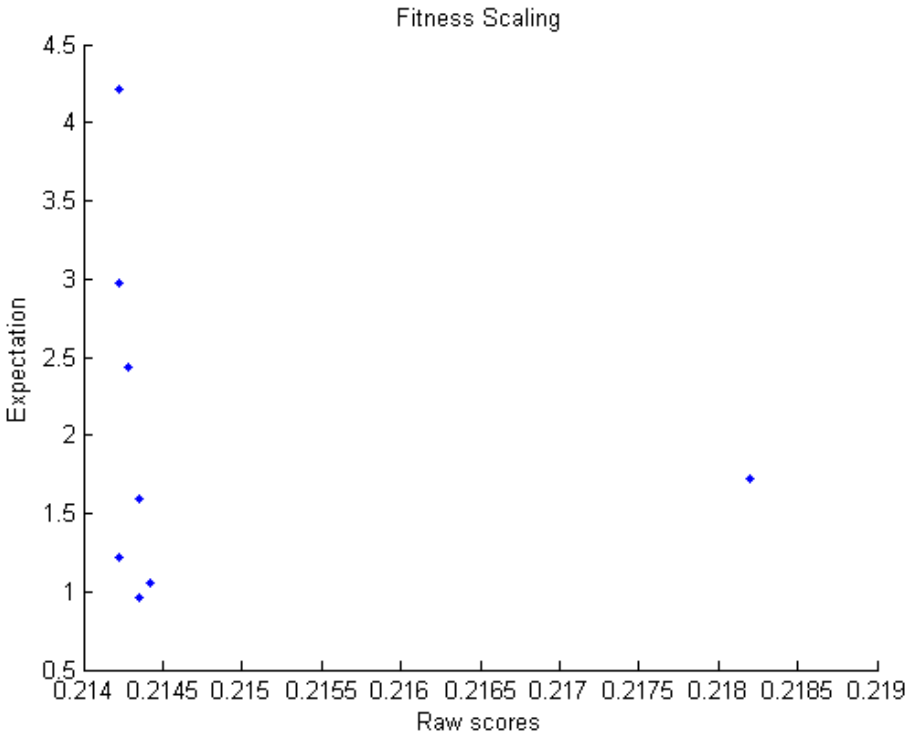

Figure 4-4: Fitness scaling

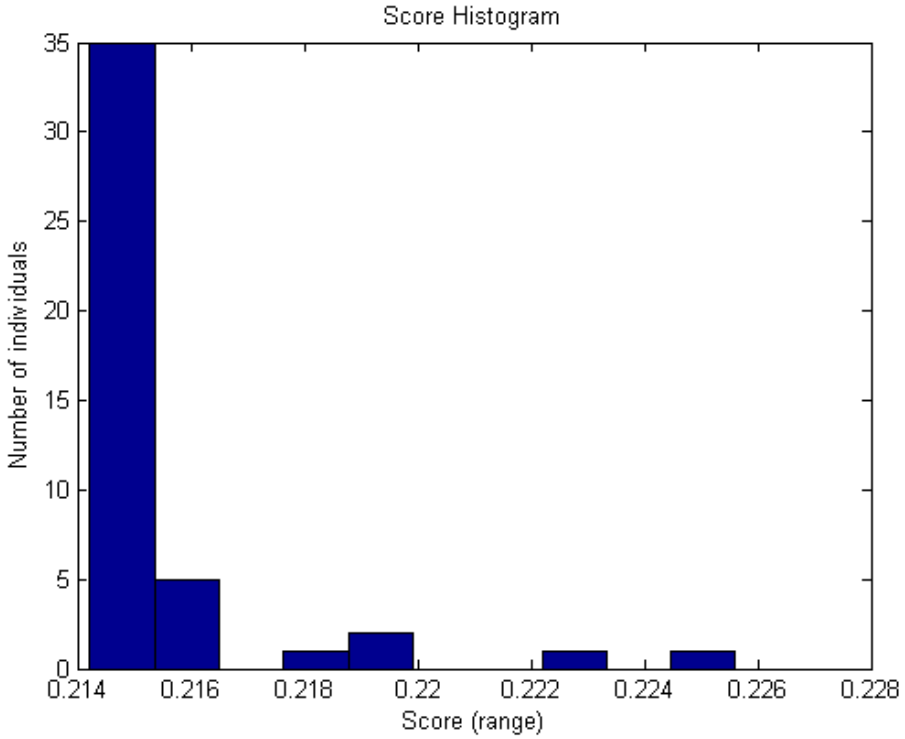

Figure 4-5: Score histogram

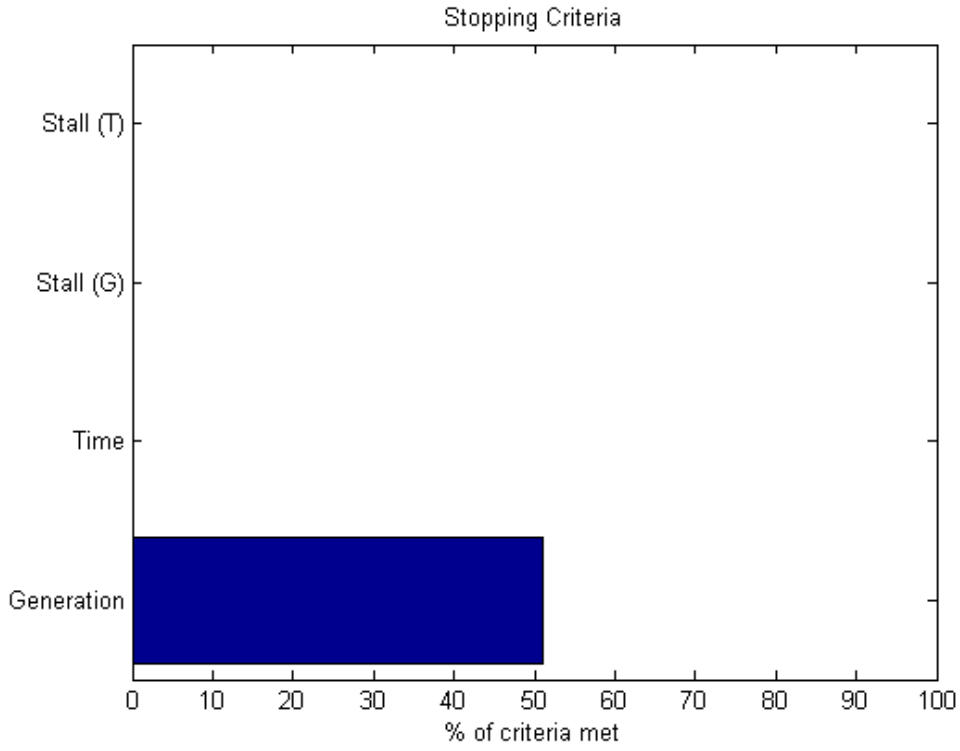

Figure 4-6: Stopping criteria

(2) Current Best Individual, land size constrained.

The procedure is repeated several times with a land size constrained boundary condition approach as explained in 3.10.3. The results of the best indidual in the search space are documented on Table 4-5. Figure 4-7, represents the fitness values across generations. Figure 4-8 shows the average distance between inviduals in the search space.Figure 4-9 shows the fitness of each individual across all subpopulations at the final iteration. Figure 4-10 shows the fitness scaling.Figure 4-11 shws the distribution of scores within the population in the form of a histogram. Figure 4-12 illustrates the satisfaction of the stopping criteria.

Table 4-5: Optimal Configuration, land size constrained

		Solar PV Panels	**Wind Turbines**	**PV Batteries**	**LPSP requirement downgrade from 5% to 10%**
d.2	Number	20311	14	66837	
	Rating	5,078 kW	3,500 kW	5,614 kWh	
	LPSP	0.0997			
	LCOE	30.03	US cents/ kWh		
	OCC	$ 101,316,278.86	$ 29,629.19	$ 14,322,214.29	**$ 115,668,122.34**

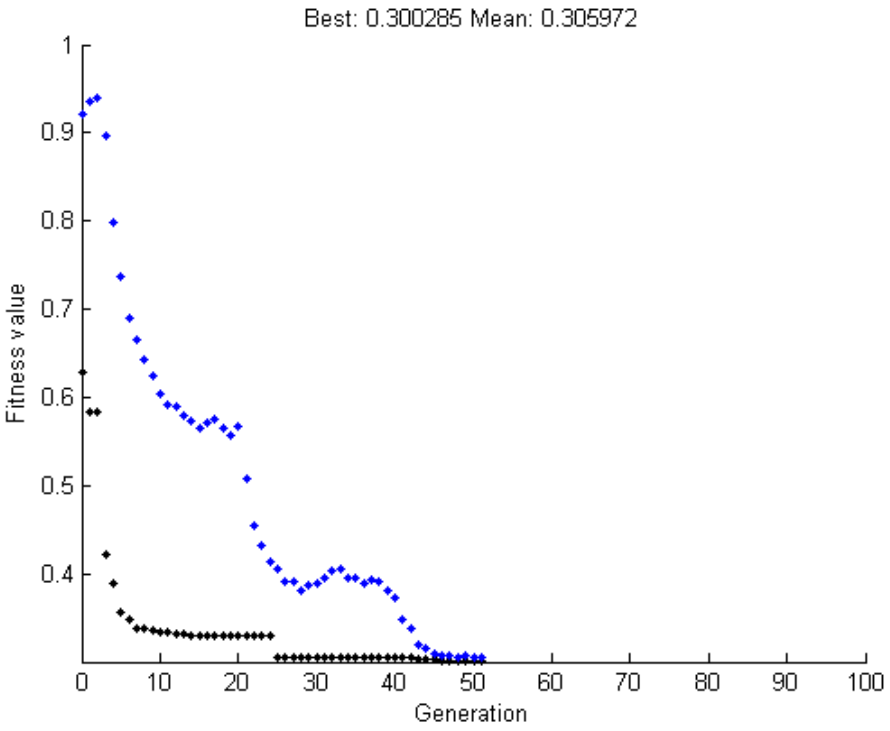

Figure 4-7: Fitness value vs generation

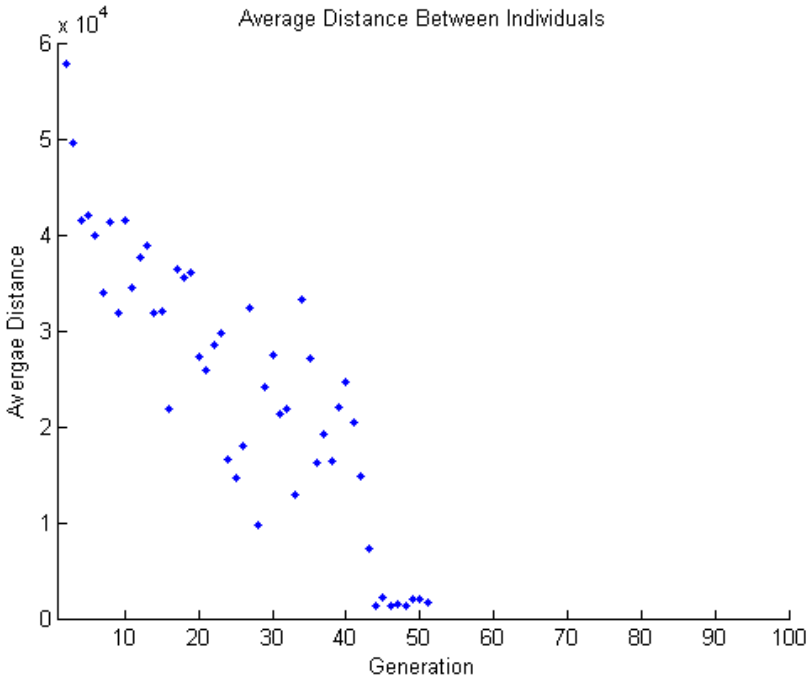

Figure 4-8: Average distance between individuals

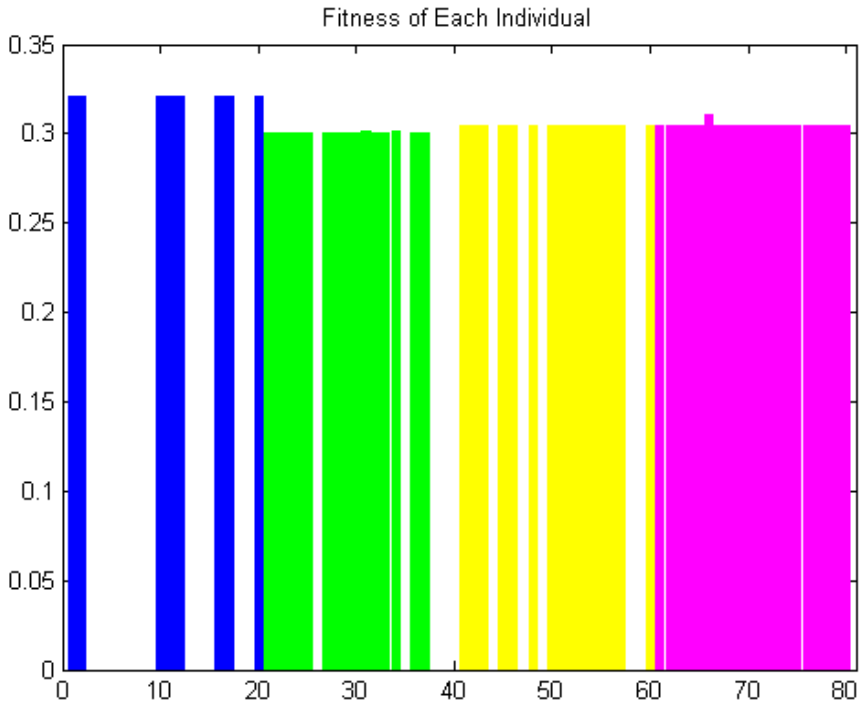

Figure 4-9: Fitness of each individual

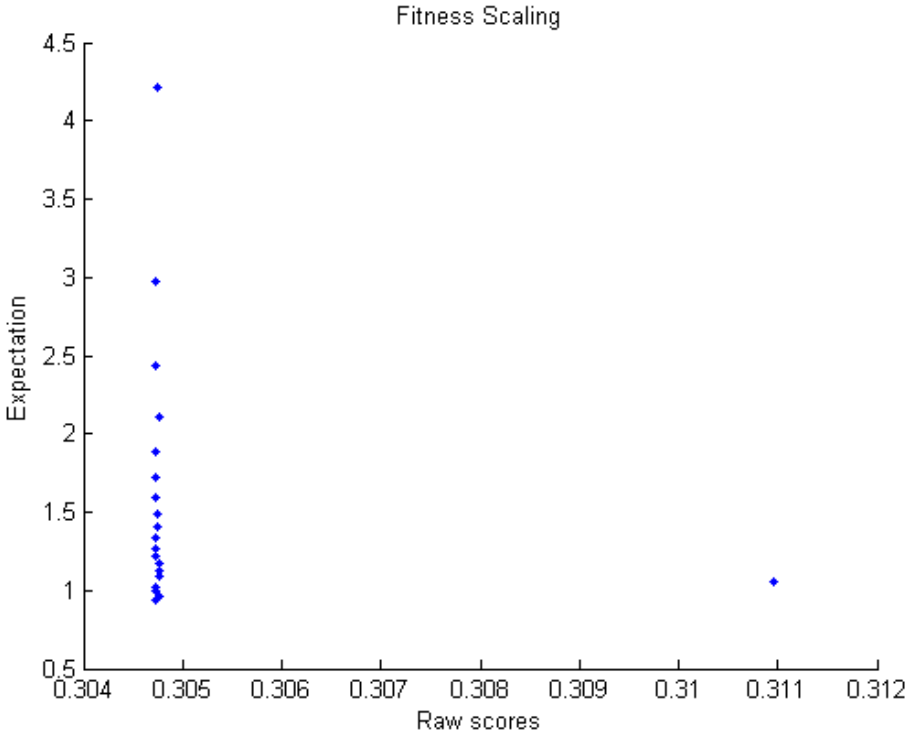

Figure 4-10: Fitness scaling

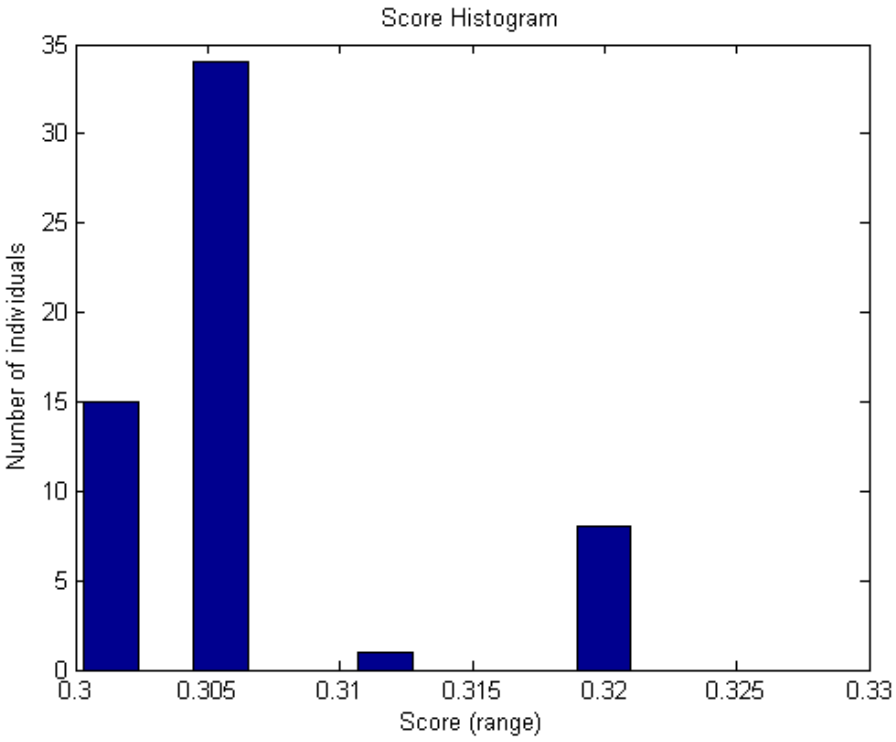

Figure 4-11: Score histogram

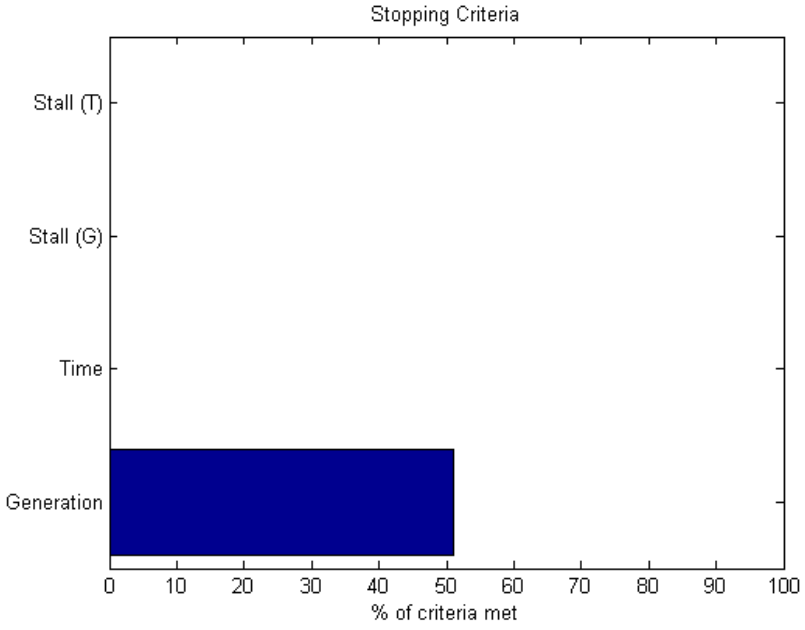

Figure 4-12: Stopping criteria

4.1.5 E: Optimal Configuration with DSM Simulation

The procedure in 4.1.4 is repeated several times on scenario B, where load is assumed to have a demand side management scheme effected and the results therefrom are simulated.

(1) Current Best Individual, algorithm constrained.

Several simulations are conducted with an algorithm defined boundary conditions as described in 3.10.3 and the best result from the search space selected. These results are displayed on Table 4-6. Figure 4-13,Figure 4-14,Figure 4-15,Figure 4-16 and Figure 4-17, have the same interpration as Figure 4-1, Figure 4-2, Figure 4-3, Figure 4-4, Figure 4-5 and Figure 4-6 respectively from the earlier results of the simulations under the procedure in 4.1.4.

Table 4-6: Optimal configuration with DSM simulation

		Solar PV Panels	Wind Turbines	PV Batteries	
e1	Number	6830	25	32243	
	Rating	1,708 kW	6,250 kW	2,708 kWh	
	LPSP	0.0491			
	LCOE	28.26	US cents/ kWh		
	OCC	$ 34,069,725.01	$ 52,909.27	$ 6,909,214.29	**$ 41,031,848.56**

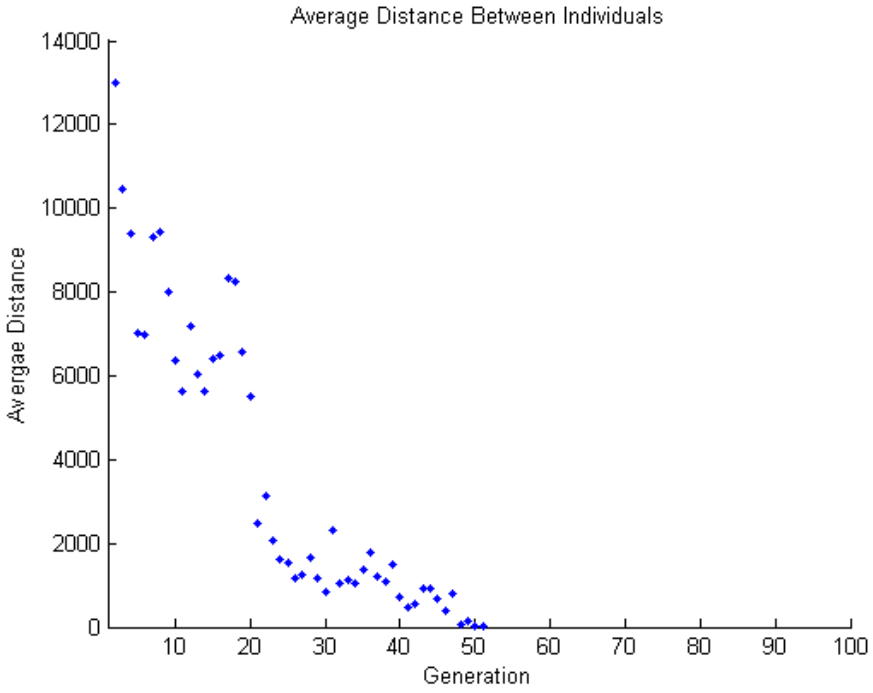

Figure 4-13: Average distance between individuals

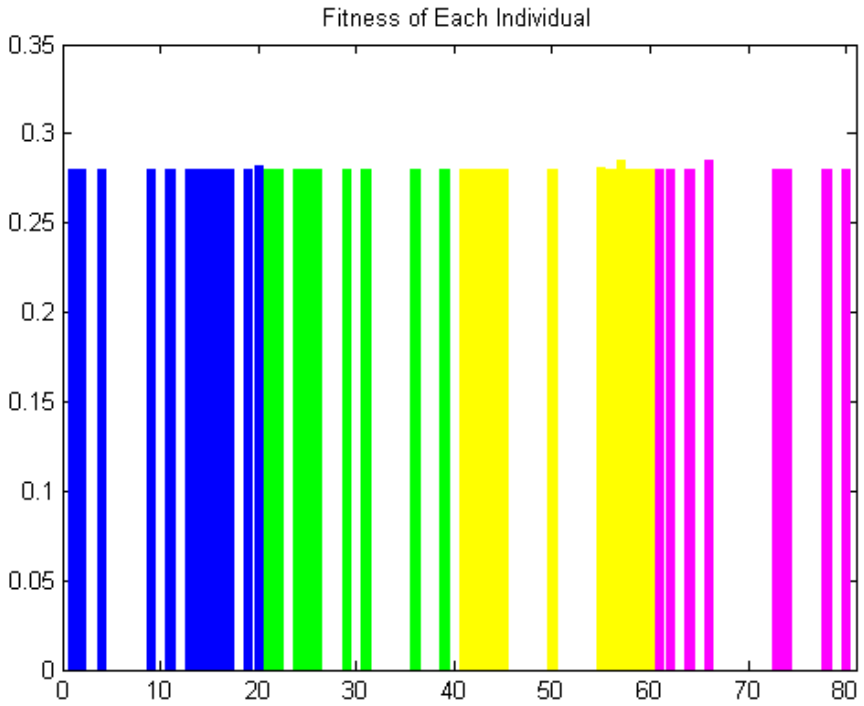

Figure 4-14: Fitness of each individual

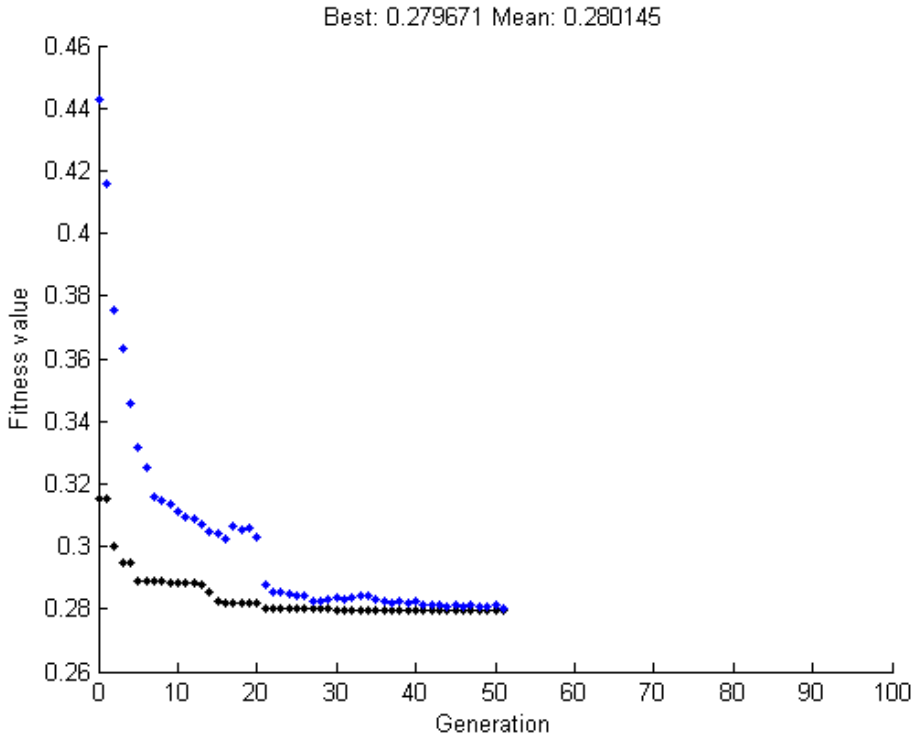

Figure 4-15: Fitness value vs generation

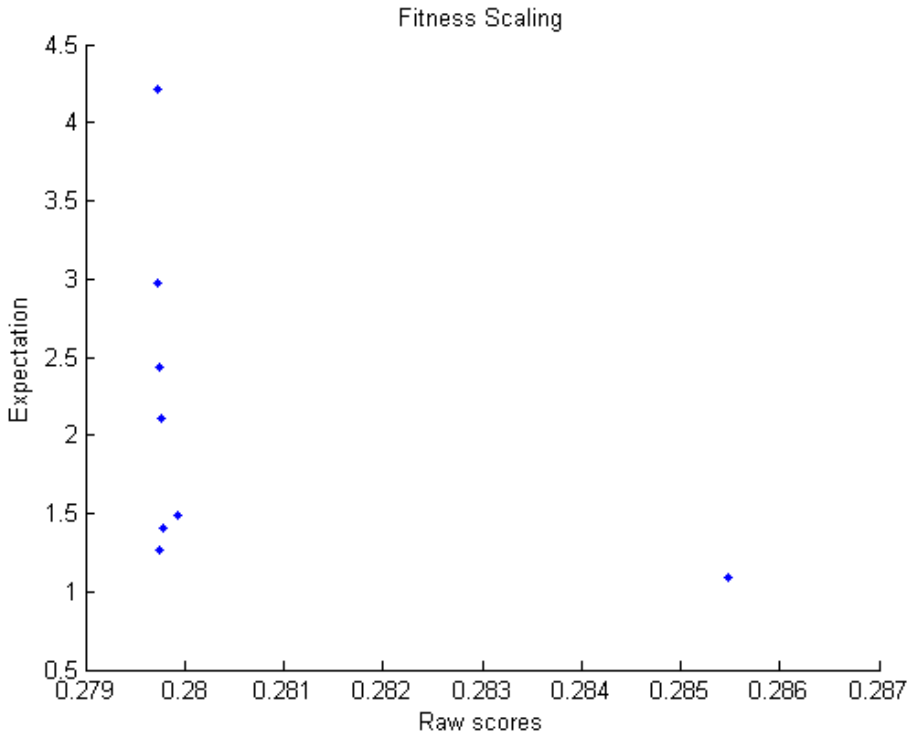

Figure 4-16: Fitness scaling

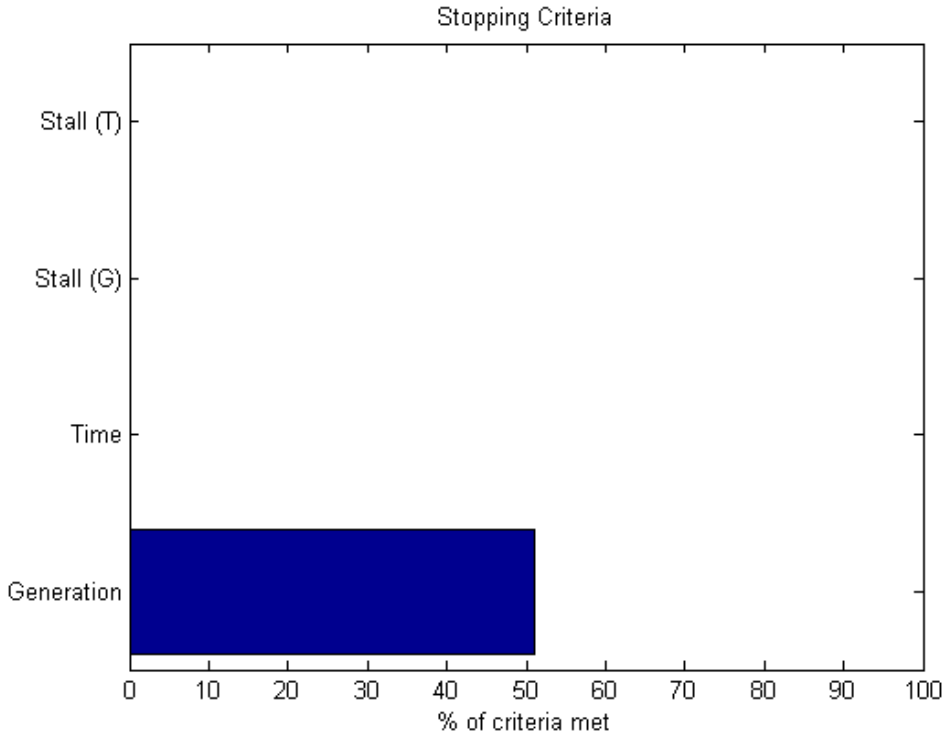

Figure 4-17: Stopping criteria

(2) Current Best Individual, land size constrained.

Several simulations are conducted with boundary conditions dependent on the land size as described in 3.10.3 and the best result from the search space selected. These results are displayed on Table 4-7.Figure 4-18, Figure 4-19, Figure 4-20, Figure 4-21, Figure 4-22 and Figure 4-23, have the same interpration as Figure 4-1, Figure 4-2, Figure 4-3, Figure 4-4, Figure 4-5 and Figure 4-6 respectively from the earlier results of the simulations under the procedure in 4.1.4.

Table 4-7: Land size constrained optimal configuration with DSM

		Solar PV Panels	**Wind Turbines**	**PV Batteries**	**LPSP requirement downgrade from 5% to 10%**
e.2	Number	1976	13	117610	
	Rating	494 kW	3,250 kW	9,879 kWh	
	LPSP	0.0882			
	LCOE	17.76	US cents/ kWh		
	OCC	$ 9,856,775.49	$ 27,512.82	$ 25,202,142.86	**$ 35,086,431.17**

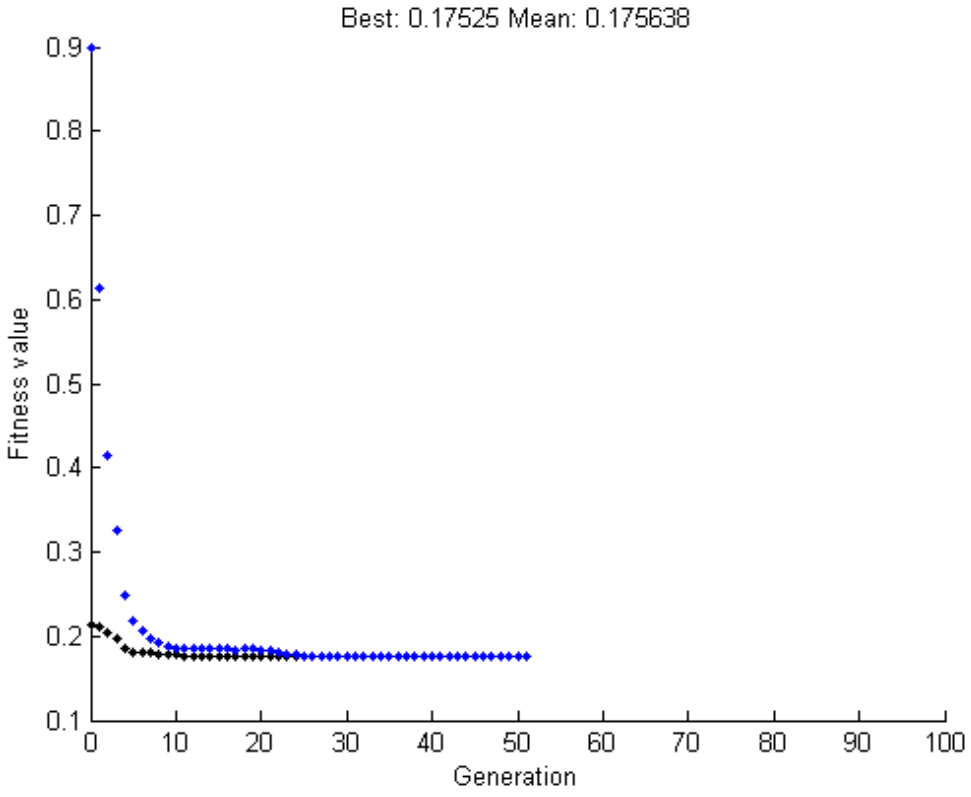

Figure 4-18: Fitness value vs generation

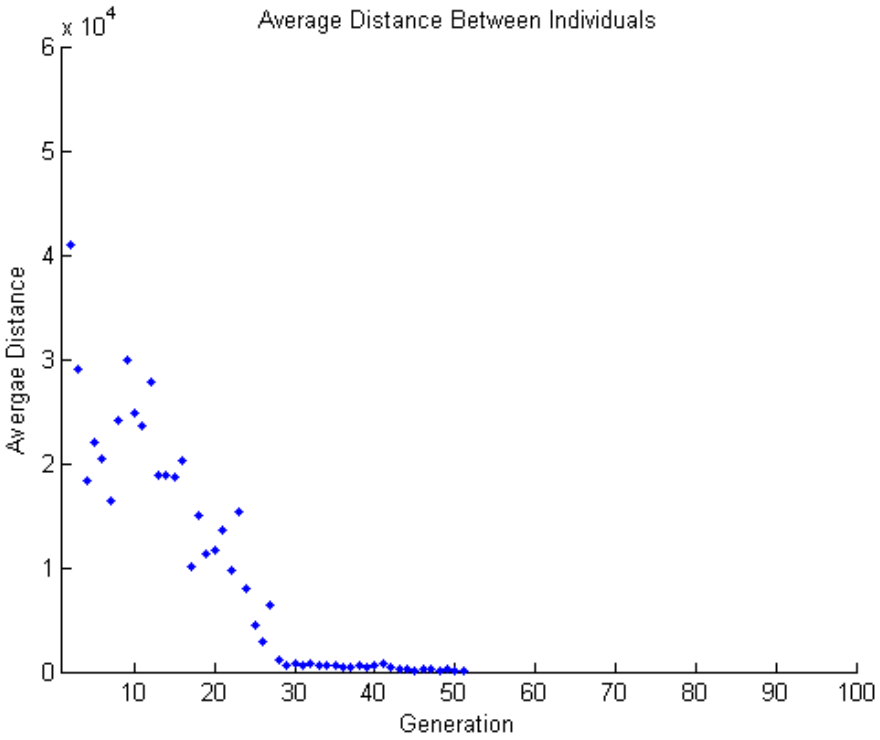

Figure 4-19: Average distance between individuals

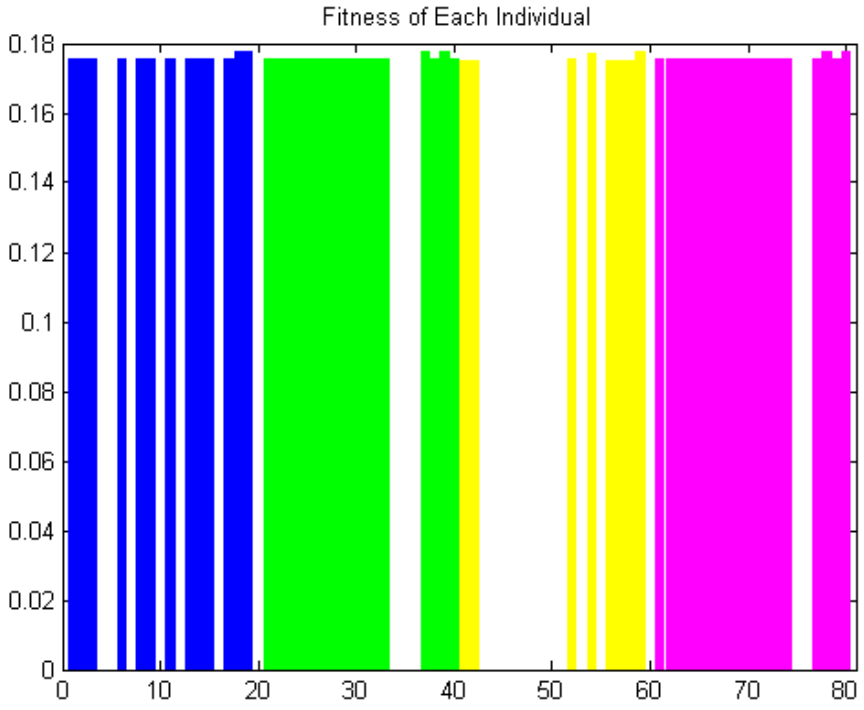

Figure 4-20: Fitness of each individual

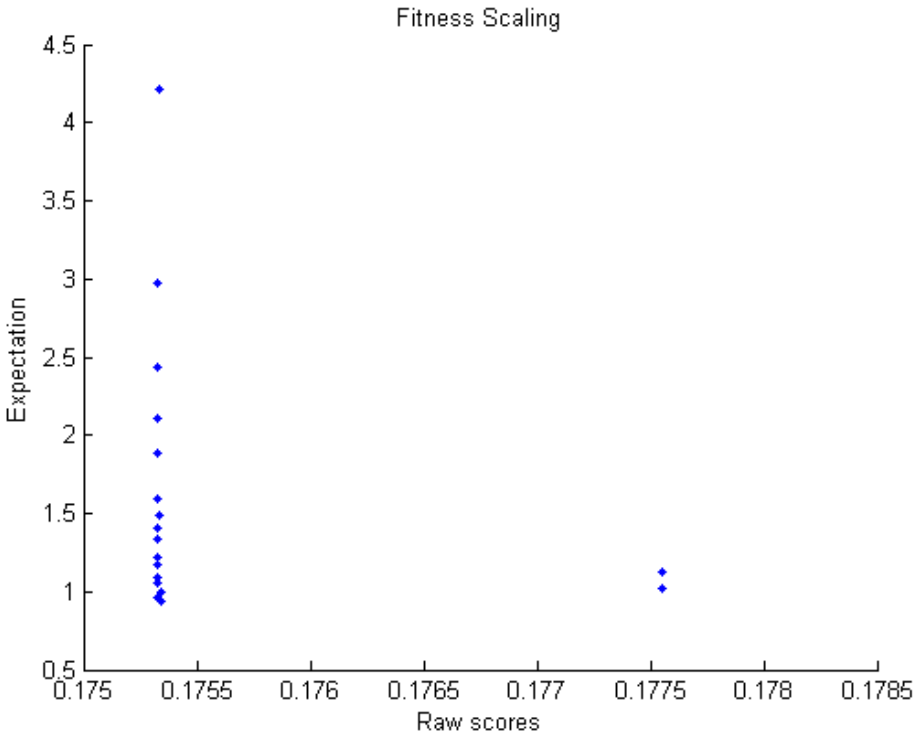

Figure 4-21: Fitness scaling

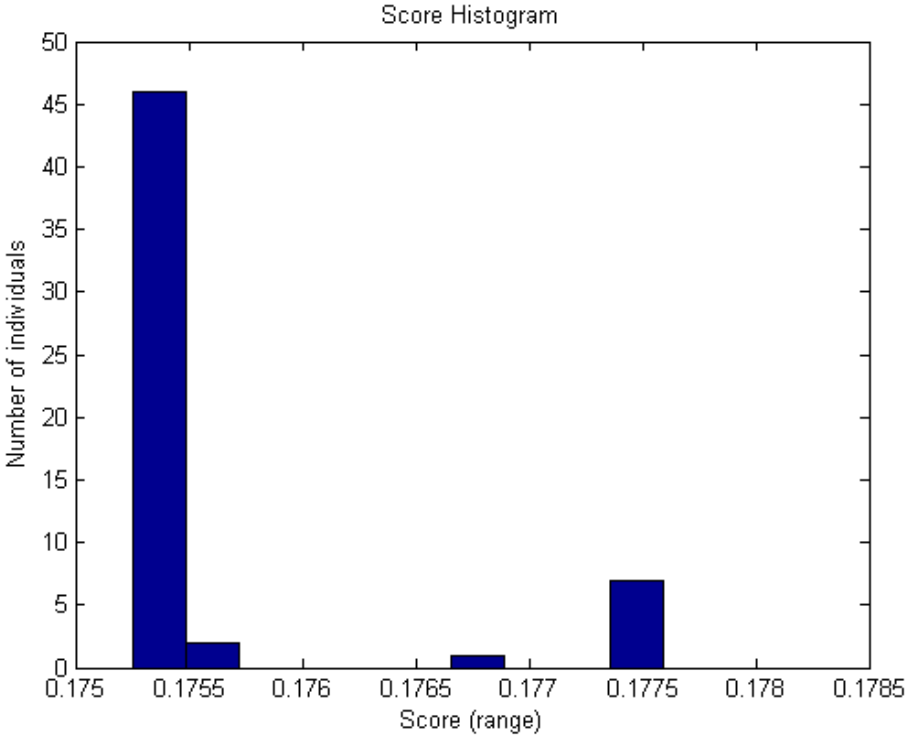

Figure 4-22: Score histogram

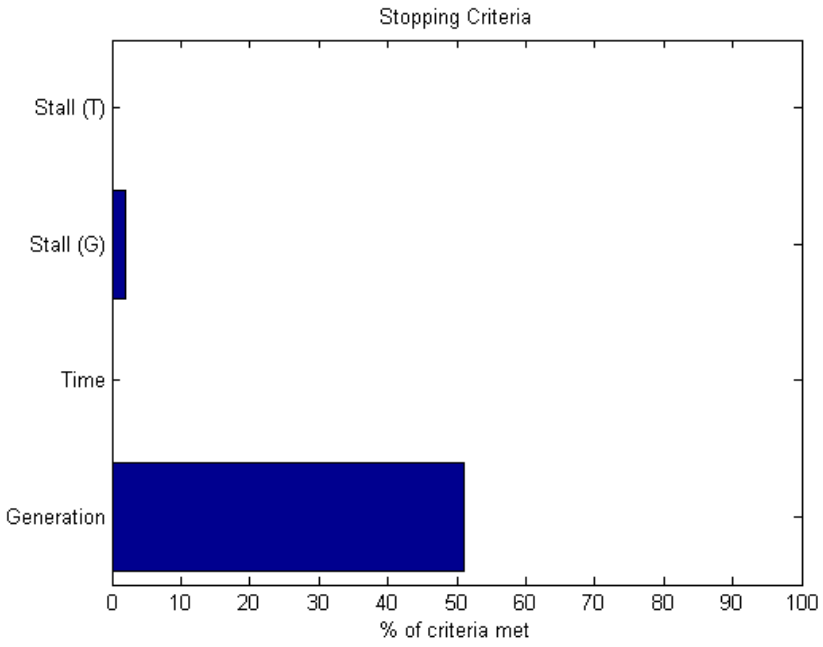

Figure 4-23: Stopping criteria

4.1.6 F: Optimal Configuration with DSM Simulation and PV Tracking

The procedure in 4.1.4 is repeated several times on scenario C, where in addition to simulating the effects of a successful demand side management scheme, single axis trackers are also implemented on the PV generators.

(1) Current Best Individual, algorithm constrained.

Several simulations are conducted with an algorithm defined boundary conditions as described in 3.10.3 and the best result from the search space selected. These results are displayed on Table 4-8Table 4-6. Figure 4-24, Figure 4-25, Figure 4-26, Figure 4-27, Figure 4-28 and Figure 4-29 have the same interpration as Figure 4-1, Figure 4-2, Figure 4-3, Figure 4-4, Figure 4-5 and Figure 4-6 respectively from the earlier results of the simulations under the procedure in 4.1.4.

Table 4-8: Optimal configuration with DSM Simulation and PV Tracking

		Solar PV Panels	**Wind Turbines**	**PV Batteries**	
f.1	Number	11047	15	20984	
	Rating	2,762 kW	3,750 kW	1,763 kWh	
	LPSP	0.0494			
	LCOE	28.02	US cents/ kWh		
	OCC	$ 55,105,161.37	$ 31,745.56	$ 4,496,571.43	**$ 59,633,478.36**

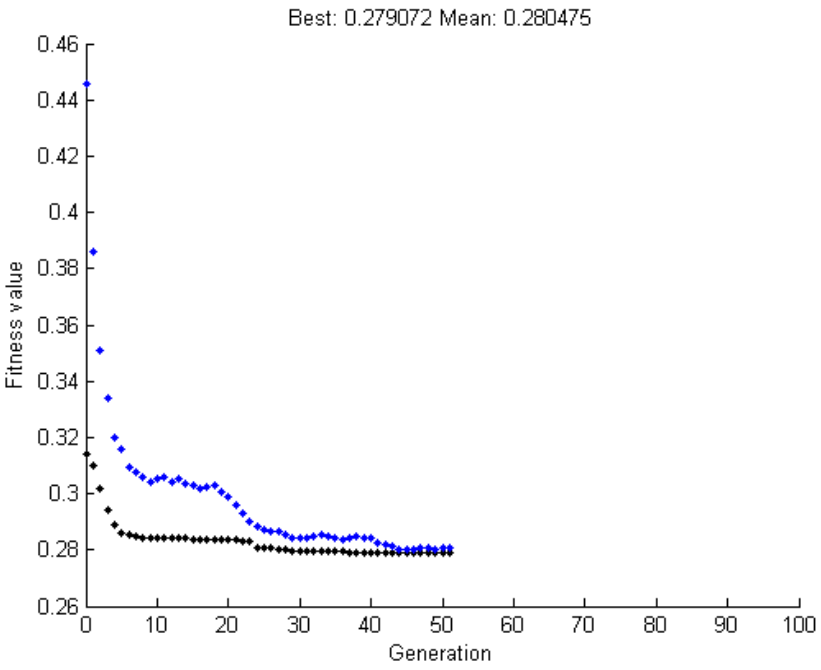

Figure 4-24: Fitness value vs generation

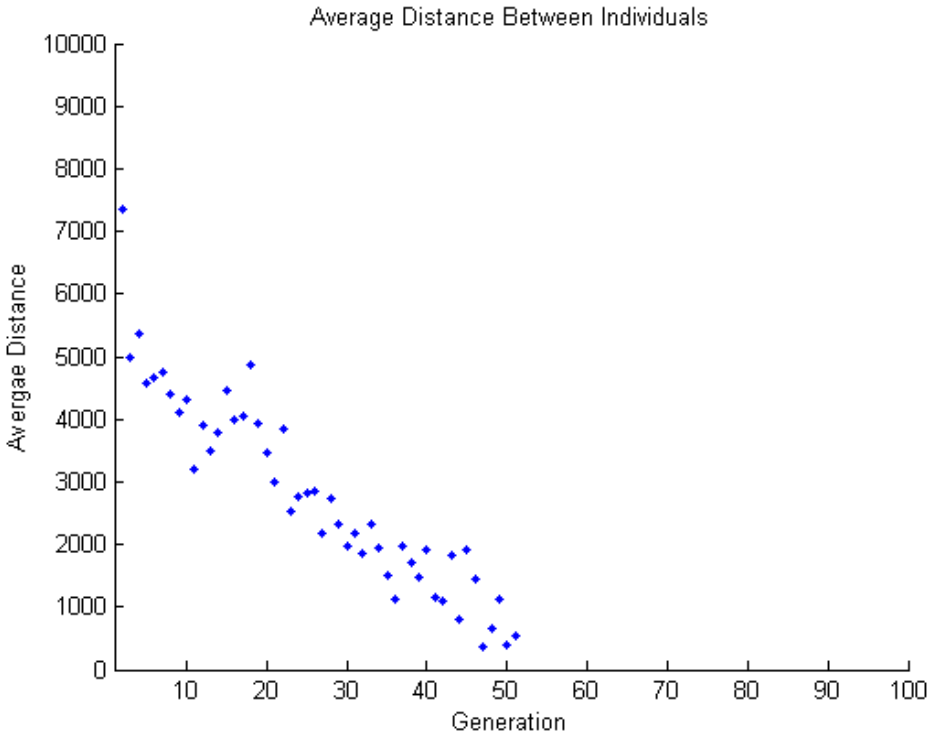

Figure 4-25: Average distance between individuals

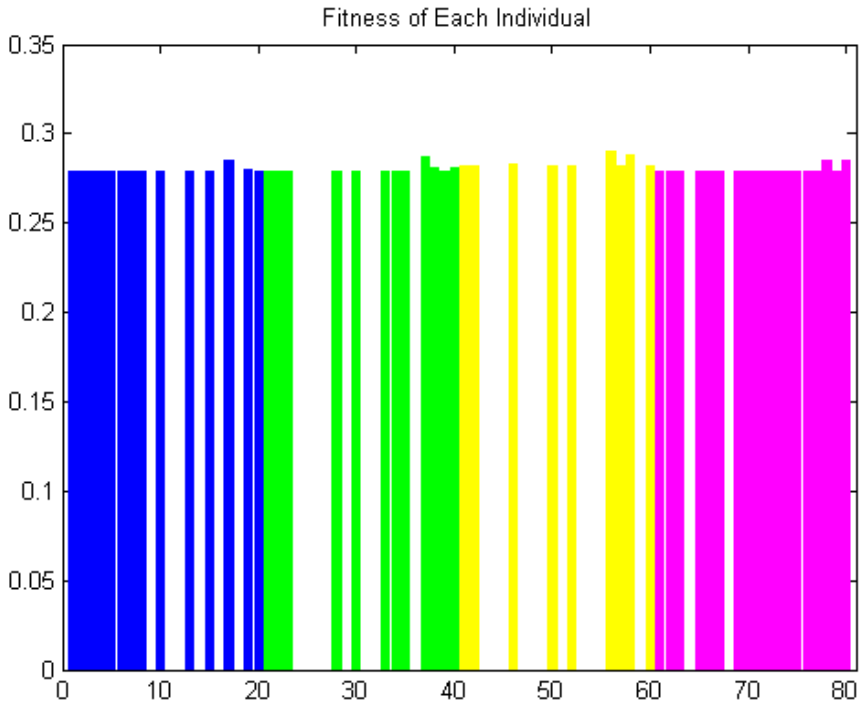

Figure 4-26: Fitness of each individual

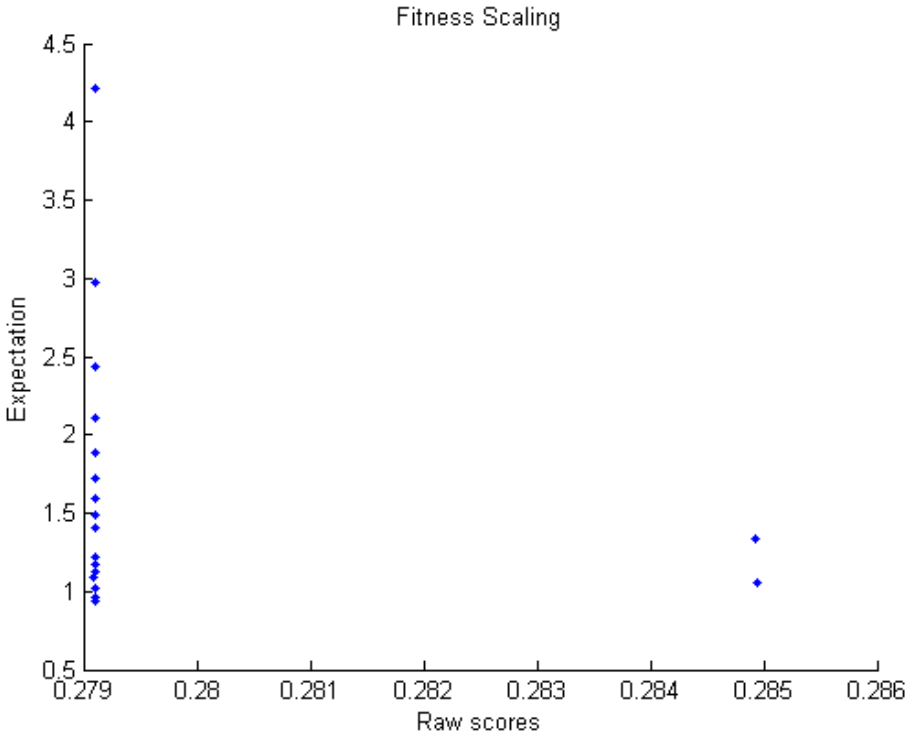

Figure 4-27: Fitness scaling

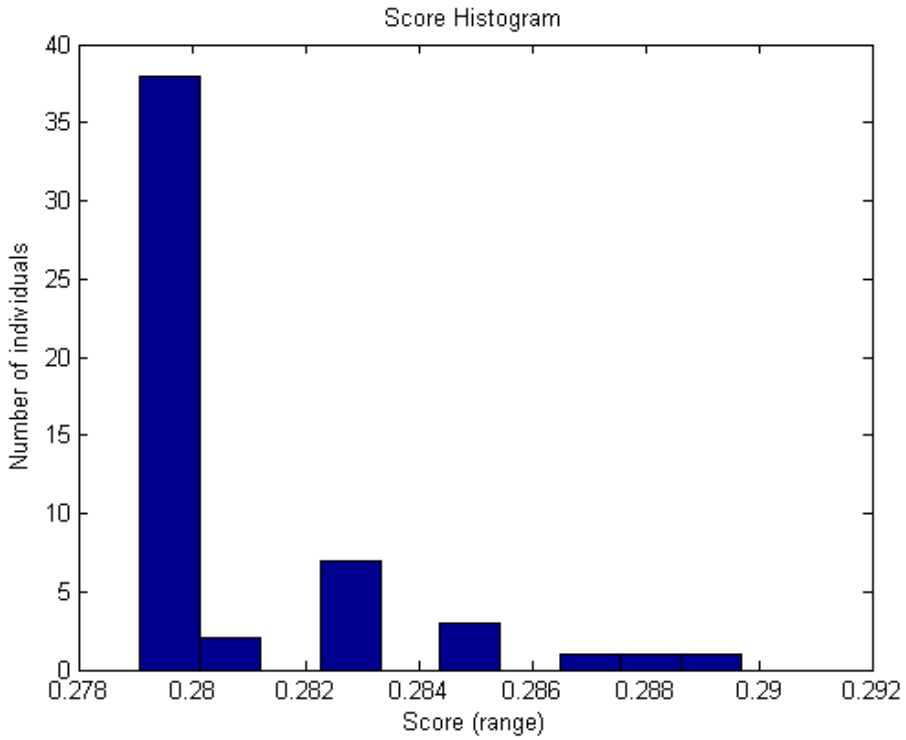

Figure 4-28: Score histogram

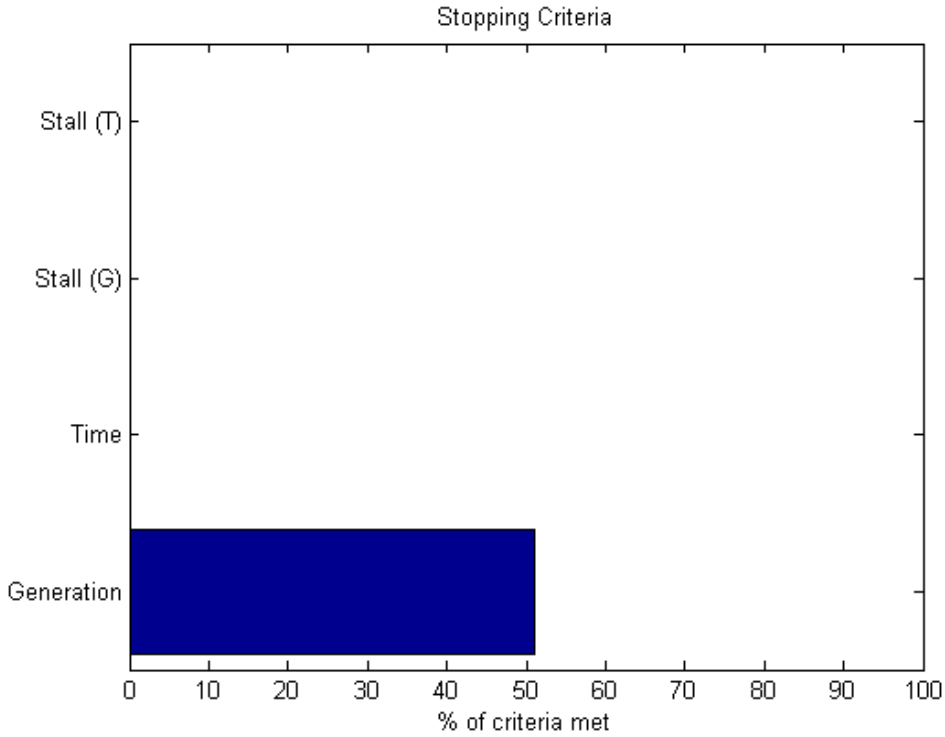

Figure 4-29: Stopping criteria

(2) Current Best Individual, land size constrained.

Several simulations are conducted with boundary conditions dependent on the land size as described in 3.10.3 and the best result from the search space selected. These results are displayed on Table 4-9.Figure 4-31, Figure 4-32, Figure 4-33, Figure 4-34 and Figure 4-35 , have the same interpration as Figure 4-1, Figure 4-2, Figure 4-3, Figure 4-4, Figure 4-5 and Figure 4-6 respectively from the earlier results of the simulations under the procedure in 4.1.4.

Table 4-9: Land constrained optimal configuration with DSM and PV trackers simulated

		Solar PV Panels	**Wind Turbines**	**PV Batteries**	**LPSP requirement downgrade from 5% to 10%**
f.2	Number	1976	13	94856	
	Rating	494 kW	3,250 kW	7,968 kWh	
	LPSP	0.0937			
	LCOE	17.62	US cents/ kWh		
	OCC	$ 9,856,775.49	$ 27,512.82	$ 20,326,285.71	**$ 30,210,574.03**

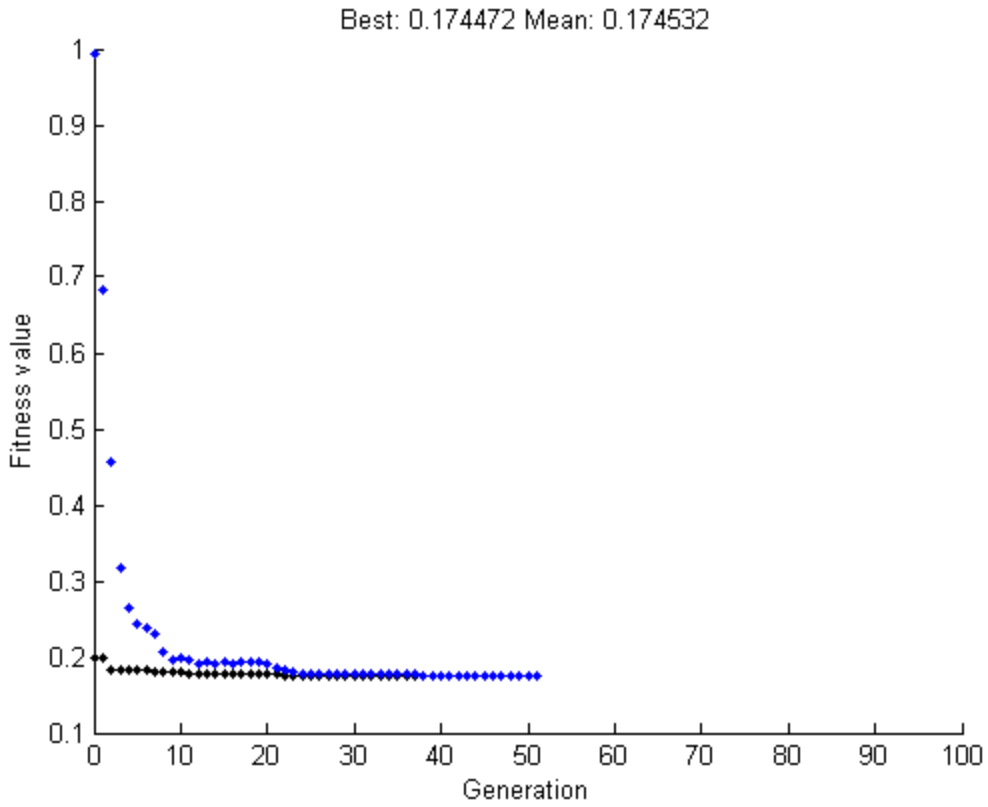

Figure 4-30: Fitness value vs. generation

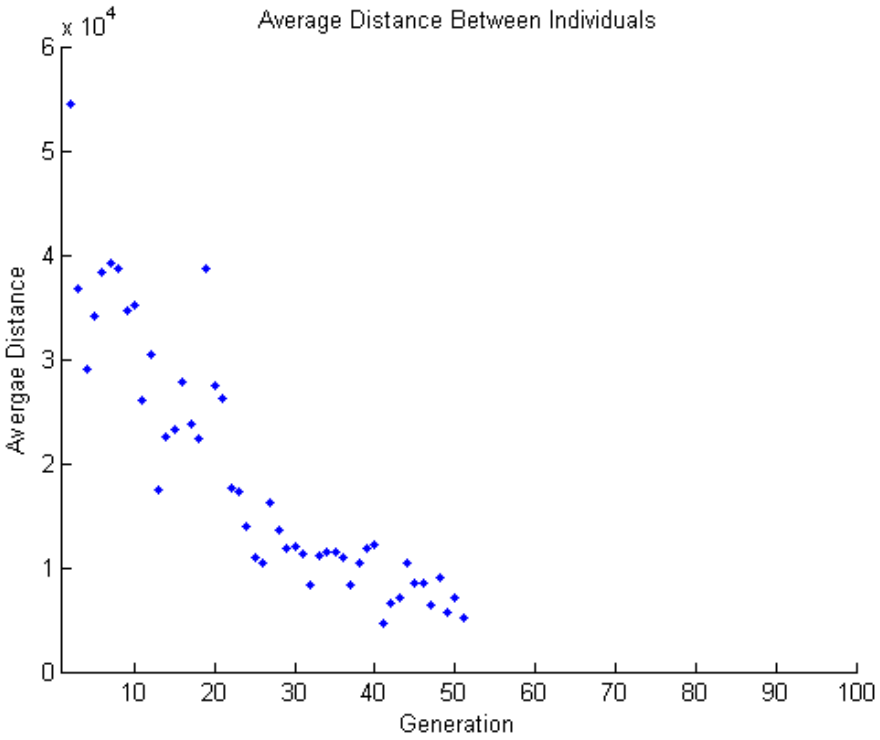

Figure 4-31: Average distance between individuals

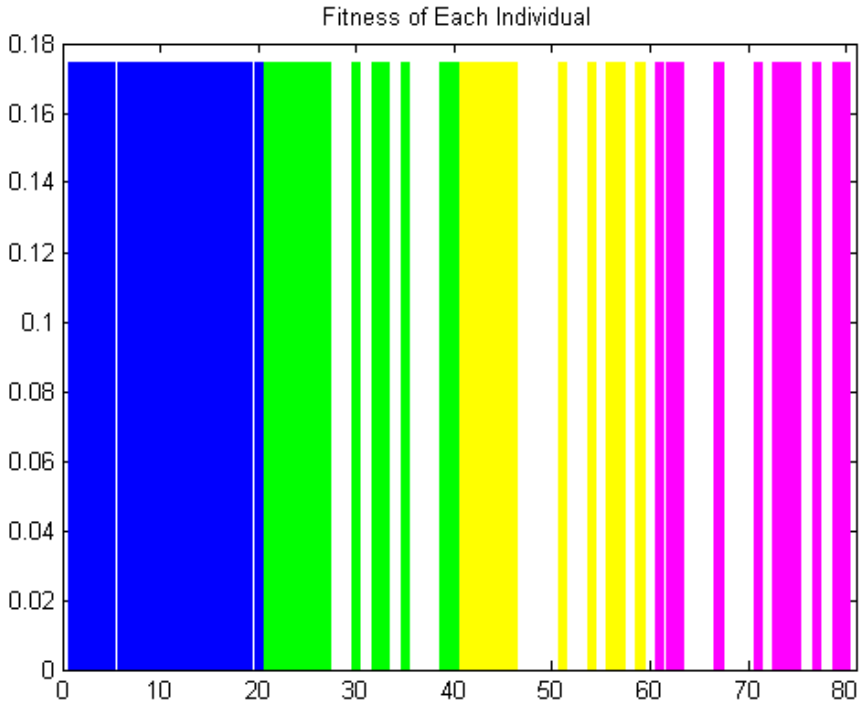

Figure 4-32: Fitness of each individual

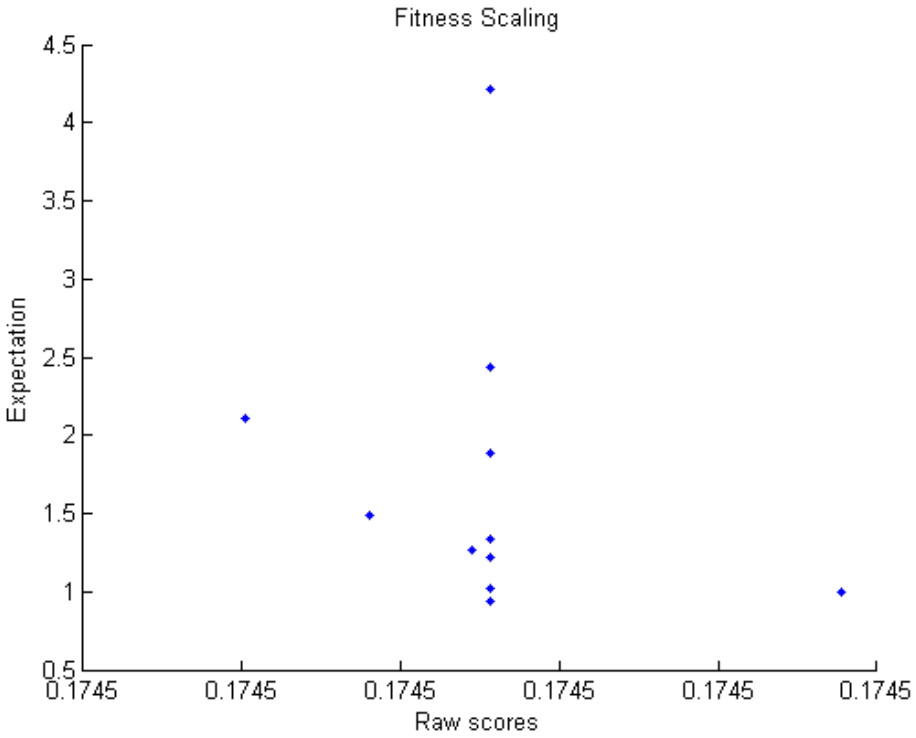

Figure 4-33: Fitness scaling

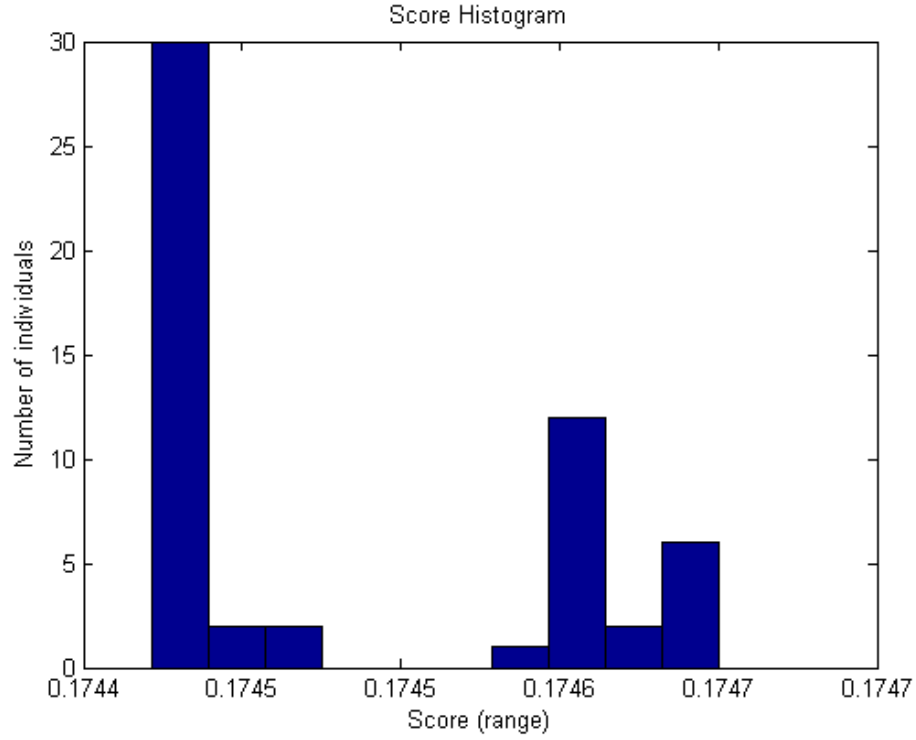

Figure 4-34: Score histogram

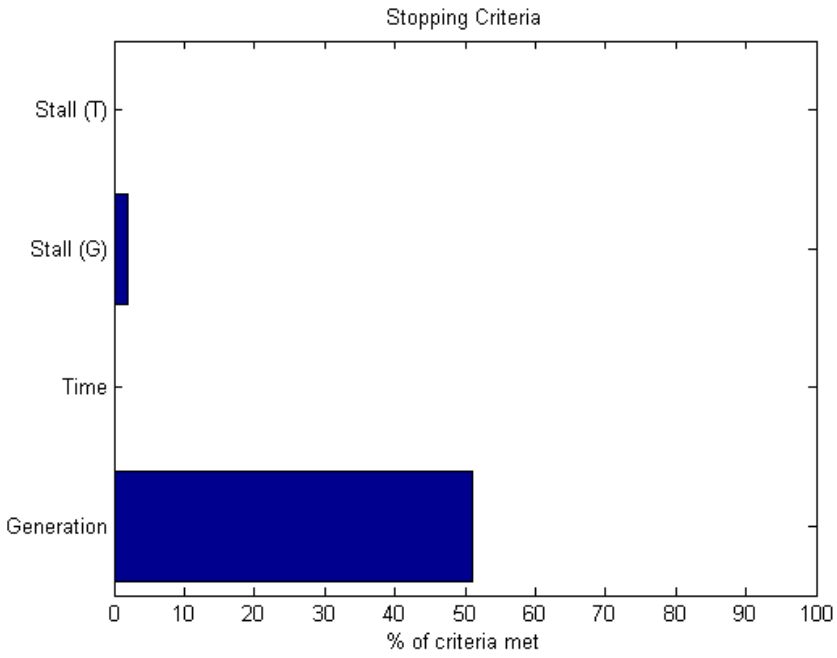

Figure 4-35: Stopping criteria

4.2 Discussion

4.2.1 Scenario A: Base case

The base case is a trivial solution involving the scaling of generation sources to match the load while allowing for a small margin in this case 20% as contingency for growth or resource shortfall. This is the approach taken in similar studies and is meant to be a control set up and is not expected to provide the optimal solution to the problem.

The base case setup consisted of 16000 photovoltaic modules with an equivalent peak power rating of 4 MWp and 10 wind turbine generator units with an equivalent rated power output of 2.5 MW and 23809 advanced lead acid battery storage units with a rated storage capacity of 2000kWh.

This set up presents an estimated overnight capital cost of approximately 85 USDM.

The overnight capital cost is developed from the transparent cost database by NREL. It is derived from average of a selection of project carried out in the USA with costs documented over a period of about 15 years. This approach has proved ineffective in determining true and reflective costs as it doesn't capture market trends in pricing. Solar PV for example has dropped down in pricing

(about 5 times) over the last decade as a result of increased production driven by demand for green energy across the globe. For a comparative analysis however, this is a sufficient approach.

The levelized cost of energy for the base case was not evaluated as the base case did not meet the set threshold for the Loss of Power Supply Probability (LPSP). The configuration delivered an LPSP of 0.2318 equivalent to about 2030 hours of unavailability per year. This would definitely not be an acceptable solution.

4.2.2 Scenario B: Base case with demand side management simulation

An attempt is made to improve the base case by introducing demand side management strategies. The actual strategy is not covered in the scope of this work, only the desired effect is simulated. The objective of the simulation is to shift demand to match the abundant resource, solar in this case.

In practice there are various ways in which this can be achieved for example via tariff structuring that makes it expensive to consume electricity at certain times of the day, via load shedding, etc.

Theoretically DSM should enable better utilization of the available resource hence a lower LPSP. This was indeed realized with an LPSP of 0.0838. This translates to about 740 hours of outage in a year which although a significant improvement, is still below the threshold of 0.05, and the levelized cost of electricity was thus not calculated.

4.2.3 Scenario C: Base Case with demand side management simulation and PV trackers

Another strategy for improving resource utilization of solar is by installation of the panels on a sun tracking racking system, simply known as trackers. Two variants of trackers are commercially available; single axis trackers and two axis trackers. Single axis trackers, track the movement of the sun along one axis – the horizontal, whereas a two axis tracker tracks along the horizontal and vertical axes. Single axis trackers have a higher cost benefit ratio and hence are more popular compared to two axis trackers. Compared to a fixed tilt installation, a single axis tracker is able to increase generation by up to 20%, but is more expensive to install and maintain. OPEX and CAPEX figures vary by manufacturer and region, for this study an assumption of 10% increase in OPEX and 10% increase in CAPEX over fixed tilt structures has been assumed in the calculation of LCOE for scenarios such as this that involve single axis trackers.

With both trackers and demand side management simulated, an LPSP of 0.0484 is achieved. This corresponds to about 430 hour of outage in a year.

The levelized cost of electricity was also evaluated and this was found to equal 31.9 USD per kWh. This is still much higher than the national average cost of electricity but is acceptable for remote installations without access to the grid. It is also cheaper than LCOE for diesel generated energy on remote sites.

4.2.4 Scenario D: Optimal Configuration without demand side management simulation

An attempt to arrive at the optimal solution is made here. The objective is to solve for an optimal plant configuration in consideration of the simulated demand and simulated resource (sunshine irradiance and wind speed). A multi deme parallel genetic algorithm implementation is used. A population of 80 individuals equal spread across 5 demes (sub populations) is used to perform the search. Two methods have been developed as observed in other literature to provide constraints to the algorithm. The first is based on a test run method, where constraints are developed programmatically in response to results of a simulation run. This method has been explained in more detail in an earlier section of this report. The method evaluates lower bounds from which upper bounds are obtained by multiplication by a scale factor. For solar PV modules, a lower bound of 1,975 units was arrived at while for wind and battery units a lower bound of 4 and 7,879 were computed respectively. A scale factor of 10 was used to obtain the upper bounds.

Figure 4-1, is a plot of the fittest individual and the mean fitness of the overall population (across all 5 demes) vs the generation. It shows how the algorithm narrows down to global minimum which is evident when the overall population fitness score and the fitness score of the fittest individual coincide. The algorithm was set up to stop iterations when the change in the mean fitness of the population between successive generations was less than 1×10^{-5}.

Figure 4-3, is also an excellent visual indication of the state of optimality of the population. It shows the different demes in different colours and individual fitness of members of a deme as well as of the whole population can be seen. It is clear that the algorithm evaluated well and converged at an optimal solution given the conditions presented to it.

The result from this run of the algorithm is recorded Table 4-4Table 4-1. An LPSP of 0.0498, which translates to about 440 hours of outage in year was achieved with this configuration. The

LCOE for this configuration was evaluated to only 21.51 US Cents per kWh at an estimated overnight capital cost of 39 MUSD. This is a stellar result compared to the only feasible solution of the base configurations earlier discussed.

The second approach simulated involved constraining the algorithm parameters by the size of land. Assuming a 10 acre parcel of land for the development of the PV/ wind farm, using equations (3.67) and (3.68), the upper bound on the number of wind turbines and PV modules that can be supported by the site are evaluated to 14 and 117,430 units respectively. The optimization algorithm fails to narrow down on an optimal solution that meets the minimum requirement of a 5 % LPSP. With a down-rating of the LPSP requirement to 10%, which translates to a maximum allowable outage rate of 876 hours annually, an optimal solution consisting of 20311 solar panels, 14 wind turbines and 66837 battery units is arrived at with an LPSP of 0.0997 and a resulting levelized cost of electricity of 30.03 US cents per kWh at an overnight capital cost of 116 Million USD.

Comparing the results from the two constraint scenarios, the effect restrictions on the search space put on the optimality of the obtained results is very clear. The conclusion drawn is that placing restriction on land size, effectively capped the contribution from the various resources. Wind was limited to only 14 units or 3.5 MW. It so happens that based on the pricing guide used, wind is cheaper than solar in terms of levelized cost of generated electricity hence resulting in a scenario where the optimal solution is a bias for wind over solar.

4.2.5 Scenario E: Optimal configuration with demand side management simulated

With Demand side simulation implemented, aimed at aligning the demand to generation and shifting peak demand away from generation troughs to generation peaks, an interesting set of results is arrived at.

In the first optimization scenario, lower bounds of 2,438, 4 and 3,320 for solar, wind and battery storage units respectively are arrived at. With these bounds, the algorithm converged to a solution, an optimal configuration of 6,830 solar PV panels, 25 wind turbines and 32,243 battery units. The configuration resulted in an LPSP of 0.0491 and an equivalent LCOE of 28.26 cents US per kWh.

Figure 4-13, Figure 4-14 and Figure 4-15 shows the convergence behaviour of the algorithm run with the current parameters.

Comparing these results to the earlier ones of scenario D, the bias action of DSM simulation is evident in the way it has promoted the adoption of solar. In the pricing scenarios used, solar being the more expensive energy source in terms of dollars per kWh has effectively ramped up the weighted average LCOE to 28.26 US Cents per kWh, nearly 7 US cent more expensive. The number of PV panels have increased from 4459 to 6830. It is thus clear that a DSM scheme will promote better utilization of a resource but that doesn't guarantee that its implementation results in the most cost optimal solution especially where more than one generation source is considered.

In the second optimization case, upper bounds of 117,430 for the PV units and 14 for the wind turbines same as in the earlier case are employed. Like the previous case, the configuration fails to arrive at an optimal solution with the LPSP threshold set to 5%. With the threshold adjusted to 10 %, the algorithm converges to an optimal configuration. The optimal configuration arrived at is constituted of 1976 PV modules, 13 wind turbines and 117,610 battery storage units. This results in a LPSP of 0.0882 and a corresponding LCOE of 17.76 US cents per kWh. The obvious explanation for the reduction in LCOE, compared with case D option two, is the reduction in the overnight capital cost made possible by a reduction in the number of panels. With DSM simulation, it is possible to reduce the installed capacity required to meet a certain energy demand. It is not valid to compare these results with those of the first option in this very case. The reasoning behind this is that, this option failed to meet the LPSP threshold.

4.2.6 Scenario F: Optimal Configuration with DSM Simulation and PV Tracking

The PV modules are usually mounted in either fixed tilt racking systems or in single axis tracker racking systems. A fixed tilt installation features panels mounted at a fixed tilt angle that is optimal to utilization of the sun's energy. Tracker racking systems are designed to track the diurnal movement of the sun across the sky as the earth rotates. Both single and two axis tracker systems are available but the latter are not as commercially popular as single axis trackers. Tracking systems cost more in both CAPEX and OPEX but with their ability to track the sun can generate up to 20% more energy from the sun's irradiation. The objective of simulating trackers in this study was to optimize solar generation which is quite costly and consequently reduce the levelized cost of electricity from the entire plant as a result of a reduction in the average cost per kWh from solar generation.

With the first set of constraints, as determined by the algorithm, the lower bound on solar PV modules, wind turbine and battery units are set at 3,041, 3 and 2,103 respectively. The algorithm

converges on an optimal configuration consisting of 11,047 PV modules, 15 wind turbines and 20,984 battery units. This configuration evaluates to an LPSP of 0.0494. With an assumed increase of 10% on both OPEX and CAPEX as result of the installation of PV trackers, an LCOE of 28.02 Us cents per kWh is obtained. These results conclusively show that a technology bias on solar, a situation brought about by the use of trackers, promotes adoption of solar in the optimal generation mix but does not necessarily guarantee a lower LCOE.

With the second set of constraints, formulated from limitations of land size, with the upper limits set as before, the algorithm converges on an optimal configuration consisting of 1976 solar modules, 13 wind turbines and 94856 battery units. Like the previous two scenarios run under these constraints, it fails to achieve the required LPSP threshold of 5%, managing only 9.37% at an LCOE of 17.62 US cents per kWh. Similar OPEX and CAPEX assumptions for the PV trackers are used as in the case above.

Comparing these two results obtained from running the algorithm under different sets of constraints, it is evident that the resource characterizes the results obtained. The second set of results is an excellent control for the first in answering the question of how much lower the LCOE can get by reducing the generation from solar. It is clear that aside from the upper bound of 14 set on the number of wind turbines which are cheaper than solar and hence contribute to a lower LCOE, there is a limit the contribution of wind to the generation mix since if this were not the case the optimal solution would consist of only 14 wind turbine units.

4.3 Validation

4.3.1 Comparison with the Transparent Cost Database (TCD)

The results obtained were validated by comparison with the transparent cost database published by openei.org. The transparent cost database is an initiative of the United States Department of Energy in association with the National Renewable Energy Laboratory (NREL). It is a public transparent database of program costs and performance estimates for energy efficiency and renewable energy programs that have been published in open literature. It has collated cost information from nearly 500 different sources in the last decade or so and is an authoritative benchmarking tool used in industry by project developers, investors, financiers, policy makers and regulators.

The database features levelized cost of energy generation for various technologies and provides a platform for comparison of results and analysis of solution optimality. An abridged form of the database used for this validation is attached in ANNEX 4: Validation – The Transparent Cost Database (Abridged form).

Below is a summary of this comparison.

Table 4-10: Comparison with the transparent cost database

		Solar	Wind	Mean LCOE	Max LCOE	Min LCOE
TCD	Photovoltaic	100%	-	28.85	$ 56.00	$ -
	Land-Based Wind	-	100%	7.18	$ 12.30	$ 5.30
Scenarios	A	62%	38%	-		-
	B	62%	38%	-	-	-
	C	62%	38%	-	-	-
	D.1	12%	88%	21.51	-	-
	D.2	59%	41%	30.03	-	-
	E.1	21%	79%	28.26	-	-
	E.2	13%	87%	17.76	-	-
	F.1	42%	58%	28.02	-	-
	F.2	13%	87%	17.62	-	-

Table 4-11: Derived worst case and nominal case compared to obtained results

		Results	TCD Nominal Case	TCD Worst Case	Adjusted TCD Nominal Case	Adjusted TCD Worst Case
Scenarios	A	-	20.52	39.19	21.75	41.54
	B	-	20.52	39.19	21.75	41.54
	C	-	20.52	39.19	21.75	41.54
	D.1	21.51	9.76	17.50	13.96	25.03
	D.2	30.03	20.01	38.17	22.49	42.90
	E.1	28.26	11.83	21.68	13.83	25.33
	E.2	17.76	10.04	18.07	17.25	31.04
	F.1	28.02	16.37	30.83	17.61	33.16
	F.2	17.62	10.04	18.07	16.80	30.22

Error! Reference source not found. is a direct comparison of the results obtained from the research with those from the transparent cost database. It is not easy to directly compare the two

results for a number of reasons. First, the TCD does not have records of hybrid renewable energy power plants and as such any comparative metric has to be derived from the measured and documented data of the TCD. Secondly, the concept of energy storage is quite different from energy generation and decoupling its contribution to the LCOE from that of the generation sources is not easy. Nonetheless, as the TCD is best open documented cost database that is freely available, an attempt has been made by the researcher to determine the quality of results obtained by comparison of these to derived metrics from the TCD. This information is presented on **Error! Reference source not found.**. The TCD Nominal Case is the LCOE derived from average LCOE values of wind and solar generation from the TCD and weighted in the same proportion as the scenario to which it is being compared. The TCD worst case is the LCOE derived from the weighted average of maximum LCOE values of wind and solar generation from the TCD, weighted in the same proportion as the scenario it is being compared to. As the derived TCD corresponding LCOE values do not factor in storage, the actual corresponding LCOEs if calculated from the TCD to factor in storage would be worse. A second pair of derived metrics attempt to include the influence of energy storage on the LCOE value from the TCD. Since the overnight capital cost component of the energy storage as a percentage of the total project overnight capital cost is known, this factor is used to dilute the quality of the derived LCOE. The two columns adjusted nominal LCOE and adjusted worst case LCOE provide this information. The obtained results can now be compared against the adjusted nominal and worst case LCOE. With the exception of scenario E.1 all the results lie within the bounds of the nominal and the worst case LCOE as derived from the TCD. These findings satisfactorily validate the results obtained from this research.

Chapter 5 Conclusion

5.1 Summary of Thesis Findings and Contributions

Multiple scenarios were simulated in this work in an attempt to find an optimal solution to the problem of sizing a hybrid renewable energy power system. The results have been documented and discussed in the previous chapter and are here below summarized ahead of drawing a conclusion to the work. Three control scenarios were set up; the base cases A, B and C and were found to be suboptimal as expected. In these control cases, a configuration of 16000 PV modules, 10 wind turbines and 23,809 battery units was used. Further, scenario B included simulation of a demand side management scheme, whereas scenario C included simulation of a demand side management scheme as well as PV units mounted on a single axis, sun tracking racking system. Scenarios D, E and F were the results from the optimal configuration of the hybrid renewable energy power system based on scenarios A, B and C respectively.

5.2 Conclusions Drawn

Three optimal configurations from three scenarios simulated have been obtained. The first objective of this study was to mathematically model the components of the hybrid renewable energy system. These were covered in **Error! Reference source not found.**, all components; the wind turbine, solar PV modules and battery storage modules were modelled and used to develop the objective function which is later minimized using a parallel, multi -deme genetic algorithm. The second objective was to develop an objective function that would be minimized by the algorithm so as to obtain the optimal sizing configuration of the plant. This as well as done in **Error! Reference source not found.**, the result of which is a two-fold objective, to minimize the loss of power supply probability (LPSP) and the levelized cost of energy (LCOE). The objective function is implemented in a Matlab function that is called by the algorithm. The third objective was to run multiple scenario analysis on the most optimal configuration as optimized by a parallel, multi-deme genetic algorithm for implementation at a specific site. The site Marsabit, which had already been pre-selected, is a wind and solar hotspot in Kenya. Data for the site was obtained from SWERA as highlighted in Chapter 3. A total of 9 scenarios were evaluated, a process that took 45 simulation runs and over 150 hours of computer runtime.

With all objectives met, conclusions can then be drawn from the results. The first conclusion based on the results of this work is that it is feasible to develop a hybrid renewable energy system at certain locations e.g. Marsabit in Kenya. It was observed that at locations where wind and solar had complementary regimes, it was possible to optimally size the individual components of the plant to meet a certain reliability requirement. It was also concluded as can be observed from the results of the land size constrained simulations that a higher reliability requirement was achievable at a higher cost. Most of the scenarios with a lower reliability requirement (10% LPSP) resulted in lower levelized cost of energy of less than 20 US cents per kWh, whereas the best scenario with a high reliability requirement (5% LPSP) resulted in a levelized cost of energy of 21.51 US cents per kWh.

A second interesting conclusion drawn is that a resource optimal configuration does not necessarily equal a cost optimal configuration where the cost of utilizing the different resources are not the same. It was observed that in a scenario where demand side management was simulated to optimize solar utilization and the solar PV modules themselves mounted on a sun tracking racking system, the resulting optimal configuration optimizes the utilization of solar energy but does not yield the lowest LCOE as solar PV systems were more expensive than wind turbines. The clear conclusion in terms of the way forward seen from the results is that a cost optimal system is one that optimally utilizes the cheapest resource to exploit. This is corroborated by the finding that wind intensive configuration resulted in lower LCOE than solar intensive configurations.

On the algorithm implementation and simulations, it was observed severally, and conclusions can be drawn that a parallel multi-deme genetic algorithm implementation, was better than a similar control experiment run in a serial generic GA in diversity of individuals in a search space and its exploration. This was measured by observing the average distance between individuals which was higher in the multi-deme parallel GA as compared to the serial generic GA. On the quality of the final solution though, clear conclusions could not be drawn on which was better as they both converged to approximately similar solutions.

From the results obtained based on the different scenarios, the recommended practical scenario for implementation would be scenario f.2 where the plant is constrained to a land size of 10 acres , demand side management is practised, and the PV modules are installed on a sun tracking racking system. Even though this option has an LPSP of only 10%, it is by far the most cost effective

resulting in an LCOE of 17.62 US cents per kWh. It could further be improved with grid storage or back up to the grid, but this has been left as a proposition for further work.

5.3 Recommendation for further Work

A number of assumptions have been made throughout this work to simplify computation and evaluation of solutions. It is recommended that on future work more detailed models be used in the modelling of the objective function. Further this work did not factor in tax in calculation of the LCOE as its purpose as for comparison, tax assumptions are a critical but complicated aspect that affects the real life levelized cost of energy. It is recommended that future researchers include this aspect in their research to obtain results that can be validated with market data.

Another key area for further investigation would be on the components of the hybrid system. It is apparent from this work that battery energy storage systems still need further technological advancements for mainstream adoption in grid applications. Researchers of the future are encouraged to look into newer battery technologies as well as alternatives. The most promising alternative proposed herein are diesel displacement solutions where the hybrid system is used to offset reliance on diesel generators for remote and isolated areas and grid backup solutions, where the hybrid system is tied to the grid for energy storage during times of surplus generation and for back feed to meet generation shortfalls. For both cases complex econometric models will have to be developed to characterize the economics of the power purchase transactions involved.

REFERENCES

[1] R. S. R. Gorla and R. Salako, "Feasibility Study of Wind Solar Hybrid System for Cleveland, Ohio, USA," *Smart Grid and Renewable Energy,* vol. 2, pp. 37-44, 2011.

[2] Potsdam Institute for Climate Impact Research and Climate Analytics, "Turn Down the Heat: Climate Extremes, Regional Impacts and the Case for Resilience," World Bank, Washington, 2013.

[3] United Nations, "United Nations Millenium Development Goals," United Nations, [Online]. Available: http://www.un.org/millenniumgoals/environ.shtml. [Accessed 4 October 2014].

[4] United Nations Development Program, "UNDP: Sustainable Energy," UNDP, [Online]. Available: http://www.undp.org/content/undp/en/home/ourwork/environmentandenergy/focus_areas/sustainable-energy.html. [Accessed 4 October 2014].

[5] L. Zhang, R. Belfkira and G. Barakat, "Wind/PV/diesel energy system: Modeling and sizing optimization," *Institute of Electrical and Electronics Engineers,* September 1, 2011.

[6] L. Zhang, G. Barakat and A. Yassine, "Design and optimal sizing of hybrid PV/wind/diesel system with battery storage by using DIRECT search algorithm," in *Power Electronics and Motion Control Conference (EPE/PEMC), 2012 15th International*, September 4, 2012.

[7] R. Belfikra, O. Hajji, C. Nichita and G. Barakat, "Optimal sizing of stand-alone hybrid wind/PV system with battery storage," in *Power Electronics and Applications, 2007 European Conference on*, Aalborg, 2007.

[8] H. Yang, W. Zhou, L. Lu and Z. Fang, "Optimal sizing method for stand-alone hybrid solar–wind system with LPSP technology by using genetic algorithm," *Elsevier Journal of Solar Energy,* vol. 82, pp. 354-367, 2008.

[9] B. O. Bilal, V. Sambou, P. A. Ndiaye, C. M. Kebe and M. Ndongo, "Optimal design of a hybrid solar–wind-battery system using the minimization of the annualized cost system and the minimization of the loss of power supply probability (LPSP)," *Elsevier Journal of Renewable Energy,* vol. 35, pp. 2388-2390, 2010.

[10] B. A. Jemaa, A. Hamzaoui, N. Essounbouli, F. Hnaien and F. Yalawi, "Optimum sizing of hybrid PV/wind/battery system using Fuzzy-Adaptive Genetic Algorithm," in *Systems and Control (ICSC), 2013 3rd International Conference on*, Algiers, 2013.

[11] M. S. Tafreshi, H. A. Zamani, S. M. Ezzati and M. Baghdadi, "Optimal unit sizing of Distributed Energy Resources in Micro Grid using genetic algorithm," in *Electrical Engineering (ICEE), 2010 18th Iranian Conference on*, Isfahan, Iran, 2010.

[12] M. Pirhaghshenasvali and B. Asaei, "Optimal modeling and sizing of a practical hybrid wind/PV/diesel generation system," in *Power Electronics, Drive Systems and Technologies Conference (PEDSTC), 2014 5th*, Tehran, 2014.

[13] M. Bashir and J. Sadeh, "Optimal sizing of hybrid wind/photovoltaic/battery considering the uncertainty of wind and photovoltaic power using Monte Carlo," in *Environment and Electrical Engineering (EEEIC), 2012 11th International Conference on*, Venice, 2012.

[14] M. Bashir and J. Sadeh, "Size optimization of new hybrid stand-alone renewable energy system considering a reliability index," in *Environment and Electrical Engineering (EEEIC), 2012 11th International Conference on*, Venice, 2012.

[15] A. Y. Saber and G. K. Venayagamoorthy, "Smart micro-grid optimization with controllable loads using particle swarm optimization," in *Power and Energy Society General Meeting (PES), 2013 IEEE*, Vancouver, 2013.

[16] A. Navaerfard, S. Tafreshi, M. Barzegari and A. Shahrood, "Optimal sizing of distributed energy resources in microgrid considering wind energy uncertainty with respect to reliability," in *Energy Conference and Exhibition (EnergyCon), 2010 IEEE International*, Manama, 2010.

[17] J. He, C. Deng and W. Huang, "Optimal sizing of distributed generation in micro-grid considering Energy Price Equilibrium point analysis model," in *Industrial Electronics and Applications (ICIEA), 2013 8th IEEE Conference on*, Melbourne, 2013.

[18] O. Ekren and B. Y. Ekren, "Size optimization of a PV/wind hybrid energy conversion system with battery storage using simulated annealing," *Journal of Applied Energy,* vol. 87, no. 2, pp. 592-598, 2010.

[19] O. Ekren and B. Y. Ekren, "Size optimization of a PV/wind hybrid energy conversion system with battery storage using response surface methodology," *Journal of Applied Energy,* vol. 85, no. 11, pp. 1086 - 1101, 2008.

[20] A. Crăciunescu, C. Popescu, M. Popescu and L. M. Florea, "Stand-alone hybrid wind-photovoltaic power generation systems optimal sizing," in *11TH INTERNATIONAL CONFERENCE OF NUMERICAL ANALYSIS AND APPLIED MATHEMATICS 2013: ICNAAM 2013*, Rhodes, 2013.

[21] A. Arabali, M. Ghofrani, M. Etezadi-Amoli and M. S. Fadali, "Stochastic Performance Assessment and Sizing for a Hybrid Power System of Solar/Wind/Energy Storage," *Sustainable Energy, IEEE Transactions on,* vol. 5, no. 2, pp. 363-371, 2014.

[22] P. C. Roy, A. Majumder and N. Chakraborty, "Optimization of a stand-alone Solar PV-Wind-DG Hybrid System for Distributed Power Generation at Sagar Island," in *INTERNATIONAL CONFERENCE ON MODELING, OPTIMIZATION, AND COMPUTING (ICMOS 20110)*, West Bengal, 2010.

[23] M. El Badawe, T. Iqbal and G. K. I. Mann, "Optimization and modeling of a stand-alone wind/PV hybrid energy system," in *Electrical & Computer Engineering (CCECE), 2012 25th IEEE Canadian Conference on*, Montreal, 2012.

[24] S. X. Chen and H. B. Gooi, "Sizing of energy storage system for microgrids," in *Probabilistic Methods Applied to Power Systems (PMAPS), 2010 IEEE 11th International Conference on*, Singapore, 2010.

[25] S. Bahramirad and W. Reder, "Islanding applications of energy storage system," in *Power and Energy Society General Meeting, 2012 IEEE*, San Diego, 2012.

[26] S. Chen, H. B. Gooi and M. Q. Wang, "Sizing of energy storage for microgrids," in *Power and Energy Society General Meeting, 2012 IEEE*, San Diego, 2012.

[27] O. Ekren, B. Y. Ekren and O. Baris, "Break-even analysis and size optimization of a PV/wind hybrid energy conversion system with battery storage – A case study," *Journal of Applied Energy,* vol. 86, no. 7-8, pp. 1043-1054, 2009.

[28] C. S. Hearn, M. C. Lewis, S. B. Pratap, R. E. Hebner, F. M. Uriarte, R. G. Longoria and C. Donmei, "Utilization of Optimal Control Law to Size Grid-Level Flywheel Energy Storage," *Sustainable Energy, IEEE Transactions on,* vol. 4, no. 3, pp. 611-618, 2013.

[29] J. S. Anagnostopoulos and D. E. Papantonis, "Simulation and size optimization of a pumped–storage power plant for the recovery of wind-farms rejected energy," *Journal of Renewable Energy,* vol. 33, no. 7, pp. 1685-1694, 2008.

[30] F. Zhang, X. Chen, X. Yin and Z. Wang, "An improved capacity ratio design method based on complementary characteristics of wind and solar," in *Electrical Machines and Systems (ICEMS), 2013 International Conference on*, Busan, 2013.

[31] L. Xu, X. Ruan, C. Mao, B. Zhang and Y. Luo, "An Improved Optimal Sizing Method for Wind-Solar-Battery Hybrid Power System," *Sustainable Energy, IEEE Transactions on,* vol. 4, no. 3, pp. 774-785, 2013.

[32] A. Kamjoo, A. Maheri and G. Putrus , "Wind Speed and Solar Irradiance Variation Simulation Using ARMA Models in Design of Hybrid Wind-PV-Battery System," *Journal of Clean Energy Technologies,* vol. 1, no. 1, 2013.

[33] Z. Benhachani, B. Azoui, R. Abdessemed and M. Chabane, "Optimal sizing of a solar-wind hybrid system supplying a farm in a semi-arid region of Algeria," in *Universities Power Engineering Conference (UPEC), 2012 47th International*, London, 2012.

[34] H. Belmili, M. Haddadi, S. Bacha, . M. F. Almi and B. Bendib, "Sizing stand-alone photovoltaic–wind hybrid system: Techno-economic analysis and optimization," *Renewable and Sustainable Energy Reviews,* vol. 30, pp. 821 -832, 2013.

[35] G. Xydis, "On the exergetic capacity factor of a wind – solar power generation system," *Journal of Cleaner Production,* vol. 47, pp. 437-445, 2013.

[36] B. Panahandeh, J. Bard, A. Outzourhit and D. Zejli, "Simulation of PV-Wind hybrid systems combined with hydrogen storage for rural electrification," *International Journal of Hydrogen Energy,* vol. 36, pp. 4185-4197, 2011.

[37] A. Testa, S. De Caro and T. Scimone, "Optimal structure selection for small-size hybrid renewable energy plants," in *Power Electronics and Applications (EPE 2011), Proceedings of the 2011-14th European Conference on*, Birmingham, 2011.

[38] S. Paudel, J. N. Shrestha and J. A. Fereira, "Optimization of hybrid PV/wind power system for remote telecom station," in *Power and Energy Systems (ICPS), 2011 International Conference on*, Chennai, 2011.

[39] S. Dial, D. Dial, M. Belhamel, M. Haddadi and A. Louche, "A methodology for optimal sizing of autonomous hybrid PV/wind system," *Energy Policy,* vol. 35, no. 11, pp. 5708-5718, 2007.

[40] F. Z. Kadda, S. Zouggar and M. L. Elhafyani, "Optimal sizing of an autonomous hybrid system," in *Renewable and Sustainable Energy Conference (IRSEC), 2013 International*, Ouarzazate, 2013.

[41] F. Scarlatache and G. Grigoras, "Optimal coordination of wind and hydro power plants in power systems," in *Optimization of Electrical and Electronic Equipment (OPTIM), 2014 International Conference on* , Bran, 2014.

[42] S. Vazquez, S. Lukic, E. Galvan, L. G. Franquelo, J. M. Carrasco and J. I. Leon, "Recent advances on Energy Storage Systems," in *IECON 2011 - 37th Annual Conference on IEEE Industrial Electronics Society*, Melbourne, 2011.

[43] N. S. Chouhan and M. Ferdowsi, "Review of energy storage systems," in *North American Power Symposium (NAPS), 2009*, Starkville, 2009.

[44] A. Puri, "Optimally sizing battery storage and renewable energy sources on an off-grid facility," in *Power and Energy Society General Meeting (PES), 2013 IEEE*, Vancouver, 2013.

[45] H. Emori, T. Ishikawa, T. Kawamura and T. Takamura, "Carbon-hydride energy storage system," in *Humanitarian Technology Conference (R10-HTC), 2013 IEEE Region 10*, Sendai, 2013.

[46] S. Y. Wang and J. L. Yu, "Optimal sizing of the CAES system in a power system with high wind power penetration," *Electric Power and Energy Systems,* vol. 37, pp. 117-125, 2012.

[47] M. Pedram, N. Chang, Y. Kim and Y. Wang, "Hybrid electrical energy storage systems," in *Proceedings of the 16th ACM/IEEE international symposium on Low power electronics and design*, Austin, 2010.

[48] A. Poullikkas, "A comparative overview of large-scale battery systems for electricity storage," *Renewable and Sustainable Energy Reviews,* vol. 27, pp. 778-788, 2013.

[49] A. Saez-de-Ibarra, A. Milo, G. Haizea, E.-O. Ion, R. Pedro, B. Seddik and V. Debusschere, "Analysis and Comparison of Battery Energy Storage technologies for grid Applications," in *IEEE PowerTech*, Grenoble, 2013.

[50] Z. Wei, L. Chengzhi, L. Zhongshi, L. Lin and Y. Hongxing, "Current Status of research on Optimum Sizing of Stand-alone hybrid solar-wind power generation systems," *Applied Energy,* vol. 87, pp. 380-389, 2010.

[51] O. Erdinc and M. Uzunoglu, "Optimum design of hybrid renewable energy systems: Overview of different approaches," *Renewable and Sustainable Energy Reviews,* vol. 16, no. 3, pp. 1412-1425, 2012.

[52] R. Dufo-Lopez and J. L. Bernal-Agustin, "Design and Control Strategies of PV-diesel Systems using Genetic Algorithms," *Solar Energy,* vol. 79, no. 1, pp. 33-46, 2005.

[53] "SWERA," openei.org, [Online]. Available: http://en.openei.org/wiki/SWERA/About. [Accessed 27 June 2015].

[54] M. G. Villalva, J. R. Gazoli and E. R. Filho, "Comprehensive Approach to Modeling and Simulation of Photovoltaic Arrays," *IEEE Transactions on Power Electronics,* vol. 24, no. 5, pp. 1198-1209, 2009.

[55] H.-L. Tsai, C.-S. Tu and Y.-J. Su, "Development of Generalized PV Model Using MATLAB/SIMULINK," in *Proceeedings of the World Congress on Engineering and Computer Science*, San Francisco, USA, 2008.

[56] C. Honsberg and S. Bowden, "Double Diode Model : PV Education," [Online]. Available: http://www.pveducation.org/pvcdrom/characterisation/double-diode-model. [Accessed 29th December 2014].

[57] Kyocera Solar, "KD 140 F SX Series Datasheet," Kyocera, 2014.

[58] Green Building Council of AUstralia, "Green Star Photovoltaic Modeling Guidelines," GBCA, Sydney, September 2013.

[59] S. Santoso and M. Singh, "Dynamic Models for Wind Turbines and Wind Power Plants," National Renewable Energy Laboratory (NREL), Golde, Colorado, October 2011.

[60] A. W. Manyonge, R. M. Ochieng, F. N. Onyango and J. M. Shichika, "Mathematical Modeling of Wind Turbine in a Wind Energy Conversion System: Power Coefficient Analysis," *Journal of Applied Mathematical Sciences,* vol. 6, no. 91, pp. 4527-4536, 2012.

[61] Electric Power Research Institute (EPRI), "WECC Type 3 Wind Turbine Generator Model," EPRI, 2014.

[62] Electric Power Research Institute (EPRI), "WECC Type 4 Wind Turbine Generator," EPRI, 2013.

[63] N. Jenkins, J. Ekanayake, L. Holdsworth and X. Wu, "Dynamic Modelling of Doubly Fed Induction Generator Wind Turbines," *IEEE Transactions on Power Systems,* vol. 18, no. 2, 2003.

[64] Y. Lei, A. Mullane, G. Lightbody and R. Yacamini, "Modeling of the Wind Turbine with a doubly fed induction generator for grid integration studies," *IEEE Transactions on Energy Conversion,* vol. 21, no. 1, pp. 257-264, 2006.

[65] S. M. Muyeen, J. Tamura and T. Murata, "Wind Turbine Modelling," in *Stability Augmentation of a Grid Connected Wind Farm*, Springer, 2009, pp. 22-65.

[66] P. Tomas, "PhD Thesis: Modelling of Wind Turbines for Power System Studies," Dept. of Electric Power Engineering, Chalmers University of Technology, Goteborg, Sweden, 2003.

[67] Electric Power Research Institute (EPRI), "Electricity Energy Storage Technology Options," EPRI, Palo Alto, 2010.

[68] A. Barin, L. N. Canha, A. D. R. Abaide, K. F. Magnago, B. Wottrich and R. Q. Machado, "Multiple Criteria Analysis for Energy Storage Selection," *Energy and Power Engineering,* vol. 3, no. 1, pp. 557-564, 2011.

[69] A. R. Sparacino, G. F. Reed, R. J. Kerestes, B. M. Grainger and Z. T. Smith, "Survey of Bateery Energy Storage Systems and Modeling Techniques," in *IEEE Power and Energy Society General Meeting*, San Diego, CA, 2012.

[70] K. Yoon-Ho and H. Hoi-Doo, "Design of Interface Circuits with Electrical Battery Models," *IEEE transactions on Industrial Electronics,* vol. 44, pp. 81-86, 1997.

[71] S. Barsali and M. Ceraolo, "Dynamical MOdels of lead-acid batteris: implementation issues," *IEEE transactions on Energy Conversion,* vol. 17, pp. 16-23, 2002.

[72] Z. F. Hussein, W. M. Cheung and A. B. Ismail, "Modeling of Sodium Sulphur Batteries for Power Systems Applications," 2007.

[73] E. Manila, C. Nasiri, C. H. Rentel and M. Hughes, "MOdelling of Zinc Bromide Energy Storage Systems for Vehicular Applications," *IEEE Transactions on Industrial Electronics,* vol. 57, pp. 624-632, 2010.

[74] J. Manwel and J. McGowan, "Evaluation of Battery Models for Wind/hybrid Power System Simulations," in *Proceedings of the 5th European Wind Energy AssociationConference (EWEC '94)*, Thessaloniki, 1994.

[75] M. R. Jongerden and B. R. Haverkot, "Which Battery Model to Use?," *Software, IET,* vol. 3, no. 6, pp. 445-457, 2009.

[76] S. M. R. Tito, T. T. Lie and T. Anderson, "A Simple Sizing Optimization Method for Wind-Photovoltaic -Battery Hybrid Renewable Energy Systems," pp. 8-12, 2013.

[77] Energy Regulatory Commission, "10 Year Power Sector Expansion Plan 2014-2024," GoK, Nairobi, June 2014.

[78] S. Ong, C. Clinton, P. Denholm, R. Margolis and G. Heath, "Land-use requirements for solar power plants in the United States," National Renewable Energy Laboratory., Golden, OC, 2013.

[79] W. Rivera, "Scallable Parallel Genetic Algorithms," *Artificial Intelligence Review,* vol. 16, pp. 153-168, 2001.

[80] B. T. Skinner, H. T. Nguyen and D. K. Liu, "Performance Study of Multi-Deme Parallel Genetic Algorithm with Adaptive Mutation," in *2nd International Conference on Autonomous Robots and Agents*, Palmerston North, New Zealand, 2004.

[81] L. Junqing, D. Wencai and C. Mei, "A New Adaptive Parallel Genetic Algorithm," in *Fifth International Conference on INtelligent Human-Machine Systems and Cybernetics*, Hangzhou, China, 2013.

[82] Communications Authority of Kenya, "Quarterly Sector Statistics Report : Third Quarter of the Financial Year 2013-2014," Communication Authority of Kenya, Nairobi, 2014.

[83] International Energy Agency, "World Energy Outlook," IEA, Paris, 2012.

[84] International Energy Agency, "World Energy Outlook : Renewable Energy Outlook," IEA, Paris, 2013.

[85] F. Geth, J. Tant, T. De Rybel, P. Tant and J. Driesen, "Techno-Economical Life Expecteancy Modelling of Battery Energy Storage Systems," in *21st International Conference on Electricity Distribution*, Frankfurt, 2011.

[86] C. J. Rydh, "Environmental Assesment of Vanadium Redox and Lead Acid Batteries for Stationery Energy Storage," *Journal of Power Sources,* vol. 80, pp. 21-29, 1999.

[87] A. Darabi, M. Hosseina, H. Gholami and M. Khakzad, "Modelling of Lead-Acid Battery Bank in the Energy Storage System," *Internatinoal Journal of Emerging Technology and Advanced Engineering,* vol. 3, no. 3, pp. 932-937, 2013.

[88] H. L. Chan and D. Sutanto, "A New Battery Model for Use with Battery Energy Storage Systems and Electric Vehicles Power Systems," in *Power Engineering Society Winter Meeting,2000 IEEE*, 2000.

[89] L. Rydberg, "RTDS Modelling of Battery Energy Storage Systems," Uppsala University - Masters Thesis, Uppsala, Sweden, 2011.

ANNEX 1: Publications Resulting from this Work

A: A Review of Techniques in Optimal Sizing of Hybrid Renewable Energy Systems

Abstract

This paper presents a review of techniques used in recent published works on optimal sizing of hybrid renewable energy sources. Hybridization of renewable energy sources is an emergent promising trend born out of the need to fully utilize and solve problems associated with the reliability of renewable energy resources such as wind and solar. Exploitation of these resources has been instrumental in tackling or mitigating present day energy problems such as price instability for fossil based fuels, global warming and climate change in addition to being seen as way of meeting future demand for power. This paper targets researchers in the renewable energy space and the general public seeking to inform them on trends in methods applied in optimal sizing of hybrid renewable energy sources as well as to provide a scope into what has been done in this field. In reviewing previous works, a two prong approach has been used focusing attention on the sizing methods used in the reviewed works as well as the performance indices used to check quality by these works. In summary there is a clear indication of increased interest in recent years in optimal sizing of hybrid renewable energy resources with metaheuristic approaches such as Genetic Algorithms and Particle Swarm Optimization coming out as very interesting to researchers. It has also been observed that resources being hybridized are those with complementary regimes on specific sites.

Citation

Journal Name: International Journal of Research in Engineering and Technology

eISSN: 2319-1163

pISSN: 2321-7308

Volume: 04

Issue: 11

Pages: 153-163

B: Modelling, Simulation and Optimal Sizing of a Hybrid Wind, Solar PV Power System in Northern Kenya

Abstract

Solar and wind, the most abundant renewable energy resources are still expensive to deploy and are unreliable as they are intermittent. It has long been postulated in open published literature that solar and wind have complementary regimes, and that their reliability can be improved by hybridization. This paper reports on the findings of research examining the problem of optimally sizing a hybrid wind and solar renewable energy power generation system.

In the research, a target site was first identified and meteorological data collected. Components of the system were then mathematically modelled from which an objective function was developed. A parallel multi-deme implementation of genetic algorithm was then used to optimize. Multiple scenarios were prepared and simulated to obtain an optimal configuration of the hybrid power system. The results obtained were validated against openly published results from real word projects. The key findings confirmed that on some locations wind and solar have complementary regimes and can thus be hybridized. To this end an optimal configuration of the system for off-grid deployment was developed with an attractive levelized cost of energy of 17 US cents per kWh. Another finding of the research decoupled resource optimal solutions from cost optimal solutions in that the least cost configuration didn't necessary maximize on the utilization of the abundant resource.

Citation

Journal Name: International Journal of Renewable Energy Research (IJRER)

eISSN: 2319-1163

pISSN: 2321-7308

Volume: To be confirmed Issue: To be confirmed Pages: To be confirmed

Journal acceptance letter received on 23rd July 2016.

ANNEX 2: Datasheets

A: Solar PV Module

Sunmodule™

SW 250 mono / Version 2.0 and 2.5 Frame

World-class quality
Fully-automated production lines and seamless monitoring of the process and material ensure the quality that the company sets as its benchmark for its sites worldwide.

SolarWorld Plus-Sorting
Plus-Sorting guarantees highest system efficiency. SolarWorld only delivers modules that have greater than or equal to the nameplate rated power.

25 years linear performance guarantee and extension of product warranty to 10 years
SolarWorld guarantees a maximum performance degression of 0.7% p.a. in the course of 25 years, a significant added value compared to the two-phase warranties common in the industry. In addition, SolarWorld is offering a product warranty, which has been extended to 10 years.*

*In accordance with the applicable SolarWorld Limited Warranty at purchase.
www.solarworld.com/warranty

Qualified, IEC 61215
Safety tested, IEC 61730
Periodic Inspection

ISO 9001
ISO 14001
Certified

Intertek

US LISTED

Made in USA

SOLARWORLD

We turn sunlight into power.

www.solarworld.com

Sunmodule™

SW 250 mono / Version 2.0 and 2.5 Frame

PERFORMANCE UNDER STANDARD TEST CONDITIONS (STC)*

		SW 250
Maximum power	P_{max}	250 Wp
Open circuit voltage	V_{oc}	37.8 V
Maximum power point voltage	V_{mpp}	31.1 V
Short circuit current	I_{sc}	8.28 A
Maximum power point current	I_{mpp}	8.05 A

*STC: 1000W/m², 25°C, AM 1.5

THERMAL CHARACTERISTICS

NOCT	46 °C
TC I_{sc}	0.004 %/K
TC V_{oc}	-0.30 %/K
TC P_{mpp}	-0.45 %/K
Operating temperature	-40°C to 85°C

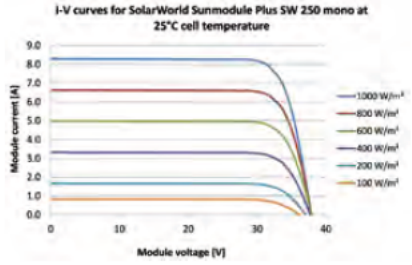

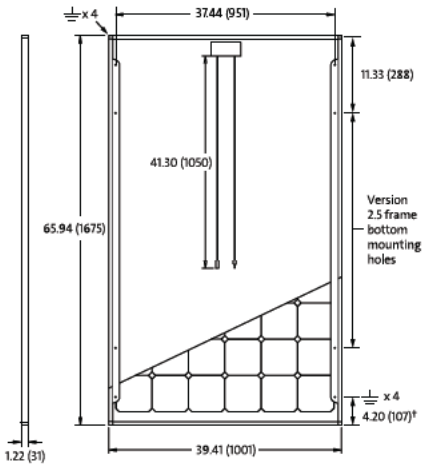

PERFORMANCE AT 800 W/m², NOCT, AM 1.5

		SW 250
Maximum power	P_{max}	183.3 Wp
Open circuit voltage	V_{oc}	34.6 V
Maximum power point voltage	V_{mpp}	28.5 V
Short circuit current	I_{sc}	6.68 A
Maximum power point current	I_{mpp}	6.44 A

Minor reduction in efficiency under partial load conditions at 25°C: at 200W/m², 95% (+/-3%) of the STC efficiency (1000 W/m²) is achieved.

COMPONENT MATERIALS

Cells per module	60
Cell type	Mono crystalline
Cell dimensions	6.14 in x 6.14 in (156 mm x 156 mm)
Front	tempered glass (EN 12150)
Frame	Clear anodized aluminum
Weight	46.7 lbs (21.2 kg)

SYSTEM INTEGRATION PARAMETERS

Maximum system voltage SC II		1000 V
Max. system voltage USA NEC		600 V
Maximum reverse current		16 A
Number of bypass diodes		3
UL Design Loads*	Two rail system	113 psf downward 64 psf upward
UL Design Loads*	Three rail system	170 psf downward 64 psf upward
IEC Design Loads*	Two rail system	113 psf downward 50 psf upward

*Please refer to the Sunmodule installation instructions for the details associated with these load cases.

ADDITIONAL DATA

Power tolerance[2]	-0 Wp / +5 Wp
J-Box	IP65
Connector	MC4
Module efficiency	14.91 %
Fire rating (UL 790)	Class C

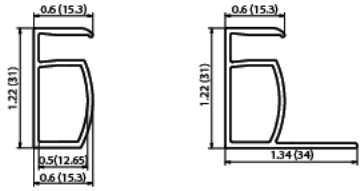

VERSION 2.0 FRAME
- Compatible with "Top-Down" mounting methods
- ⏚ Grounding Locations: 4 corners of the frame

VERSION 2.5 FRAME
- Compatible with both "Top-Down" and "Bottom" mounting methods
- ⏚ Grounding Locations:
  - 4 corners of the frame
  - 4 locations along the length of the module in the extended flange†

1) Sunmodules dedicated for the United States and Canada are tested to UL 1703 Standard and listed by a third party laboratory. The laboratory may vary by product and region. Check with your SolarWorld representative to confirm which laboratory has a listing for the product.
2) Measuring tolerance traceable to TUV Rheinland: +/- 2% (TUV Power Controlled).
3) All units provided are imperial. SI units provided in parentheses.

SolarWorld AG reserves the right to make specification changes without notice.

B: Wind Turbine Generator

rm energy

Wind Technik Nord

WTN250: Turbine Summary

Delivering reliable energy solutions

Wind Technik Nord 250 kW Turbine

WTN250 Key Benefits

- Well-engineered, solid turbine that delivers what it promises
- GL Certified to perform reliably over 20 years
- Global track record with proven 99% availability over 22 years in northern European conditions
- Robust warranty, guarantees and O&M packages
- Based on 100% European, off-the-shelf components from major suppliers and German engineering standards
- Manufacturer is closely linked to the customer through the Warranty
- Product built in Germany by highly experienced engineers
- UK Distributor with bases across Scotland brings 8 years experience of 200+ turbine installations and strong service and maintenance terms
- UK bank approved, UK insurance provider approved, OfGem approved, DNO approved
- Four and a half months delivery times
- Family-owned company that is approachable, located within easy reach and offers you the opportunity to see your turbine being made

RM Energy Ltd, 8 Atholl Crescent, Perth PH1 5NG, T: 0800 046 9843, E: enquiries@rm-energy.co.uk

www.rm-energy.co.uk Delivering reliable energy solutions

Wind Technik Nord WTN250

The WTN250 is a class-leading wind turbine. It is designed and manufactured by Wind Technik Nord (WTN) for the harsh physical environments of northern Europe. It is an ideal solution for UK sites with medium or medium-to-high wind resource and will quality as a 250kW machine for the Feed-in Tariff (FiT). Two turbines can be sited in close proximity to maximise income at the 500kW FiT threshold.

RM Energy is an authorised WTN Distributor with bases across Scotland. The company brings together a staff of 50 with the experience of installing over 200 small and medium scale turbines in the last 8 years. It has been through a rigorous process of WTN training and provides a full-range of services from site design and planning to installation and on-going maintenance and support. With a 2 or 5 year warranty directly with WTN, RM Energy also offers a 10+ year Support and Maintenance package giving complete peace-of-mind. This includes 95% performance and availability guarantees, further re-assurance based on the robustness of the product.

The turbine has evolved over a period of 25 years with upgraded components whilst retaining its reliable construction and high manufacturing quality. To underline this it has been certified under GL 2004 and will soon be certified to the latest GL 2010 standard. This independent certification by a globally recognised wind body is highly onerous on manufacturers. It remains rare at this scale of turbine and demonstrates the WTN commitment to quality, performance and safety.

The track record of the turbine is unrivalled at this scale. Early versions are still spinning after 22 years with more than 99% availability over this period and no major component failures. There is no better measure to demonstrate its proven performance and reliability.

WTN was established in 1986 as a family-owned business in northern Germany committed to the highest standards of wind engineering. It still remains so today. Its size means it is easily approachable and cares deeply about its reputation for quality products that stand the test of time. Its ownership structure means it is financially stable, has a long-term outlook and a sustainable approach to growth in a global market. Its location means it is at the heart of the Danish-German wind industry. Its off-the-shelf components are sourced from high quality manufacturing firms in Germany and Denmark that can guarantee GL certified products.

There is no complex chain of companies involved in supplying and supporting this turbine – components are 100% European, it is manufactured at WTN HQ and sold and supported through RM Energy as an authorised Distributor. Should there ever be a need, it is re-assuring to know that the manufacturer is within easy reach for expert advice, direct support and access to parts. WTN also welcomes visits and can offer tours of the factory and warm German hospitality.

So whether you are a landowner, a business or a wind developer, we invite you to take the 225/250kW Test on our website (www.rm-energy.co.uk) to understand why the WTN250 is a market leader at this scale.

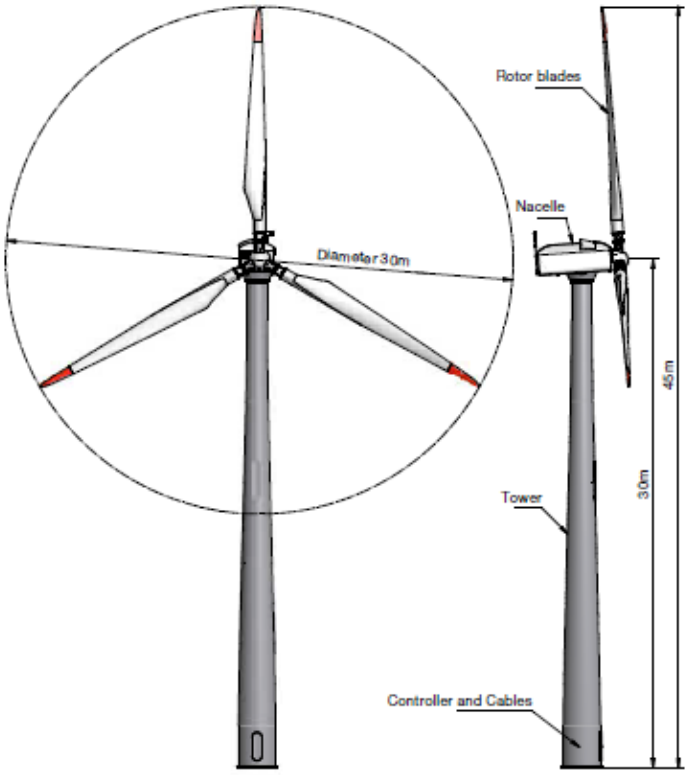

RM Energy Ltd, 8 Atholl Crescent, Perth PH1 5NG, T: 0800 046 9843, E: enquiries@rm-energy.co.uk

Wind Technik Nord WTN250 Turbine Components

Blades and Rotor

The WTN 250 is equipped with a 3-blade, up-wind, stall-regulated rotor. The blades are made of reinforced polyester and are equipped with "fail-safe" tip-brakes, which are activated simultaneously by centrifugal forces. The projected area of the blades ensures the turbine is suited to sites with medium-to-high average wind speeds and means it has a high survival wind speed. With a blade length of 13.4 m and a diameter of 30 m the rotor of the WTN 250 has a swept area of 707 m². The rotor speed is 40 rpm.

Hub

The hub is made of casted steel GGG 40.3 and mounted to the rotor shaft-flange. Correction of the pitch angel of the blades is possible by oval holes in the blade flanges.

Main shaft

The main shaft is a forged piece and made of high-grade alloyed steel. It is mounted in two bearings and able to transfer all forces and moments to the frame and gears.

Main bearings

Two long-time grease lubricated bearings are the basis for a nearly noiseless operation of the main shaft.

Gearbox

A heavy three-stage helical gear transforms the 40 revolutions of the rotor to the 1500 rpm of the generator. This gear is specially designed for the WTN 250 with a gear ratio of 1:37.9. An oil cooler is separately located.

Coupling

The power of the rotor, transformed in the gearbox, is transmitted to the generator by an elastic coupling. With this method no vibrations will reach the bearings of the generator, ensuring minimal wear and a longer lifetime.

Brakes

The turbine is equipped with two independent fail-safe systems. The blades are equipped with a simultaneously activated safety tip-brake and, in addition, the turbine is equipped with a disc brake. The disk braking mechanism is supplied through two hydraulic fail-safe brake callipers which are activated by a loss of supply (grid) voltage.

The tip brakes, in normal operation, and held in position by a hydraulic cylinder. In emergency situations a hydraulic valve is activated by centrifugal forces, and both brake systems are engaged, independently of each other.

Generator

The generator is a pole-changing asynchronous machine with a nominal output of 250 kW at 1500 rpm and 50 kW at 1000 rpm. It is operating on 400V AC level. A ventilator cools the outside of the machine.

Yaw System

The yaw-system is a key technology that differentiates the WTN 250 from many of its rivals. It is based on arranging two gears in a way that eliminates any space in the system. The yaw gear system incorporates both a damping system to decrease forces induced by the turning forces of the rotor, and a brake system, while the yaw motors are stopped.

The system is means the WTN 250 can operate more effectively in situations where there is one or more turbines upwind that can cause exposure to dynamic turning loads.

Nacelle

The hot dip galvanised nacelle is constructed of welded steel beams that support the main shaft, gear and generator. The yaw ring is fitted to the bottom of the frame and allows the connection to the tower. The nacelle can be reached by a ladder inside the tower. The nacelle cover is fully noise insulated and recently re-designed to support 3 metres depth of snow to meet GL 2010 guidelines. Innovative design enables lightning protection to be built into the nacelle cover (together with the blades and tower) to minimise the risk of damage to major components – the WTN 250 is lightning protection Class I meaning it offers the highest level of protection.

Tower

A 30m and 40m welded tubular tower is available. The microprocessor control system is placed at the bottom of the tower. The ladder is supported by a Climbing Support system called LW 50. This is licensed to other larger-scale turbine manufacturers and enables engineers to get themselves, their tools and spare parts up to the nacelle with the minimum of effort. The climbing aid is fully certified to safety standards.

Control panel

All functions of the turbine are controlled through a microprocessor control system inside the bottom of the tower. While the turbine is operational and connected to the grid, the computer stores all operational data. This makes it possible for end-customers to monitor actual performance and authorised engineers to continuously check all sensors and system safety.

RM Energy Ltd, 8 Atholl Crescent, Perth PH1 5NG, T: 0800 046 9843, E: enquiries@rm-energy.co.uk

Wind Technik Nord WTN250

Technical Data

GENERAL	
Nominal Output	250 kW
Number of blades	3
Wind class	Class II A (29m rotor) Class III A (30m rotor)
Avg. wind speed suitability	Medium-to-high avg wind speeds
Wind turbulence suitability	Medium-to-high turbulence (18%)
Certifications	GL 2004, GL 2010 (early 2013)
Rotor shaft arrangement	horizontal
Arrangement of rotor	upwind
Effect limitation	Stall
Mode of operation	Grid connected
Hub height	30 m or 40 m
50 year peak gust	59.5 resp. 52.5 m/s
Lightning class	I (the highest)
Calculated design life	20 years
Service regime	Twice annually
POWER	
Cut in windspeed	4 m/s
Rated windspeed	14 m/s
Power at 10 m/s	151.8 kW
Cut off windspeed	25 m/s
Max. shaft power	300 kW
Specified output	378 W/m²
ROTOR	
Diameter	29 m or 30 m
Swept area	661 m² or 707 m²
Arrangement of rotor	upwind
Rotor speed	26 / 40 rpm
BLADE	
Type	LM 13.4
Material	Glass fibre
Length of blade	13.39 m
YAW SYSTEM	
Type (active / passive)	active
Actuation	electrical
GENERATOR	
Type	asynchronous, pole-changeable
Rated output	250 kW
Rated speed	1515 rpm
Voltage	400 V ±10%
Frequency	50 Hz ±5%
TOWER	
Type	Tubular steel monopole
Length	30 m or 40 m
Safety ladder	Internal and power assisted
CONTROL SYSTEM	
Kind of output control	Stall regulation
Remote control system	via telephone line
Scada system	Gateway
BRAKES	
Aerodynamic brakes	Tip brakes
Mechanical brakes	Disc brake
WEIGHTS	
Rotor (with hub)	3.550 kg + 650 kg (30 m)
Nacelle (without rotor)	9.750 kg
Tower weight	11.500 kg (30m) or 21.000 kg (40m)
Total without foundation	25.200 kg (30m) or 34.700 kg (40m)

Energy Production

WTN250 Power Curve

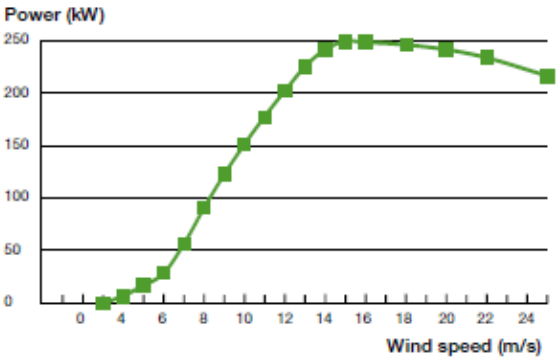

Wind at hub height (m/s)	Output kW	Wind at hub height (m/s)	Output kW	Wind at hub height (m/s)	Output kW
3	0.0	9	123.3	15	250.0
4	7.5	10	151.8	16	249.1
5	17.3	11	178.4	18	246.7
6	28.9	12	202.7	20	242.1
7	56.9	13	225.9	22	234.4
8	91.1	14	242.2		

Annual Energy Production (AEP)

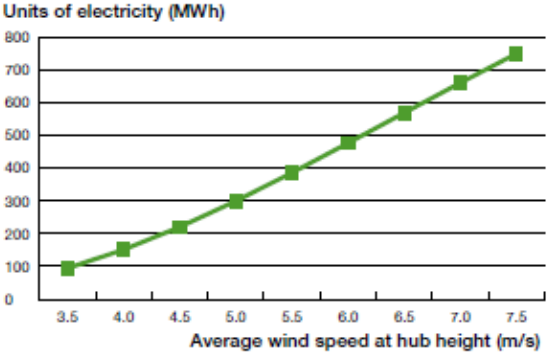

Average Wind speed at hub height m/s	Approx energy yield per annum MWh	Capacity factor % / year full load	Average Wind speed at hub height m/s	Approx energy yield per annum MWh	Capacity factor % / year full load
3.5	95	4.4%	6.0	478	22.1%
4.0	152	7.0%	6.5	571	26.4%
4.5	221	10.2%	7.0	667	30.7%
5.0	301	13.9%	7.5	752	34.8%
5.5	387	17.9%			

Figures based on 360 days/yr availability and the 30m rotor diameter.

All output figures provided above are GL certified and a result of rigorous, independent tests.

RM Energy Ltd, 8 Atholl Crescent, Perth PH1 5NG, T: 0800 046 9843, E: enquiries@rm-energy.co.uk

C: Battery Unit

NP SERIES - **NP7-12**

Reliability is your Security

Yuasa NP, NPC and NPH Batteries. Utilising the latest advance design Oxygen Recombination Technology, Yuasa have applied their 80 years experience in the lead acid battery field to produce the optimum design of Sealed Lead Acid batteries.

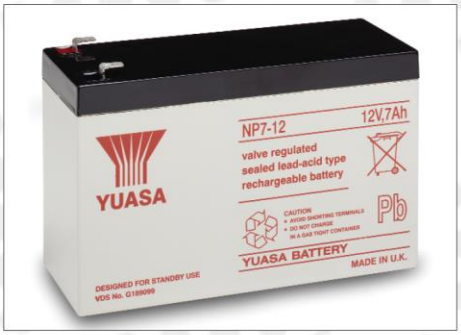

FEATURES

- Superb recovery from deep discharge.
- Electrolyte suspension system.
- Gas Recombination.
- Multipurpose: Float or Cyclic use.
- Usable in any orientation (except continuous inverted).
- Superior energy density.
- Lead calcium grids for extended life.
- Manufactured World wide.
- Application specific designs.

Technical Features

Sealed Construction
Yuasa's unique construction and sealing technique ensures no electrolyte leakage from case or terminals

Electrolyte Suspension System
All NP batteries utilize Yuasa's unique electrolyte suspension system incorporating a microfine glass mat to retain the maximum amount of electrolyte in the cells. The electrolyte is retained in the separator material and there is no free electrolyte to escape from the cells. No gels or other contaminants are added.

Control of Gas Generation
The design of Yuasa's NP batteries incorporates the very latest oxygen recombination technology to effectively control the generation of gas during normal use.

Low Maintenance Operation
Due to the perfectly sealed construction and the recombination of gasses within the cell, the battery is almost maintenance free.

Terminals
NP batteries are manufactured using a range of terminals which vary in size and type. Please refer to details as shown.

Operation in any Orientation
The combination of sealed construction and Yuasa's unique electrolyte suspension system allows operation in any orientation, with no loss of performance or fear of electrolyte leakage. (Excluding continuous use inverted)

Valve Regulated Design
The batteries are equipped with a simple, safe low pressure venting system which releases excess gas and automatically reseals should there be a build up of gas within the battery due to severe overcharge. Note. On no account should the battery be charged in a sealed container.

Layout

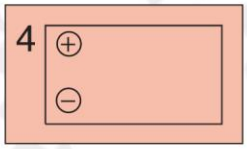

General Specifications

Nominal Capacity (Ah)	NP7-12
20hr to 1.75vpc 30°C	7
10hr to 1.75vpc 20°C	6.4
5hr to 1.70vpc 20°C	5.9
1hr to 1.60vpc 20°C	4.2
Voltage	12
Energy Density (Wh.L.20hr)	91
Specific Energy (Wh.kg.20hr)	32
Int. Resistance (m.Ohms)	25
Maximum discharge (A)	40/75
Short Circuit current (A)	210
Dimensions (mm)	
Length	151
Width	65
Height overall	97.5
Weight (Kg)	2.65
Terminal	A/D
Layout	4
Terminal Torque Nm	-

Terminals

Faston tab: 187 **A**

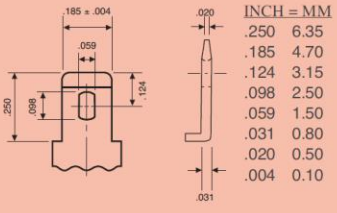

INCH	= MM
.250	6.35
.185	4.70
.124	3.15
.098	2.50
.059	1.50
.031	0.80
.020	0.50
.004	0.10

Faston tab: 250 **D**

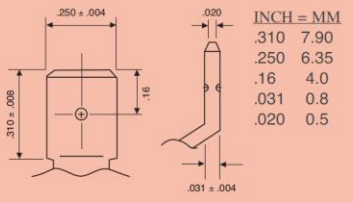

INCH	= MM
.310	7.90
.250	6.35
.16	4.0
.031	0.8
.020	0.5

NP SERIES - **NP7-12**

Data Sheet

Lead Calcium Grids
The heavy duty lead calcium alloy grids provide an extra margin of performance and life in both cyclic and float applications and give unparalleled recovery from deep discharge.

Long Cycle Service Life
Depending upon the average depth of discharge, over a thousand discharge/charge cycles can be expected.

Float Service Life
The expected service life is five years in float standby applications.

Separators
The use of the special separator material provides a very efficient insulation between plates preventing inter-plate short circuits and prohibiting the shedding of active materials.

Long shelf Life
The extremely low self discharge rate allows the battery to be stored for extended periods up to one year at normal ambient temperatures with no permanent loss of capacity.

Operating Temperature Range
The batteries can be used over a broad temperature range permitting considerable flexibility in system design and location.

Charge	– 15°C to 50°C
Discharge	– 20°C to 60°C
Storage	– 20°C to 50°C (fully charged battery)

CYCLIC RECHARGE REGIME

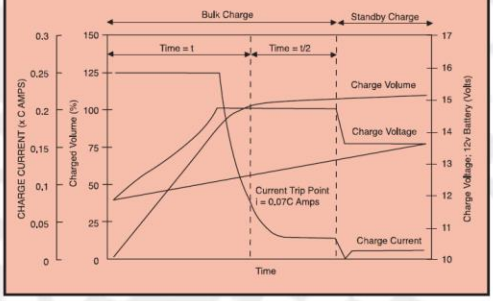

NP DISCHARGE CHARACTERISTICS CURVES AT 25ºC (77ºF)

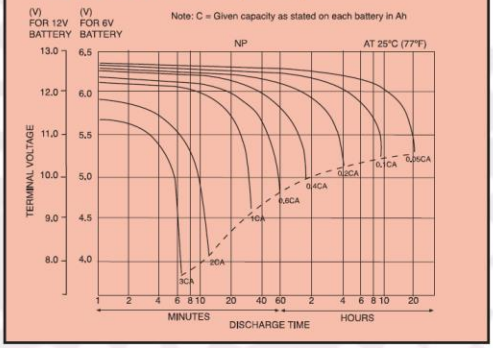

FLOAT SERVICE LIFE NP RANGE

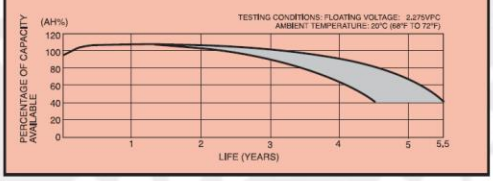

SELF DISCHARGE CHARACTERISTICS

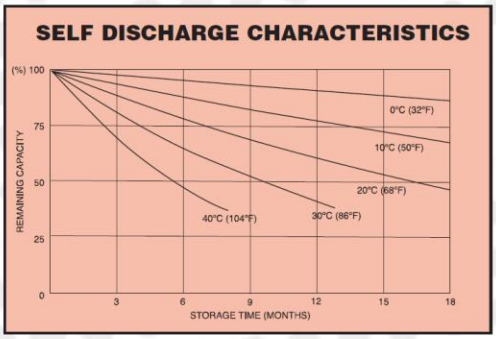

FLOAT CHARGE CHARACTERISTICS

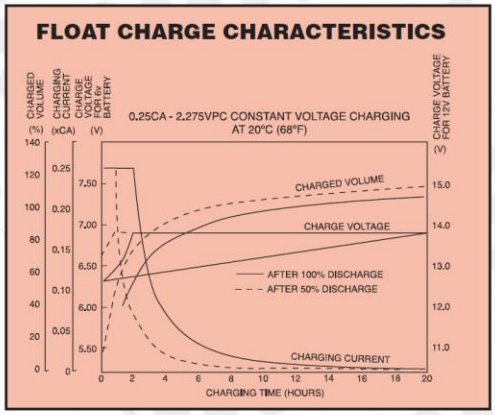

TYPICAL DISCHARGE CHARACTERISTICS NP RANGE

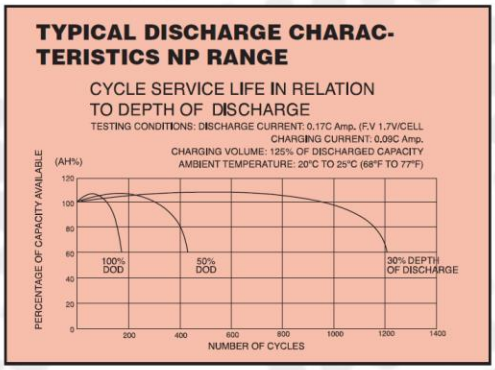

NP SERIES - **NP7-12**

Data Sheet

INTELLIGENT BATTERY CHARGERS

Manufactured to BS3456, IEC335, UL 1236, EN60335, CE mark to EN5008-1

Features

Micro processor controlled
Short circuit protection
Reverse polarity protection
High temperature protection
Soft start current control
Fast constant current bulk charge
3 stage charging CI-CV-float
Constant voltage float/standby
Proportional timing
Flexibility, to match battery specification.

Standard Range

YCP03A12	300mA 12v
YCP03A24	300mA 24v
YCP03A6	300mA 6v
YCP06A12	600mA 12v
YCP06A6	600mA 6v
YCP1.5A12	1.5A 12v
YCP1.5A24	1.5A 24v
YCP1.5A6	1.5A 6v
YCP1A12	1A 12v
YCP1A6	1A 6v
YCP2A12	2A 12v
YCP2A24	2A 24v
YCP2A6	2A 6v
YCP3A12	3A 12v
YCP4A12	4A 12v
YCP6A12	6A 12v
YCP8A12	8A 12v
YCP10A12	10A 12v
YCP8A24	8A 24v

RELATIONSHIP BETWEEN CHARGING VOLTAGE AND TEMPERATURE

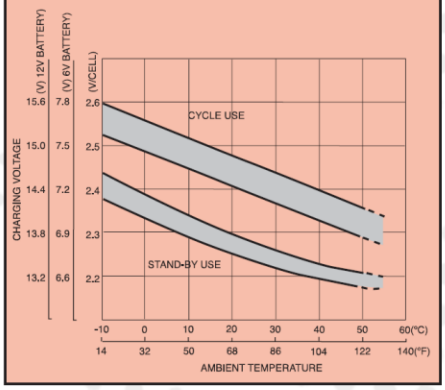

NPH DISCHARGE CHARACTERISTIC CURVES

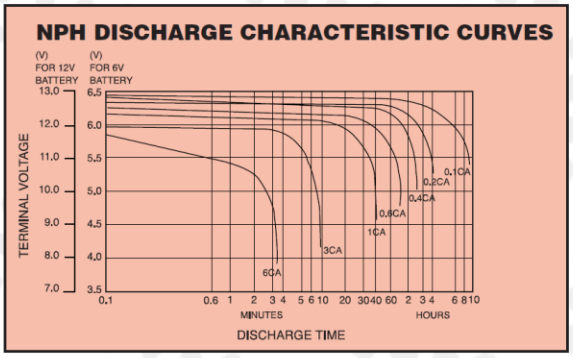

Standard NP

Available in a wide range of sizes to suit general applications.

NPH/NPW

High performance batteries specially designed for applications requiring high rate discharge, supplying up to 50% (NPH), (NPW) more power (Watts) for short durations when compared to conventional NP models.

NPC

Specifically designed to suit the arduous requirements of cyclic applications allowing increased cycle life (at least double that of conventional types). (NPC Shortform refers)

NPL

Long Life Model also to BS6290pt4 (FR Options)
Dedicated literature available on request. (NPL Shortform refers).

Applications

Yuasa NP batteries, having excellent deep discharge recovery characteristics coupled with long life on float standby, are ideal for numerous applications in both cyclic and standby modes. For advice on the use of NP batteries in your particular application please contact our Sales Office.

Charging For Float Standby Applications

Charged at 2.275 volts per cell continuous. The battery will seek its own current level and float fully charged. However, users should be aware that when charging from fully discharged, the battery can draw an initial charge current of approximately 2cA. Care should therefore be taken to ensure that this initial charge current (if ungoverned) is within the output capability of the equipment. Final charge current at 2.275 volts per cell is typically between 0.0005cA to 0.004cA.

Charging For Cyclic Applications

See cyclic recharge regime graph.

CAUTION

- Do not Short Circuit
- Do not charge in a sealed container
- Service life and operational characteristics will be affected by temperature
- AC Ripple reduces service life.

Yuasa Battery Corp
Unit 22 Rassau Industrial Estate
Ebbw Vale, Gwent, NP23 5SD
Tel: 08708 506312 Fax: 08708 506317
Registered number 1548820

Cat. No.	NP7-12 February 07

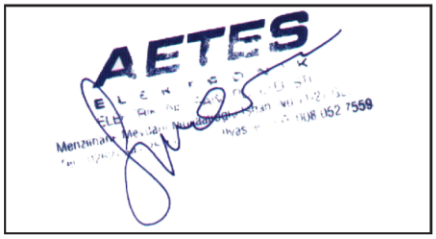

ANNEX 3: MATLAB code

Runner.m

```
%%Call optimization function
% Syntax:: [x,fval,exitflag,output,population,score] =
optim_ga(nvars,lb,ub,PopulationSize_Data,EliteCount_Data,CrossoverFraction_Da
ta,MigrationInterval_Data,MigrationFraction_Data,TolFun_Data)
%Function params
nvars = 3;
lb=[1358 3 7280];
ub = [13580 30 12800];
PopulationSize_Data=[20 20 20 20];
EliteCount_Data = 3;
CrossoverFraction_Data = 0.75;
MigrationInterval_Data = 10;
MigrationFraction_Data = 0.1;
TolFun_Data = 1e-5;
% call function
[x,fval,exitflag,output,population,score] =
optim_ga(nvars,lb,ub,PopulationSize_Data,EliteCount_Data,CrossoverFraction_Da
ta,MigrationInterval_Data,MigrationFraction_Data,TolFun_Data);
```

Optimga.m

```
function [x,fval,exitflag,output,population,score] =
optim_ga(nvars,lb,ub,PopulationSize_Data,EliteCount_Data,CrossoverFraction_Da
ta,MigrationInterval_Data,MigrationFraction_Data,TolFun_Data)
%% Preload Data and Configurations.
[HWSPSData,HWSPSConf] = loader('Data-Matrix.xlsx');
%% Start with the default options
options = gaoptimset;

%% Modify options setting
options = gaoptimset(options,'PopulationSize', PopulationSize_Data);
options = gaoptimset(options,'EliteCount', EliteCount_Data);
options = gaoptimset(options,'CrossoverFraction', CrossoverFraction_Data);
options = gaoptimset(options,'MigrationDirection', 'both');
options = gaoptimset(options,'MigrationInterval', MigrationInterval_Data);
options = gaoptimset(options,'MigrationFraction', MigrationFraction_Data);
options = gaoptimset(options,'TolFun', TolFun_Data);
options = gaoptimset(options,'CreationFcn', @gacreationlinearfeasible);
options = gaoptimset(options,'SelectionFcn', @selectionroulette);
options = gaoptimset(options,'CrossoverFcn', {  @crossoverheuristic [] });
options = gaoptimset(options,'MutationFcn', @mutationadaptfeasible);
options = gaoptimset(options,'Display', 'iter');
options = gaoptimset(options,'PlotFcns', {  @gaplotbestf @gaplotbestindiv
@gaplotdistance @gaplotexpectation @gaplotgenealogy @gaplotrange
@gaplotscorediversity @gaplotscores @gaplotselection @gaplotstopping
@gaplotmaxconstr });
options = gaoptimset(options,'OutputFcns', { @outputfunc });
options = gaoptimset(options,'Vectorized', 'off');
options = gaoptimset(options,'UseParallel', 'always');
[x,fval,exitflag,output,population,score] = ...
```

```
ga(@(x)(fitnessfunc_ser(x,HWSPSData,HWSPSConf)),nvars,[],[],[],[],lb,ub,[],[]
,options);
```

loader.m

```
function [HWSPSData,HWSPSConf] = loader (File)
%This script preloads all necessary data to the workspace
%%Preload Data preprocessing Matrix
%   Sheets
%   1&2. Demand  "Load"
    Demand = xlsread(File,'Load','D2:E8761');
%   3&4&5. Solar Resource "Solar"
    Solar = xlsread(File,'Solar','G2:I8761');
%   6. Wind  Resource "Wind"
    Wind = xlsread(File,'Wind','D2:D8761');
%Output Data
   HWSPSData = cat(2,Demand,Solar, Wind);
%% Load configuration
   HWSPSConf = xlsread(File,'Conf','B1:B50');
end
```

gaOptimSet.m

```
function options = gaoptimset(varargin)
%GAOPTIMSET Create/alter GA OPTIONS structure.
%   GAOPTIMSET returns a listing of the fields in the options structure as
%   well as valid parameters and the default parameter.

if (nargin == 0) && (nargout == 0)
    fprintf('          PopulationType: [ ''bitstring''      | ''custom''    |
{''doubleVector''} ]\n');
    fprintf('            PopInitRange: [ matrix           | {[0;1]} ]\n');
    fprintf('          PopulationSize: [ positive scalar ]\n');
    fprintf('             EliteCount: [ positive scalar  | {2} ]\n');
    fprintf('       CrossoverFraction: [ positive scalar  | {0.8} ]\n\n');
    fprintf('          ParetoFraction: [ positive scalar  | {0.35} ]\n\n');

    fprintf('      MigrationDirection: [ ''both''           | {''forward''}
]\n');
    fprintf('       MigrationInterval: [ positive scalar  | {20} ]\n');
    fprintf('       MigrationFraction: [ positive scalar  | {0.2} ]\n\n');

    fprintf('             Generations: [ positive scalar ]\n');
    fprintf('               TimeLimit: [ positive scalar  | {Inf} ]\n');
    fprintf('            FitnessLimit: [ scalar           | {-Inf} ]\n');
    fprintf('           StallGenLimit: [ positive scalar ]\n');
    fprintf('          StallTimeLimit: [ positive scalar  | {Inf} ]\n');
    fprintf('                  TolFun: [ positive scalar ]\n\n');
    fprintf('                  TolCon: [ positive scalar  | {1e-6} ]\n\n');

    fprintf('       InitialPopulation: [ matrix           | {[]} ]\n');
    fprintf('           InitialScores: [ column vector    | {[]} ]\n\n');
```

```
    fprintf('          InitialPenalty: [ positive scalar | {10} ]\n');
    fprintf('           PenaltyFactor: [ positive scalar | {100} ]\n\n');

    fprintf('             CreationFcn: [ function_handle  |
@gacreationuniform | @gacreationlinearfeasible ]\n');
    fprintf('       FitnessScalingFcn: [ function_handle  |
@fitscalingshiftlinear  | @fitscalingprop  | \n');
    fprintf('                            @fitscalingtop   | {@fitscalingrank}
]\n');
    fprintf('           SelectionFcn: [ function_handle  |
@selectionremainder    | @selectionuniform | \n');
    fprintf('                            @selectionroulette |
@selectiontournament   | @selectionstochunif ]\n');
    fprintf('           CrossoverFcn: [ function_handle  |
@crossoverheuristic  | @crossoverintermediate | \n');
    fprintf('                            @crossoversinglepoint |
@crossovertwopoint | @crossoverarithmetic | \n');
    fprintf('                            @crossoverscattered ]\n');
    fprintf('             MutationFcn: [ function_handle  | @mutationuniform
| @mutationadaptfeasible | \n');
    fprintf('                            @mutationgaussian ]\n');
    fprintf('      DistanceMeasureFcn: [ function_handle  |
{@distancecrowding} ]\n');
    fprintf('               HybridFcn: [ @fminsearch | @patternsearch |
@fminunc | @fmincon | {[]} ]\n\n');

    fprintf('                 Display: [ ''off'' | ''iter'' | ''diagnose'' |
{''final''} ]\n');
    fprintf('              OutputFcns: [ function_handle  | {[]} ]\n');
    fprintf('                PlotFcns: [ function_handle  | @gaplotbestf |
@gaplotbestindiv | @gaplotdistance | \n');
    fprintf('                            @gaplotexpectation |
@gaplotgenealogy | @gaplotselection | @gaplotrange | \n');
    fprintf('                            @gaplotscorediversity  |
@gaplotscores | @gaplotstopping  | \n');
    fprintf('                            @gaplotmaxconstr | @gaplotrankhist |
@gaplotpareto | @gaplotspread | \n');
    fprintf('                            @gaplotparetodistance |{[]} ]\n');
    fprintf('            PlotInterval: [ positive scalar  | {1} ]\n\n');

    fprintf('              Vectorized: [ ''on''  | {''off''} ]\n\n');
    fprintf('             UseParallel: [ ''always'' | {''never''} ]\n');
    return;
end

numberargs = nargin;

%Return options with default values and return it when called with one output
argument
options=struct('PopulationType', [], ...
               'PopInitRange', [], ...
               'PopulationSize', [], ...
               'EliteCount', [], ...
               'CrossoverFraction', [], ...
               'ParetoFraction', [], ...
               'MigrationDirection',[], ...
```

```
                'MigrationInterval',[], ...
                'MigrationFraction',[], ...
                'Generations', [], ...
                'TimeLimit', [], ...
                'FitnessLimit', [], ...
                'StallGenLimit', [], ...
                'StallTimeLimit', [], ...
                'TolFun', [], ...
                'TolCon', [], ...
                'InitialPopulation',[], ...
                'InitialScores', [], ...
                'InitialPenalty', [], ...
                'PenaltyFactor', [], ...
                'PlotInterval',[], ...
                'CreationFcn',[], ...
                'FitnessScalingFcn', [], ...
                'SelectionFcn', [], ...
                'CrossoverFcn',[], ...
                'MutationFcn',[], ...
                'DistanceMeasureFcn',[], ...
                'HybridFcn',[], ...
                'Display', [], ...
                'PlotFcns', [], ...
                'OutputFcns', [], ...
                'Vectorized',[], ...
                'UseParallel', []);


% If we pass in a function name then return the defaults.
if (numberargs==1) && (ischar(varargin{1}) ||
isa(varargin{1},'function_handle') )
    if ischar(varargin{1})
        funcname = lower(varargin{1});
        if ~exist(funcname)

error(message('globaloptim:GAOPTIMSET:functionNotFound',funcname));
        end
    elseif isa(varargin{1},'function_handle')
        funcname = func2str(varargin{1});
    end
    try
        optionsfcn = feval(varargin{1},'defaults');
    catch
        error(message('globaloptim:GAOPTIMSET:noDefaultOptions',funcname));
    end
    % To get output, run the rest of psoptimset as if called with
gaoptimset(options, optionsfcn)
    varargin{1} = options;
    varargin{2} = optionsfcn;
    numberargs = 2;
end

Names = fieldnames(options);
m = size(Names,1);
names = lower(Names);
```

```
i = 1;
while i <= numberargs
    arg = varargin{i};
    if ischar(arg)                          % arg is an option name
        break;
    end
    if ~isempty(arg)                       % [] is a valid options argument
        if ~isa(arg,'struct')
            error(message('globaloptim:GAOPTIMSET:invalidArgument', i));
        end
        for j = 1:m
            if any(strcmp(fieldnames(arg),Names{j,:}))
                val = arg.(Names{j,:});
            else
                val = [];
            end
            if ~isempty(val)
                if ischar(val)
                    val = deblank(val);
                end
                checkfield(Names{j,:},val);
                options.(Names{j,:}) = val;
            end
        end
    end
    i = i + 1;
end

% A finite state machine to parse name-value pairs.
if rem(numberargs-i+1,2) ~= 0
    error(message('globaloptim:GAOPTIMSET:invalidArgPair'));
end
expectval = 0;                           % start expecting a name, not a value
while i <= numberargs
    arg = varargin{i};

    if ~expectval
        if ~ischar(arg)
            error(message('globaloptim:GAOPTIMSET:invalidArgFormat', i));
        end

        lowArg = lower(arg);
        j = strmatch(lowArg,names);
        if isempty(j)                         % if no matches
            error(message('globaloptim:GAOPTIMSET:invalidParamName', arg));
        elseif length(j) > 1                  % if more than one match
            % Check for any exact matches (in case any names are subsets of
others)
            k = strmatch(lowArg,names,'exact');
            if length(k) == 1
                j = k;
            else
                allNames = ['(' Names{j(1),:}];
                for k = j(2:length(j))'
                    allNames = [allNames ', ' Names{k,:}];
                end
```

```
                allNames = sprintf('%s).', allNames);

error(message('globaloptim:GAOPTIMSET:ambiguousParamName',arg,allNames));
            end
        end
        expectval = 1;                      % we expect a value next

    else
        if ischar(arg)
            arg = (deblank(arg));
        end
        checkfield(Names{j,:},arg);
        options.(Names{j,:}) = arg;
        expectval = 0;
    end
    i = i + 1;
end

if expectval
    error(message('globaloptim:GAOPTIMSET:invalidParamVal', arg));
end


%---------------------------------------------------
function checkfield(field,value)
%CHECKFIELD Check validity of structure field contents.
%   CHECKFIELD('field',V) checks the contents of the specified
%   value V to be valid for the field 'field'.
%

% empty matrix is always valid
if isempty(value)
    return
end

switch field
    case {'PopulationType','MigrationDirection'}
        if ~isa(value,'char')

error(message('globaloptim:GAOPTIMSET:checkfield:NotAString','OPTIONS',field)
);
        end

    case {'FitnessScalingFcn','SelectionFcn','CrossoverFcn','MutationFcn',...

'CreationFcn','HybridFcn','PlotFcns','OutputFcns','DistanceMeasureFcn'}
        if ~(iscell(value) ||  isa(value,'function_handle'))

error(message('globaloptim:GAOPTIMSET:checkfield:NotAFunctionOrCellArray','OP
TIONS',field));
        end

    case
{'ParetoFraction','EliteCount','CrossoverFraction','MigrationInterval','PlotI
nterval','TolCon', ...
```

```
'TolFun','MigrationFraction','TimeLimit','StallTimeLimit','FitnessLimit','Sta
llGenLimit'}
        if ~isa(value,'double')
            if ischar(value)

error(message('globaloptim:GAOPTIMSET:checkfield:NotAPosRealNumButString','OP
TIONS',field));
            else

error(message('globaloptim:GAOPTIMSET:checkfield:NotAPosRealNum','OPTIONS',fi
eld));
            end
        end
    case
{'PopInitRange','InitialPopulation','InitialScores','InitialPenalty','Penalty
Factor'}
       % The content is checked elsewhere.
    case {'Display'}
        if ~isa(value,'char') ||
~any(strcmpi(value,{'off','none','iter','diagnose','final'}))

error(message('globaloptim:GAOPTIMSET:checkfield:NotADisplayType','OPTIONS',f
ield,'off','iter','diagnose','final'));
        end
    case {'Vectorized'}
        if ~isa(value,'char') || ~any(strcmp(value,{'on','off'}))

error(message('globaloptim:GAOPTIMSET:checkfield:NotOnOrOff','OPTIONS',field,
'off','on'));
        end
     case {'Generations'} % integer including inf or default string
        if ~(isscalar(value) && isa(value,'double') && value >= 0) && ...
                ~strcmpi(value, '200*numberOfVariables')
            if ischar(value)

error(message('globaloptim:GAOPTIMSET:checkfield:NotAPosNumericScalarButStrin
g','OPTIONS',field));
            else

error(message('globaloptim:GAOPTIMSET:checkfield:NotAPosNumericScalar','OPTIO
NS',field));
            end
        end

    case {'PopulationSize'} % integer including inf or default string
        if ~(isa(value,'double') && all(value(:) >= 0)) && ...
                ~strcmpi(value,'15*numberOfVariables')
            if ischar(value)

error(message('globaloptim:GAOPTIMSET:checkfield:NotAPosNumericButString','OP
TIONS',field));
            else

error(message('globaloptim:GAOPTIMSET:checkfield:NotAPosNumeric','OPTIONS',fi
eld));
            end
```

```
        end

    case 'UseParallel'
        if ~ischar(value)

error(message('globaloptim:GAOPTIMSET:checkfield:NotNeverOrAlways','OPTIONS',
field,'never','always'));
        end

    otherwise
        error(message('globaloptim:GAOPTIMSET:unknownOptionsField'))
end
```

fitnessfunc_ser.m

```
function LCOE  = fitnessfunc_ser(x,HWSPSData,HWSPSConf)
%fitnessfunc Function to evaluate solution fitness
%   evaluates suitability of a configuration.
%   evaluates LPSP and LCOE

%Layouts
Npv = x(1);Nwtg = x(2);Nbess=x(3);
%Declare globals
%global HWSPSData; global HWSPSConf;
%%   1. Read configuration
        PVConf = HWSPSConf(2:10);WTGConf = HWSPSConf(12:20); BESSConf =
HWSPSConf(22:30); CRF = HWSPSConf(34);EFF = HWSPSConf(37:40);
        LPSPThrshld = HWSPSConf(43);DSM = HWSPSConf(44);SPT=HWSPSConf(45);
%   Panel constants
%       (1)Ppvr - rated unit capacity (W),(2)fpv - derating factor,(3)Gstc -
STC irradiance,(4) Tstc - STC temperature,(5)alpha_t -
%       temperature coefficient (7) -  (8)CCPV - Overnight
%       Capital Cost, (9)FOMPV - Fixed O&M Costs, (10) IEF - Inverter
%       Efficiency
%       Costs.
        Ppvr = PVConf(1);fpv
=PVConf(2);Gstc=PVConf(3);Tstc=PVConf(4);alpha_t=PVConf(5);CCPV=PVConf(7);FOM
PV=PVConf(8);
%   WTG Constants
%       (1)Pwtgr - rated unit capacity (W),(2)v_in - Cut In speed (m/s),(3)
v_r - Rated
%       Speed (m/s),(4) v_out - Cut Off Speed (m/s), (5)CCWTG - Overnight
%       Capital Cost, (6) FOMWTG - Fixed O&M , (7) VOMWTG - Variable O&M
%       (8) - Hub Height, (9) TEF - Transformer Efficiency
        Pwtgr =
WTGConf(1);v_in=WTGConf(2);v_r=WTGConf(3);v_out=WTGConf(4);CCWTG=WTGConf(5);F
OMWTG = WTGConf(6); VOMWTG = WTGConf(7);

%   BESS constants
%       (1)PBr - unit BESS size (kW),(2)SDR - Self Discharge Rate,(3)Cbess -
BESS rating
%       in AH, (4)Vbess - BESS Voltage rating, (5) DOD_Max - Maximum Depth
%       of Discharge, (6) CCBESS - Overnight Capital Cost (7)FOMBESS -
%       Fixed O&M
```

```
        PBr = BESSConf(1);SDR = BESSConf(2);Cbess = BESSConf(3);Vbess =
BESSConf(4);DOD_max = BESSConf(5);CCBESS =
BESSConf(6);FOMBESS=BESSConf(7);RTEF = BESSConf(8);

% Converters
%       DCDC - DC to DC Boost converter, ACDC - AC to Dc Power rectifiers,
%       DCAC - Inverter, ACAC - Step up transformer.
        DCDC = EFF(1);ACDC = EFF(2);DCAC = EFF(3);ACAC=EFF(4);

%%   2. Load Data
        switch DSM
            case 1
                Demand = HWSPSData(:,2); % Simulate Demand Side Management
            case 0
                Demand = HWSPSData(:,1);% No Demand Side Management
        end
        switch SPT
            case 1
                Solar = HWSPSData(:,4:5);% simulate PV trackers
            case 0
                Solar = cat(2,HWSPSData(:,3),HWSPSData(:,5));% Do NOT
simulate PV trackers
        end
        Wind=HWSPSData(:,6);


%%   3. Calculate LPSP
%      a. Iterative loop through all timesteps
        %prep matrices
        Pg = zeros(8760,1);SOC=zeros(8760,1);Ppvg=zeros(8760,1);
        Pwtg = zeros(8760,1);Pbess=zeros(8760,1);Pl=zeros(8760,1);
        %prep sum values
        SPlPg = 0; SPl=0;LPSP=0;LCOE=0;SPwtg=0;SPpvg=0;SPbess=0;LPS=0;
        %Demand adjusted as seen on DC Bus
        Pl = Demand/(DCAC*ACAC);
        % initial charge set to 1-DOD_max
        SOC(1) = 1-DOD_max;
        for t=1:8760
%           ii. Evaluate Pg(ti) - All calculation on DC Bus
%                   Evaluate Ppvg
                    Ppvg(t) =
DCDC*fpv*Npv*Ppvr*(Solar(t,1)/Gstc)*(1+alpha_t*(Solar(t,2)-Tstc));

%                   Evaluate Pwtg
                    if  Wind(t) < v_in
                            Pwtg(t)=0;
                    elseif (Wind(t)>v_in)&&(Wind(t)<v_r)
                            Pwtg(t) = ACDC*Nwtg*Pwtgr*((Wind(t)-v_in)/(v_r-
v_in));
                    else
                            Pwtg(t) =
ACDC*Nwtg*Pwtgr*rectangularPulse((Wind(t)-(v_out+v_r)/2)/(v_out-v_r));
                    end;

%                   Evaluate Pg
                    Pg(t) = Pwtg(t)+Ppvg(t);
```

```
%                   Energy Summations
                    SPl = SPl + Pl(t);
%                   Check if Pg is greater than Demand
                  if t>1
                    if Pg(t)>Pl(t)
                        % Demand met, extra power to charge BESS
                        SOC(t) = SOC(t-1)*(1-SDR/24)+ (DCDC*RTEF*(Pg(t)-
Pl(t)))/(Nbess*PBr);
                        SOC(t) = limits(1-DOD_max,SOC(t),1);
                        %calculate actual power delivered from wind
                        SPwtg = SPwtg + (Pwtg(t)/Pg(t)*(Pl(t)+(SOC(t)-SOC(t-
1))*1/(DCDC*RTEF)*Nbess*PBr));
                        %calculate actual power delivered from solar
                        SPpvg = SPpvg + (Ppvg(t)/Pg(t)*(Pl(t)+(SOC(t)-SOC(t-
1))*1/(DCDC*RTEF)*Nbess*PBr));
                    else
                        %Check if Demand will be met with input from BESS
                        if (Pg(t)+DCDC*Nbess*PBr*(SOC(t-1)+DOD_max-1))>Pl(t)
                            %Demand met, update SOC
                            SOC(t) = SOC(t-1)*(1-SDR/24)-(Pl(t)-
Pg(t))/(DCDC*Nbess*PBr);
                            SOC(t) = limits(1-DOD_max,SOC(t),1);
                            SPbess = SPbess + (Pl(t)-Pg(t));
                            %check that DOD-max not violated
                            if SOC(t)<1-DOD_max
                                %Demand will not be met without violation, DO
not Discharge from
                                %batteries, overwrite calculate present
                                %state of charge
                                LPS = LPS+1;
                                SOC(t) = SOC(t-1)*(1-SDR/24);
                            else
                                SOC(t) = limits(1-DOD_max,SOC(t),1);
                                if Pg~=0
                                %calculate actual power delivered from wind
                                SPwtg = SPwtg + (Pwtg(t)/Pg(t)*(Pl(t)-(SOC(t-
1)-SOC(t))*DCDC*Nbess*PBr));
                                %calculate actual power delivered from solar
                                SPpvg = SPpvg + (Ppvg(t)/Pg(t)*(Pl(t)-(SOC(t-
1)-SOC(t))*DCDC*Nbess*PBr));
                                end
                            end

                        else
                            %Demand not met
                            LPS = LPS+1;
                            SOC(t) = SOC(t-1)*(1-SDR/24);
                        end

                    end
                  else
                      if Pg(t)> Pl(t)
                        %Calculate actual power delivered from wind
                        SPwtg = SPwtg +
(Pwtg(t)/Pg(t)*(Pl(t)+(SOC(t)+DOD_max-1)*1/(DCDC*RTEF)*Nbess*PBr));
                        %calculate actual power delivered from solar
```

```
                            SPpvg = SPpvg +
(Ppvg(t)/Pg(t)*(Pl(t)+(SOC(t)+DOD_max-1)*1/(DCDC*RTEF)*Nbess*PBr));
                        end
                    end


        end
%       Evaluate LPSP
        LPSP = LPS/8760;
%%   4. (Optional) Check if LPSP within allowed range and proceed or quit
        if LPSP > LPSPThrshld
            %THreshold not met, exit no need to calculate LCOE, return
            %negative LCOE, solution will be discarded.
            LCOE = NaN;
        else
%%  5. Calculate LCOE
%       a. Solar PV (SLCOE)
        SLCOE = Npv*Ppvr*(CCPV*CRF+FOMPV)/SPpvg;
%       b. Wind TG (WLCOE)
        WLCOE = (Nwtg*Pwtgr*(CCWTG*CRF+FOMWTG)/SPwtg)+VOMWTG;
        %Combine Solar and Wind LCOE
        SWLCOE = (SPpvg*SLCOE+SPwtg*WLCOE)/(SPpvg+SPwtg);
%       c. BESS (BLCOE)
        BLCOE = Nbess*PBr*(CCBESS*CRF+FOMBESS)/SPbess+SWLCOE;
%       d. Weighted Average LCOE
            if SPbess ~= 0
                LCOE =
(SPpvg*SLCOE+SPwtg*WLCOE+SPbess*BLCOE)/(SPpvg+SPwtg+SPbess);
            else
                LCOE =
(SPpvg*SLCOE+SPwtg*WLCOE+SPbess*1)/(SPpvg+SPwtg+SPbess);
            end
        end
end
```

limits.m

```
function [ limit ] = limits( LB,val,UB )
%limits Enforce limits on outputs of calculations
%   Returns the value (val) if it is not more than the upper bound (UB) and
%   not less than the lower bound(LB).
%   Returns the lower bound LB, if the value is less than LB and returns
%   UB, the upper bound if the value exceeds the UB.

if val < LB
    limit = LB;
elseif val >UB
    limit = UB;
else
    limit = val;
end

end
```

outputfunc.m

```
function [state, options,optchanged] = outputfunc(options,state,flag)
%output Save output statistics of an algorithm run for post optimization
%analysis
optchanged = false;
switch flag
case 'init'
disp('Starting the algorithm');
case {'iter','interrupt'}
disp('Iterating ...')
fname=[pwd,'\log\',num2str(state.Generation),'.mat'];
save(fname,'state')
case 'done'
disp('Performing final task');
fname=[pwd,'\log\',num2str(state.Generation),'.mat'];
save(fname,'state');
end
```

ga.m

```
function [x,fval,exitFlag,output,population,scores] =
ga(fun,nvars,Aineq,bineq,Aeq,beq,lb,ub,nonlcon,intcon,options)
%GA    Constrained optimization using genetic algorithm.
defaultopt = struct('PopulationType', 'doubleVector', ...
    'PopInitRange', [0;1], ...
    'PopulationSize', 20, ...
    'EliteCount', 2, ...
    'CrossoverFraction', 0.8, ...
    'MigrationDirection','forward', ...
    'MigrationInterval',20, ...
    'MigrationFraction',0.2, ...
    'Generations', 100, ...
    'TimeLimit', inf, ...
    'FitnessLimit', -inf, ...
    'StallGenLimit', 50, ...
    'StallTimeLimit', inf, ...
    'TolFun', 1e-6, ...
    'TolCon', 1e-6, ...
    'InitialPopulation',[], ...
    'InitialScores', [], ...
    'InitialPenalty', 10, ...
    'PenaltyFactor', 100, ...
    'PlotInterval',1, ...
    'CreationFcn',@gacreationuniform, ...
    'FitnessScalingFcn', @fitscalingrank, ...
    'SelectionFcn', @selectionstochunif, ...
    'CrossoverFcn',@crossoverscattered, ...
    'MutationFcn',{{@mutationgaussian 1  1}}, ...
    'HybridFcn',[], ...
    'Display', 'final', ...
    'PlotFcns', [], ...
    'OutputFcns', [], ...
    'Vectorized','off', ...
```

```
    'UseParallel', 'never');

% Check number of input arguments
errmsg = nargchk(1,11,nargin);
if ~isempty(errmsg)
    error(message('globaloptim:ga:numberOfInputs', errmsg));
end

% If just 'defaults' passed in, return the default options in X
if nargin == 1 && nargout <= 1 && isequal(fun,'defaults')
    x = defaultopt;
    return
end

if nargin < 11, options = [];
    if nargin < 10,  intcon = [];
        if nargin < 9,  nonlcon = [];
            if nargin < 8, ub = [];
                if nargin < 7, lb = [];
                    if nargin <6, beq = [];
                        if nargin <5, Aeq = [];
                            if nargin < 4, bineq = [];
                                if nargin < 3, Aineq = [];
                                end
                            end
                        end
                    end
                end
            end
        end
    end
end

% Is third argument a structure
if nargin == 3 && isstruct(Aineq) % Old syntax
    options = Aineq; Aineq = [];
end

% Is tenth argument a structure? If so, integer constraints have not been
% specified
if nargin == 10 && isstruct(intcon)
    options = intcon;
    intcon = [];
end

% One input argument is for problem structure
if nargin == 1
    if isa(fun,'struct')
        [fun,nvars,Aineq,bineq,Aeq,beq,lb,ub,nonlcon,intcon,rngstate,options]
= separateOptimStruct(fun);
        % Reset the random number generators
        resetDfltRng(rngstate);
    else % Single input and non-structure.
        error(message('globaloptim:ga:invalidStructInput'));
    end
end
```

```
% If fun is a cell array with additional arguments get the function handle
if iscell(fun)
    FitnessFcn = fun{1};
else
    FitnessFcn = fun;
end

% Only function handles or inlines are allowed for FitnessFcn
if isempty(FitnessFcn) ||  ~(isa(FitnessFcn,'inline') ||
isa(FitnessFcn,'function_handle'))
    error(message('globaloptim:ga:needFunctionHandle'));
end

% We need to check the nvars here before we call any solver
valid =  isnumeric(nvars) && isscalar(nvars)&& (nvars > 0) ...
    && (nvars == floor(nvars));
if ~valid
    error(message('globaloptim:ga:notValidNvars'));
end

% Specific checks and modification of options for mixed integer GA
if ~isempty(intcon)
    % Check whether the user has specified options that the mixed integer
    % solver will either ignore or error.
    gaminlpvalidateoptions(options);
    % If a user doesn't specify PopInitRange, we want to set it to the
    % bounds when we create the initial population. Need to store a flag
    % that indicates whether the user has specified PopInitRange so we can
    % do this in the creation function.
    UserSpecPopInitRange = isa(options, 'struct') && ...
        isfield(options, 'PopInitRange') && ~isempty(options.PopInitRange);
    % Change the default options for PopulationSize and EliteCount here.
    defaultopt.PopulationSize = max(min(10*nvars, 100), 40);
    defaultopt.EliteCount = floor(0.05*defaultopt.PopulationSize);
end

user_options = options;
% Use default options if empty
if ~isempty(options) && ~isa(options,'struct')
        error(message('globaloptim:ga:optionsNotAStruct'));
elseif isempty(options)
    options = defaultopt;
end
% Take defaults for parameters that are not in options structure
options = gaoptimset(defaultopt,options);

% Check for non-double inputs
msg = isoptimargdbl('GA', {'NVARS','A',   'b',   'Aeq','beq','lb','ub'}, ...
                           nvars,  Aineq, bineq, Aeq,  beq,  lb,  ub);
if ~isempty(msg)
    error('globaloptim:ga:dataType',msg);
end
```

```
[x,fval,exitFlag,output,population,scores,FitnessFcn,nvars,Aineq,bineq,Aeq,be
q,lb,ub, ...
    NonconFcn,options,Iterate,type] =
gacommon(nvars,fun,Aineq,bineq,Aeq,beq,lb,ub,nonlcon,intcon,options,user_opti
ons);

if exitFlag < 0
    return;
end

% Turn constraints into right size if they are empty.
if isempty(Aineq)
    Aineq = zeros(0,nvars);
end
if isempty(bineq)
    bineq = zeros(0,1);
end
if isempty(Aeq)
    Aeq = zeros(0,nvars);
end
if isempty(beq)
    beq = zeros(0,1);
end

% Call appropriate single objective optimization solver
if ~isempty(intcon)
    [x,fval,exitFlag,output,population,scores] = gaminlp(FitnessFcn,nvars,
...
        Aineq,bineq,Aeq,beq,lb,ub,NonconFcn,intcon,options,output,Iterate,...
        UserSpecPopInitRange);
else
    switch (output.problemtype)
        case 'unconstrained'
            [x,fval,exitFlag,output,population,scores] =
gaunc(FitnessFcn,nvars, ...
                options,output,Iterate);
        case {'boundconstraints', 'linearconstraints'}
            [x,fval,exitFlag,output,population,scores] =
galincon(FitnessFcn,nvars, ...
                Aineq,bineq,Aeq,beq,lb,ub,options,output,Iterate);
        case 'nonlinearconstr'
            [x,fval,exitFlag,output,population,scores] =
gacon(FitnessFcn,nvars, ...

Aineq,bineq,Aeq,beq,lb,ub,NonconFcn,options,output,Iterate,type);
    end
end
```

galincon.m

```
function [x,fval,exitFlag,output,population,scores] =
galincon(FitnessFcn,GenomeLength, ...
    Aineq,bineq,Aeq,beq,lb,ub,options,output,Iterate)
%GALINCON Genetic algorithm linear constrained solver.
%   GALINCON solves problems of the form:
%           min F(X)    subject to:      A*x <= b
```

```
%            X                          Aeq*x = beq
%                                      LB <= X <= UB
%   Private function to GA

%   Copyright 2005-2011 The MathWorks, Inc.
%   $Revision: 1.1.6.7 $  $Date: 2012/08/21 00:23:49 $

% Initialize output args
x = []; fval = []; exitFlag = [];
LinearConstr = options.LinearConstr;

% Create initial state: population, scores, status data
state =
makeState(GenomeLength,FitnessFcn,Iterate,output.problemtype,options);
% Determine who is the caller
callStack = dbstack;
caller = callStack(2).file(1:end-2);

% Set state for plot and output functions (only gacon will have
% 'interrupt' state)
if ~strcmp(caller,'gacon')
    currentState = 'init';
else
    currentState = 'interrupt';
end
% Give the plot/output Fcns a chance to do any initialization they need.
state = gadsplot(options,state,currentState,'Genetic Algorithm');
[state,options] = gaoutput(FitnessFcn,options,state,currentState);

% Setup display header
if  options.Verbosity > 1
    fprintf('\n                                  Best           Mean
Stall\n');
    fprintf('Generation      f-count        f(x)           f(x)
Generations\n');
end

% Set state for plot and output functions (only gacon will have
% 'interrupt' state)
if ~strcmp(caller,'gacon')
    currentState = 'iter';
else
    currentState = 'interrupt';
end
% Run the main loop until some termination condition becomes true
while isempty(exitFlag)
    state.Generation = state.Generation + 1;
    % Repeat for each subpopulation (element of the populationSize vector)
    offset = 0;
    totalPop = options.PopulationSize;
    % Each sub-population loop
    for pop = 1:length(totalPop)
        populationSize =  totalPop(pop);
        thisPopulation = 1 + (offset:(offset + populationSize - 1));
        population = state.Population(thisPopulation,:);
        score = state.Score( thisPopulation );
```

```
        % Empty population is also possible
        if isempty(thisPopulation)
            continue;
        end
        [score,population,state] =
stepGA(score,population,options,state,GenomeLength,FitnessFcn);
        % Store the results for this sub-population
        state.Population(thisPopulation,:) = population;
        state.Score(thisPopulation) = score;
        offset = offset + populationSize;
    end

    % Remember the best score
    best = min(state.Score);
    generation = state.Generation;
    state.Best(generation) = best;
    % Keep track of improvement in the best
    if((generation > 1) && isfinite(best))
        if(state.Best(generation-1) > best)
            state.LastImprovement = generation;
            state.LastImprovementTime = cputime;
        end
    end
    % Do any migration
    state = migrate(FitnessFcn,GenomeLength,options,state);
    % Update the Output
    state = gadsplot(options,state,currentState,'Genetic Algorithm');
    [state,options,optchanged] =
gaoutput(FitnessFcn,options,state,currentState);
    if optchanged
        options.LinearConstr = LinearConstr;
    end
    % Check to see if any stopping criteria have been met
    [exitFlag,output.message] = isItTimeToStop(options,state);
end % End while loop

% Find and return the best solution
[fval,best] = min(state.Score);
x = state.Population(best,:);

% Update output structure
output.generations = state.Generation;
output.funccount   = state.FunEval;
output.maxconstraint = norm([Aeq*x'-beq; max([Aineq*x' - bineq;x' -
ub(:);lb(:) - x'],0)],Inf);
population = state.Population;
scores = state.Score;

% Call hybrid function
if ~isempty(options.HybridFcn)
    if  strcmpi(options.PopulationType,'doubleVector')
        [x,fval] = callHybridFunction;
    else
        warning(message('globaloptim:galincon:notValidHybrid'));
    end
end
```

```
% Set state for plot and output functions (only gacon will have
% 'interrupt' state)
if ~strcmp(caller,'gacon')
    currentState = 'done';
else
    currentState = 'interrupt';
end
% give the Output functions a chance to finish up
gadsplot(options,state,currentState,'Genetic Algorithm');
gaoutput(FitnessFcn,options,state,currentState);

%------------------------------------------------------------------
% Hybrid function
    function [xhybrid,fhybrid] = callHybridFunction
        xhybrid = x;
        fhybrid = fval;
        % Who is the hybrid function
        if isa(options.HybridFcn,'function_handle')
            hfunc = func2str(options.HybridFcn);
        else
            hfunc = options.HybridFcn;
        end
        % Inform about hybrid scheme
        if   options.Verbosity > 1
            fprintf('%s%s%s\n','Switching to the hybrid optimization
algorithm (',upper(hfunc),').');
        end
        % Create functions handle to be passed to hybrid function
        FitnessHybridFcn = @(x) FitnessFcn(x,options.FitnessFcnArgs{:});
        ConstrHybridFcn = [];
        if ~any(strcmpi(hfunc,{'fmincon', 'patternsearch'}))

warning(message('globaloptim:galincon:unconstrainedHybridFcn',upper(hfunc),'F
MINCON'));
            hfunc = 'fmincon';
        end
        [x_temp,f_temp,funccount,theMessage,conviol_temp] = ...

callHybrid(hfunc,FitnessHybridFcn,x,options.HybridFcnArgs,Aineq,bineq,Aeq,beq
,lb,ub,ConstrHybridFcn);
        output.funccount = output.funccount + funccount;
        output.message   = sprintf([output.message '\n', theMessage '\n']);
        hybridPointFeasible = isHybridPointFeasible(conviol_temp, ...
            hfunc, options.HybridFcnArgs{:});
        % We have to recheck whether the final point returned from GA is
        % feasible because GA asserts that the final point is always
        % feasible. If a user supplies their own operators, this may not be
        % the case. We could replace this code if output.maxconstraint
        % reflects the true constraint violation.
        tol = max(sqrt(eps),sqrt(options.TolCon));
        gaPointFeasible = isTrialFeasible(x(:), Aineq, bineq, ...
            Aeq, beq, lb, ub, tol);
        if hybridPointFeasible && (~gaPointFeasible || f_temp < fhybrid)
            fhybrid = f_temp;
            xhybrid = x_temp;
        end
        % Inform about hybrid scheme termination
```

```
        if  options.Verbosity > 1
            fprintf('%s%s\n',upper(hfunc), ' terminated.');
        end
    end % End of callHybridFunction
end  % End of galincon
```

Constraints_estimator

```
%%Estimation of Lower and Upper Bounds
disp('------First run sizing check-------');
disp('-----------------------------------');
dispX=['Peak load: ', num2str(max(Pl))];disp(dispX);
disp('Initial bounds:');
dispX=['Solar = ', num2str(round( max(Pl)/Ppvr))];disp(dispX);
dispX=['Wind = ', num2str(round(max(Pl)/Pwtgr))];disp(dispX);
disp('BESS = 0');
disp('-----------------------------------');
disp('---Calculating Approximate Bounds---');
SLB = SPpvg/(SPpvg+SPwtg)*(1-LPSP)*max(Pl);
WLB = SPwtg/(SPpvg+SPwtg)*(1-LPSP)*max(Pl);
BLB = LPSP*max(Pl);
scaleFactor = 10;
dispX=['Solar Bounds [ ', num2str(round(SLB/Ppvr)), '---' ,
num2str(scaleFactor*round(SLB/Ppvr)), ' ]'];disp(dispX);
dispX=['Wind Bounds [ ', num2str(round(WLB/Pwtgr)), '---' ,
num2str(scaleFactor*round(WLB/Pwtgr)), ' ]'];disp(dispX);
dispX=['BESS Bounds [ ', num2str(round(BLB/PBr)), '---' ,
num2str(scaleFactor*round(BLB/PBr)), ' ]'];disp(dispX);
disp('-----------------------------------');
disp('-----------End of Report------------');
```

ANNEX 4: Validation – The Transparent Cost Database (Abridged form)

#	Technology	Year	Calculated LCOE	Overnight Capital Cost dollar per kW including Contingency	Fixed O&M dollar per kW	Variable O&M dollar per MWh	Reference Name	Publication Year	Dataset name
1	Land-Based Wind	2010	$ 0.06		18	6	DOE 2013	2013	DOE Program Estimate
2	Land-Based Wind	2014	$ 0.05		51	0	NREL_ATB 2015	2015	NREL Annual Technology Baseline 2015
3	Land-Based Wind	2013	$ 0.05		51	0	NREL_ATB 2015	2015	NREL Annual Technology Baseline 2015
4	Land-Based Wind	2009	$ 0.05	$ 1,435.00	26.79		GPRA 2009	2009	Government Performance and Results Act (2009). Data from Market Allocation (MARKAL) model, International Energy Agency and Brookhaven National Laboratory
5	Land-Based Wind	2009	$ 0.04	$ 1,435.00	26.79		GPRA 2009	2009	Government Performance and Results Act (2009). Data from Market Allocation (MARKAL) model, International Energy Agency and Brookhaven National Laboratory
6	Land-Based Wind	2009	$ 0.04	$ 1,435.00	26.79		GPRA 2009	2009	Government Performance and Results Act (2009). Data from Market Allocation (MARKAL) model, International Energy Agency and Brookhaven National Laboratory
7	Land-Based Wind	2009	$ 0.07	$ 1,922.99	30.3	0	AEO 2009	2009	Annual Energy Outlook 2009
8	Land-based Wind	2009	$ 0.08				USOWC	2009	U.S. Offshore Wind Energy: A Path Forward
9	Land-Based Wind	2010	$ 0.07	$ 1,964.39			AEO 2010	2010	Annual Energy Outlook 2010
10	Land-Based Wind	2009	$ 0.07	$ 1,965.56			AEO 2010	2010	Annual Energy Outlook 2010
11	Land-Based Wind	2010	$ 0.07	$ 2,034.20			EPA 2010	2010	Environmental Protection Agency (2010). Data from Integrated Power Model (IPM), ICF International.
12	Land-based Wind	2009	$ 0.05		10.28	4.82	Klein et al 2010	2010	Comparate Costs of California Central Station Electricity Generation. Final Staff Report
13	Land-based Wind	2009	$ 0.04		10.28	4.82	Klein et al 2010	2010	Comparate Costs of California Central Station Electricity Generation. Final Staff Report
14	Land-Based Wind	2009	$ 0.07				E3 2010	2010	Capital Cost Recommendations for 2009 TEPPC Study.
15	Land-based Wind	2009	$ 0.07		13.7	5.5	Klein et al 2010	2010	Comparate Costs of California Central Station Electricity Generation. Final Staff Report

#	Technology	Year	Calculated LCOE	Overnight Capital Cost dollar per kW including Contingency	Fixed O&M dollar per kW	Variable O&M dollar per MWh	Reference Name	Publication Year	Dataset name
16	Land-based Wind	2009	$ 0.06		13.7	5.5	Klein et al 2010	2010	Comparate Costs of California Central Station Electricity Generation. Final Staff Report
17	Land-Based Wind	2009	$ 0.09				Wiser and Bolinger, 2010	2010	2009 Wind Technologies Market Report, U.S. Department of Energy.
18	Land-Based Wind	2009	$ 0.07		60	0	Lazard 2010	2010	Lazard Levelized Cost of Energy Analysis, version 4.0
19	Land-Based Wind	2009	$ 0.09		50	0	E3 2010	2010	Capital Cost Recommendations for 2009 TEPPC Study.
20	Land-Based Wind	2009	$ 0.08				E3 2010	2010	Capital Cost Recommendations for 2009 TEPPC Study.
21	Land-Based Wind	2009	$ 0.11		60	0	Lazard 2010	2010	Lazard Levelized Cost of Energy Analysis, version 4.0
22	Land-based Wind	2009	$ 0.09		17.13	7.66	Klein et al 2010	2010	Comparate Costs of California Central Station Electricity Generation. Final Staff Report
23	Land-based Wind	2009	$ 0.09		17.13	7.66	Klein et al 2010	2010	Comparate Costs of California Central Station Electricity Generation. Final Staff Report
24	Land-Based Wind	2011	$ 0.08	$ 2,402.77			AEO 2011	2011	Annual Energy Outlook 2011
25	Land-Based Wind	2010	$ 0.07	$ 2,408.76	27.73	0	AEO 2011	2011	Annual Energy Outlook 2011
26	Land-Based Wind	2009	$ 0.05				Wiser et al, 2011	2011	Wind Energy, Chapter 7, an IPPCC Special Report on Renewable Energy Sources and Climate Change Mitigation.
27	Land-Based Wind	2011	$ 0.05			12	IPCC 2011	2011	IPCC Annex 3
28	Land-Based Wind	2011	$ 0.07			17.5	IPCC 2011	2011	IPCC Annex 3
29	Land-Based Wind	2009	$ 0.06				Wiser et al, 2011	2011	Wind Energy, Chapter 7, an IPPCC Special Report on Renewable Energy Sources and Climate Change Mitigation.
30	Land-Based Wind	2009	$ 0.07				McCalley et al, 2011	2011	A Wider Horizon. IEEE Power & Energy Magazine. May/June 2011
31	Land-Based Wind	2011	$ 0.07		11.7	6	DOE 2011	2011	DOE Program Estimate
32	Land-Based Wind	2009	$ 0.07				Wiser et al, 2011	2011	Wind Energy, Chapter 7, an IPPCC Special Report on Renewable Energy Sources and Climate Change Mitigation.
33	Land-Based Wind	2011	$ 0.09			23	IPCC 2011	2011	IPCC Annex 3

#	Technology	Year	Calculated LCOE	Overnight Capital Cost dollar per kW including Contingency	Fixed O&M dollar per kW	Variable O&M dollar per MWh	Reference Name	Publication Year	Dataset name
34	Land-Based Wind	2012	$ 0.06		60	0	Tegan et al, 2012	2012	2010 Cost of Wind Energy Review
35	Land-based Wind	2010	$ 0.09		36		IEA 2012	2012	Energy Technology Perspectives 2012 Pathways to a Clean Energy System
36	Land-Based Wind	2010	$ 0.06		12.24	7.45	Mai et al, 2012	2012	Renewable Electricity Futures
37	Land-Based Wind	2010	$ 0.07		59.41	0	Black and Veatch 2012	2012	COST AND PERFORMANCE DATA FOR POWER GENERATION TECHNOLOGIES
38	Land-Based Wind	2010	$ 0.07		34	0	Tegan et al, 2012	2012	2010 Cost of Wind Energy Review
39	Land-based Wind	2010	$ 0.08				Hubbell et al 2012	2012	Renewable Energy Finance Tracking Initiative
40	Land-based Wind	2010	$ 0.10				Hubbell et al 2012	2012	Renewable Energy Finance Tracking Initiative
41	Land-based Wind	2011	$ 0.11				Hubbell et al 2012	2012	Renewable Energy Finance Tracking Initiative
42	Land-based Wind	2010	$ 0.11				Hubbell et al 2012	2012	Renewable Energy Finance Tracking Initiative
43	Land-based Wind	2009	$ 0.12				Hubbell et al 2012	2012	Renewable Energy Finance Tracking Initiative
44	Land-based Wind	2010	$ 0.12				Hubbell et al 2012	2012	Renewable Energy Finance Tracking Initiative
45	Land-based Wind	2013	$ 0.05		31.72	6.34	McCann RE 2013	2013	Cost of Generation Workshop: Non-solar Renewables
46	Land-based Wind	2013	$ 0.05		31.72	6.34	McCann RE 2013	2013	Cost of Generation Workshop: Non-solar Renewables
47	Land-based Wind	2013	$ 0.06		31.72	8.46	McCann RE 2013	2013	Cost of Generation Workshop: Non-solar Renewables
48	Land-based Wind	2013	$ 0.06		31.72	8.46	McCann RE 2013	2013	Cost of Generation Workshop: Non-solar Renewables
49	Land-based Wind	2013	$ 0.09		31.72	10.57	McCann RE 2013	2013	Cost of Generation Workshop: Non-solar Renewables
50	Land-based Wind	2013	$ 0.07				Tegen et al 2013	2013	2011 Cost of Wind Energy Review
51	Land-based Wind	2013	$ 0.11		31.72	10.57	McCann RE 2013	2013	Cost of Generation Workshop: Non-solar Renewables
52	Land-based Wind	2010	$ 0.05				IIASA 2014	2014	AMPERE DB
53	Land-Based Wind	2014	$ 0.04		35		Lazard 2014	2014	Lazard Levelized Cost of Energy Analysis, version 8.0

#	Technology	Year	Calculated LCOE	Overnight Capital Cost dollar per kW including Contingency	Fixed O&M dollar per kW	Variable O&M dollar per MWh	Reference Name	Publication Year	Dataset name
54	Land-based Wind	2013	$ 0.06				Wisner et al 2014	2014	2013 Wind Technologies Market Report
55	Land-Based Wind	2014	$ 0.08		40		Lazard 2014	2014	Lazard Levelized Cost of Energy Analysis, version 8.0
56	Land-based Wind	2012	$ 0.07				Wisner et al 2014	2014	2013 Wind Technologies Market Report
57	Land-based Wind	2010	$ 0.07				Mai et al 2014	2014	Envisioning a renewable electricty future for the United States
58	Land-based Wind	2010	$ 0.07				Mai et al 2014	2014	Envisioning a renewable electricty future for the United States
59	Land-based Wind	2011	$ 0.07				Wisner et al 2014	2014	2013 Wind Technologies Market Report
60	Land-based Wind	2010	$ 0.08				Wisner et al 2014	2014	2013 Wind Technologies Market Report
61	Land-based Wind	2009	$ 0.08				Wisner et al 2014	2014	2013 Wind Technologies Market Report
62	Wind-Offshore	2010	$ 0.16		67	17	DOE 2013	2013	DOE Program Estimate
63	Wind-Offshore	2013	$ 0.17		132	0	NREL_ATB 2015	2015	NREL Annual Technology Baseline 2015
64	Wind-Offshore	2014	$ 0.17		132	0	NREL_ATB 2015	2015	NREL Annual Technology Baseline 2015
65	Wind-Offshore	2013	$ 0.17		132	0	NREL_ATB 2015	2015	NREL Annual Technology Baseline 2015
66	Wind-Offshore	2014	$ 0.17		132	0	NREL_ATB 2015	2015	NREL Annual Technology Baseline 2015
67	Wind-Offshore	2013	$ 0.19		162	0	NREL_ATB 2015	2015	NREL Annual Technology Baseline 2015
68	Wind-Offshore	2014	$ 0.19		162	0	NREL_ATB 2015	2015	NREL Annual Technology Baseline 2015
69	Wind-Offshore	2009	$ 0.16	$ 2,838.75	180		GPRA 2009	2009	Government Performance and Results Act (2009). Data from Market Allocation (MARKAL) model, International Energy Agency and Brookhaven National Laboratory
70	Wind-Offshore	2009	$ 0.13	$ 2,838.75	180		GPRA 2009	2009	Government Performance and Results Act (2009). Data from Market Allocation (MARKAL) model, International Energy Agency and Brookhaven National Laboratory
71	Wind-Offshore	2009	$ 0.12	$ 2,838.75	180		GPRA 2009	2009	Government Performance and Results Act (2009). Data from Market Allocation (MARKAL) model, International Energy Agency and Brookhaven National Laboratory

#	Technology	Year	Calculated LCOE	Overnight Capital Cost dollar per kW including Contingency	Fixed O&M dollar per kW	Variable O&M dollar per MWh	Reference Name	Publication Year	Dataset name
72	Wind-Offshore	2009	$ 0.13	$ 3,851.50	89.48	0	AEO 2009	2009	Annual Energy Outlook 2009
73	Wind-Offshore	2009	$ 0.13	$ 3,936.77	86.92	0	AEO 2010	2010	Annual Energy Outlook 2010
74	Wind-Offshore	2009	$ 0.11		60	13	Lazard 2010	2010	Lazard Levelized Cost of Energy Analysis, version 4.0
75	Wind-Offshore	2009	$ 0.21		100	18	Lazard 2010	2010	Lazard Levelized Cost of Energy Analysis, version 4.0
76	Wind-Offshore	2009	$ 0.18		90	0	E3 2010	2010	Capital Cost Recommendations for 2009 TEPPC Study.
77	Wind-Offshore	2010	$ 0.18	$ 6,055.75	86.98	0	AEO 2011	2011	Annual Energy Outlook 2011
78	Wind-Offshore	2011	$ 0.10			20	IPCC 2011	2011	IPCC Annex 3
79	Wind-Offshore	2009	$ 0.13		86.92		McCalley et al, 2011	2011	A Wider Horizon. IEEE Power & Energy Magazine. May/June 2011
80	Wind-Offshore	2011	$ 0.14			30	IPCC 2011	2011	IPCC Annex 3
81	Wind-Offshore	2011	$ 0.12				Schwabe et al 2011	2011	Multi-national Case Study of the Financial Cost of wind Energy
82	Wind-Offshore	2011	$ 0.17			40	IPCC 2011	2011	IPCC Annex 3
83	Wind-Offshore	2011	$ 0.17		40	19.7	DOE 2011	2011	DOE Program Estimate
84	Wind-Offshore	2010	$ 0.13		107	0	Tegan et al, 2012	2012	2010 Cost of Wind Energy Review
85	Wind-Offshore	2010	$ 0.12		15.96	22.35	Mai et al, 2012	2012	Renewable Electricity Futures
86	Wind-Offshore	2010	$ 0.12		99.01	0	Black and Veatch 2012	2012	COST AND PERFORMANCE DATA FOR POWER GENERATION TECHNOLOGIES
87	Wind-Offshore	2010	$ 0.14		114		IEA 2012	2012	Energy Technology Perspectives 2012 Pathways to a Clean Energy System
88	Wind-Offshore	2014	$ 0.10		60	13	Lazard 2014	2014	Lazard Levelized Cost of Energy Analysis, version 8.0
89	Wind-Offshore	2014	$ 0.20		100	18	Lazard 2014	2014	Lazard Levelized Cost of Energy Analysis, version 8.0
90	Photovoltaic	2012	$ 0.20		30	0	DOE 2013	2013	DOE Program Estimate
91	Photovoltaic	2014	$ 0.11		17	0	NREL_ATB 2015	2015	NREL Annual Technology Baseline 2015

#	Technology	Year	Calculated LCOE	Overnight Capital Cost dollar per kW including Contingency	Fixed O&M dollar per kW	Variable O&M dollar per MWh	Reference Name	Publication Year	Dataset name
92	Photovoltaic	2013	$ 0.14		18	0	NREL_ATB 2015	2015	NREL Annual Technology Baseline 2015
93	Photovoltaic	2009	$ 0.21	$ 4,591.94	7.56		GPRA 2009	2009	Government Performance and Results Act (2009). Data from Market Allocation (MARKAL) model, International Energy Agency and Brookhaven National Laboratory
94	Photovoltaic	2009	$ 0.29	$ 5,161.67	16.46		GPRA 2009	2009	Government Performance and Results Act (2009). Data from Market Allocation (MARKAL) model, International Energy Agency and Brookhaven National Laboratory
95	Photovoltaic	2009	$ 0.37	$ 6,096.26	39.49		GPRA 2009	2009	Government Performance and Results Act (2009). Data from Market Allocation (MARKAL) model, International Energy Agency and Brookhaven National Laboratory
96	Photovoltaic	2009	$ 0.29	$ 6,037.52	11.68	0	AEO 2009	2009	Annual Energy Outlook 2009
97	Photovoltaic	2010	$ 0.41	$ 6,110.55			AEO 2010	2010	Annual Energy Outlook 2010
98	Photovoltaic	2009	$ 0.41	$ 6,171.18	11.94	0	AEO 2010	2010	Annual Energy Outlook 2010
99	Photovoltaic	2009	$ 0.17				Barbose et al, 2010	2010	Tracking the Sun III. The Installed Cost of Photovoltaics in the US from 1998-2009.
100	Photovoltaic	2009	$ 0.14		25	0	Lazard 2010	2010	Lazard Levelized Cost of Energy Analysis, version 4.0
101	Photovoltaic	2009	$ 0.16		37.5	0	Lazard 2010	2010	Lazard Levelized Cost of Energy Analysis, version 4.0
102	Photovoltaic	2009	$ 0.22		50	0	Lazard 2010	2010	Lazard Levelized Cost of Energy Analysis, version 4.0
103	Photovoltaic	2009	$ 0.19		25	0	Lazard 2010	2010	Lazard Levelized Cost of Energy Analysis, version 4.0
104	Photovoltaic	2009	$ 0.23		37.5	0	Lazard 2010	2010	Lazard Levelized Cost of Energy Analysis, version 4.0
105	Photovoltaic	2009	$ 0.17		60	0	Klein et al 2010	2010	Comparate Costs of California Central Station Electricity Generation. Final Staff Report
106	Photovoltaic	2009	$ 0.24		25	0	Lazard 2010	2010	Lazard Levelized Cost of Energy Analysis, version 4.0
107	Photovoltaic	2009	$ 0.20		68	0	Klein et al 2010	2010	Comparate Costs of California Central Station Electricity Generation. Final Staff Report
108	Photovoltaic	2009	$ 0.34				E3 2010	2010	Capital Cost Recommendations for 2009 TEPPC Study.
109	Photovoltaic	2009	$ 0.24		92	0	Klein et al 2010	2010	Comparate Costs of California Central Station Electricity Generation. Final Staff Report
110	Photovoltaic	2009	$ 0.34				Barbose et al, 2010	2010	Tracking the Sun III. The Installed Cost of Photovoltaics in the US from 1998-2009.
111	Photovoltaic	2009	$ 0.24		65	0	E3 2010	2010	Capital Cost Recommendations for 2009 TEPPC Study.
112	Photovoltaic	2009	$ 0.43				E3 2010	2010	Capital Cost Recommendations for 2009 TEPPC Study.

#	Technology	Year	Calculated LCOE	Overnight Capital Cost dollar per kW including Contingency	Fixed O&M dollar per kW	Variable O&M dollar per MWh	Reference Name	Publication Year	Dataset name
113	Photovoltaic	2011	$ 0.31	$ 4,634.63			AEO 2011	2011	Annual Energy Outlook 2011
114	Photovoltaic	2010	$ 0.32	$ 4,697.26	25.73	0	AEO 2011	2011	Annual Energy Outlook 2011
115	Photovoltaic	2011	$ 0.16		14		IPCC 2011	2011	IPCC Annex 3
116	Photovoltaic	2011	$ 0.16		16		IPCC 2011	2011	IPCC Annex 3
117	Photovoltaic	2011	$ 0.24		18		IPCC 2011	2011	IPCC Annex 3
118	Photovoltaic	2011	$ 0.25		19		IPCC 2011	2011	IPCC Annex 3
119	Photovoltaic	2011	$ 0.15		26	0	DOE 2011	2011	DOE Program Estimate
120	Photovoltaic	2011	$ 0.25		41.5		IPCC 2011	2011	IPCC Annex 3
121	Photovoltaic	2011	$ 0.25		45.5		IPCC 2011	2011	IPCC Annex 3
122	Photovoltaic	2011	$ 0.36		59		IPCC 2011	2011	IPCC Annex 3
123	Photovoltaic	2011	$ 0.34		69		IPCC 2011	2011	IPCC Annex 3
124	Photovoltaic	2011	$ 0.38		64.5		IPCC 2011	2011	IPCC Annex 3
125	Photovoltaic	2011	$ 0.29		30	0	DOE 2011	2011	DOE Program Estimate
126	Photovoltaic	2011	$ 0.34		75		IPCC 2011	2011	IPCC Annex 3
127	Photovoltaic	2011	$ 0.35		41	0	DOE 2011	2011	DOE Program Estimate
128	Photovoltaic	2011	$ 0.49		100		IPCC 2011	2011	IPCC Annex 3
129	Photovoltaic	2011	$ 0.51		110		IPCC 2011	2011	IPCC Annex 3
130	Photovoltaic	2012	$ 0.10		26	0	DOE 2012	2012	DOE Program Estimate
131	Photovoltaic	2012	$ 0.18		30	0	DOE 2012	2012	DOE Program Estimate
132	Photovoltaic	2011	$ 0.25				Hubbell et al 2012	2012	Renewable Energy Finance Tracking Initiative
133	Photovoltaic	2012	$ 0.26	$ -	0	0	Goodrich et al, 2012	2012	Residential, Commercial, and Utility-Scale Photovoltaic (PV) System Prices in the United States: Current Drivers and Cost-Reduction Opportunities
134	Photovoltaic	2010	$ 0.26				Hubbell et al 2012	2012	Renewable Energy Finance Tracking Initiative
135	Photovoltaic	2011	$ 0.27				Hubbell et al 2012	2012	Renewable Energy Finance Tracking Initiative

#	Technology	Year	Calculated LCOE	Overnight Capital Cost dollar per kW including Contingency	Fixed O&M dollar per kW	Variable O&M dollar per MWh	Reference Name	Publication Year	Dataset name
136	Photovoltaic	2010	$ 0.27				Hubbell et al 2012	2012	Renewable Energy Finance Tracking Initiative
137	Photovoltaic	2010	$ 0.16		19.93		DOE SETP 2012	2012	Sunshot Solar Vision
138	Photovoltaic	2010	$ 0.24		40		IEA 2012	2012	Energy Technology Perspectives 2012 Pathways to a Clean Energy System
139	Photovoltaic	2010	$ 0.15		20.69	0	Mai et al, 2012	2012	Renewable Electricity Futures
140	Photovoltaic	2010	$ 0.17		50	0	Black and Veatch 2012	2012	COST AND PERFORMANCE DATA FOR POWER GENERATION TECHNOLOGIES
141	Photovoltaic	2011	$ 0.28				Hubbell et al 2012	2012	Renewable Energy Finance Tracking Initiative
142	Photovoltaic	2012	$ 0.24		41	0	DOE 2012	2012	DOE Program Estimate
143	Photovoltaic	2012	$ 0.30	$ -	0	0	Goodrich et al, 2012	2012	Residential, Commercial, and Utility-Scale Photovoltaic (PV) System Prices in the United States: Current Drivers and Cost-Reduction Opportunities
144	Photovoltaic	2012	$ 0.31	$ -	0	0	Goodrich et al, 2012	2012	Residential, Commercial, and Utility-Scale Photovoltaic (PV) System Prices in the United States: Current Drivers and Cost-Reduction Opportunities
145	Photovoltaic	2010	$ 0.32				Hubbell et al 2012	2012	Renewable Energy Finance Tracking Initiative
146	Photovoltaic	2010	$ 0.30		50	0	Black and Veatch 2012	2012	COST AND PERFORMANCE DATA FOR POWER GENERATION TECHNOLOGIES
147	Photovoltaic	2010	$ 0.33				Hubbell et al 2012	2012	Renewable Energy Finance Tracking Initiative
148	Photovoltaic	2010	$ 0.33		49		IEA 2012	2012	Energy Technology Perspectives 2012 Pathways to a Clean Energy System
149	Photovoltaic	2010	$ 0.33				Hubbell et al 2012	2012	Renewable Energy Finance Tracking Initiative
150	Photovoltaic	2012	$ 0.33	$ -	0	0	Feldman et al, 2012	2012	Photovoltaic (PV) Pricing Trends: Historical, Recent, and Near-Term Projections
151	Photovoltaic	2010	$ 0.26		23.5		DOE SETP 2012	2012	Sunshot Solar Vision
152	Photovoltaic	2009	$ 0.34				Hubbell et al 2012	2012	Renewable Energy Finance Tracking Initiative
153	Photovoltaic	2010	$ 0.34				Hubbell et al 2012	2012	Renewable Energy Finance Tracking Initiative
154	Photovoltaic	2012	$ 0.34	$ -	0	0	Feldman et al, 2012	2012	Photovoltaic (PV) Pricing Trends: Historical, Recent, and Near-Term Projections

#	Technology	Year	Calculated LCOE	Overnight Capital Cost dollar per kW including Contingency	Fixed O&M dollar per kW	Variable O&M dollar per MWh	Reference Name	Publication Year	Dataset name
155	Photovoltaic	2010	$ 0.30		23.27	0	Mai et al, 2012	2012	Renewable Electricity Futures
156	Photovoltaic	2010	$ 0.35				Hubbell et al 2012	2012	Renewable Energy Finance Tracking Initiative
157	Photovoltaic	2012	$ 0.36	$ -	0	0	Feldman et al, 2012	2012	Photovoltaic (PV) Pricing Trends: Historical, Recent, and Near-Term Projections
158	Photovoltaic	2009	$ 0.37				Hubbell et al 2012	2012	Renewable Energy Finance Tracking Initiative
159	Photovoltaic	2012	$ 0.38	$ -	0	0	Goodrich et al, 2012	2012	Residential, Commercial, and Utility-Scale Photovoltaic (PV) System Prices in the United States: Current Drivers and Cost-Reduction Opportunities
160	Photovoltaic	2012	$ 0.39	$ -	0	0	Feldman et al, 2012	2012	Photovoltaic (PV) Pricing Trends: Historical, Recent, and Near-Term Projections
161	Photovoltaic	2012	$ 0.40	$ -	0	0	Feldman et al, 2012	2012	Photovoltaic (PV) Pricing Trends: Historical, Recent, and Near-Term Projections
162	Photovoltaic	2010	$ 0.37		50	0	Black and Veatch 2012	2012	COST AND PERFORMANCE DATA FOR POWER GENERATION TECHNOLOGIES
163	Photovoltaic	2010	$ 0.32		32.8		DOE SETP 2012	2012	Sunshot Solar Vision
164	Photovoltaic	2010	$ 0.42				Hubbell et al 2012	2012	Renewable Energy Finance Tracking Initiative
165	Photovoltaic	2011	$ 0.42				Hubbell et al 2012	2012	Renewable Energy Finance Tracking Initiative
166	Photovoltaic	2012	$ 0.42	$ -	0	0	Feldman et al, 2012	2012	Photovoltaic (PV) Pricing Trends: Historical, Recent, and Near-Term Projections
167	Photovoltaic	2010	$ 0.39		32.47	0	Mai et al, 2012	2012	Renewable Electricity Futures
168	Photovoltaic	2012	$ 0.17				Feldman et al 2013	2013	Photovoltaic System Pricing Trends: Historical, Recent, and Near-Term Projections 2013 Edition
169	Photovoltaic	2012	$ 0.22				Feldman et al 2013	2013	Photovoltaic System Pricing Trends: Historical, Recent, and Near-Term Projections 2013 Edition
170	Photovoltaic	2011	$ 0.25				Feldman et al 2013	2013	Photovoltaic System Pricing Trends: Historical, Recent, and Near-Term Projections 2013 Edition
171	Photovoltaic	2012	$ 0.29				Feldman et al 2013	2013	Photovoltaic System Pricing Trends: Historical, Recent, and Near-Term Projections 2013 Edition
172	Photovoltaic	2010	$ 0.29				Feldman et al 2013	2013	Photovoltaic System Pricing Trends: Historical, Recent, and Near-Term Projections 2013 Edition
173	Photovoltaic	2011	$ 0.31				Feldman et al 2013	2013	Photovoltaic System Pricing Trends: Historical, Recent, and Near-Term Projections 2013 Edition

#	Technology	Year	Calculated LCOE	Overnight Capital Cost dollar per kW including Contingency	Fixed O&M dollar per kW	Variable O&M dollar per MWh	Reference Name	Publication Year	Dataset name
174	Photovoltaic	2010	$ 0.34				Feldman et al 2013	2013	Photovoltaic System Pricing Trends: Historical, Recent, and Near-Term Projections 2013 Edition
175	Photovoltaic	2011	$ 0.40				Feldman et al 2013	2013	Photovoltaic System Pricing Trends: Historical, Recent, and Near-Term Projections 2013 Edition
176	Photovoltaic	2010	$ 0.45				Feldman et al 2013	2013	Photovoltaic System Pricing Trends: Historical, Recent, and Near-Term Projections 2013 Edition
177	Photovoltaic	2014	$ 0.06		13		Lazard 2014	2014	Lazard Levelized Cost of Energy Analysis, version 8.0
178	Photovoltaic	2014	$ 0.06		13		Lazard 2014	2014	Lazard Levelized Cost of Energy Analysis, version 8.0
179	Photovoltaic	2014	$ 0.10		20		Lazard 2014	2014	Lazard Levelized Cost of Energy Analysis, version 8.0
180	Photovoltaic	2014	$ 0.10		20		Lazard 2014	2014	Lazard Levelized Cost of Energy Analysis, version 8.0
181	Photovoltaic	2013	$ 0.14				Feldman et al 2014	2014	Photovoltaic (PV) Pricing Trends: Historical, Recent, and Near-Term Projections 2014 Edition
182	Photovoltaic	2014	$ 0.12		13		Lazard 2014	2014	Lazard Levelized Cost of Energy Analysis, version 8.0
183	Photovoltaic	2012	$ 0.18				Feldman et al 2014	2014	Photovoltaic (PV) Pricing Trends: Historical, Recent, and Near-Term Projections 2014 Edition
184	Photovoltaic	2013	$ 0.18				Feldman et al 2014	2014	Photovoltaic (PV) Pricing Trends: Historical, Recent, and Near-Term Projections 2014 Edition
185	Photovoltaic	2013	$ 0.22		30	0	LBNL 2014	2014	Tracking the Sun VII
186	Photovoltaic	2014	$ 0.16		20		Lazard 2014	2014	Lazard Levelized Cost of Energy Analysis, version 8.0
187	Photovoltaic	2012	$ 0.22		30	0	LBNL 2014	2014	Tracking the Sun VII
188	Photovoltaic	2012	$ 0.22				Feldman et al 2014	2014	Photovoltaic (PV) Pricing Trends: Historical, Recent, and Near-Term Projections 2014 Edition
189	Photovoltaic	2014	$ 0.17		25		Lazard 2014	2014	Lazard Levelized Cost of Energy Analysis, version 8.0
190	Photovoltaic	2011	$ 0.25		30	0	LBNL 2014	2014	Tracking the Sun VII
191	Photovoltaic	2010	$ 0.25				IIASA 2014	2014	AMPERE DB
192	Photovoltaic	2013	$ 0.25				Bollinger-Weaver 2014	2014	Utility-Scale Solar 2013: An Empirical Analysis of Project Cost, Performance, and Pricing Trends in the United States
193	Photovoltaic	2013	$ 0.25				Feldman et al 2014	2014	Photovoltaic (PV) Pricing Trends: Historical, Recent, and Near-Term Projections 2014 Edition
194	Photovoltaic	2011	$ 0.25				Feldman et al 2014	2014	Photovoltaic (PV) Pricing Trends: Historical, Recent, and Near-Term Projections 2014 Edition
195	Photovoltaic	2010	$ 0.27		30	0	LBNL 2014	2014	Tracking the Sun VII

#	Technology	Year	Calculated LCOE	Overnight Capital Cost dollar per kW including Contingency	Fixed O&M dollar per kW	Variable O&M dollar per MWh	Reference Name	Publication Year	Dataset name
196	Photovoltaic	2012	$ 0.26				Bollinger-Weaver 2014	2014	Utility-Scale Solar 2013: An Empirical Analysis of Project Cost, Performance, and Pricing Trends in the United States
197	Photovoltaic	2013	$ 0.27		30	0	LBNL 2014	2014	Tracking the Sun VII
198	Photovoltaic	2010	$ 0.27				Mai et al 2014	2014	Envisioning a renewable electricty future for the United States
199	Photovoltaic	2010	$ 0.28				Mai et al 2014	2014	Envisioning a renewable electricty future for the United States
200	Photovoltaic	2012	$ 0.29				Feldman et al 2014	2014	Photovoltaic (PV) Pricing Trends: Historical, Recent, and Near-Term Projections 2014 Edition
201	Photovoltaic	2013	$ 0.30		30	0	LBNL 2014	2014	Tracking the Sun VII
202	Photovoltaic	2010	$ 0.29				Feldman et al 2014	2014	Photovoltaic (PV) Pricing Trends: Historical, Recent, and Near-Term Projections 2014 Edition
203	Photovoltaic	2014	$ 0.25		30		Lazard 2014	2014	Lazard Levelized Cost of Energy Analysis, version 8.0
204	Photovoltaic	2012	$ 0.32		30	0	LBNL 2014	2014	Tracking the Sun VII
205	Photovoltaic	2013	$ 0.32		30	0	LBNL 2014	2014	Tracking the Sun VII
206	Photovoltaic	2011	$ 0.32				Feldman et al 2014	2014	Photovoltaic (PV) Pricing Trends: Historical, Recent, and Near-Term Projections 2014 Edition
207	Photovoltaic	2011	$ 0.34		30	0	LBNL 2014	2014	Tracking the Sun VII
208	Photovoltaic	2012	$ 0.35		30	0	LBNL 2014	2014	Tracking the Sun VII
209	Photovoltaic	2010	$ 0.34				Feldman et al 2014	2014	Photovoltaic (PV) Pricing Trends: Historical, Recent, and Near-Term Projections 2014 Edition
210	Photovoltaic	2012	$ 0.37		30	0	LBNL 2014	2014	Tracking the Sun VII
211	Photovoltaic	2011	$ 0.40		30	0	LBNL 2014	2014	Tracking the Sun VII
212	Photovoltaic	2010	$ 0.40		30	0	LBNL 2014	2014	Tracking the Sun VII
213	Photovoltaic	2011	$ 0.40				Feldman et al 2014	2014	Photovoltaic (PV) Pricing Trends: Historical, Recent, and Near-Term Projections 2014 Edition
214	Photovoltaic	2011	$ 0.43		30	0	LBNL 2014	2014	Tracking the Sun VII
215	Photovoltaic	2010	$ 0.45		30	0	LBNL 2014	2014	Tracking the Sun VII
216	Photovoltaic	2010	$ 0.46				Feldman et al 2014	2014	Photovoltaic (PV) Pricing Trends: Historical, Recent, and Near-Term Projections 2014 Edition
217	Photovoltaic	2010	$ 0.48		30	0	LBNL 2014	2014	Tracking the Sun VII

#	Technology	Year	Calculated LCOE	Overnight Capital Cost dollar per kW including Contingency	Fixed O&M dollar per kW	Variable O&M dollar per MWh	Reference Name	Publication Year	Dataset name
218	Photovoltaic	2009	$ 0.53		30	0	LBNL 2014	2014	Tracking the Sun VII
219	Photovoltaic	2009	$ 0.54		30	0	LBNL 2014	2014	Tracking the Sun VII
220	Photovoltaic	2009	$ 0.56		30	0	LBNL 2014	2014	Tracking the Sun VII
221	Solar Thermal	2011	$ 0.24		71	0	DOE 2013	2013	DOE Program Estimate
222	Solar Thermal	2014	$ 0.21		71	3	NREL_ATB 2015	2015	NREL Annual Technology Baseline 2015
223	Solar Thermal	2013	$ 0.21		75	3	NREL_ATB 2015	2015	NREL Annual Technology Baseline 2015
224	Solar Thermal	2014	$ 0.16		71	3	NREL_ATB 2015	2015	NREL Annual Technology Baseline 2015
225	Solar Thermal	2013	$ 0.17		75	3	NREL_ATB 2015	2015	NREL Annual Technology Baseline 2015
226	Solar Thermal	2009	$ 0.14	$ 5,219.08	56.6		GPRA 2009	2009	Government Performance and Results Act (2009). Data from Market Allocation (MARKAL) model, International Energy Agency and Brookhaven National Laboratory
227	Solar Thermal	2009	$ 0.19	$ 5,021.14	56.78	0	AEO 2009	2009	Annual Energy Outlook 2009
228	Solar Thermal	2009	$ 0.17		50	0.71	Staley et al, 2009	2009	Juice from Concentrate - Reducing Emissions with Concentrating Solar Thermal Power. World Resources Institute in conjunction with Goldman Sachs. 2009
229	Solar Thermal	2010	$ 0.14	$ 4,932.80			AEO 2010	2010	Annual Energy Outlook 2010
230	Solar Thermal	2010	$ 0.16	$ 6,001.63			EPA 2010	2010	Environmental Protection Agency (2010). Data from Integrated Power Model (IPM), ICF International.
231	Solar Thermal	2009	$ 0.14	$ 5,132.31	58.05	0	AEO 2010	2010	Annual Energy Outlook 2010
232	Solar Thermal	2009	$ 0.15		60	0	Klein et al 2010	2010	Comparate Costs of California Central Station Electricity Generation. Final Staff Report
233	Solar Thermal	2009	$ 0.17		68	0	Klein et al 2010	2010	Comparate Costs of California Central Station Electricity Generation. Final Staff Report
234	Solar Thermal	2009	$ 0.19		92	0	Klein et al 2010	2010	Comparate Costs of California Central Station Electricity Generation. Final Staff Report
235	Solar Thermal	2009	$ 0.20		66	0	Lazard 2010	2010	Lazard Levelized Cost of Energy Analysis, version 4.0
236	Solar Thermal	2009	$ 0.24		66	0	Lazard 2010	2010	Lazard Levelized Cost of Energy Analysis, version 4.0

#	Technology	Year	Calculated LCOE	Overnight Capital Cost dollar per kW including Contingency	Fixed O&M dollar per kW	Variable O&M dollar per MWh	Reference Name	Publication Year	Dataset name
237	Solar Thermal	2009	$ 0.15		50	3	Lazard 2010	2010	Lazard Levelized Cost of Energy Analysis, version 4.0
238	Solar Thermal	2009	$ 0.21		60	3	Lazard 2010	2010	Lazard Levelized Cost of Energy Analysis, version 4.0
239	Solar Thermal	2009	$ 0.21		70	3	Lazard 2010	2010	Lazard Levelized Cost of Energy Analysis, version 4.0
240	Solar Thermal	2009	$ 0.25		60	3	Lazard 2010	2010	Lazard Levelized Cost of Energy Analysis, version 4.0
241	Solar Thermal	2010	$ 0.21		70	3	Turchi 2010	2010	Parabolic Trough Reference Plant for Cost Modeling with the Solar Advisor Model
242	Solar Thermal	2010	$ 0.23		70	3	Turchi 2010	2010	Parabolic Trough Reference Plant for Cost Modeling with the Solar Advisor Model
243	Solar Thermal	2011	$ 0.13	$ 4,574.59			AEO 2011	2011	Annual Energy Outlook 2011
244	Solar Thermal	2010	$ 0.13	$ 4,636.41	63.23	0	AEO 2011	2011	Annual Energy Outlook 2011
245	Solar Thermal	2009	$ 0.21		80	3	DOE SETP 2011	2011	US DOE Energy Efficiency & Renewable Energy (EERE). Solar Energy Technologies Program. Accessed August 2011.
246	Solar Thermal	2011	$ 0.18		60		IPCC 2011	2011	IPCC Annex 3
247	Solar Thermal	2011	$ 0.17				McCalley et al, 2011	2011	A Wider Horizon. IEEE Power & Energy Magazine. May/June 2011
248	Solar Thermal	2011	$ 0.20		71		IPCC 2011	2011	IPCC Annex 3
249	Solar Thermal	2011	$ 0.22		82		IPCC 2011	2011	IPCC Annex 3
250	Solar Thermal	2009	$ 0.22		80	3	DOE SETP 2011	2011	US DOE Energy Efficiency & Renewable Energy (EERE). Solar Energy Technologies Program. Accessed August 2011.
251	Solar Thermal	2011	$ 0.25		71	11	DOE 2011	2011	DOE Program Estimate
252	Solar Thermal	2009	$ 0.07				Hubbell et al 2012	2012	Renewable Energy Finance Tracking Initiative
253	Solar Thermal	2010	$ 0.11				Hubbell et al 2012	2012	Renewable Energy Finance Tracking Initiative
254	Solar Thermal	2010	$ 0.20		70		DOE SETP 2012	2012	Sunshot Solar Vision
255	Solar Thermal	2010	$ 0.19		49.5	0	Black and Veatch 2012	2012	COST AND PERFORMANCE DATA FOR POWER GENERATION TECHNOLOGIES

#	Technology	Year	Calculated LCOE	Overnight Capital Cost dollar per kW including Contingency	Fixed O&M dollar per kW	Variable O&M dollar per MWh	Reference Name	Publication Year	Dataset name
256	Solar Thermal	2010	$ 0.14				Hubbell et al 2012	2012	Renewable Energy Finance Tracking Initiative
257	Solar Thermal	2010	$ 0.21		80	3	Mai et al, 2012	2012	Renewable Electricity Futures
258	Solar Thermal	2010	$ 0.15				Hubbell et al 2012	2012	Renewable Energy Finance Tracking Initiative
259	Solar Thermal	2010	$ 0.16		65		IEA 2012	2012	Energy Technology Perspectives 2012 Pathways to a Clean Energy System
260	Solar Thermal	2010	$ 0.18		49.5	0	Black and Veatch 2012	2012	COST AND PERFORMANCE DATA FOR POWER GENERATION TECHNOLOGIES
261	Solar Thermal	2010	$ 0.22		80	3	Mai et al, 2012	2012	Renewable Electricity Futures
262	Solar Thermal	2013	$ 0.14		65	4	Turchi and Heath 2013	2013	Molten Salt Power Tower Cost Model for the System Advisor Model (SAM)
263	Solar Thermal	2013	$ 0.15		65	4	Turchi and Heath 2013	2013	Molten Salt Power Tower Cost Model for the System Advisor Model (SAM)
264	Solar Thermal	2013	$ 0.18		65	4	Turchi and Heath 2013	2013	Molten Salt Power Tower Cost Model for the System Advisor Model (SAM)
265	Solar Thermal	2010	$ 0.15				Mai et al 2014	2014	Envisioning a renewable electricty future for the United States
266	Solar Thermal	2014	$ 0.10		80		Lazard 2014	2014	Lazard Levelized Cost of Energy Analysis, version 8.0
267	Solar Thermal	2010	$ 0.19				Mai et al 2014	2014	Envisioning a renewable electricty future for the United States
268	Solar Thermal	2014	$ 0.22		115		Lazard 2014	2014	Lazard Levelized Cost of Energy Analysis, version 8.0
269	Geothermal	2013	$ 0.08		115	0	NREL_ATB 2015	2015	NREL Annual Technology Baseline 2015
270	Geothermal	2013	$ 0.10		115	0	NREL_ATB 2015	2015	NREL Annual Technology Baseline 2015
271	Geothermal	2009	$ 0.04	$ 3,050.96	69.59		GPRA 2009	2009	Government Performance and Results Act (2009). Data from Market Allocation (MARKAL) model, International Energy Agency and Brookhaven National Laboratory
272	Geothermal	2009	$ 0.06	$ 4,281.00	112.16		GPRA 2009	2009	Government Performance and Results Act (2009). Data from Market Allocation (MARKAL) model, International Energy Agency and Brookhaven National Laboratory
273	Geothermal	2009	$ 0.04	$ 1,711.11	164.64	0	AEO 2009	2009	Annual Energy Outlook 2009
274	Geothermal	2010	$ 0.07	$ 5,268.24			AEO 2010	2010	Annual Energy Outlook 2010

#	Technology	Year	Calculated LCOE	Overnight Capital Cost dollar per kW including Contingency	Fixed O&M dollar per kW	Variable O&M dollar per MWh	Reference Name	Publication Year	Dataset name
275	Geothermal	2009	$ 0.04	$ 1,748.99	168.33	0	AEO 2010	2010	Annual Energy Outlook 2010
276	Geothermal	2009	$ 0.03		40.32	4.31	Klein et al 2010	2010	Comparate Costs of California Central Station Electricity Generation. Final Staff Report
277	Geothermal	2009	$ 0.04		49.62	4.85	Klein et al 2010	2010	Comparate Costs of California Central Station Electricity Generation. Final Staff Report
278	Geothermal	2009	$ 0.05		58.38	5.06	Klein et al 2010	2010	Comparate Costs of California Central Station Electricity Generation. Final Staff Report
279	Geothermal	2009	$ 0.06		47.44	4.55	Klein et al 2010	2010	Comparate Costs of California Central Station Electricity Generation. Final Staff Report
280	Geothermal	2009	$ 0.07		67.14	5.28	Klein et al 2010	2010	Comparate Costs of California Central Station Electricity Generation. Final Staff Report
281	Geothermal	2009	$ 0.09		54.65	5.12	Klein et al 2010	2010	Comparate Costs of California Central Station Electricity Generation. Final Staff Report
282	Geothermal	2010	$ 0.05	$ 2,481.75	107.27	9.52	AEO 2011	2011	Annual Energy Outlook 2011
283	Geothermal	2011	$ 0.05		150		IPCC 2011	2011	IPCC Annex 3
284	Geothermal	2011	$ 0.05		150		IPCC 2011	2011	IPCC Annex 3
285	Geothermal	2011	$ 0.06		170		IPCC 2011	2011	IPCC Annex 3
286	Geothermal	2011	$ 0.08		190		IPCC 2011	2011	IPCC Annex 3
287	Geothermal	2011	$ 0.08		170		IPCC 2011	2011	IPCC Annex 3
288	Geothermal	2011	$ 0.10		190		IPCC 2011	2011	IPCC Annex 3
289	Geothermal	2010	$ 0.07		229	0	Mai et al, 2012	2012	Renewable Electricity Futures
290	Geothermal	2010	$ 0.10		229	0	Black and Veatch 2012	2012	COST AND PERFORMANCE DATA FOR POWER GENERATION TECHNOLOGIES
291	Geothermal	2013	$ 0.05		86.15	0	McCann RE 2013	2013	Cost of Generation Workshop: Non-solar Renewables
292	Geothermal	2013	$ 0.06		89.79	0	McCann RE 2013	2013	Cost of Generation Workshop: Non-solar Renewables
293	Geothermal	2013	$ 0.08		89.79	0	McCann RE 2013	2013	Cost of Generation Workshop: Non-solar Renewables
294	Geothermal	2013	$ 0.08		89.79	0	McCann RE 2013	2013	Cost of Generation Workshop: Non-solar Renewables
295	Geothermal	2013	$ 0.11		154.78	0	McCann RE 2013	2013	Cost of Generation Workshop: Non-solar Renewables

#	Technology	Year	Calculated LCOE	Overnight Capital Cost dollar per kW including Contingency	Fixed O&M dollar per kW	Variable O&M dollar per MWh	Reference Name	Publication Year	Dataset name
296	Geothermal	2013	$ 0.14		182.58	0	McCann RE 2013	2013	Cost of Generation Workshop: Non-solar Renewables
297	Geothermal	2010	$ 0.08		0	17.099	DOE 2013	2013	DOE Program Estimate
298	Geothermal	2011	$ 0.10		222.9761	0	DOE 2011	2011	DOE Program Estimate
299	Geothermal	2010	$ 0.09		0	32.3142	DOE 2013	2013	DOE Program Estimate
300	Geothermal	2013	$ 0.09		115	0	NREL_ATB 2015	2015	NREL Annual Technology Baseline 2015
301	Geothermal	2013	$ 0.09		115	0	NREL_ATB 2015	2015	NREL Annual Technology Baseline 2015
302	Geothermal	2013	$ 0.15		115	0	NREL_ATB 2015	2015	NREL Annual Technology Baseline 2015
303	Geothermal	2013	$ 0.15		115	0	NREL_ATB 2015	2015	NREL Annual Technology Baseline 2015
304	Geothermal	2009	$ 0.06	$ 3,904.14	136.54		GPRA 2009	2009	Government Performance and Results Act (2009). Data from Market Allocation (MARKAL) model, International Energy Agency and Brookhaven National Laboratory
305	Geothermal	2009	$ 0.06				E3 2010	2010	Capital Cost Recommendations for 2009 TEPPC Study.
306	Geothermal	2009	$ 0.08		0	30	Lazard 2010	2010	Lazard Levelized Cost of Energy Analysis, version 4.0
307	Geothermal	2009	$ 0.09		180	5	E3 2010	2010	Capital Cost Recommendations for 2009 TEPPC Study.
308	Geothermal	2009	$ 0.09				E3 2010	2010	Capital Cost Recommendations for 2009 TEPPC Study.
309	Geothermal	2009	$ 0.13		0	40	Lazard 2010	2010	Lazard Levelized Cost of Energy Analysis, version 4.0
310	Geothermal	2011	$ 0.03				McCalley et al, 2011	2011	A Wider Horizon. IEEE Power & Energy Magazine. May/June 2011
311	Geothermal	2010	$ 0.15		223	0	DOE 2011	2011	DOE Program Estimate
312	Geothermal	2014	$ 0.08			30	Lazard 2014	2014	Lazard Levelized Cost of Energy Analysis, version 8.0
313	Geothermal	2014	$ 0.13			40	Lazard 2014	2014	Lazard Levelized Cost of Energy Analysis, version 8.0
314	Small Hydro	2009	$ 0.02		9.88	1.9	Klein et al 2010	2010	Comparate Costs of California Central Station Electricity Generation. Final Staff Report
315	Small Hydro	2009	$ 0.07		17.57	3.48	Klein et al 2010	2010	Comparate Costs of California Central Station Electricity Generation. Final Staff Report
316	Small Hydro	2009	$ 0.26		28.83	5.54	Klein et al 2010	2010	Comparate Costs of California Central Station Electricity Generation. Final Staff Report
317	Small Hydro	2011	$ 0.14		130	0	DOE 2011	2011	DOE Program Estimate

#	Technology	Year	Calculated LCOE	Overnight Capital Cost dollar per kW including Contingency	Fixed O&M dollar per kW	Variable O&M dollar per MWh	Reference Name	Publication Year	Dataset name
318	Hydroelectric	2010	$ 0.09		90	0	DOE 2013	2013	DOE Program Estimate
319	Hydroelectric	2009	$ 0.04	$ 2,241.84	13.63	2.43	AEO 2009	2009	Annual Energy Outlook 2009
320	Hydroelectric	2009	$ 0.06	$ 2,291.48	13.93	2.49	AEO 2010	2010	Annual Energy Outlook 2010
321	Hydroelectric	2009	$ 0.01		8.77	1.6	Klein et al 2010	2010	Comparate Costs of California Central Station Electricity Generation. Final Staff Report
322	Hydroelectric	2009	$ 0.04		12.59	2.39	Klein et al 2010	2010	Comparate Costs of California Central Station Electricity Generation. Final Staff Report
323	Hydroelectric	2009	$ 0.19		27.05	5	Klein et al 2010	2010	Comparate Costs of California Central Station Electricity Generation. Final Staff Report
324	Hydroelectric	2009	$ 0.12		25	0	E3 2010	2010	Capital Cost Recommendations for 2009 TEPPC Study.
325	Hydroelectric	2009	$ 0.08		25	0	E3 2010	2010	Capital Cost Recommendations for 2009 TEPPC Study.
326	Hydroelectric	2010	$ 0.06	$ 2,221.23	13.55	2.42	AEO 2011	2011	Annual Energy Outlook 2011
327	Hydroelectric	2011	$ 0.03		25		IPCC 2011	2011	IPCC Annex 3
328	Hydroelectric	2011	$ 0.07		50		IPCC 2011	2011	IPCC Annex 3
329	Hydroelectric	2011	$ 0.10		75		IPCC 2011	2011	IPCC Annex 3
330	Hydroelectric	2010	$ 0.09		14.85	3	Mai et al, 2012	2012	Renewable Electricity Futures
331	Hydroelectric	2010	$ 0.09		14.85	5.94	Black and Veatch 2012	2012	COST AND PERFORMANCE DATA FOR POWER GENERATION TECHNOLOGIES
332	Ocean	2011	$ 0.23		100		IPCC 2011	2011	IPCC Annex 3
333	Ocean	2011	$ 0.24		100		IPCC 2011	2011	IPCC Annex 3
334	Ocean	2011	$ 0.25		100		IPCC 2011	2011	IPCC Annex 3
335	Biopower	2009	$ 0.07	$ 2,542.97	114.25	0.01	AEO 2009	2009	Annual Energy Outlook 2009
336	Biopower	2009	$ 0.08	$ 3,765.70	64.45	6.71	AEO 2009	2009	Annual Energy Outlook 2009
337	Biopower	2009	$ 0.06	$ 3,849.07	65.89	6.86	AEO 2010	2010	Annual Energy Outlook 2010
338	Biopower	2009	$ 0.05	$ 2,599.27	116.8	0.01	AEO 2010	2010	Annual Energy Outlook 2010

#	Technology	Year	Calculated LCOE	Overnight Capital Cost dollar per kW including Contingency	Fixed O&M dollar per kW	Variable O&M dollar per MWh	Reference Name	Publication Year	Dataset name
339	Biopower	2009	$ 0.04		0	17	Lazard 2010	2010	Lazard Levelized Cost of Energy Analysis, version 4.0
340	Biopower	2009	$ 0.05		70	3	Klein et al 2010	2010	Comparate Costs of California Central Station Electricity Generation. Final Staff Report
341	Biopower	2009	$ 0.06		107.8	4.7	Klein et al 2010	2010	Comparate Costs of California Central Station Electricity Generation. Final Staff Report
342	Biopower	2009	$ 0.04		0	17	Lazard 2010	2010	Lazard Levelized Cost of Energy Analysis, version 4.0
343	Biopower	2009	$ 0.08		160.1	6.98	Klein et al 2010	2010	Comparate Costs of California Central Station Electricity Generation. Final Staff Report
344	Biopower	2009	$ 0.07		125	3	Klein et al 2010	2010	Comparate Costs of California Central Station Electricity Generation. Final Staff Report
345	Biopower	2009	$ 0.08		130	0	E3 2010	2010	Capital Cost Recommendations for 2009 TEPPC Study.
346	Biopower	2009	$ 0.09		150	4	Klein et al 2010	2010	Comparate Costs of California Central Station Electricity Generation. Final Staff Report
347	Biopower	2009	$ 0.09		95	15	Lazard 2010	2010	Lazard Levelized Cost of Energy Analysis, version 4.0
348	Biopower	2009	$ 0.08		99.5	4.47	Klein et al 2010	2010	Comparate Costs of California Central Station Electricity Generation. Final Staff Report
349	Biopower	2009	$ 0.11		200	8.73	Klein et al 2010	2010	Comparate Costs of California Central Station Electricity Generation. Final Staff Report
350	Biopower	2009	$ 0.11		175	4.5	Klein et al 2010	2010	Comparate Costs of California Central Station Electricity Generation. Final Staff Report
351	Biopower	2009	$ 0.11		95	15	Lazard 2010	2010	Lazard Levelized Cost of Energy Analysis, version 4.0
352	Biopower	2009	$ 0.11		155	4	E3 2010	2010	Capital Cost Recommendations for 2009 TEPPC Study.
353	Biopower	2009	$ 0.12		150	10	Klein et al 2010	2010	Comparate Costs of California Central Station Electricity Generation. Final Staff Report
354	Biopower	2009	$ 0.12		165	0	E3 2010	2010	Capital Cost Recommendations for 2009 TEPPC Study.
355	Biopower	2010	$ 0.07	$ 3,723.89	99.3	6.94	AEO 2011	2011	Annual Energy Outlook 2011
356	Biopower	2010	$ 0.16	$ 8,236.87	369.28	8.23	AEO 2011	2011	Annual Energy Outlook 2011
357	Biopower	2011	$ 0.01		12	1.8	IPCC 2011	2011	IPCC Annex 3
358	Biopower	2011	$ 0.01		12	1.8	IPCC 2011	2011	IPCC Annex 3
359	Biopower	2011	$ 0.01		12	1.8	IPCC 2011	2011	IPCC Annex 3
360	Biopower	2011	$ 0.01		18		IPCC 2011	2011	IPCC Annex 3
361	Biopower	2011	$ 0.01		18		IPCC 2011	2011	IPCC Annex 3

#	Technology	Year	Calculated LCOE	Overnight Capital Cost dollar per kW including Contingency	Fixed O&M dollar per kW	Variable O&M dollar per MWh	Reference Name	Publication Year	Dataset name
362	Biopower	2011	$ 0.02		18		IPCC 2011	2011	IPCC Annex 3
363	Biopower	2011	$ 0.05		84	3.4	IPCC 2011	2011	IPCC Annex 3
364	Biopower	2011	$ 0.05		87	4	IPCC 2011	2011	IPCC Annex 3
365	Biopower	2011	$ 0.06		86	3.5	IPCC 2011	2011	IPCC Annex 3
366	Biopower	2011	$ 0.06		84	3.4	IPCC 2011	2011	IPCC Annex 3
367	Biopower	2011	$ 0.06		87	4	IPCC 2011	2011	IPCC Annex 3
368	Biopower	2011	$ 0.06		86	3.5	IPCC 2011	2011	IPCC Annex 3
369	Biopower	2011	$ 0.07		84	3.4	IPCC 2011	2011	IPCC Annex 3
370	Biopower	2011	$ 0.07		87	4	IPCC 2011	2011	IPCC Annex 3
371	Biopower	2011	$ 0.07		86	3.5	IPCC 2011	2011	IPCC Annex 3
372	Biopower	2012	$ 0.05		56.4	3.8	IRENA Biomass 2012	2012	IRENA Biomass 2012
373	Biopower	2012	$ 0.07		210.87		IRENA Biomass 2012	2012	IRENA Biomass 2012
374	Biopower	2012	$ 0.06		64.2	3.8	IRENA Biomass 2012	2012	IRENA Biomass 2012
375	Biopower	2012	$ 0.06		65.1	3.8	IRENA Biomass 2012	2012	IRENA Biomass 2012
376	Biopower	2012	$ 0.11		487.2		IRENA Biomass 2012	2012	IRENA Biomass 2012
377	Biopower	2012	$ 0.06		54.054	4.2	IRENA Biomass 2012	2012	IRENA Biomass 2012
378	Biopower	2012	$ 0.08		106.5	3.8	IRENA Biomass 2012	2012	IRENA Biomass 2012
379	Biopower	2010	$ 0.10		94.06	14.85	Black and Veatch 2012	2012	COST AND PERFORMANCE DATA FOR POWER GENERATION TECHNOLOGIES
380	Biopower	2010	$ 0.09		102.6	4.6	Mai et al, 2012	2012	Renewable Electricity Futures
381	Biopower	2012	$ 0.11		255.6	4.7	IRENA Biomass 2012	2012	IRENA Biomass 2012
382	Biopower	2012	$ 0.11		270	4.7	IRENA Biomass 2012	2012	IRENA Biomass 2012
383	Biopower	2012	$ 0.11		167.1	3.7	IRENA Biomass 2012	2012	IRENA Biomass 2012

#	Technology	Year	Calculated LCOE	Overnight Capital Cost dollar per kW including Contingency	Fixed O&M dollar per kW	Variable O&M dollar per MWh	Reference Name	Publication Year	Dataset name
384	Biopower	2012	$ 0.14		342	4.7	IRENA Biomass 2012	2012	IRENA Biomass 2012
385	Biopower	2012	$ 0.15		427.28	4.2	IRENA Biomass 2012	2012	IRENA Biomass 2012
386	Biopower	2012	$ 0.15		392.7	3.7	IRENA Biomass 2012	2012	IRENA Biomass 2012
387	Biopower	2012	$ 0.16		409.2	4.7	IRENA Biomass 2012	2012	IRENA Biomass 2012
388	Biopower	2013	$ 0.09		106.26	5.29	McCann RE 2013	2013	Cost of Generation Workshop: Non-solar Renewables
389	Biopower	2013	$ 0.11		106.26	5.29	McCann RE 2013	2013	Cost of Generation Workshop: Non-solar Renewables
390	Biopower	2013	$ 0.14		100.44	15.86	McCann RE 2013	2013	Cost of Generation Workshop: Non-solar Renewables
391	Biopower	2014	$ 0.09		95	15	Lazard 2014	2014	Lazard Levelized Cost of Energy Analysis, version 8.0
392	Biopower	2014	$ 0.11		95	15	Lazard 2014	2014	Lazard Levelized Cost of Energy Analysis, version 8.0
393	Distributed Generation	2009	$ 0.09	$ 1,369.74	16.03	7.12	AEO 2009	2009	Annual Energy Outlook 2009
394	Distributed Generation	2009	$ 0.48	$ 1,644.72	16.03	7.12	AEO 2009	2009	Annual Energy Outlook 2009
395	Distributed Generation	2011	$ 0.05		65	11	IPCC 2011	2011	IPCC Annex 3
396	Distributed Generation	2011	$ 0.06		68	15	IPCC 2011	2011	IPCC Annex 3
397	Distributed Generation	2011	$ 0.06		71	19	IPCC 2011	2011	IPCC Annex 3
398	Distributed Generation	2011	$ 0.11		54	35	IPCC 2011	2011	IPCC Annex 3
399	Distributed Generation	2011	$ 0.13		54	35	IPCC 2011	2011	IPCC Annex 3
400	Distributed Generation	2011	$ 0.14		54	35	IPCC 2011	2011	IPCC Annex 3
401	Distributed Generation	2011	$ 0.16		59	43	IPCC 2011	2011	IPCC Annex 3
402	Distributed Generation	2011	$ 0.19		70	47	IPCC 2011	2011	IPCC Annex 3
403	Distributed Generation	2011	$ 0.22		80	51	IPCC 2011	2011	IPCC Annex 3

#	Technology	Year	Calculated LCOE	Overnight Capital Cost dollar per kW including Contingency	Fixed O&M dollar per kW	Variable O&M dollar per MWh	Reference Name	Publication Year	Dataset name
404	Distributed Generation	2014	$ 0.01		15		Lazard 2014	2014	Lazard Levelized Cost of Energy Analysis, version 8.0
405	Distributed Generation	2014	$ 0.04		15		Lazard 2014	2014	Lazard Levelized Cost of Energy Analysis, version 8.0
406	Distributed Generation	2014	$ 0.09			18	Lazard 2014	2014	Lazard Levelized Cost of Energy Analysis, version 8.0
407	Distributed Generation	2014	$ 0.13			22	Lazard 2014	2014	Lazard Levelized Cost of Energy Analysis, version 8.0
408	Fuel Cell	2010	$ 0.10		140	8	DOE 2013	2013	DOE Program Estimate
409	Fuel Cell	2009	$ 0.15	$ 5,359.52	5.65	47.92	AEO 2009	2009	Annual Energy Outlook 2009
410	Fuel Cell	2009	$ 0.07	$ 5,478.18	49	5.78	AEO 2010	2010	Annual Energy Outlook 2010
411	Fuel Cell	2009	$ 0.10		169	11	Lazard 2010	2010	Lazard Levelized Cost of Energy Analysis, version 4.0
412	Fuel Cell	2009	$ 0.22		850	11	Lazard 2010	2010	Lazard Levelized Cost of Energy Analysis, version 4.0
413	Fuel Cell	2010	$ 0.11	$ 6,752.47	345.8	0	AEO 2011	2011	Annual Energy Outlook 2011
414	Fuel Cell	2011	$ 0.12		140	8	DOE 2011	2011	DOE Program Estimate
415	Fuel Cell	2011	$ 0.15		188	8	DOE 2011	2011	DOE Program Estimate
416	Fuel Cell	2014	$ 0.10			30	Lazard 2014	2014	Lazard Levelized Cost of Energy Analysis, version 8.0
417	Fuel Cell	2014	$ 0.16			50	Lazard 2014	2014	Lazard Levelized Cost of Energy Analysis, version 8.0
418	Combined Cycle	2009	$ 0.05	$ 947.50	11.7	2	AEO 2009	2009	Annual Energy Outlook 2009
419	Combined Cycle	2009	$ 0.05	$ 962.43	12.48	2.07	AEO 2009	2009	Annual Energy Outlook 2009
420	Combined Cycle	2009	$ 0.07	$ 1,889.91	19.9	2.94	AEO 2009	2009	Annual Energy Outlook 2009
421	Combined Cycle	2009	$ 0.02	$ 968.48	11.96	2.04	AEO 2010	2010	Annual Energy Outlook 2010
422	Combined Cycle	2009	$ 0.02	$ 983.74	12.76	2.11	AEO 2010	2010	Annual Energy Outlook 2010
423	Combined Cycle	2009	$ 0.03	$ 1,931.75	20.35	3.01	AEO 2010	2010	Annual Energy Outlook 2010
424	Combined Cycle	2009	$ 0.05		5.76	2.19	Klein et al 2010	2010	Comparate Costs of California Central Station Electricity Generation. Final Staff Report
425	Combined Cycle	2009	$ 0.04		5.01	1.95	Klein et al 2010	2010	Comparate Costs of California Central Station Electricity Generation. Final Staff Report

#	Technology	Year	Calculated LCOE	Overnight Capital Cost dollar per kW including Contingency	Fixed O&M dollar per kW	Variable O&M dollar per MWh	Reference Name	Publication Year	Dataset name
426	Combined Cycle	2009	$ 0.04		5.76	2.19	Klein et al 2010	2010	Comparate Costs of California Central Station Electricity Generation. Final Staff Report
427	Combined Cycle	2009	$ 0.05		5.5	2	Lazard 2010	2010	Lazard Levelized Cost of Energy Analysis, version 4.0
428	Combined Cycle	2009	$ 0.05		7.17	2.69	Klein et al 2010	2010	Comparate Costs of California Central Station Electricity Generation. Final Staff Report
429	Combined Cycle	2009	$ 0.06		8.3	3.02	Klein et al 2010	2010	Comparate Costs of California Central Station Electricity Generation. Final Staff Report
430	Combined Cycle	2009	$ 0.05		8.62	3.02	Klein et al 2010	2010	Comparate Costs of California Central Station Electricity Generation. Final Staff Report
431	Combined Cycle	2009	$ 0.07		6.2	3.5	Lazard 2010	2010	Lazard Levelized Cost of Energy Analysis, version 4.0
432	Combined Cycle	2009	$ 0.06		10.97	3.42	Klein et al 2010	2010	Comparate Costs of California Central Station Electricity Generation. Final Staff Report
433	Combined Cycle	2009	$ 0.02		8	4.9	E3 2010	2010	Capital Cost Recommendations for 2009 TEPPC Study.
434	Combined Cycle	2009	$ 0.07		12.62	3.84	Klein et al 2010	2010	Comparate Costs of California Central Station Electricity Generation. Final Staff Report
435	Combined Cycle	2009	$ 0.07		12.62	3.84	Klein et al 2010	2010	Comparate Costs of California Central Station Electricity Generation. Final Staff Report
436	Combined Cycle	2010	$ 0.02	$ 966.82	14.22	3.37	AEO 2011	2011	Annual Energy Outlook 2011
437	Combined Cycle	2010	$ 0.02	$ 990.79	14.44	3.07	AEO 2011	2011	Annual Energy Outlook 2011
438	Combined Cycle	2010	$ 0.04	$ 2,036.13	29.89	6.37	AEO 2011	2011	Annual Energy Outlook 2011
439	Combined Cycle	2010	$ 0.02		20		IEA 2012	2012	Energy Technology Perspectives 2012 Pathways to a Clean Energy System
440	Combined Cycle	2010	$ 0.05		6.31	3.67	Black and Veatch 2012	2012	COST AND PERFORMANCE DATA FOR POWER GENERATION TECHNOLOGIES
441	Combined Cycle	2013	$ 0.07		34.56	0.61	McCann and Walters 2013	2013	Cost of Generation Workshop: Natural Gas Technologies
442	Combined Cycle	2013	$ 0.07		34.56	0.61	McCann and Walters 2013	2013	Cost of Generation Workshop: Natural Gas Technologies
443	Combined Cycle	2014	$ 0.05		5.5	2	Lazard 2014	2014	Lazard Levelized Cost of Energy Analysis, version 8.0
444	Combined Cycle	2014	$ 0.08		6.2	3.5	Lazard 2014	2014	Lazard Levelized Cost of Energy Analysis, version 8.0
445	Combustion Turbine	2009	$ 0.06	$ 634.17	10.53	3.17	AEO 2009	2009	Annual Energy Outlook 2009

#	Technology	Year	Calculated LCOE	Overnight Capital Cost dollar per kW including Contingency	Fixed O&M dollar per kW	Variable O&M dollar per MWh	Reference Name	Publication Year	Dataset name
446	Combustion Turbine	2009	$ 0.06	$ 670.26	12.11	3.57	AEO 2009	2009	Annual Energy Outlook 2009
447	Combustion Turbine	2009	$ 0.03	$ 648.21	10.77	3.24	AEO 2010	2010	Annual Energy Outlook 2010
448	Combustion Turbine	2009	$ 0.04	$ 685.10	12.38	3.65	AEO 2010	2010	Annual Energy Outlook 2010
449	Combustion Turbine	2009	$ 0.08		6.27	0.79	Klein et al 2010	2010	Comparate Costs of California Central Station Electricity Generation. Final Staff Report
450	Combustion Turbine	2009	$ 0.16		16.33	3.67	Klein et al 2010	2010	Comparate Costs of California Central Station Electricity Generation. Final Staff Report
451	Combustion Turbine	2009	$ 0.15		6.68	0.88	Klein et al 2010	2010	Comparate Costs of California Central Station Electricity Generation. Final Staff Report
452	Combustion Turbine	2009	$ 0.16		6.68	0.88	Klein et al 2010	2010	Comparate Costs of California Central Station Electricity Generation. Final Staff Report
453	Combustion Turbine	2009	$ 0.35		39.82	8.05	Klein et al 2010	2010	Comparate Costs of California Central Station Electricity Generation. Final Staff Report
454	Combustion Turbine	2009	$ 0.05		14	5	E3 2010	2010	Capital Cost Recommendations for 2009 TEPPC Study.
455	Combustion Turbine	2009	$ 0.37		17.4	4.17	Klein et al 2010	2010	Comparate Costs of California Central Station Electricity Generation. Final Staff Report
456	Combustion Turbine	2009	$ 0.40		23.94	4.17	Klein et al 2010	2010	Comparate Costs of California Central Station Electricity Generation. Final Staff Report
457	Combustion Turbine	2009	$ 0.94		42.44	9.05	Klein et al 2010	2010	Comparate Costs of California Central Station Electricity Generation. Final Staff Report
458	Combustion Turbine	2009	$ 0.98		42.44	9.05	Klein et al 2010	2010	Comparate Costs of California Central Station Electricity Generation. Final Staff Report
459	Combustion Turbine	2010	$ 0.05	$ 961.49	9.75	8.15	AEO 2011	2011	Annual Energy Outlook 2011
460	Combustion Turbine	2010	$ 0.04	$ 657.58	14.52	6.9	AEO 2011	2011	Annual Energy Outlook 2011
461	Combustion Turbine	2010	$ 0.05		10		IEA 2012	2012	Energy Technology Perspectives 2012 Pathways to a Clean Energy System
462	Combustion Turbine	2010	$ 0.11		5.26	29.9	Black and Veatch 2012	2012	COST AND PERFORMANCE DATA FOR POWER GENERATION TECHNOLOGIES
463	Combustion Turbine	2013	$ 0.19		25.24	0	McCann and Walters 2013	2013	Cost of Generation Workshop: Natural Gas Technologies
464	Combustion Turbine	2013	$ 0.33		27.44	0	McCann and Walters 2013	2013	Cost of Generation Workshop: Natural Gas Technologies
465	Combustion Turbine	2013	$ 0.34		28.39	0	McCann and Walters 2013	2013	Cost of Generation Workshop: Natural Gas Technologies

#	Technology	Year	Calculated LCOE	Overnight Capital Cost dollar per kW including Contingency	Fixed O&M dollar per kW	Variable O&M dollar per MWh	Reference Name	Publication Year	Dataset name
466	Combustion Turbine	2014	$ 0.15		5	4.7	Lazard 2014	2014	Lazard Levelized Cost of Energy Analysis, version 8.0
467	Combustion Turbine	2014	$ 0.20		25	7.5	Lazard 2014	2014	Lazard Levelized Cost of Energy Analysis, version 8.0
468	Coal	2009	$ 0.06	$ 2,057.84	27.53	4.59	AEO 2009	2009	Annual Energy Outlook 2009
469	Coal	2009	$ 0.06		20.4	2	Lazard 2010	2010	Lazard Levelized Cost of Energy Analysis, version 4.0
470	Coal	2009	$ 0.14		31.6	5.9	Lazard 2010	2010	Lazard Levelized Cost of Energy Analysis, version 4.0
471	Coal	2010	$ 0.04		46		IEA 2012	2012	Energy Technology Perspectives 2012 Pathways to a Clean Energy System
472	Coal	2010	$ 0.07		23	3.71	Black and Veatch 2012	2012	COST AND PERFORMANCE DATA FOR POWER GENERATION TECHNOLOGIES
473	Coal	2014	$ 0.06		40	2	Lazard 2014	2014	Lazard Levelized Cost of Energy Analysis, version 8.0
474	Coal	2014	$ 0.15		80	5	Lazard 2014	2014	Lazard Levelized Cost of Energy Analysis, version 8.0
475	Coal	2009	$ 0.06	$ 2,378.34	38.67	2.92	AEO 2009	2009	Annual Energy Outlook 2009
476	Coal	2009	$ 0.08	$ 3,495.95	46.12	4.44	AEO 2009	2009	Annual Energy Outlook 2009
477	Coal	2009	$ 0.06	$ 2,568.84	39.53	2.99	AEO 2010	2010	Annual Energy Outlook 2010
478	Coal	2009	$ 0.08	$ 3,776.17	47.15	4.54	AEO 2010	2010	Annual Energy Outlook 2010
479	Coal	2009	$ 0.09		26.4	6.8	Lazard 2010	2010	Lazard Levelized Cost of Energy Analysis, version 4.0
480	Coal	2009	$ 0.12		28.2	7.3	Lazard 2010	2010	Lazard Levelized Cost of Energy Analysis, version 4.0
481	Coal	2009	$ 0.18		25	10	E3 2010	2010	Capital Cost Recommendations for 2009 TEPPC Study.
482	Coal	2010	$ 0.08	$ 3,182.10	58.52	6.79	AEO 2011	2011	Annual Energy Outlook 2011
483	Coal	2010	$ 0.12	$ 5,286.63	68.47	8.83	AEO 2011	2011	Annual Energy Outlook 2011
484	Coal	2010	$ 0.09		31.1	6.54	Black and Veatch 2012	2012	COST AND PERFORMANCE DATA FOR POWER GENERATION TECHNOLOGIES
485	Coal	2014	$ 0.10		62.25	7	Lazard 2014	2014	Lazard Levelized Cost of Energy Analysis, version 8.0
486	Coal	2014	$ 0.17		73	8.5	Lazard 2014	2014	Lazard Levelized Cost of Energy Analysis, version 8.0
487	Nuclear	2009	$ 0.06	$ 3,317.80	90.02	0.49	AEO 2009	2009	Annual Energy Outlook 2009
488	Nuclear	2009	$ 0.06	$ 3,820.23	92.04	0.51	AEO 2010	2010	Annual Energy Outlook 2010
489	Nuclear	2009	$ 0.08		12.8	0	Lazard 2010	2010	Lazard Levelized Cost of Energy Analysis, version 4.0

#	Technology	Year	Calculated LCOE	Overnight Capital Cost dollar per kW including Contingency	Fixed O&M dollar per kW	Variable O&M dollar per MWh	Reference Name	Publication Year	Dataset name
490	Nuclear	2009	$ 0.12		70	6	E3 2010	2010	Capital Cost Recommendations for 2009 TEPPC Study.
491	Nuclear	2009	$ 0.11		12.8	0	Lazard 2010	2010	Lazard Levelized Cost of Energy Analysis, version 4.0
492	Nuclear	2010	$ 0.08	$ 5,274.51	87.69	2	AEO 2011	2011	Annual Energy Outlook 2011
493	Nuclear	2011	$ 0.06		87.31	0.62	Rothwell 2011	2011	The Economics of Future Nuclear Power: An update of The Economic Future of Nuclear Power (2004). Department of Economics. Stanford University. Feb 22, 2011
494	Nuclear	2011	$ 0.07		109.34	0.48	Rothwell 2011	2011	The Economics of Future Nuclear Power: An update of The Economic Future of Nuclear Power (2004). Department of Economics. Stanford University. Feb 22, 2011
495	Nuclear	2010	$ 0.08		115		IEA 2012	2012	Energy Technology Perspectives 2012 Pathways to a Clean Energy System
496	Nuclear	2010	$ 0.10		127		Black and Veatch 2012	2012	COST AND PERFORMANCE DATA FOR POWER GENERATION TECHNOLOGIES
497	Nuclear	2014	$ 0.09		95	0.25	Lazard 2014	2014	Lazard Levelized Cost of Energy Analysis, version 8.0
498	Nuclear	2014	$ 0.13		115	0.75	Lazard 2014	2014	Lazard Levelized Cost of Energy Analysis, version 8.0

ANNEX 5: Data Visualization

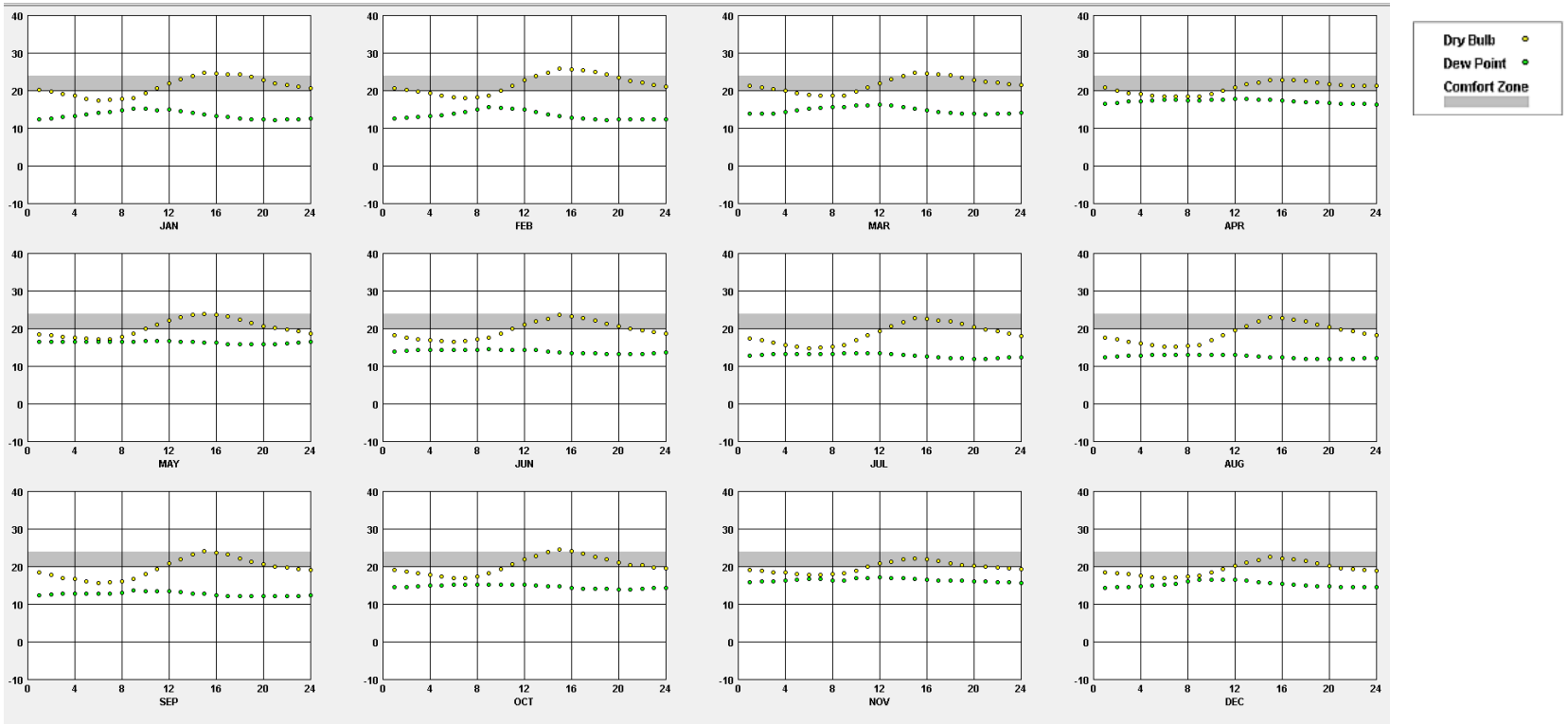

Figure 0-1: Monthly variation of Dry Bulb and Dew point for a TMY at station 636410

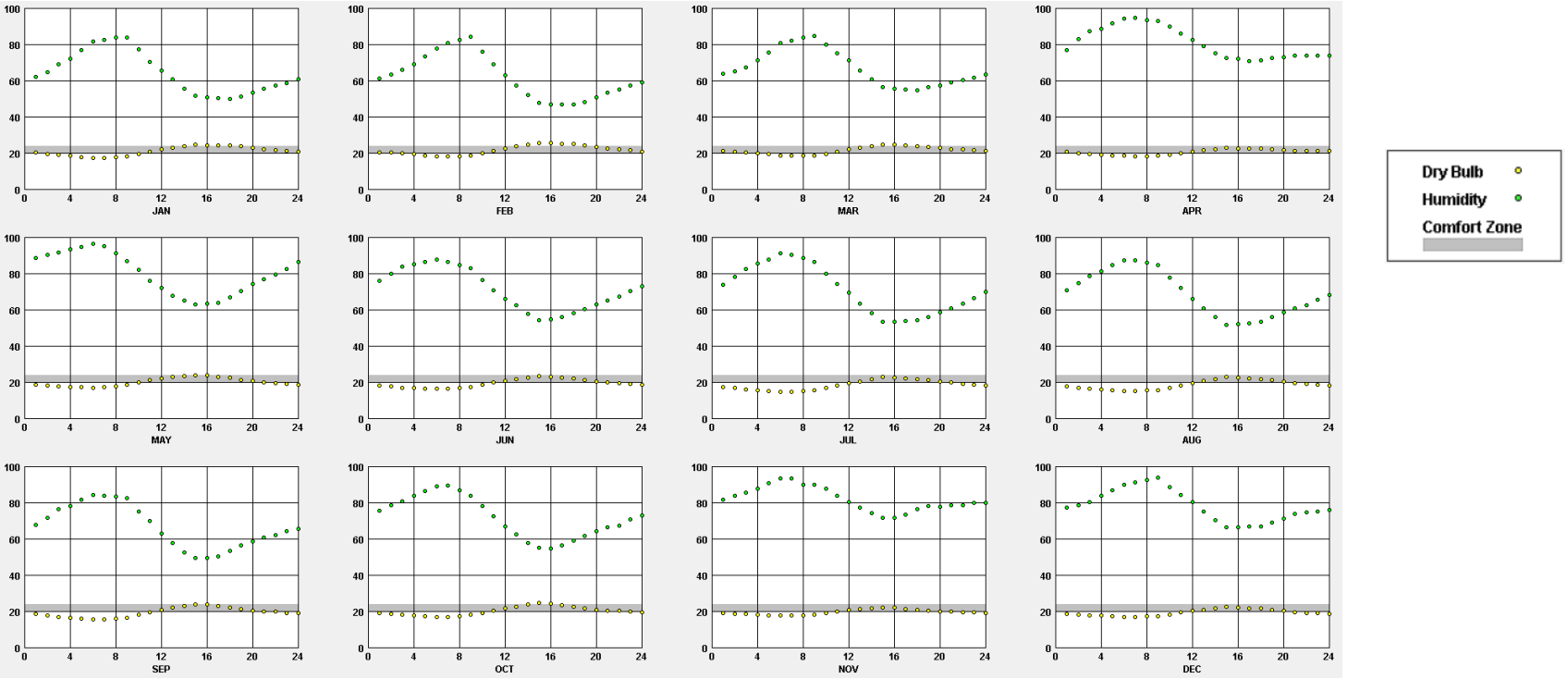

Figure 0-2: Monthly variation of relative humidity and Dry Bulb Temperature over a TMY at station 636410

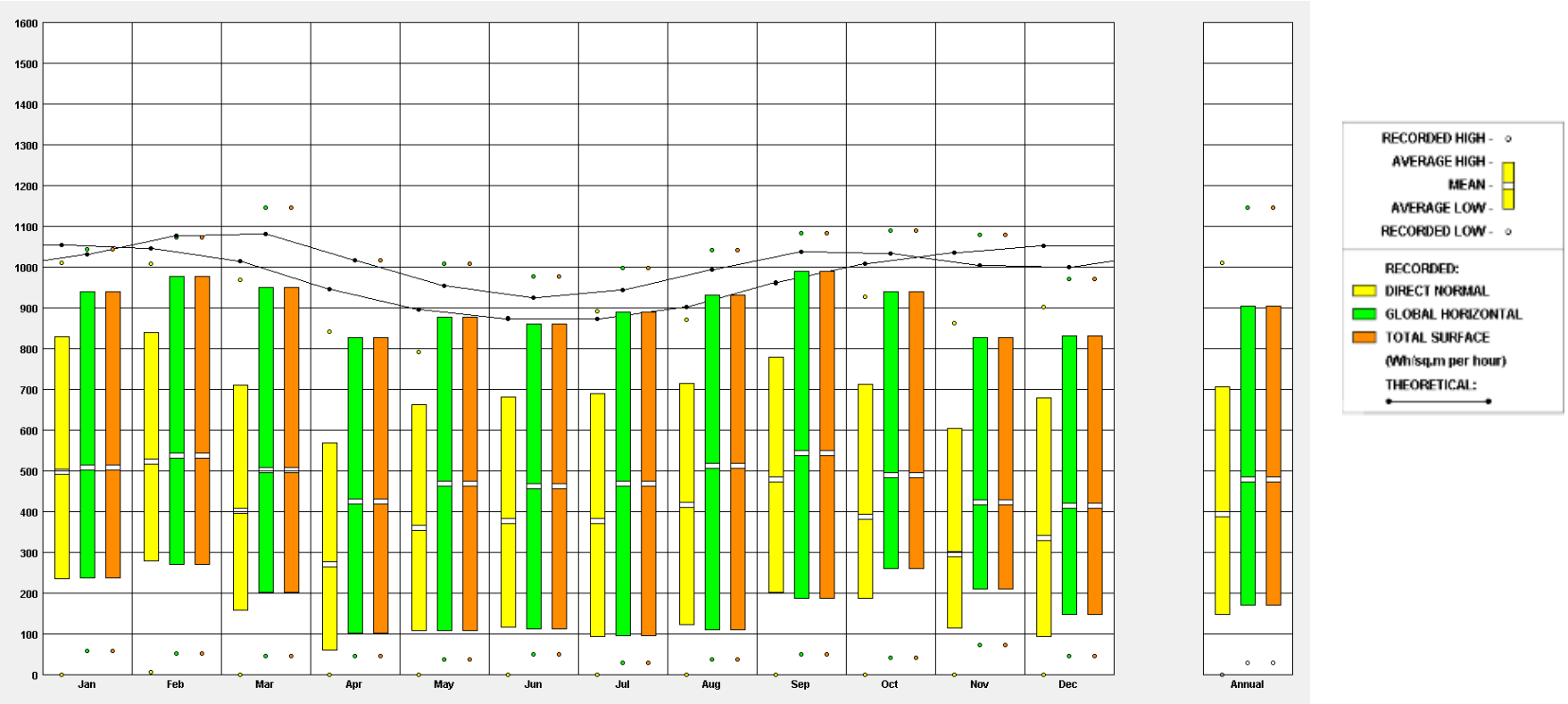

Figure 0-3: Hourly Average Radiation range for Day lit Hours over a TMY at station 636410

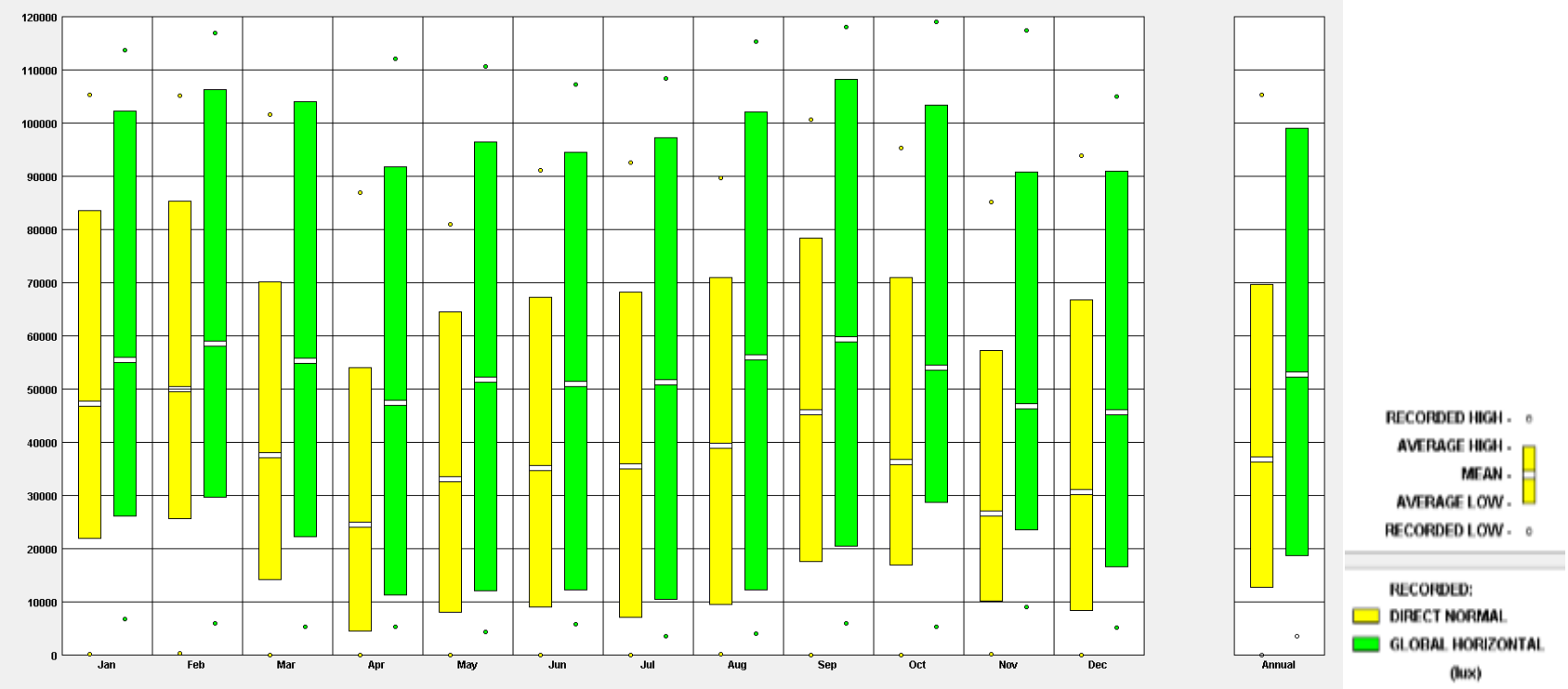

Figure 0-4: Hourly day lit hour's illumination over a TMY at station 636410

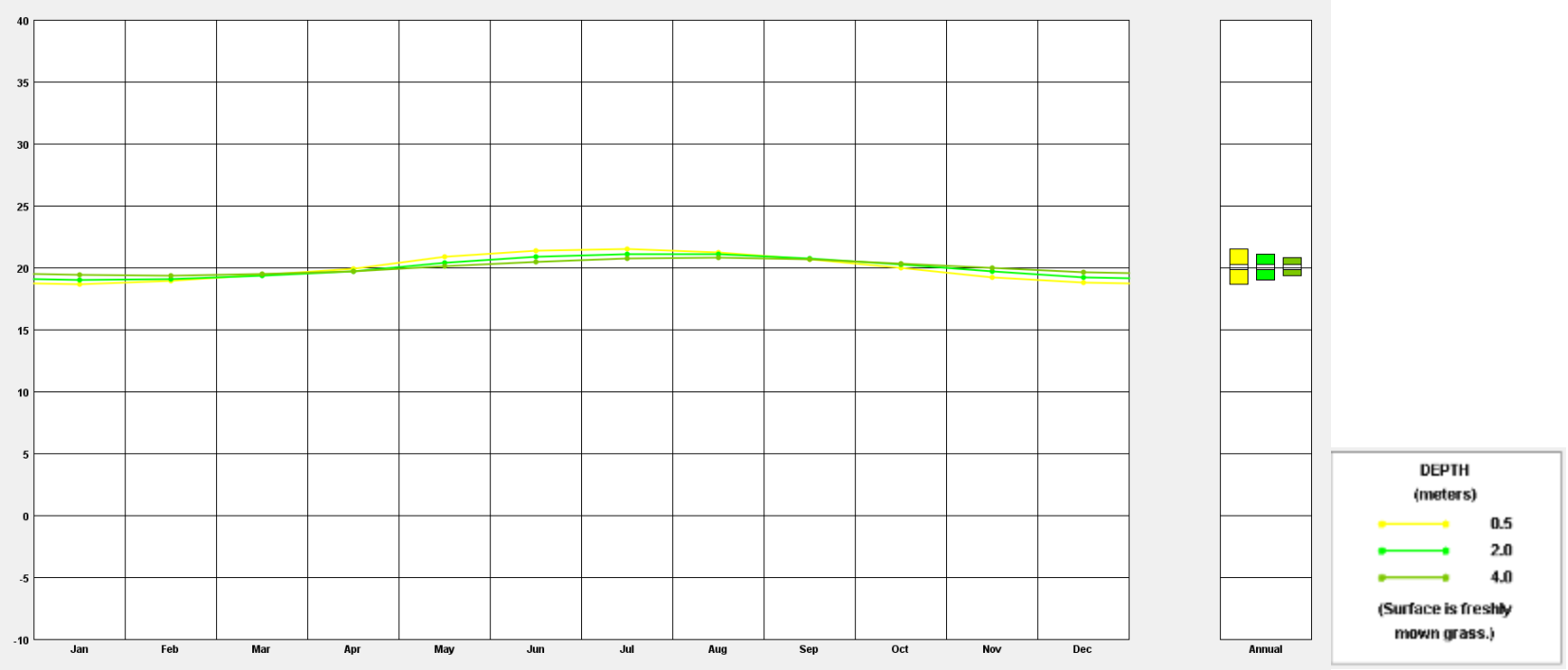

Figure 0-5: Monthly average ground temperature over a TMY at station 636410

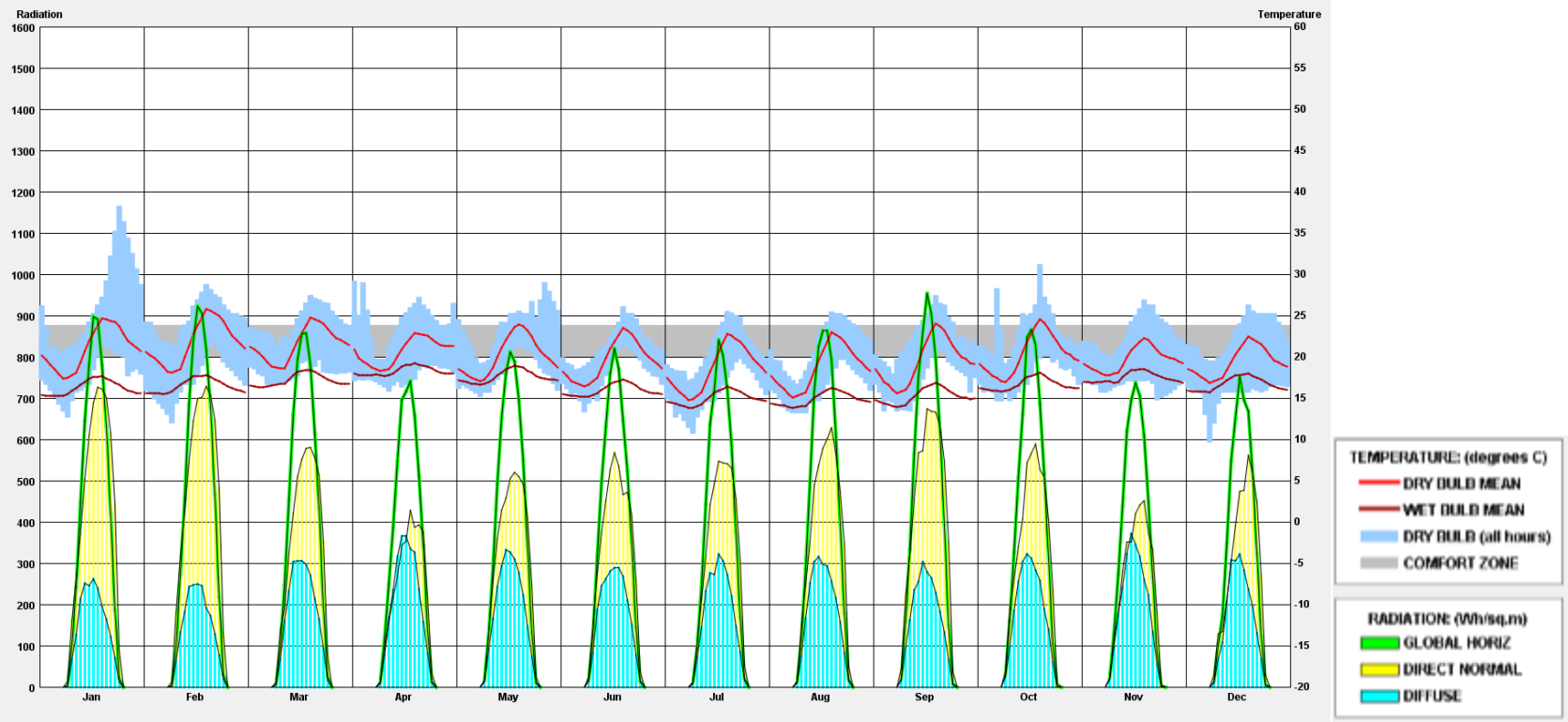

Figure 0-6: Diurnal hourly averages for various radiation and temperature parameters over a TMY at station 636410

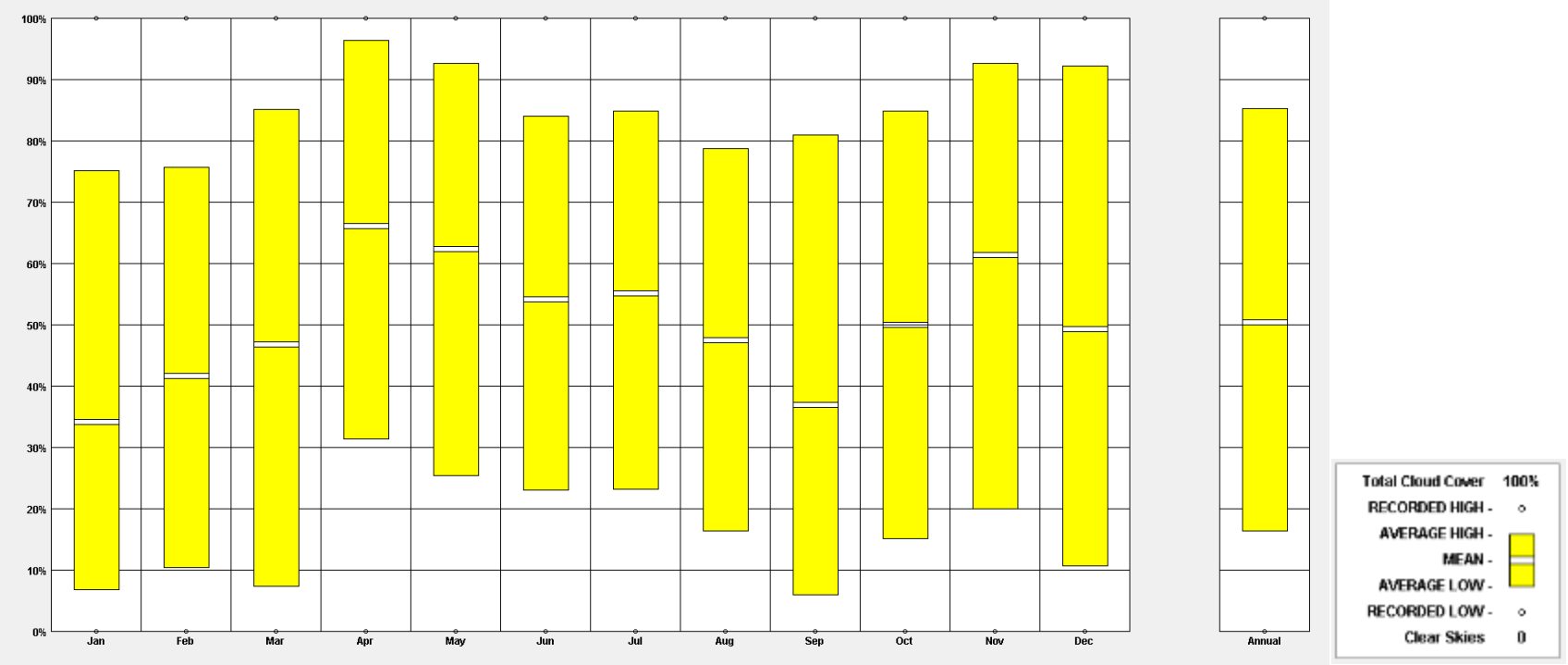

Figure 0-7: Sky cover range in percentage over a TMY for station 636410

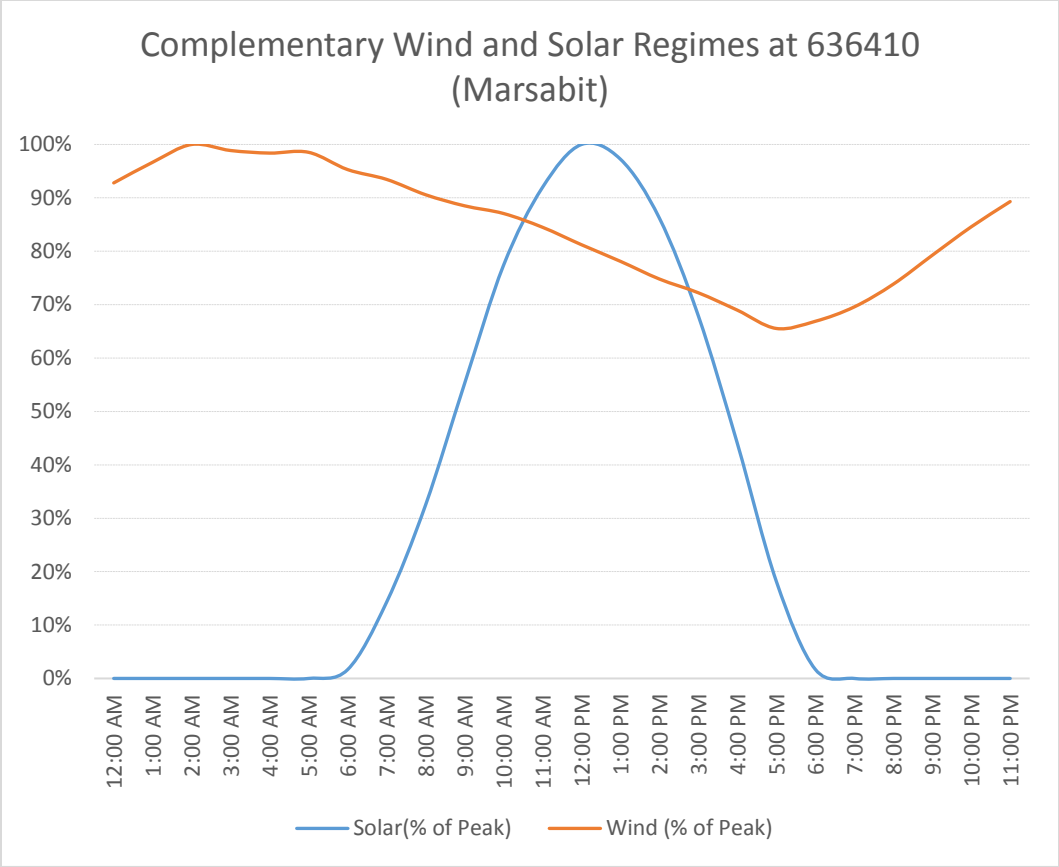

Figure 0-8: Complementary wind and solar regimes – analysis in data matrix

END